

**THE QUANTITATIVE ISOLATION OF 'INSOLUBLE ORGANIC MATTER'
(IOM) FROM SEDIMENTS AND BACTERIA, AND ITS ATTEMPTED
DISSOLUTION USING THE IONIC LIQUID 1-ETHYL-3-
METHYLIMIDAZOLIUM CHLORIDE-ALUMINIUM (III) CHLORIDE**

by

PAUL ANTONY SUTTON

A thesis submitted to the University of Plymouth
in partial fulfilment for the degree of

DOCTOR OF PHILOSOPHY

Department of Environmental Sciences
Faculty of Science

2000

90 0451855 6



UNIVERSITY OF PLYMOUTH	
Item No.	900 4518556
Date	- 4 DEC 2000
Class No.	T 552.5 SUT
Contl. No.	X 70416 8366
LIBRARY SERVICES	

REFERENCE ONLY

LIBRARY STORE

British Library thesis no. DX235857

This copy of the thesis has been supplied on condition that anyone who consults it is understood to recognise that its copyright rests with its author and that no quotation and no information derived from it may be published without the authors prior consent.

Signed Paul Latta

Dated 16/11/00



THE QUANTITATIVE ISOLATION OF 'INSOLUBLE ORGANIC MATTER' (IOM) FROM SEDIMENTS AND BACTERIA, AND ITS ATTEMPTED DISSOLUTION USING THE IONIC LIQUID 1-ETHYL-3-METHYLIMIDAZOLIUM CHLORIDE-ALUMINIUM (III) CHLORIDE

by

Paul Antony Sutton

ABSTRACT

Organic matter which is insoluble in common solvents and non-oxidising acids often comprises the quantitatively most important fraction of organic matter in sediments. This operationally defined material is usually simply termed 'insoluble organic matter' (IOM) or 'kerogen' when it is isolated from ancient sediments. Indeed, kerogen is regarded as the most abundant form of carbon on the planet. The molecular character of this generic material has not been fully elucidated, principally because of its insolubility which limits instrumental methods of analysis to those applicable to solid substrates. This thesis describes the quantitative isolation of IOM from lacustrine and marine sediments and two species of methanogenic bacteria using a sequential isolation procedure. A range of synthetic IOMs (melanoidins) was also prepared. The dissolution of IOM and melanoidins obtained in this manner was then attempted using the acidic ionic liquid 1-ethyl-3-methylimidazolium chloride-aluminium (III) chloride. Two synthetic dendrimers containing similar functional groups to those observed in sedimentary IOM were used to try and assess the mode of action of the ionic liquid. Ionic liquid treatment of the DCM soluble dendrimers resulted in the formation of 7 - 62 % of material that was no longer soluble in DCM, whilst the soluble components had been substantially altered. The ionic liquid was found to non-quantitatively promote ether cleavage, protonation and rearrangement reactions.

IOM was isolated from lacustrine Rostherne Mere, UK, sediments (7 - 30 % dry weight), Kimmeridge Clay, Dorset (11 - 12 %) and methanogenic bacteria (*Methanococcus jannaschii*, 3 %; *Methanobacterium thermoautotrophicum*, 0.1 %) using a time-consuming isolation procedure involving over forty separate chemical manipulations. Monitoring of the sequential isolation of IOM and characterisation of the final isolates was carried out using solid-state NMR, IR, elemental analysis, pyrolysis-gas chromatography-mass spectrometry (Py-GC-MS), scanning electron microscopy, and the newer surface sensitive technique of time of flight-secondary ion mass spectrometry (ToF-SIMS). Less than 1 % of sedimentary IOM and 5 % of Kimmeridge Clay IOM was soluble in DCM following ionic liquid treatment, whilst alkyl chains were lost from the insoluble portion which also increased in aromaticity. The poor yield recovered following ionic liquid treatment of *M. jannaschii* IOM (5 %) was attributed to loss of volatile material during hydrolysis. Following ionic liquid treatment 93 - 96 % of the melanoidins remained insoluble in DCM although their character had been altered, becoming more condensed. This ionic liquid dissolution procedure has not provided the substantial progress in elucidating the molecular character of IOM promised by earlier reports.

CONTENTS

ABSTRACT	i
CONTENTS	ii
LIST OF FIGURES	v
LIST OF TABLES	ix
AUTHORS DECLARATION	xi
ACKNOWLEDGEMENTS	xii
LIST OF COMMON ABBREVIATIONS	xiii
1.0 Introduction and aims	1
1.1 Introduction	2
1.1.1 Organic matter inputs to sediments	4
1.1.2 Quantitative sequential isolation of biochemical classes	5
1.1.2.1 Lipids	7
1.1.2.2 Proteins	9
1.1.2.3 Carbohydrates	10
1.1.2.4 Insoluble organic matter	10
1.2 Instrumental techniques routinely used to characterise IOM (kerogen)	11
1.2.1 Chemolysis techniques	13
1.2.2 ¹³ C Solid-state nuclear magnetic resonance spectroscopy	14
1.2.3 Elemental analysis	15
1.2.4 Infrared spectroscopy	16
1.2.5 Microscopy	17
1.3 Previous studies of IOM	18
1.4 Aims of the present study	25
2.0 Quantitative isolation of 'insoluble organic matter' (IOM)	26
2.1 Introduction	27
2.2 Experimental substrates	27
2.2.1 Sediments from Rostherne Mere, Cheshire, UK	28
2.2.2 Kimmeridge Clay	29
2.2.3 Bacteria	30
2.2.4 Algae	33
2.3 Experimental procedures	34
2.3.1 General laboratory procedures	35
2.3.2 Extraction of 'aqueous soluble' material	35
2.3.3 Extraction of 'free lipids'	35
2.3.4 Removal of 'proteins'	36
2.3.4.1 'Protein' determination	36
2.3.5 Removal of 'carbohydrates'	37
2.3.6 Removal of 'bound lipids'	38
2.3.7 Removal of 'minerals'	38
2.4 Results	39
2.4.1 Extraction efficiencies of 'aqueous-solubles', 'free lipids' and 'proteins' from Rostherne Mere sediments	39
2.4.2 Isolation of IOM from Rostherne Mere sediments	42
2.4.2.1 'Aqueous soluble' fraction	43
2.4.2.2 'Free lipid' fraction	44
2.4.2.3 'Protein' fraction	46
2.4.2.4 'Carbohydrate' fraction	48
2.4.2.5 'Bound lipid' fraction	48
2.4.2.6 'Mineral' fraction	49

2.4.2.7	'Insoluble organic matter' (IOM)	51
2.4.3	Isolation of IOM from Kimmeridge Clay	52
2.4.4	Isolation of IOM from bacterial necromass	53
2.4.5	Isolation of IOM from algae	56
2.5	Summary	58
3.0	Instrumental characterisation of IOM from sediments and biota	60
3.1	Introduction	61
3.2	Experimental procedures	61
3.2.1	Scanning electron microscopy	61
3.2.2	Elemental analysis	61
3.2.3	¹³ C Solid-state nuclear magnetic resonance spectroscopy (ss-NMR)	61
3.2.4	Infrared spectroscopy	62
3.3	Results	62
3.3.1	Scanning electron microscopy	62
3.3.2	Elemental analysis	69
3.3.3	¹³ C Solid-state nuclear magnetic resonance spectroscopy (ss-NMR)	72
3.3.4	Infrared spectroscopy	79
3.4	Summary	88
4.0	Monitoring the sequential isolation of 'insoluble organic matter' (IOM) using pyrolysis-gas chromatography-mass spectrometry (Py-GC-MS) and time of flight-secondary ion mass spectrometry (ToF-SIMS)	90
4.1	Introduction	91
4.1.1	Pyrolysis-gas chromatography-mass spectrometry (Py-GC-MS) applied to insoluble organic matter	91
4.1.2	Time of flight-secondary ion mass spectrometry (ToF-SIMS) techniques	94
4.2	Experimental procedures	96
4.2.1	Pyrolysis-Gas Chromatography-Mass Spectrometry (Py-GC-MS)	96
4.2.1.1	Instrumental details	97
4.2.1.2	Data collection	97
4.2.1.3	Quality control and quantitation	98
4.2.2	Time of flight-secondary ion mass spectrometry (ToF-SIMS)	98
4.3	Results	99
4.3.1	Py-GC-MS reproducibility	99
4.3.2	Monitoring sequential digestion of Rostherne Mere sediments	102
4.3.3	Monitoring isolation of IOM from Kimmeridge Clay	115
4.3.4	Monitoring isolation of IOM from <i>M. jannaschii</i>	122
4.4	Summary	130
5.0	Synthesis and characterisation of insoluble melanoidins	133
5.1	Introduction	134
5.2	Experimental procedures	136
5.2.1	Aqueous synthesis of insoluble melanoidins	137
5.2.2	Acidic synthesis of insoluble melanoidins	138
5.2.3	Pyrolysis-Gas Chromatography-Mass Spectrometry	138
5.2.4	Infrared Spectroscopy	138
5.3	Results	138
5.3.1	Insoluble melanoidins synthesised in water	138
5.3.2	Melanoidins synthesised in acid	139
5.3.3	Analysis of amino acids, glucose and melanoidins using Pyrolysis-Gas Chromatography-Mass Spectrometry	141

5.3.4	Analysis of melanoidins using Infrared Spectroscopy	147
5.4	Summary	149
6.0	Attempted dissolution of 'insoluble organic matter' (IOM) using the ionic liquid 1-ethyl-3-methylimidazolium chloride/ aluminium (III) chloride	151
6.1	Introduction	152
6.1.1	Review of ionic liquids	153
6.1.2	Review of dendrimer compounds	171
6.2	Experimental work	173
6.2.1	Preparation of [emim]Cl-AlCl ₃ {X(AlCl ₃), X = 0.65}	173
6.2.2	Dissolution protocol	175
6.2.3	Addition of [emim]Cl-AlCl ₃ {X(AlCl ₃), X = 0.65} to samples	176
6.2.4	Microwave heating	177
6.2.5	Pre-hydrolysis	178
6.2.6	Hydrolysis	178
6.2.7	Solvent extraction of retentate	178
6.2.8	Solvent extraction of filtrate	179
6.2.9	¹ H and ¹³ C NMR analysis	179
6.2.10	Pyrolysis-Gas Chromatography-Mass Spectrometry (Py-GC-MS) of solvent-extracted retentate	179
6.2.11	Gas Chromatography-Mass Spectrometry (GC-MS) of retentate and filtrate solvent extracts	180
6.2.14	Analysis of solvent-extracted retentates using Time of Flight – Secondary Ion Mass Spectrometry (TOF-SIMS)	180
6.2.15	Analysis of solvent-extracted filtrates using Electrospray Ionisation-Mass Spectrometry (ESI-MS)	181
6.3	Results	181
6.3.1	[emim]Cl-AlCl ₃ {X(AlCl ₃), X = 0.65} procedural blank	181
6.3.2	Ionic liquid-treated aromatic compounds	185
6.3.3	Ionic liquid-treated dendrimers	191
6.3.4	Ionic liquid-treated IOM from Rostherne Mere sediments	201
6.3.5	Ionic liquid-treated Kimmeridge Clay IOM	206
6.3.6	Ionic liquid-treated bacterial IOM from <i>M. jannaschii</i>	210
6.3.7	Ionic liquid-treated acid-synthesised insoluble melanoidins	214
6.4	Summary	216
7.0	Conclusions and future work	218
7.1	Conclusions	219
7.2	Suggestions for future work	222
	References	225

List of Figures

1.0	Introduction	
Figure 1.1	Sedimentary diagenetic pathways	6
Figure 1.2	Relationship between the total bacterial population and percentage uncharacterised organic matter with sediment depth	23
2.0	Quantitative isolation of 'insoluble organic matter' (IOM) from sediments and biota	
Figure 2.1	Outline of the sequential procedure used to isolate IOM from sediments and biota	28
Figure 2.2	Site location map for Kimmeridge Clay samples used in this study	30
Figure 2.3	Taxonomic relationship between <i>Archaea</i> , <i>Bacteria</i> and <i>Eucarya</i> emphasising hyperthermophiles within the 16S rRNA-based phylogenetic tree	32
Figure 2.4	Cumulative percentage of 'aqueous soluble' material extracted from Rostherne Mere sediments (5 - 6 cm and 95 - 96 cm)	41
Figure 2.5	Gravimetric results and cumulative percentage of 'free lipids' extracted from Rostherne Mere sediments (5 - 6 cm and 95 - 96 cm)	41
Figure 2.6	Gravimetric results and cumulative percentage of 'proteins' extracted from Rostherne Mere sediments (5 - 6 cm and 95 - 96 cm)	42
Figure 2.7	'Aqueous soluble' fractions removed from Rostherne Mere sediments as mean percentages of original sample weight	44
Figure 2.8	Comparison of 'free lipid' concentrations obtained in this study with those obtained by Crotty (1994)	45
Figure 2.9	'Free lipid' fractions removed from Rostherne Mere sediments as mean percentages of original sample weight	45
Figure 2.10	Protein equivalent concentrations obtained from 'protein' fractions in this study compared with those obtained by Crotty (1994)	47
Figure 2.11	'Protein' fractions removed from Rostherne Mere sediments as mean percentages of original sample weight	47
Figure 2.12	'Carbohydrate' fractions removed from Rostherne Mere sediments as mean percentages of original sample weight	48
Figure 2.13	'Bound lipid' fractions removed from Rostherne Mere sediments as mean percentages of original sample weight	49
Figure 2.14	'Mineral' fractions removed from Rostherne Mere sediments as a percentage of original sample weight	50
Figure 2.15	IOM fraction isolated from Rostherne Mere sediments as a percentage of original sample weight	51
Figure 2.16	Kimmeridge Clay: range of gravimetric results for operationally defined fractions	53
Figure 2.17	<i>M. jannaschii</i> : gravimetric results for operationally defined fractions	54
Figure 2.18	<i>M. thermoautotrophicum</i> : gravimetric results for operationally defined fractions	55
Figure 2.19	<i>D. postgatei</i> : gravimetric results for operationally defined fractions	55
Figure 2.20	<i>S. costatum</i> : gravimetric results for operationally defined fractions	57
Figure 2.21	<i>H. ostrearia</i> : gravimetric results for operationally defined fractions	58

Figure 2.22	Proportion of IOM isolated from lacustrine Rostherne Mere sediments, Kimmeridge Clay, and methanogenic bacteria	59
3.0	Instrumental characterisation of IOM from sediments and biota	
Figure 3.1	SEM micrograph of Rostherne Mere sediment (a) Untreated (b) IOM	64
Figure 3.2	SEM micrographs of <i>M. jannaschii</i> (a) Untreated (b) IOM	65
Figure 3.3	SEM micrographs of <i>M. thermoautotrophicum</i> (a) Untreated (b) IOM	66
Figure 3.4	SEM micrographs of <i>S. costatum</i> (a) Untreated (b) IOM	67
Figure 3.5	SEM micrographs of <i>H. ostrearia</i> (a) Untreated (b) IOM	68
Figure 3.6	Change in CHN content (mg g ⁻¹ dry weight sediment) in Rostherne Mere sediments following each digestion stage (a) 6 - 7 cmbswi (b) 94 - 95 cmbswi	71
Figure 3.7	Change in sedimentary atomic H/C and N/C ratios after each sequential digestion stage	72
Figure 3.8	Solid-state CP-MAS ¹³ C NMR spectra of Rostherne Mere sediment from 6 - 7 cm below sediment-water interface (a) untreated (b) IOM	73
Figure 3.9	Solid-state CP-MAS ¹³ C NMR spectra of Rostherne Mere sediment from 94 - 95 cm below sediment-water interface (a) untreated (b) IOM	74
Figure 3.10	Summary of carbon distributions (%) from ss-NMR ¹³ C spectra of untreated Rostherne Mere sediments (6 - 7 and 94 - 95 cmbswi) and IOM isolated from the same sediments	75
Figure 3.11	Change in carbon fractions following sequential digestion (mg C g ⁻¹ dry sediment) (a) 6 - 7 cm (b) 94 - 95 cm	77
Figure 3.12	Percentage change in calculated mass of carbon environments between untreated Rostherne Mere sediments (6 - 7 and 94 - 95 cmbswi) and respective IOMs using ss-NMR CP-MAS and SPE experiments	78
Figure 3.13	Solid-state NMR spectra of untreated <i>M. jannaschii</i> bacterial necromass (a) CP 3 ms (c) CPDD 3 ms	79
Figure 3.14	Infrared absorbance spectra of Rostherne Mere sediment, 6 - 7 cmbswi (a) untreated (b) IOM	81
Figure 3.15	Infrared absorbance spectra of Rostherne Mere sediment, 94 - 95 cmbswi (a) untreated (b) IOM	81
Figure 3.16	Infrared absorbance spectra of Rostherne Mere sediment (5 - 6 cmbswi) a) IOM b) DCM extracted IOM	82
Figure 3.17	Infrared spectra of Kimmeridge Clay (a) untreated (b) IOM	83
Figure 3.18	Infrared spectra of <i>M. jannaschii</i> (a) untreated (b) IOM	85
Figure 3.19	Infrared spectra of <i>M. thermoautotrophicum</i> (a) untreated (b) IOM	86
Figure 3.20	Infrared absorbance spectra of <i>S. costatum</i> (a) untreated (b) IOM	87
Figure 3.21	Infrared spectra of <i>H. ostrearia</i> (a) untreated (b) IOM	88
4.0	Monitoring sequential isolation of insoluble organic matter using Pyrolysis-Gas Chromatography-Mass Spectrometry (Py-GC-MS) and Time of Flight-Secondary Ion Mass Spectrometry (ToF-SIMS)	
Figure 4.1	Schematic layout of ToF-SIMS instrument and process used in the current study	94
Figure 4.2	Chronological variability in chromatographic response (peak	100

Figure 4.3	area) of PtBS internal standard used in Py-GC-MS analyses Reconstructed total ion chromatograms from the Py-GC-MS of Rostherne Mere sediment following each stage of the sequential digestion procedure normalised to the toluene peak	105
Figure 4.4	Typical mass spectrum (RT = 6:03 min) from the series of fluorinated compounds identified in the Py-GC-MS chromatogram of IOM isolated from Rostherne Mere sediment	104
Figure 4.5	Ion chromatograms from the Py-GC-MS of IOM isolated from Rostherne Mere sediment differentiating the series of fluorinated compounds from the <i>n</i> -alkane/alk-1-ene series	108
Figure 4.6	Generic structure of Teflon® PFA	108
Figure 4.7	Averaged mass spectra from the Py-GC-MS analyses of 0.4 mg of untreated Rostherne Mere sediment and sedimentary IOM	110
Figure 4.8	Partial ToF-SIMS positive ion mass spectra of untreated Rostherne Mere sediments	112
Figure 4.9	Partial ToF-SIMS positive ion mass spectra of IOM isolated from Rostherne Mere sediments	114
Figure 4.10	Reconstructed total ion chromatograms from the Py-GC-MS of untreated Kimmeridge Clay and 'IOM' isolated from the same sample	117
Figure 4.11	Background subtracted averaged mass spectra of pyrograms obtained from the Py-GC-MS of untreated Kimmeridge clay and 'IOM' isolated from the same sample	120
Figure 4.12	Partial ToF-SIMS positive ion mass spectra of untreated Kimmeridge Clay and IOM isolated from the same material	122
Figure 4.13	Reconstructed total ion chromatogram from the Py-GC-MS of untreated <i>M. jannaschii</i> and 'IOM' isolated from the same sample	124
Figure 4.14	Alkane and alk-1-ene ion chromatograms from the Py-GC-MS analysis of untreated <i>M. Jannaschii</i> and IOM isolated from the sample	127
Figure 4.15	Background subtracted averaged mass spectra from the Py-GC-MS of untreated <i>M. jannaschii</i> and IOM isolated from the same sample	128
Figure 4.16	Partial ToF-SIMS positive ion mass spectra of untreated <i>M. jannaschii</i> and IOM isolated from the same material	130
5.0	Synthesis and characterisation of insoluble melanoidins	
Figure 5.1	Py-GC-MS TIC of glycine	142
Figure 5.2	Py-GC-MS TIC of histidine	143
Figure 5.3	Py-GC-MS TIC of glucose	144
Figure 5.4	Py-GC-MS TIC of acid synthesised Gly/Glu melanoidin	145
Figure 5.5	Py-GC-MS TIC of acid synthesised His/Glu melanoidin	147
Figure 5.6	Infrared absorbance spectra of acid synthesised Gly/Glu and His/Glu melanoidins	149
6.0	Attempted dissolution of 'insoluble organic matter' (IOM) using the ionic liquid 1-ethyl-3-methylimidazolium chloride/aluminium (III) chloride	
Figure 6.1	Phase diagram for [emim]Cl-AlCl ₃ (Fannin <i>et al.</i> , 1984)	155
Figure 6.2	Schematic of electrophilic aromatic substitution: Friedel-Crafts alkylation and acylation	156
Figure 6.3	Schematic of the Fries rearrangement	157
Figure 6.4	Schematic of the Scholl reaction, (a) intermolecular, (b)	157

	intramolecular	
Figure 6.5	Proposed reaction scheme for the acetylation of anthracene (Adams <i>et al.</i> , 1998)	162
Figure 6.6	Reaction equilibrium for the protonation of anthracene in superacidic [emim]Cl-AlCl ₃ with [emim]HCl ₂ as the proton source (Carlin <i>et al.</i> , 1992)	163
Figure 6.7	Flow chart of ionic liquid 'dissolution' procedure used by Patell (1994) and Dutta (1994)	167
Figure 6.8	Mass distribution of traditional polymers and dendrimers	171
Figure 6.9	Simplified divergent and convergent dendrimer synthesis	172
Figure 6.10	Structure of dendrimer G ₁ P-[6]-Obn	174
Figure 6.11	Structure of dendrimer G ₂ P-[12]-Obn	174
Figure 6.12	Experimental protocol for the attempted dissolution of IOM	175
Figure 6.13	¹ H and ¹³ C NMR spectra of [emim]Cl-AlCl ₃	182
Figure 6.14	Partial GC-MS TIC of anthracene retentate solvent extract	186
Figure 6.15	Partial Py-GC-MS TIC of anthracene solvent-extracted retentate	187
Figure 6.16	Positive ion ESI-MS mass spectra of methanol, and solvent-extracted filtrates from [emim]Cl-AlCl ₃ and phenanthrene	189
Figure 6.17	Partial GC TIC of phenanthrene retentate solvent extract	190
Figure 6.18	Partial Py-GC-MS TIC of phenanthrene solvent-extracted retentate	191
Figure 6.19	Py-GC-MS TIC of G ₁ P-[6]-Obn (a) Before ionic liquid treatment (b) Solvent-extracted retentate	193
Figure 6.20	Hypothesised fragmentation routes for major products formed during the pyrolysis of untreated G ₁ P-[6]-Obn	194
Figure 6.21	Formation pathway of phenanthrene from <i>cis</i> -stilbene by UV irradiation in the presence of molecular oxygen (from March, 1985)	195
Figure 6.22	Partial GC TIC of G ₁ P-[6]-Obn retentate solvent extract	196
Figure 6.23	Partial GC-MS TIC of G ₂ P-[12]-Obn retentate solvent extract	198
Figure 6.24	Py-GC-MS TIC of G ₂ P-[12]-Obn (a) Before ionic liquid treatment (b) Solvent-extracted retentate	199
Figure 6.25	Typical partial Py-GC-MS TIC of Rostherne Mere sedimentary IOM (a) Before ionic liquid treatment (b) Solvent-extracted retentate	203
Figure 6.26	Partial positive ion ToF-SIMS mass spectrum of Rostherne Mere sediment IOM solvent-extracted retentate	205
Figure 6.27	Partial Py-GC-MS TIC of ionic liquid-treated Kimmeridge clay (a) IOM (b) Solvent-extracted retentate	208
Figure 6.28	Background subtracted averaged mass spectrum of ionic liquid-treated Kimmeridge Clay IOM solvent-extracted retentate	209
Figure 6.29	Partial positive ion ToF-SIMS mass spectrum of ionic liquid-treated Kimmeridge clay IOM solvent-extracted retentate	210
Figure 6.30	Time averaged positive ion ESI-MS mass spectrum of <i>M. jannaschii</i> solvent-extracted filtrate	211
Figure 6.31	Py-GC-MS TIC of <i>M. jannaschii</i> (a) IOM (b) Solvent-extracted retentate	213
Figure 6.32	Partial Py-GC-MS TIC of (a) Insoluble Gly/Glu melanoidin (b) Solvent-extracted retentate following ionic liquid treatment	215
Figure 6.33	Background subtracted averaged mass spectrum of Py-GC-MS analysis of Gly/Glu solvent-extracted retentate	216

List of Tables

1.0	Introduction	
Table 1.1	Summary of typical analytical instrumental techniques routinely applied to the analysis of solid samples	12
Table 1.2	Principal chemolysis techniques applied to kerogens	14
Table 1.3	Principal absorption band assignments used in IR analysis of kerogen	17
Table 1.4	Relative contribution of organic fractions from Lower St. Lawrence Estuary as percentage of Total Organic Carbon and Total Nitrogen	19
Table 1.5	Summary of recent quantitative sequential studies into major biochemical classes isolated from sediments	21
Table 1.6	Proportion of non-hydrolysable material obtained from nine species of bacteria	24
Table 1.7	Yield of non-hydrolysable organic matter from Actinomycetes	24
Table 1.8	Yields of melanoidin-like polymers	25
2.0	Quantitative Isolation of 'Insoluble Organic Matter' (IOM)	
Table 2.1	Gross biochemical composition of <i>S. costatum</i> previously reported	57
3.0	Instrumental characterisation of IOM from sediments and biota	
Table 3.1	Elemental carbon, hydrogen and nitrogen content of Rostherne Mere sediment (6 - 7 cmbswi) following each stage of the sequential isolation procedure	69
Table 3.2	Elemental carbon, hydrogen and nitrogen content of Rostherne Mere sediment (94 - 95 cmbswi) following each stage of the sequential isolation procedure	70
4.0	Monitoring sequential isolation of insoluble organic matter using Pyrolysis-Gas Chromatography-Mass Spectrometry (Py-GC-MS) and Time of Flight-Secondary Ion Mass Spectrometry (ToF-SIMS)	
Table 4.1	Summary of parent-like positive and negative secondary ion species observed in mass spectra from the SIMS analysis of organic substrates (from Benninghoven <i>et al.</i> , 1987)	96
Table 4.2	Chromatographic response quantified as a percentage of the sample mass subjected to Py-GC-MS	101
5.0	Synthesis and characterisation of insoluble melanoidins	
Table 5.1	Composition and pH of mixtures of amino acids and glucose used in the attempted aqueous synthesis of insoluble melanoidins	137
Table 5.2	Product yields of melanoidins synthesised in aqueous solution	139
Table 5.3	Product yields of melanoidins synthesised in acid solution	140
6.0	Attempted dissolution of 'insoluble organic matter' (IOM) using the ionic liquid 1-ethyl-3-methylimidazolium chloride/aluminium (III) chloride	
Table 6.1	Ionic species present in purified and hydrolysed [emim]Cl-AlCl ₃	158
Table 6.2	Yields and reaction conditions for the Friedel-Crafts acetylation of aromatic compounds in [emim]Cl-AlCl ₃ {X(AlCl ₃), X = 0.67} (Adams <i>et al.</i> (1998)	161
Table 6.3	Yields and reaction conditions for the Friedel-Crafts acetylation	161

	of anthracene at 0 °C in [emim]Cl-AlCl ₃ {X(AlCl ₃), X = 0.67} (Adams <i>et al.</i> (1998)	
Table 6.4	Degree of protonation of arenes in the superacidic HCl-containing [emim]Cl-AlCl ₃ ionic liquid	163
Table 6.5	Relative proportion (%) of compound classes released during each stage of the sequential extraction of reprecipitated Green River (Type I) kerogen after treatment with [emim]Cl-AlCl ₃ (Patell, 1994)	169
Table 6.6	Relative proportion (%) of compound classes released during each stage of the sequential extraction of reprecipitated Kimmeridge Clay (Type II) kerogen after treatment with [emim]Cl-AlCl ₃ (Patell, 1994)	169
Table 6.7	Relative proportion of carbon environments in Type I and II kerogens before and after treatment with [emim]Cl-AlCl ₃ determined by ¹³ C CPMAS NMR (Patell, 1994)	170
Table 6.8	Relative proportion of carbon environments in Type II and Northumberland coal before and after treatment with [emim]Cl-AlCl ₃ determined by ¹³ C CPMAS NMR (Dutta, 1994)	170
Table 6.9	Ratios of substrates and ionic liquid mixtures	177
Table 6.10	NMR ¹ H assignments of [emim]Cl-AlCl ₃	183
Table 6.11	NMR ¹³ C assignments of [emim]Cl-AlCl ₃	183
Table 6.12	Percentage of initial sample weight in each of the fractions obtained following hydrolysis of substrate/ionic liquid mixtures and solvent extraction of the retentates and filtrates	184

AUTHORS DECLARATION

At no time during the registration for the degree of Doctor of Philosophy has the author been registered for any other University award.

This study was financed with the aid of a studentship from the University of Plymouth and a research award from the Natural Environment Research Council, Ancient Biomolecules Initiative (Grant No. GST/02/1385).

Relevant scientific seminars and conferences were attended at which work was often presented.

Publications:

Sutton, P.A., Lewis, C.A. and Rowland, S.J. (1996) Solving the insoluble? *Ancient Biomolecules Initiative (ABI) Newsletter*, 3, 80 - 81.

Sutton, P.A., Lewis, C.A. and Rowland, S.J. (1998) Solving the insoluble? PR handout for ABI Grand Finale, The Natural History Museum, London, January 1998.

Sutton, P.A., Lewis, C.A. and Rowland, S.J. (1998) Attempted dissolution of 'insoluble organic matter' from *Methanococcus jannaschii* and Rostherne Mere (UK) sediment with 1-ethyl-3-methylimidazolium chloride/aluminium (III) chloride. *Ancient Biomolecules*, 2, 195 - 207.

Oral presentations and Conferences attended:

Sutton, P.A., Lewis, C.A. and Rowland, S.J. Isolation of 'insoluble organic matter' (IOM) from sediments (oral presentation). Departmental seminar, University of Plymouth, April 1996.

Sutton, P.A., Lewis, C.A. and Rowland, S.J. The isolation of major biochemical and mineral classes from lacustrine sediment using a mass balance sequential digestion procedure (poster presentation). 7th Annual Meeting of the British Organic Geochemical Society, University of Liverpool, July 1996.

Sutton, P.A., Lewis, C.A. and Rowland, S.J. Isolation of IOM from sediments and bacteria. (oral presentation). Ancient Biomolecules Initiative Workshop, University of Bristol, June 1996.

Sutton, P.A., Lewis, C.A. and Rowland, S.J. Attempting the dissolution of IOM isolated from sediments and bacteria. (oral presentation). Ancient Biomolecules Initiative Workshop, University of Leicester, September 1996.

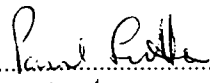
Sutton, P.A., Lewis, C.A. and Rowland, S.J. Attempted dissolution of sedimentary and bacterial IOM using a novel solvent, 1-ethyl-3-methylimidazolium chloride/aluminium (III) chloride. (oral presentation). Ancient Biomolecules Initiative meeting, Cambridge University, January 1997.

Sutton, P.A., Lewis, C.A. and Rowland, S.J. Attempted dissolution of 'insoluble organic matter' (IOM) isolated from sediments and bacteria, using a novel ionic liquid. Departmental seminar, University of Plymouth, May 1997.

Sutton, P.A., Lewis, C.A. and Rowland, S.J. Isolation and characterisation of sedimentary and bacterial "insoluble organic matter" (IOM) using dissolution in a novel ionic liquid (oral presentation). 9th Meeting of the British Organic Geochemical Society, University of Newcastle upon Tyne. July 1997.

Sutton, P.A., Lewis, C.A. and Rowland, S.J. Isolation and characterisation of sedimentary and bacterial "insoluble organic matter" (IOM) using dissolution in a novel ionic liquid (poster presentation). 18th International Meeting of the European Association of Organic Geochemistry, Maastricht, The Netherlands, September 1997.

Sutton, P.A., Lewis, C.A. and Rowland, S.J. Solving the insoluble? (oral presentation). Departmental seminar, University of Plymouth, March 1998.

Signed 

Dated 16/11/00

Acknowledgements

The difficult task of trying to 'solve the insoluble' has been an interesting and challenging philosophical, conceptual, practical and personal journey that would not have been completed without the welcome contributions of others whose help is readily and gratefully acknowledged. First and foremost I wish to thank my supervisors, Prof. Steve Rowland and Dr Anthony Lewis, for their invaluable assistance and patience throughout the course of this work and for their comments and advice in the preparation of this thesis.

I would like to thank Prof. Ken Seddon and Dr Yasmin Patell of Queen's University, Belfast for providing the ionic liquid, allowing me to work in their laboratory, and for making my trips to Belfast so memorable. Thanks are extended to Dr Andy Steele for undertaking ToF-SIMS analyses whilst working for NASA and for our useful and enlightening discussions. Prof. Colin Snape (University of Strathclyde) and Dr David Appleby are gratefully acknowledged for carrying out solid-state NMR experiments. Dendrimer molecules were supplied courtesy of Prof. David Haddleton of the University of Warwick.

Many thanks are owed to Roger Shrodzinski for maintaining and assisting with analyses using Py-GC-MS and GC-MS instrumentation. In addition, Paul McCormack and Roger are thanked for their help with ESI-MS analyses, Dr Roger Evens for showing me how to operate the NMR, Dr Roy Moate and staff for their assistance with SEM work, and Geology staff for their provision of facilities and assistance in HF dissolution work. Technical staff, including Ian Doidge, Andrew Tonkin and Andrew Arnold also merit thanks for the professional way in which they have helped, not only myself, but other students within the Environmental Sciences Department.

I wish to thank the NERC Ancient Biomolecules Initiative for funding the second year of study and the University of Plymouth for providing the initial studentship award.

All the 601 'crew' deserve thanks, especially Emma, Helen and Stewart, for helping me to "always look on the bright side of life". I wish my family, especially my gran, and friends (Jeanette, Steve and Alyn, and Elaine, Richard, Richard, Amie and Nicholas) to know that I am grateful for their continued support. Finally, I would like to thank my girlfriend Anita for her continuing support and encouragement, long may it continue.

LIST OF COMMON ABBREVIATIONS

^{13}C NMR	Carbon nuclear magnetic resonance spectroscopy
CP	Cross polarisation
DCM	Dichloromethane
DEPT	Distortionless enhancement by polarisation transfer
DD	Dipolar dephasing
EI	Electron impact
[emim]Cl-AlCl ₃	1-ethyl-3-methylimidazolium chloride-aluminium (III) chloride
{X(AlCl ₃), X = 0.65}	Mole fraction aluminium (III) chloride
GC-MS	Gas chromatography-mass spectrometry
G ₁ P-[6]-Obn	Generation 1 dendrimer with phloroglucinol core and six benzyl terminal groups
G ₂ P-[12]-Obn	Generation 2 dendrimer with phloroglucinol core and twelve benzyl terminal groups
^1H ^{13}C 2-D NMR	Two dimensional proton-carbon nuclear magnetic resonance spectroscopy
HCl	Hydrochloric acid
HF	Hydrofluoric acid
^1H NMR	Proton nuclear magnetic resonance spectroscopy
H ₂ SO ₄	Sulphuric acid
IOM	Operationally defined insoluble organic matter
IR	Infra-red spectroscopy
KOH	Potassium hydroxide
MAS	Magic angle spinning
MeOH	Methanol
M _r	Relative molecular mass
MS	Mass spectrometry
N ₂	Nitrogen
NMR	Nuclear magnetic resonance spectroscopy
OM	Organic matter
Py-GC-MS	Pyrolysis-gas chromatography-mass spectrometry
RSD	Relative standard deviation
SEM	Scanning electron microscopy
ss-NMR	Solid state nuclear magnetic resonance spectroscopy
TIC	Total ion chromatogram
ToF-SIMS	Time of flight-secondary ion mass spectrometry

Chapter 1: Introduction and aims

1.1. Introduction

Kerogen, the poorly described, heterogeneous macromolecular organic matter found in ancient sediments, is extremely important since most scientists accept that it is the source material from which petroleum is generated (Durand, 1980)^a. Possibly the factor which most impedes the molecular characterisation of kerogen, and of the somewhat analogous 'insoluble organic matter' (IOM) found in more recent sediments, is its insolubility in common solvents and in non-oxidising acids and bases. This thesis therefore describes the quantitative sequential isolation of IOM from contemporaneous lacustrine sediments, *Archaea*, algae and a marine shale, and subsequent attempts to dissolve the IOM in an unusual solvent known as an ionic liquid. Sequential isolation and attempted dissolution was monitored using pyrolysis-gas chromatography-mass spectrometry, time of flight-secondary ion mass spectrometry, elemental analysis, solid-state ¹³C nuclear magnetic resonance and infrared spectroscopy. The possibility that artefactual melanoidin-like material may form during the sequential isolation procedure was also investigated by synthesising a range of melanoidins and subjecting them to the same ionic liquid treatment. Relatively high molecular weight (1075 and 2454 Daltons) dendritic molecules and lower molecular weight compounds were used to assess the mode of action of the ionic liquid on known organic matter. Any components solubilised following the ionic liquid treatments were determined using gas chromatography-mass spectrometry after extraction into dichloromethane.

Fossil fuel deposits (*e.g.* coal, oil and gas) formed by biological, physical and chemical alteration of organic matter (Section 1.1) are amongst the commercially most important natural resources on Earth. However, the exact modes of formation of such deposits have yet to be fully elucidated. A major hindrance to progress in this area is the fact that the major portion of precursor material remains insoluble in normal solvents, non-oxidising

^a A contrasting view is described by Gold (1999) and references therein.

acids and bases. This insolubility precludes analysis using commonplace solution instrumental analytical techniques. Analytical instrumentation capable of providing information on solid samples does not provide data of the same quality as that provided by solution techniques (Section 1.4).

In addition to its occurrence in sediments and sedimentary rocks, IOM has also been isolated from a number of organisms (*e.g.* from algae, Atkinson *et al.*, 1972; Good & Chapman, 1978; Honegger & Brunner, 1981; Berkaloff *et al.*, 1983; Aken & Pienaar, 1985; Puel *et al.*, 1987; Burczyk, 1987; Zelibor *et al.*, 1988; Kadouri *et al.*, 1988; Derenne *et al.*, 1989; Gelin *et al.*, 1994, and algal spores, De Vries *et al.*, 1983, plant cuticles, Nip *et al.*, 1986a, 1986b; Tegelaar *et al.*, 1989a, and periderm tissue, Tegelaar *et al.*, 1993, the inner seed coat of fossil water plants, Van Bergen *et al.*, 1994, spores and pollen grains, Beckett, 1976; Guilford *et al.*, 1988; Hemsley *et al.*, 1996, and possibly from bacteria, Strohl *et al.*, 1977; Le Berre *et al.*, 1991). Many of these studies have utilised a retro-structural approach to IOM characterisation, based on chemolysis techniques, to try to determine the structure of the refractory IOM components but the isolation methods used have sometimes also resulted in artefactual IOM formation (Allard *et al.*, 1997). The formation of such artefacts (*e.g.* melanoidins; Chapter 5), during isolation and subsequent chemical treatments may produce misleading data from which incorrect interpretations of IOM structure may then be made. Development of a new dissolution technique that would allow solubilisation of previously insoluble organic matter, especially without artefact formation, would enable rapid progress to be made in discovering the true nature of IOM and may make the organic matter more amenable to analysis using powerful instrumental solution techniques.

Ionic liquids, which are liquid mixtures that are comprised entirely of ionic species, have been studied for a number of years. However, until recently those known were difficult to

work with because they were only liquid at elevated temperatures (*e.g.* sodium chloride is an ionic liquid at 803 °C, Seddon, 1996). Recent advances in ionic liquid chemistry have resulted in the development of ionic liquids that are liquid at room temperature (Chapter 6) and are much easier to work with. Whilst this field of chemistry is still in its infancy, ionic liquids have shown great promise in a wide range of applications, including solvents and catalysts (Koch *et al.*, 1976; Appleby *et al.*, 1986; Boon *et al.*, 1986; Surette *et al.*, 1996; Seddon, 1997; Adams *et al.*, 1998). Indeed, in geochemical research, two preliminary studies have reported that the ionic liquid, 1-ethyl-3-methylimidazolium chloride/aluminium (III) chloride (I) solubilises up to 95 % of certain kerogens (Dutta, 1994; Patell, 1994). These latter studies provided the impetus for the present more thorough investigation into the dissolution of IOM isolated from recent sediments, bacteria and algae, and into the solubility of authentic high molecular weight compounds. Few high molecular mass, polyfunctional, compounds of suitable purity and known chemical composition for controlled dissolution studies are presently available, but the rapid expansion of dendrimer chemistry has recently led to synthesis of some well-defined compounds. These have been used in the present study to test the modes of action of the ionic liquid (Chapter 6). The two compounds used in this study, abbreviated here and throughout the text to G₁P-[6]-Obn and G₂P-[12]-Obn, were selected primarily because their major functional groups reflect the functionality often observed by infrared spectroscopy in sedimentary IOM (*e.g.* ester groups, ether linkages and benzyl moieties).

1.1.1. Organic matter inputs to sediments

Organic matter (OM) from a variety of sources (*e.g.* algae, higher plants and bacteria) is deposited in sediments and subject to various biological, chemical and physical transformations during burial (diagenesis, catagenesis and metagenesis). The dominant sources of organic matter to sediments are dependent upon the environmental conditions existing at the time of deposition. To cite extreme examples, Type I kerogens have a

dominant algal source whilst coal deposits principally result from the alteration of higher plant remains (Tissot & Welte, 1984; de Leeuw & Largeau, 1993). Thus, the principal biotic source of organic matter to sediments is one of the major determinants in the type of fossil fuel deposit formed. Generally, organic material reaching the sediment surface undergoes rapid reworking by benthic organisms and bacteria. The formation of kerogen in ancient sediments has variously been attributed to the degradation of labile biomolecules and/or to their subsequent polycondensation (Tissot & Welte, 1984), or to the selective preservation of refractory biomolecules from the contributing organisms (Tegelaar *et al.*, 1989b), or to the protective adsorption of biomolecules to mineral grains (Hedges & Keil, 1995; Figure 1.1). It is likely that these reactions are not mutually exclusive but rather operate in parallel with the dominant mechanism dependent upon environmental conditions prevailing during and after burial. For example, selective preservation of non-hydrolysable components of algae (algaenans), similar to those in *Botryococcus braunii*, and bacteria (bacterans) has been indicated in algal kerogens (Hatcher *et al.*, 1983; Derenne *et al.*, 1988) and amorphous kerogens (Flaviano *et al.*, 1994), respectively. Upon burial, biological processes become a less dominant factor in OM alteration with depth, although viable bacterial communities have been identified from marine sediments at depths exceeding 500 m below the ocean floor (Parkes *et al.*, 1994, 2000).

1.1.2. Quantitative sequential isolation of biochemical classes

The soft parts of all living organisms are composed of the same groups of biochemicals: lipids, proteins, carbohydrates and in higher plants, lignin. Although the investigation of these classes of biochemicals is not the primary focus of this thesis, a broad overview of each biochemical class is provided in Sections 1.2.1 to 1.2.4 in order to provide an appreciation of the materials removed during the sequential digestion procedure employed in this work (Section 2.1). Many previous investigations of the biochemicals found in sediments have concentrated on relatively easily isolated fractions, such as lipids (*e.g.*

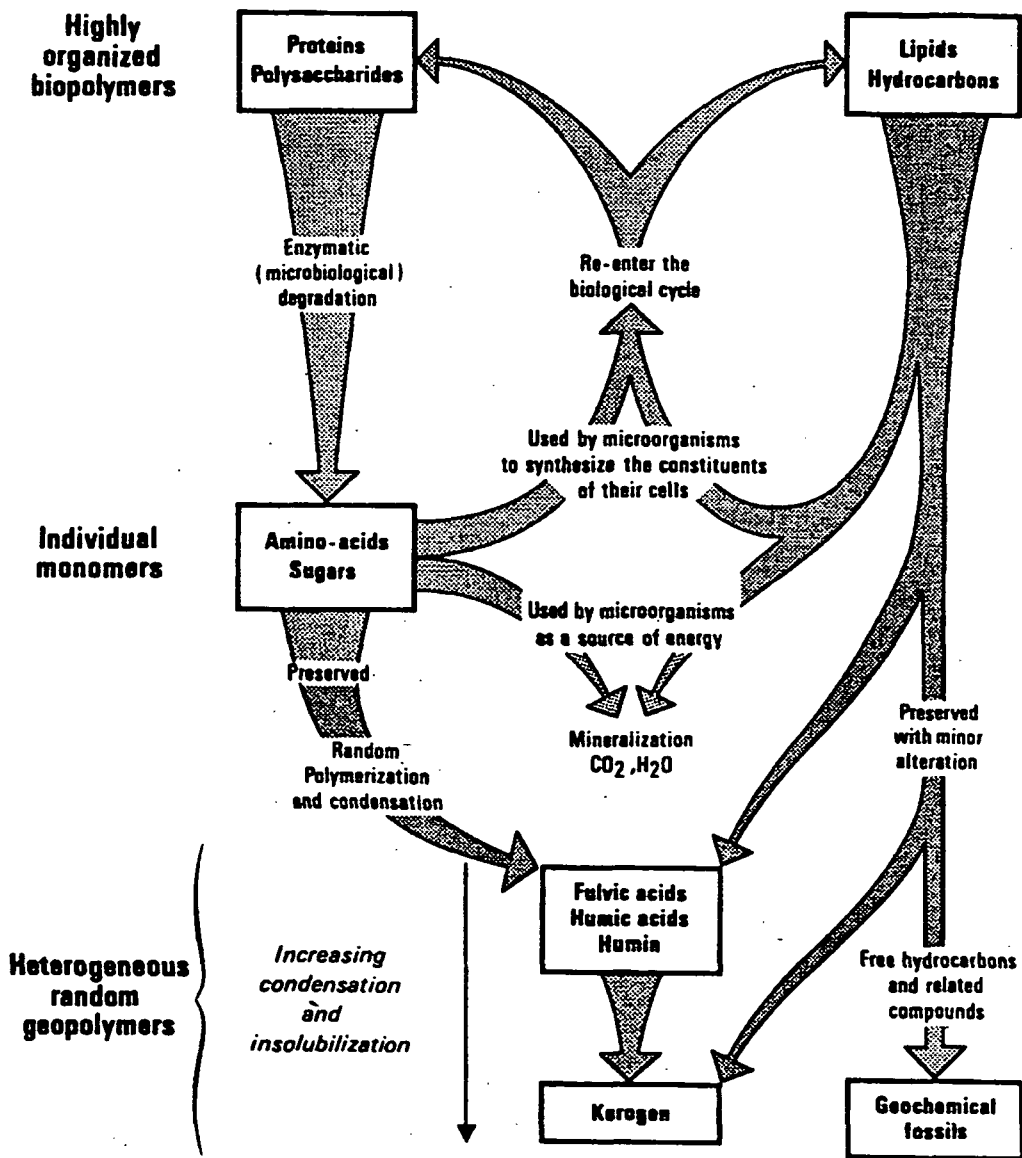


Figure 1.1. Sedimentary diagenetic pathways (from Tissot & Welte, 1984)

Volkman *et al.*, 1983; Leenheer & Meyers, 1983; Cranwell, 1990), proteins and amino acids (*e.g.* Emery *et al.*, 1964; Clarke, 1967; Rosenfield, 1979; Henrichs & Farrington, 1979, 1987; Burdige & Martens, 1984) and carbohydrates (*e.g.* Klok *et al.*, 1984a; Moers *et al.*, 1994). Determination of the precise chemical composition of organisms contributing to sedimentary organic matter has not yet been achieved. This primarily reflects the complex chemical nature of living matter and intra-species and intra-organism variability. Indeed, substantial post-mortem alteration of organic material during and after deposition makes full chemical characterisation of organisms somewhat fruitless. Notwithstanding

this, some chemical compounds specific to individual species (biomarkers) are preserved with little alteration in the sedimentary record and can provide useful information regarding the organisms contributing to sedimentary organic matter and environmental conditions prevailing during deposition (*e.g.* Philp, 1985; Johns, 1986; Peters & Moldowan, 1993).

In the present study, the major classes of biochemicals (*i.e.* lipids, proteins and carbohydrates) and mineral matter were sequentially removed from various substrates, including sediments, resulting in the isolation of that organic matter which is insoluble in normal solvents, non-oxidising acids and bases, *i.e.* IOM. A few previous studies have also quantified such insoluble fractions (*e.g.* Klok *et al.*, 1983, 1984; Reimers & Suess, 1983; Patience *et al.*, 1990; Parkes *et al.*, 1993; Lewis & Rowland, 1993; Ripley, 1994; Colombo *et al.*, 1996a; Fabiano & Danovaro, 1994), but this comparative paucity of studies of IOM, which belies the quantitative importance of the fraction, probably mainly reflects the difficulties in isolating and fully characterising the material using (currently) available instrumental techniques.

1.1.2.1. Lipids

Lipids, which include fats, oils and waxes, are compounds that are soluble in non-polar organic solvents but are practically insoluble in water. They are used by organisms for energy storage and some form components of cell membranes. Fats and oils comprise mixtures of triacylglycerides and are operationally distinguished, the former being a solid at room temperature and the latter, liquid. The carboxylic acid components of natural fats have an even number of carbon atoms, as they are biosynthesised from acetate units. Waxes, which generally fulfil a protective function in organisms, have similar structures to fats and oils but glycerol is replaced by complex alcohols of the sterol series or by aliphatic alcohols (C₁₆ – C₃₆) with even carbon number chains. In addition to the lipids mentioned

thus far, lipid-like materials (*e.g.* oil-soluble pigments, terpenoids, steroids, and complex fats) also merit inclusion because they can be extracted using solvent or following alkaline hydrolysis. The structures of terpenoid, and steroid compounds are based on the conjugation of isoprene units. Terpenoids can be categorised by the number of component isoprene units, *e.g.* mono- (2 units, C₁₀), sequi- (3 units, C₁₅), di- (4 units, C₂₀), tri- (6 units, C₃₀), tetra- (8 units, C₄₀), and poly- (>8 units). The isoprene units of terpenoids may be arranged linearly or in cyclic systems of one or more rings which may have varying degrees of saturation and occur with a variety of functionalities (*e.g.* hydrocarbons, alcohols or their esters, aldehydes, ketones, acids, or lactones).

Highly chemically resistant organic material obtained from a variety of organisms is thought to form *via* the ether cross-linking of lipidic fragments such as unsaturated acids, either on their own or in combination with polysaccharides. These materials have been given trivial names, generally according to their source organisms. For example, 'sporopollenins' from spores pollen grains, and vascular plants (*e.g.* Guilford *et al.*, 1988), 'algaenans' from algae (*e.g.* Tegelaar *et al.*, 1989b), 'cutans' and 'suberans' from the leaves and woody flesh of higher plants, respectively (*e.g.* Nip *et al.*, 1986a, 1986b; Tegelaar *et al.*, 1995), and 'bacterans' from bacteria (*e.g.* Le Berre *et al.*, 1991). Although these insoluble isolates apparently have a generic character (*i.e.* ether cross-linked hydrocarbon backbones) there has been some debate about how similar they really are. For example, sporopollenin which survives drastic non-oxidative chemical treatment such as acetolysis, has been suggested to originate from carotenoid-type tetraterpene precursors (Brooks, 1971). This view is not universally accepted (Berkaloff *et al.*, 1983; Guilford *et al.*, 1988; de Leeuw & Largeau, 1993). Algaenans which are comprised of non-hydrolysable ether cross-linked methylenic, isoprenoid or polyester chains are considered to form from acetate units or unsaturated or partially unsaturated acids (Berkaloff *et al.*, 1983; Kadouri *et al.*, 1988; Derenne *et al.*, 1989; Gelin *et al.*, 1997; Blokker *et al.*, 1998).

In the sequential digestion used in this study (Chapter 2) a distinction is made between 'free' and 'bound' lipids. 'Free' lipids are extracted by cold solvent extraction and 'bound' lipids are released upon hot alkaline hydrolysis. Alkaline hydrolysis will cleave triacylglycerides to give glycerol and the component unsaturated acids.

1.1.2.2. Proteins

Proteins, or polypeptides, are polymeric compounds comprising amino acids linked by peptide bonds and are important constituents of cells. Twenty amino acids commonly occur in nature. These can be combined in a number of different sequences. The inherent biological function of each protein is determined by the amino acid bonding sequence that confers different chemical properties on the resultant protein. Thus, proteins can act as enzymes, transporters, regulators, storage substances, defence substances or structural substances (de Leeuw & Largeau, 1993). Proteins can also be differentiated on a morphological basis into globular and fibrous proteins. Generally, globular proteins are water-soluble because they contain tightly folded chains with hydrophilic amino acid residues outermost and hydrophobic amino acid residues centred within the globule. In contrast, fibrous proteins, which account for most of the structural and protective functions, are elongated, stringy and water-insoluble. Water-insoluble proteins can be broken down in the presence of water by enzymatic processes into their aqueous soluble amino acid monomers (Tissot & Welte, 1984).

Free and enzymatically released amino acids present in samples subjected to the sequential digestion procedure used in this study should be extracted during the initial aqueous extraction stages. Non-aqueous-soluble proteins present in analytical substrates can be broken down to their constituent amino acids by the action of a mineral acid (*e.g.* 6M HCl,

110 °C; Bock, 1979) which cleaves the peptide bonds. Proteins released by peptide bond cleavage are then removed with the acid supernatant.

1.1.2.3. Carbohydrates

Carbohydrates are polyhydroxy aldehydes or polyhydroxy ketones that generally have the formula $C_n(H_2O)_m$ and yield water-soluble monosaccharides upon hydrolysis (*e.g.* with H_2SO_4). Depending on the number of monomeric units released on hydrolysis, carbohydrates are referred to as mono- (1 unit), di- (2 units), oligo- (3 – 10 units) or poly- (>10 units) saccharides. In excess of two hundred monosaccharides are known (Carey, 1992). Carbohydrates are major components of plants, present as supporting tissues and as energy sources. Cellulose for example, comprises 2000 – 8000 monomers and makes up 40 – 60 % of wood tissue. Pertinent sources and structures of naturally occurring geochemically important carbohydrates have been reviewed by de Leeuw & Largeau (1993).

1.1.2.4. Insoluble organic matter

The term ‘insoluble organic matter’ (IOM) is used throughout this text to refer to material remaining after the sequential removal of ‘lipids’, ‘proteins’ and ‘carbohydrates’, and ‘minerals’ from sediments. IOM isolated in the present study is somewhat analogous to refractory material isolated by other authors using fundamentally the same isolation procedure, albeit excluding a ‘mineral’ removal stage (*e.g.* Patience *et al.*, 1990; Parkes *et al.*, 1993; Ripley, 1994). However, direct comparison of data in this study with results obtained using alternative isolation procedures should be treated cautiously because different isolation protocols are likely to yield differing amounts of residual material which may also differ qualitatively. A distinction is made here between the **insoluble organic matter** isolated after removal of major biochemical classes, and **kerogen** which is the organic matter remaining after demineralisation and solvent extraction. Generally, kerogen

is isolated from organic-rich sediments by demineralisation using a mixture of acids (HF/HCl) followed by washing (H₂O) and solvent extraction of the residue (Durand, 1980). This method is often referred to as the 'classical method' of kerogen isolation (Boussafir *et al.*, 1995). Some researchers have used a modified method utilising ammonium carbonate and boric acid in order to prevent the formation of neo-fluorides (Boucher *et al.*, 1990). Not all researchers have used the same methods. Furthermore, the insolubility of kerogen combined with the lack of instrumentation capable of generating molecular information directly from this material has also limited progress in this field (Rullkötter & Michaelis, 1990).

At present, kerogen models are presented as complex macromolecules (*e.g.* Faulon *et al.*, 1990) although they may actually comprise a complexity of macromolecules, none of which is soluble. In addition, like IOM from biota and recent sediments, this macromolecular material does not have a unique formula, as evidenced by the various sources of organic matter which characterise kerogen types and the variety of means of classifying kerogens (*e.g. via* elemental ratios and hydrocarbon indices). Since few studies of IOM have been published (Patience *et al.*, 1990; Parkes *et al.*, 1993; Ripley, 1994) comparison of the structures of IOM and kerogens is currently impossible.

1.2. Instrumental techniques routinely used to characterise IOM (kerogen)

The insolubility of the bulk of sedimentary organic matter in normal solvents, non-oxidising acids and bases means that it is not amenable to commonplace solution instrumental analytical techniques. Routine instrumental analytical characterisation of insoluble organic matter is limited to a few techniques that provide only bulk information about the substrate (Table 1.1), including infrared spectroscopy (IR), solid-state nuclear magnetic resonance spectroscopy (ss-NMR) and elemental analysis, or to techniques that provide comprehensive information about altered parts of the substrate such as pyrolysis

techniques (*e.g.* pyrolysis coupled to mass spectrometry, gas chromatography, gas chromatography-mass spectrometry, or hydrous pyrolysis). With the exception of ss-NMR, and arguably IR spectroscopy and microscopy techniques, all other techniques applied to the elucidation of insoluble organic matter are destructive. Finally, before further considering the principal methods used in the analysis of insoluble organic material it is worth noting that most studies rely on the application of a number of complementary techniques in order to verify their conclusions (Rullkötter & Michaelis, 1990).

Table 1.1. Summary of typical analytical instrumental techniques routinely applied to the analysis of solid samples

Analytical technique	Chemical information	Comments
Infrared spectroscopy	Functional groups	Semi-quantitative
Solid-state ^{13}C NMR	Carbon environments and carbon-linked substituents	Semi-quantitative
Elemental analysis	Bulk C, H, N, S, O concentrations	Quantitative
Pyrolysis techniques	Pyrolysable material	(Semi)-quantitative
SEM (linked to X-ray analyser)	Morphological features (elemental composition)	Qualitative (quantitative)

Difficulties encountered in the instrumental characterisation of an insoluble solid are compounded when the substrate is macromolecular or is a mixture and contains polyfunctional substituents or linkages. Spectroscopic analysis of such materials often results in signal broadening, *e.g.* broad resonances and band broadening in solid-state NMR and IR, respectively, whilst the outcome of thermolytic cleavage and subsequent separation (*e.g.* Py-GCMS) is the production of a plethora of fragments that are often difficult to piece back together retrospectively. Furthermore, some molecular information may be ‘lost’ to these techniques, *e.g.* carbon atoms within macromolecules that cannot be made to resonate or respond to IR excitation, or which is non-pyrolysable material. In the

latter case, subsequent elemental analysis has shown that non-pyrolisable residual material can be strongly aromatic (Derenne *et al.*, 1990). Microscopy techniques are generally limited to morphological analysis although the coupling of an X-ray analyser to a SEM can be used to provide atomic information. This latter technique cannot be used for carbon analysis.

1.2.1. Chemolysis techniques

Chemical techniques applied to the determination of the structure of recalcitrant organic matter can be divided into three groups: those based on oxidation, reduction or cleavage. The purpose of chemical degradation is to release fragments from the refractory matrix that can subsequently be fully characterised using solution instrumental techniques and then related back to the parent material. However, chemical degradation techniques may not be sufficiently specific, may yield an assortment of products, or provide little information regarding how the fragment was initially attached to the parent 'molecule'. In addition, the inherent inhomogeneous nature of kerogens (between and within different kerogens) and steric protection of inner core 'reactive' sites, is recognised to be problematic in chemical degradation procedures (Vitorović, 1980; Rullkötter & Michaelis, 1990). To date, even multiple step-wise selective chemical degradation experiments have not been able to define fully the molecular structure of any kerogen. The principal chemolysis techniques applied to the structural elucidation of kerogens have been summarised by Rullkötter & Michaelis (1990; Table 1.2).

Table 1.2. Principal chemolysis techniques applied to kerogens (Rullkötter & Michaelis, 1990).

Bond type	Method	Bond site labelling
Ester	Base hydrolysis: OH ⁻ , crown ethers, trimethylsilyliodide (TMSI)	-COOH, -OH
Amide	Acid hydrolysis	-COOH, -NH ₂
Ether	BCl ₃ , BBr ₃ , TMSI/LiAlH ₄	LiAlD ₄
Sulphur	Raney Ni/H ₂	(D ₂)
Ar-C-	RuO ₄	-COOH
-C=C-	O ₃	-COOH
Ar-O-C- (lignins)	Hydrogenolysis (Rh-C/H ₂), sodium bis-(2-methoxyethoxy)-aluminium dihydride (SMEAH)	D ₂

1.2.2. ¹³C Solid-state nuclear magnetic resonance spectroscopy

The application of nuclear magnetic resonance (NMR) spectroscopy to solid organic-rich geochemical samples has broadened the understanding of these materials and the alteration processes that they undergo when deposited in sediments. Fundamentally, NMR differentiates atoms in different chemical environments (*i.e.* different substituent groups) on the basis of their interaction with an applied radiofrequency irradiation within a magnetic field or *vice versa*. Fourier transformation of data so obtained is plotted in terms of chemical shift on the NMR spectrum. Chemical shift for the same atomic species in different chemical environments varies primarily owing to the shielding effects of electrons around the nucleus which alter the magnetic field experienced by that nucleus. Early applications of NMR to solid organic-rich samples were hampered by the fact that nuclear spin resonance cannot be induced in ¹²C whilst ¹³C has low natural abundance. In addition, broad spectral resonances resulted from the transfer of applied energy through the

solid lattice rather than the simple relaxation observed in samples in solution. The development of cross-polarisation (CP), magic-angle-spinning (MAS) and dipolar-dephasing (DD) techniques has alleviated some of these problems. Basically, CP in solid state NMR occurs by excitation of the more abundant protons and subsequent energy transfer to the less abundant carbon atoms. The ^{13}C signal acquired after CP is enhanced approximately fourfold in comparison to experiments that rely purely on carbon atom relaxation (Wilson, 1987). MAS involves rapidly spinning the sample at the 'magic angle' (54.7°) in order to remove dipolar interactions (*e.g.* between carbon and hydrogen atoms) caused by the attached substituents being in different energy states (*e.g.* protons). Consequently, MAS operates in an analogous way to suppression of dipolar interactions by irradiation and suffers from similar averaging effects where amorphous materials are studied (Wilson, 1987), *i.e.* signal overlap. DD is achieved either by a brief cessation of excitation pulse or by applying an opposite pulse with the result that CH and CH_2 groups are lost from the spectrum whilst methyl and non-protonated carbons are not (Wilson, 1987).

Despite the development of advanced techniques in ss-NMR the quality and utility of information obtained has been questioned (Rullkötter & Michaelis, 1990). These authors suggest that basic suppositions drawn from solid-state NMR spectra, such as the aromaticity factor (f_a), may be erroneous owing to overlap from different chemical groups. Similarly, they describe results of any further subdivision of spectra as artificial for the same reasons.

1.2.3. Elemental analysis

Elemental analysis is routinely used in organic geochemical studies to determine the bulk composition of substrates in terms of the major elements comprising organic matter, *i.e.* carbon and hydrogen, and to a lesser extent nitrogen, sulphur and less reliably oxygen

(Rullkötter & Michaelis, 1990). High mineral content (>50 %) is known to interfere with O, H and N determinations whilst sulphur determinations may be affected when the pyrite content exceeds 10 % (Huc and Durand, 1977; Durand and Monin, 1980). Although elemental composition can be quantitatively related back to the substrate it does not provide precise molecular information. Furthermore, erroneous suppositions about the bulk character of organic matter may be made where mixtures of solid compounds are analysed together. Notwithstanding this, the use of atomic ratios based on elemental analyses, *e.g.* H/C, O/C ratios, has enabled researchers to relate sedimentary organic matter to its degree of evolution and degree of aromaticity (Durand & Monin, 1980).

1.2.4. Infrared spectroscopy

Infrared spectroscopic analysis of insoluble sedimentary organic matter, such as kerogen, is commonly used to identify the presence and relative importance of functional groups. The most common absorption bands encountered in geochemical studies are included in Table 1.3. However, there is substantial overlap in the absorption bands of functional groups in complex solid samples, such that spectroscopic resolution is generally poor. Principally, the utility of IR spectroscopy has been limited to demonstrating that sedimentary organic matter becomes depleted in aliphatic components and relatively enriched in aromatic character with increasing maturity or thermal stress (Rullkötter & Michaelis, 1990). Notwithstanding this generalisation, IR spectroscopy is a useful tool in monitoring changes in the chemical character of substrates subjected to chemical degradation procedures (*e.g.* Standen *et al.*, 1991).

Table 1.3. Principal absorption band assignments used in IR analysis of kerogen (from Tissot & Welte, 1984 and references therein)

Absorption band (cm ⁻¹)	Assignment
3430	OH (phenol, alcohol, carboxyl)
3100 - 3000	CH aromatic stretching
2920 and 2855	CH ₂ , CH ₃ aliphatic
1710	C=O (ketone, acid, ester)
1630	aromatic C=C, olefinic C=C, bridged quinone carbonyl C=O, free H ₂ O
1455	CH ₃ , linear and cyclic CH ₂
1400 - 1040	C-O stretching, OH bending
1375	CH ₃ only
930 - 700	aromatic CH out of plane bending, dependent on number of adjacent protons
720	aliphatic chains of four or more C atoms

1.2.5. Microscopy

Microscopy techniques do not directly yield chemical information *per se*, but they do assist in defining potential sources of insoluble organic matter based on morphologically identifiable biological remains, *e.g.* plant and algal debris, inorganic mineral components, or structural changes following chemical treatments. Two principal forms of microscopy are used in geochemical studies, light microscopy and electron microscopy. Of the different methods of light microscopy (transmitted, fluorescence or reflectance), reflectance is most commonly applied to the study of kerogen maturity (*i.e.* vitrinite reflectance). It provides a relatively easy means of estimating the thermal evolution and hydrocarbon potential of kerogens by assessment of the relative proportions of source-identifiable contributing particles (Tissot & Welte, 1984), *e.g.* algae (alginite) and plants

(vitrinite and inertinite). Electron microscopy (scanning and transmission) is capable of significantly greater magnification than light microscopy and can provide information down to the molecular level (Whelan & Thompson-Rizer, 1993). Basically, these techniques involve subjecting a material to a focused beam of electrons and interpreting the degree of electron transparency as a monochromatic picture. Electron microscopy has previously been used to identify particular microorganisms in marine detritus (Peulvé *et al.*, 1996) and kerogen-rich deposits (Goth *et al.*, 1988 Derenne *et al.*, 1992), mineral structures such as pyritic framboids (Combaz, 1980; Zegouagh *et al.*, 1999), and to confirm the location of sporopollenins and algaenans, following drastic chemical treatments, in the outer cell walls of spores (Atkinson *et al.*, 1972; Beckett, 1976) and algae (Puel *et al.*, 1987; Berkaloff *et al.*, 1983; Kadouri *et al.*, 1988; Derenne *et al.*, 1989; Gelin *et al.*, 1999).

1.3. Previous studies of IOM

The majority of previous studies of sedimentary IOM (kerogen) have generally concentrated on the characterisation of this material using bulk parameters (*e.g.* elemental content, degree of aromaticity/aliphaticity and functionality) or the importance of specific components (*e.g.* alkane odd/even predominance). Others have focused on the relative quantitative importance of the insoluble fraction in relation to other biochemical fractions. These latter more relevant studies are briefly reviewed here.

Investigation into the nature of settling particles in the Lower St. Lawrence Estuary (Colombo *et al.*, 1996, 1996a) using a non-sequential procedure (Table 1.4) showed that 40 – 60 % of the TOC and 58 – 76 % of the total nitrogen was present as non-characterised organic matter in the water column. The authors speculated that much of this non-characterised material was probably refractory in nature and suggested that its source may have been humic compounds and, to a lesser extent, lignin. Colombo *et al.* (1996a) also

examined the bulk composition of sediments in the same area and found that non-characterised organic matter accounted for 62 – 74 % of the TOC and 51 – 78 % of the total nitrogen. There were no obvious down-core trends in the 0 – 35 cm below sediment-water interface of sediment sampled. Thus it appears that this non-characterised, and possibly refractory, organic matter may reach sediments directly from the water column and be selectively preserved there.

Table 1.4. Relative contribution of organic fractions from Lower St. Lawrence Estuary as percentage of Total Organic Carbon (TOC) and Total Nitrogen (TN), from Colombo *et al.* (1996, 1996a)

fraction	Water column (sediment trap)		Sediment (0 –35 cm)	
	% TOC	% TN	% TOC	% TN
Lipids	17 – 37	-	1 – 5	-
Carbohydrates	8 – 16	-	15 – 22	-
Hydrolysable amino acids	8 – 16	24 – 42	7 – 13	21 – 43
Labile proteins	<1 – 3	1 – 10	<1 – 1	1 – 4
Non-characterised	40 – 64	58 – 76	62 – 74	51 – 78

The observations of Colombo *et al.* (1996, 1996a) provide support for the theory of selective preservation of inherently recalcitrant biomolecules which are subsequently deposited to sediments, as suggested by Hatcher *et al.* (1983). Hatcher *et al.* (1983) also recognised the potential for a significant bacterial contribution to precursors of refractory organic matter in sediments.

Cranwell (1990) used a sequential extraction procedure involving solvent extraction, base hydrolysis and acid hydrolysis in order to release 'free' and 'bound' lipids from recent

lacustrine sediment from Loch Affric, N. Scotland. The total lipid extract accounted for 1.2 % of the sediment dry weight. 'Free' lipids, extracted with chloroform-methanol (1: 2, 1: 1 and 1: 2 v/v, respectively) and chloroform, accounted for 60 % of the total lipid extract and base and acid liberated lipids each accounted for around 30 % of the total lipids extracted.

Peru Margin sediments (0 – 220 cm) were sequentially digested (desalting; solvent extraction; alkaline hydrolysis; acid hydrolysis; demineralisation) by Reimers & Suess (1983) to isolate the insoluble amorphous 'proto-kerogen' fraction. Their 'proto-kerogen' fraction may have included carbohydrate material not removed using an oxidising acid, *e.g.* H₂SO₄. In near-surface sediments (0 to around 50 cm) this 'proto-kerogen' was comprised of carbon (40 – 52 %), hydrogen (5 – 6 %), nitrogen (4 – 5 %), oxygen (18 – 24 %) and sulphur (3 – 8 %). In deeper sediments (180 – 225 cm) the elemental composition was much less certain (total CHNOS 34 – 57 %).

Klok *et al.* (1983) used a limited sequential digestion procedure (H₂O, 0 and 100 °C; EDTA, 100 °C; HCl, 2M, 4M and 6M, 100 °C, 100 °C and 105 °C, respectively) to extract classes of biochemicals from a diatomaceous ooze of the Namibian Shelf (Table 1.5). Carbohydrates as mono- and polysaccharides were released at each stage except the 6M HCl hydrolysis whilst amino acids were present in all extracts except the cold water extract. Residual material accounted for 63 % of the original dry weight sediment and contained 40 % of the initial total carbon. Some of the residual material was presumed to be lipidic as lipid extraction was not carried out. In a later study on a similar substrate (40 – 75 cm section) using essentially the same procedure, Klok *et al.* (1984; Table 1.5) reported 66 % of the original dry weight sediment, containing 54 % of the initial total carbon, remained after sequential extraction. Lipids detected in the aqueous and acid extracts were found to be hydrolysis products of lipopolysaccharides solubilised during the main extraction stages. In parallel experiments in both of these studies Klok *et al.* (1983,

1984) found that material remaining after direct acid attack (6M HCl, 105 °C) was richer in organic carbon than residues obtained following sequential digestion (43 % cf. 40 % TOC and 54 % cf. 60 % TOC, respectively). They suggested that these discrepancies demonstrated the greater efficiency of the sequential procedure whilst Maillard-type condensation reactions in the direct attack could have accounted for the formation of acid-insoluble (melanoidin-like) material.

Table 1.5. Summary of recent quantitative sequential studies into major biochemical classes isolated from sediments (% TOC)

Fraction	Klok <i>et al.</i> (1983)^a	Klok <i>et al.</i> (1984)^b	Patience <i>et al.</i> (1990)^c	Lewis & Rowland (1993)^d
Proteins	10	11	6 – 17	7 – 52
Lipids	nd	4	12 – 46	23 – 63
Carbohydrates	39	22	2 – 9	1 – 14
Residual	40	50	27 - 79	<i>ca</i> 20

a. TOC = 5.66 % dry weight sediment; b. TOC = 5.76 % dry weight sediment; c. TOC = 2 – 11 % dry weight sediment; d. TOC = 4 – 10 % dry weight sediment.

A sequential digestion procedure, similar to that in the present study, was used by Patience *et al.* (1990) to determine the contributions of major biochemical classes to the total organic matter in Peru Margin sediments (Table 1.5). The organic carbon content of the extractable fractions was estimated using conversion factors (0.45, protein; 0.75, lipid; and 0.40, carbohydrates) which resulted in calculated yields of organic carbon up to 135 %. ‘Uncharacterised’ organic matter formed the largest single class of organic matter even in surficial sediments (40 % TOC in near surface sediments to 80 % TOC at 22 m below the sediment-water interface).

Lewis & Rowland (1993) used the methods of Patience *et al.* (1990) to determine the organic carbon mass balance, in terms of major biochemical classes, of 0 – 10 cm sediments from the Peru Margin (Table 1.5). Similar to Patience *et al.* (1990), the use of conversion factors produced an overestimation of TOC (up to 125 %). These authors demonstrated the presence of uncharacterised organic matter (*ca* 20 %) in surface sediments as shallow as 6 cm below the sediment water interface.

Parkes *et al.* (1993) noted an inverse relationship between the decreasing total bacterial population and the increasing percentage of uncharacterised organic matter with depth to around 100 m in recent sediments from the Peru Margin (Figure 1.2). They interpreted this to suggest that reducing bacterial population with depth was associated with a concomitant increase in bacterial necromass that may have directly contributed to the proportion of refractory organic matter *via* selective preservation of bacterial constituents, *i.e.* bacterans. To date, the presence of refractory components in methanogenic bacteria has not been unequivocally demonstrated.

Le Berre *et al.* (1991) subjected nine species of bacteria to a sequential digestion procedure involving, in the following order: lyophilisation, organic solvent extraction, saponification (6h reflux in 6 % KOH) and acid treatment (H₃PO₄, 55°C, 13 days). Non-hydrolysable material was obtained from the cell walls of six of the nine species (Table 1.6). The three species with the highest content of non-hydrolysable material (*ca.* 2 % total biomass) were from the same group, the *Actinomycetes*, and were found to have comparable H/C ratios (*ca* 1.1), FTIR and ¹³C solid-state NMR spectra. After subsequent investigation into non-hydrolysable organic matter from three members of the *Actinomycetes* group (*Mycobacterium phlei*, *Mycobacterium tuberculosis*, and *Mycobacterium smegmatis*; Table 1.7; Allard *et al.*, 1997, 1998) it was suggested that this material was purely artefactual and formed during the isolation procedure. Based on the synthesis of melanoidin-like polymers

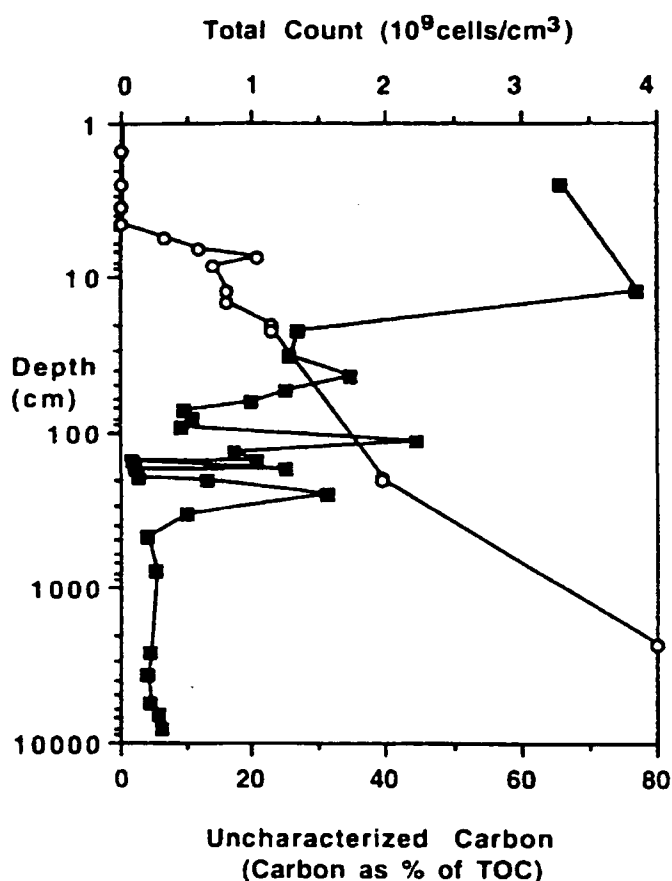


Figure 1.2. Relationship between the total bacterial population and percentage uncharacterised organic matter with sediment depth (from Parkes *et al.*, 1993)
 ■ bacterial population, ○ uncharacterised carbon.

under basic (direct treatment; base then acid hydrolysis) and acid (inverted treatment; acid then base hydrolysis) conditions from mixtures of monosaccharides and amino acids or arabinogalactan and polypeptide (Table 1.8), these workers related 'bacterans' to melanoidin-like polymers on the basis of spectroscopic (FTIR, ¹³C NMR), pyrolytic, thermogravimetric, elemental, and chemical oxidation (KMnO₄) characteristics. However, their interpretations should be treated cautiously because they did not remove aqueous soluble saccharides and amino acids prior to lipid extraction and hydrolysis. This omission was also evident in the isolation of non-hydrolysable algaenan from *B. braunii* (*e.g.* Berkaloff *et al.*, 1983). Failure to remove aqueous-soluble melanoidin precursor material (*i.e.* saccharides, amino acids and lipids) prior to more drastic hydrolysis suggests that even

their new isolation techniques may have been accompanied by the formation of artefactual melanoidin-like material.

Table 1.6. Proportion (% dry weight) of non-hydrolysable material obtained from nine species of bacteria (Le Berre *et al.*, 1991)

species	type	Proportion of non-hydrolysable macromolecular material
<i>Rhodospirillum rubrum</i>	Photosynthetic	No significant amount
<i>Halococcus morrhuae</i>	Halophilic	ca. 0.1 %
<i>Beggiatoa alba</i>	Sulphur-reducing	No significant amount
<i>Pseudomonas putida</i>	Aerobic	No significant amount
<i>Corynebacterium glutamicum</i>	Aerobic	ca. 2 %
<i>Nocardia opaca</i>	Aerobic	ca. 2 %
<i>Mycobacterium smegmatis</i>	Aerobic	ca. 2 %
<i>Methanosarcina barkeri</i>	Methanogenic	ca. 0.1 %
<i>Methanosarcina thermophila</i>	Methanogenic	ca. 0.1 %

Table 1.7. Yield (% dry weight) of non-hydrolysable organic matter from Actinomycetes and Chlorophyceae (Derenne *et al.*, 1989; Allard *et al.*, 1997, 1998)

Organism	Yield (% lipid free biomass)
<i>Mycobacterium phlei</i> [†]	3.2 (4.2)
<i>Mycobacterium tuberculosis</i> [†]	3.0 (4.3)
<i>Mycobacterium smegmatis</i> [†]	1.8 (no data)
<i>Botryococcus braunii</i> L race [‡]	11.4* (24 – 26)
<i>Scenedesmus communis</i> [‡]	2.6 (4.8)

[†]Allard *et al.*, 1997; [‡]Allard *et al.*, 1998 and Derenne *et al.*, 1989 (figures in brackets); * % initial dry biomass

Table 1.8. Yields of melanoidin-like polymers (Allard *et al.*, 1997)

Mixture	Yield (% initial weight of reactants)	
	Direct treatment	Inverted treatment
Monosaccharides + amino acids	16	37
Arabinogalactan + polypeptide (BSA)	4	5

Preliminary studies into the dissolution of kerogens by Dutta (1994) and Patell (1994) suggested that the ionic liquid 1-ethyl-3-methylimidazolium chloride-aluminium (III) chloride could be used to dissolve substantial amounts of these previously insoluble materials. Following this initial semi-quantitative work, there was an important need to undertake a more detailed quantitative investigation into the dissolution of insoluble organic matter using this ionic liquid. That research forms the basis of the current thesis.

1.4. Aims of the present study

The aims of this study were:

- To determine whether ‘insoluble organic matter’ is present in a range of sediments, bacteria and algae, and characterise isolated material using a range of instrumental techniques.
- To attempt the quantitative dissolution of isolated IOM using the acidic ionic liquid, 1-ethyl-3-methylimidazolium chloride/aluminium (III) chloride $\{X(\text{AlCl}_3), X = 0.65\}$.
- To characterise the quantitatively important fractions obtained following ionic liquid treatment and assess whether IOM subject to ionic liquid treatment has been substantially chemically altered.
- To assess the mode of action of the ionic liquid on organic compounds which are, or contain functionalities that are, commonly found in many kerogens.

**Chapter 2: Quantitative isolation of 'insoluble organic matter' (IOM) from sediments
and biota**

2.1. Introduction

The foregoing introductory chapter emphasises the two key requirements for progress in the elucidation of the chemical nature of IOM and kerogens *viz.* (i) isolation of substantial quantities of IOM from substrates including biota and recent and ancient sediments (ii) discovery of a method of dissolving IOM (*sic*) and kerogens. The present chapter describes the quantitative isolation of operationally defined 'insoluble organic matter' (IOM) from freeze-dried sediments (Rostherne Mere, UK; Section 2.4.2), Kimmeridge Clay (Section 2.4.3), methanogenic bacteria (*Methanococcus jannaschii* and *Methanobacterium thermoautotrophicum*; Section 2.4.4), sulphate-reducing bacteria (*Desulfobacter postgatei*; Section 2.4.4) and two species of marine algae (*Skeletonema costatum* and *Haslea ostrearia*; Section 2.4.5) following a lengthy sequential digestion procedure (Figure 2.1 and Section 2.3). IOM obtained in this manner was characterised using SEM, elemental analysis, and ss-NMR and IR spectroscopy (Chapter 3), and more comprehensively using Py-GC-MS and ToF-SIMS (Chapter 4). Dissolution of the IOM in an ionic liquid was then attempted (Chapter 6).

2.2. Experimental substrates

A range of experimental substrates: lacustrine sediments (Section 2.2.1), marine shale (Section 2.2.2) methanogenic bacteria (Section 2.2.3), and algae (Section 2.2.4), were selected to investigate whether they contained 'insoluble organic matter' (IOM). IOM isolated from some of these substrates, along with synthetic melanoidins (Chapter 5) and dendrimers (Chapter 6), was subsequently used to investigate their solubility in 1-ethyl-3-methylimidazolium chloride/aluminium (III) chloride ionic liquid (Chapter 6) and to assess its mode of action.

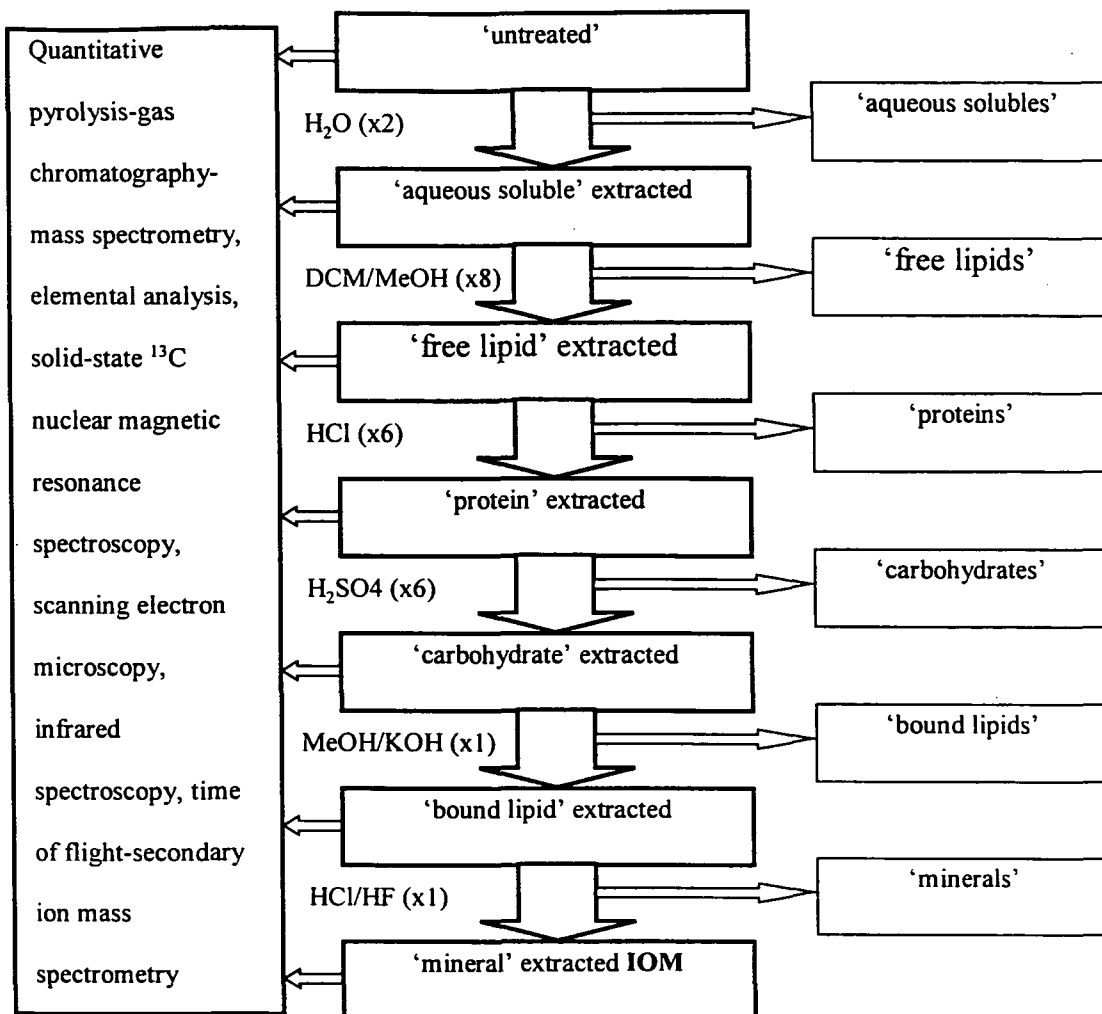


Figure 2.1. Outline of the sequential procedure used to isolate IOM from sediments and biota.

2.2.1. Sediments from Rostherne Mere, Cheshire, UK

Rostherne Mere is one of the largest (*ca.* 48.7 ha) and deepest (maximum depth about 30 m) in a series of more than 60 freshwater meres across the Shropshire-Cheshire Plain (Reynolds, 1979). It is a highly productive eutrophic lake subject to seasonal stratification during summer months when the bottom waters become anoxic. Increasing eutrophy since around 1960, variously ascribed to sewage effluent and increased inputs of agricultural fertilisers and guantrophy (Brinkhurst & Walsh, 1967; Moss *et al.*, 1997), has been cited as the main cause of change in the phytoplankton population which is now dominated by seasonal blooms of relatively few algae, *e.g.* *Microcystis aeruginosa* (Reynolds, 1979). Although organic matter inputs to Rostherne Mere sediment have been reported to be

dominated by algal remains (Livingstone, 1984), such that it is similar to depleted sapropel deposits, with a lesser contribution from allochthonous material (Livingstone & Cambray, 1978), the importance of allochthonous inputs is disputed by Prariono (1995). Livingstone & Reynolds (1981) noted that algal deposits to sediments were related to the periodicity of algal blooms whilst Cardoso *et al.* (1983) demonstrated that the blue-green alga *Microcystis aeruginosa* provided a major contribution to surface sediment lipid concentrations. At greater depth, contributions from higher-plants became the dominant lipid source suggesting that algal lipids were rapidly reworked in the surface sediment. Prariono & Wolff (1997) reported similar lipid distributions, but with the aid of elemental and isotopic data ascribed these variations to greater deposition of phytoplankton to surficial sediments resulting from increased eutrophy of the Mere. The sedimentation rate has been estimated at between 10 – 12 mm yr⁻¹ (Reynolds, 1979) and 20 mm yr⁻¹ (Livingstone & Cambray, 1978) with preservation of organic matter in the sediment favoured owing to stratification, a limited euphotic zone, and a poorly developed community of benthic fauna (Cardoso *et al.*, 1983). Sediment from Rostherne Mere therefore provides a good lacustrine analogue of organic-rich marine sediments and provided a suitable substrate for the investigation of IOM formation and subsequent attempted dissolution using an ionic liquid.

2.2.2. Kimmeridge Clay

Kimmeridge Clay samples used in this study were collected from Burning Cliff, Dorset (Figure 2.2) by Bertenshaw (1996). Dorset Kimmeridge Clay is composed of laminated organic-rich black shale formed under anoxic and cyclic deposition conditions during the Upper Jurassic period (Stoneley & Selley, 1986). Organic matter, which generally comprises up to 20.5 % of the total organic carbon (TOC), originates principally from autochthonous marine phytoplankton and zooplankton, although some terrestrial material may be present. Kerogen obtained from this formation is Type II (up to 16.3 %) and is of

good source potential. Work on Kimmeridge Clay from Yorkshire showed carbon enrichments (up to 9.5 % TOC) to occur towards the top of each 90 cm thick microcycle (Bousaffir *et al.*, 1995). These organic enrichments were explained as a consequence of repeated increases in deposition of resistant biomolecules (*e.g.* algaenans) associated with upsurges in biomass production, cyclic anoxia, and the natural ‘vulcanisation’ of lipidic material.

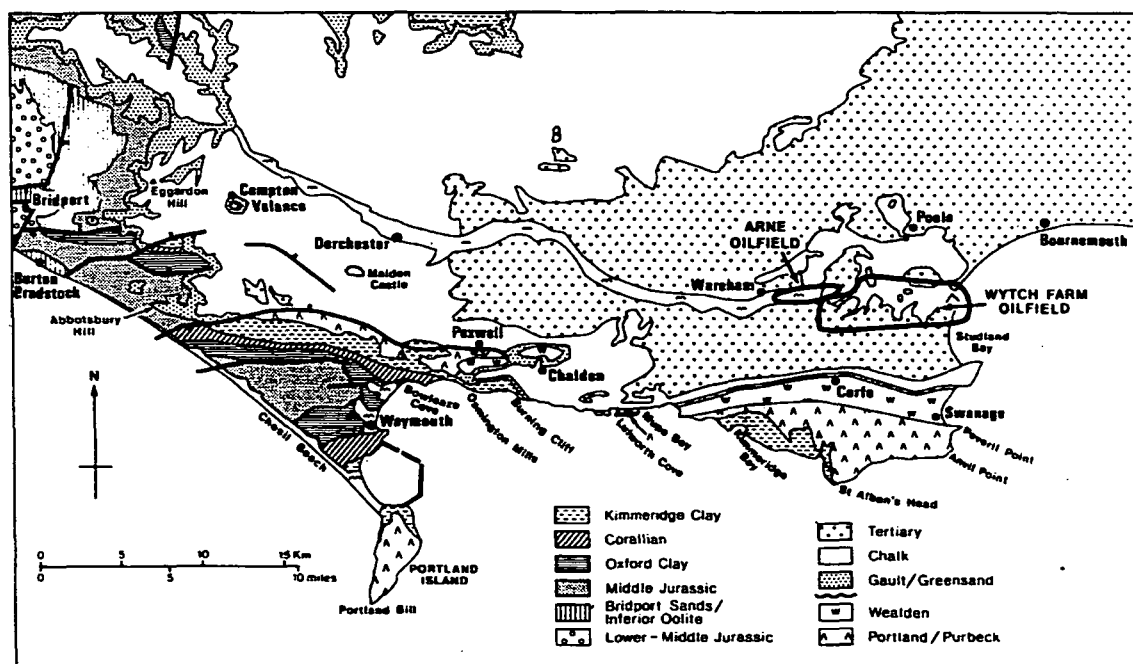


Figure 2.2. Site location map for Kimmeridge Clay samples used in this study obtained from Burning Cliff (from Stoneley & Selley, 1986).

2.2.3. Bacteria

Bacterial samples used in this study included: *Methanobacterium thermoautotrophicum*, *Methanococcus jannaschii* and *Desulfobacter postgatei*. The first two species are methanogens and belong to the kingdom *Euryarchaeota* of the domain *Archaea* (formerly Archaeobacteria; Stetter, 1998), the latter is a sulphate-reducing bacterium belonging to the domain *Bacteria* (often referred to as Eubacteria or ‘true bacteria’). *Archaea* and *Bacteria* differ in that the *Archaea* do not contain peptidoglycan in their cell walls; have membrane lipids comprising isoprene units ether linked to glycerol or other carbohydrates rather than

ester linked to carboxylic acids; have a single large RNA polymerase enzyme with many sub-units rather than a single small enzyme with four sub-units; and during protein synthesis the initiation codon always specifies methionine rather than N-formylmethionine (Koga *et al.*, 1993; Ni & Boone, 1998). The means by which thermophilic bacterial cell components are able to withstand extreme conditions of temperature, pressure and acidity have yet to be resolved (Stetter, 1998). However, their inherent ability to resist degradation under such conditions suggests that they may not break down rapidly under normal sedimentary burial conditions or perhaps during chemical isolation procedures.

M. jannaschii and *M. thermoautotrophicum* are members of the *Archaea*, first recognised as a separate taxonomic group in 1977 (Woese & Fox, 1977). Where previously bacteria had been identified principally on morphological features, the *Archaea* were shown to be a distinct domain based on their genetic make-up, *e.g.* 16/18S rRNA sequences (Woese & Fox, 1977; Woese *et al.*, 1990; Stetter, 1998; Figure 2.3). Recently, elucidation of the complete genome sequence of *M. jannaschii* (Bult *et al.*, 1996) has confirmed that they lack the necessary genes to utilise methanol or acetate in methanogenesis but instead appear to use H₂ and formate as substrates. In addition, *M. jannaschii* also has all the genes necessary to fix nitrogen. Whilst this difficult genome sequencing work has been completed, the gross biochemical composition of *M. jannaschii*, or *M. thermoautotrophicum*, has not yet been reported. Indeed, much of the literature relating to the composition of these methanogens has been focused on solvent soluble aliphatic, diether and tetraether lipid molecules (*e.g.* Rowland *et al.*, 1982; Sprott *et al.*, 1991; Koga *et al.*, 1993) and extractable osmolytes and metabolic by-products (Robertson *et al.*, 1990; White, 1997).

Methanococcus jannaschii is a gram-negative hyperthermophilic obligate anaerobic methanogenic bacteria that grows chemolithoautotrophically in the presence of H₂ and CO₂

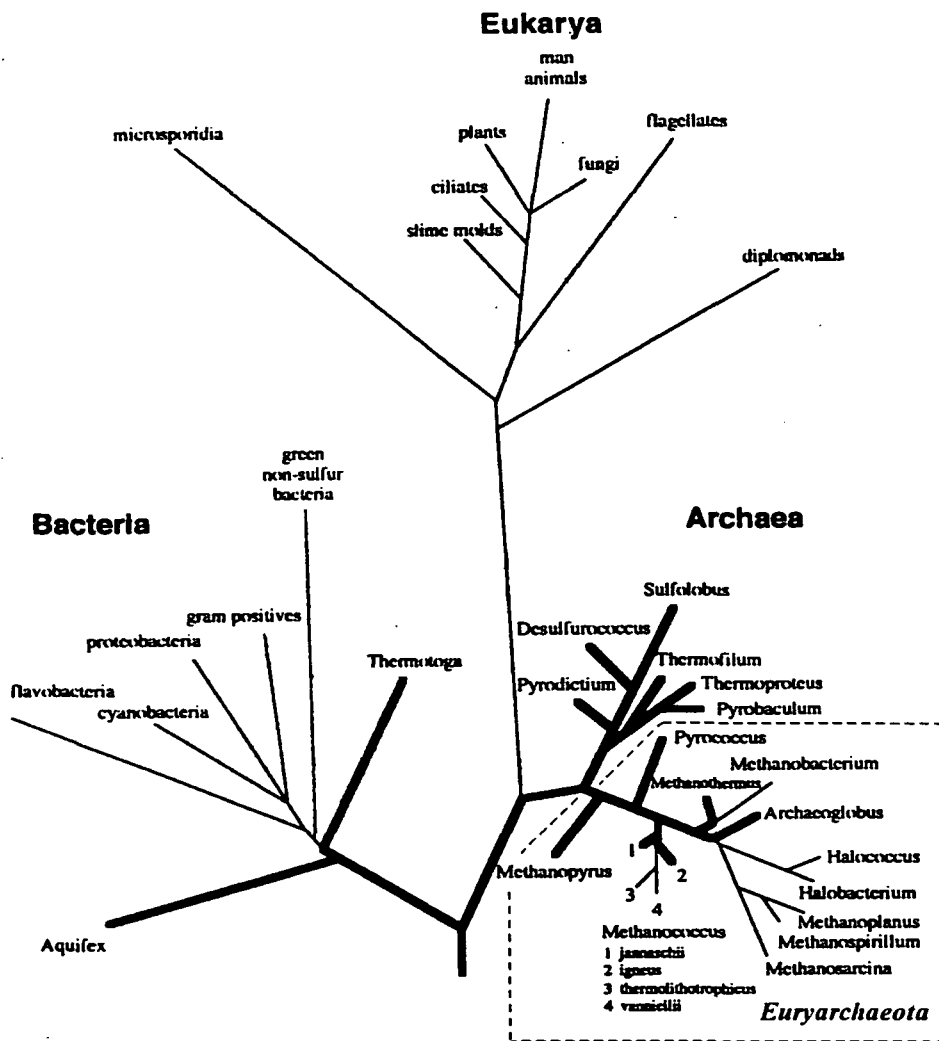


Figure 2.3. Taxonomic relationship between *Archaea*, *Bacteria* and *Eucarya* emphasising hyperthermophiles within the 16S rRNA-based phylogenetic tree (schematically redrawn and modified from Woese *et al.*, 1990, by Stetter, 1998).

over a temperature range of 48 – 94 °C (optimum 85 °C) and at pressures of up to greater than 200 atmospheres (Stetter, 1998; Ni & Boone, 1998). The cells are motile, irregularly coccoid shape and surrounded by a single S-layer envelope (Jones *et al.*, 1983; Stetter, 1998) with a plasma membrane containing variable amounts of diether, tetraether and macrocyclic diether lipids dependent upon growth conditions (Spratt *et al.*, 1991; Beveridge & Schultze-Lam, 1996). *M. jannaschii* was first isolated from a sea floor

sediment (2600 m water depth) at the base of a 'white smoker' chimney on the East Pacific Rise (Jones *et al.*, 1983). Samples of *M. thermoautotrophicum* and *M. jannaschii* used in the present study were cultured by Risatti (USGS, 1982). Culture conditions for *M. thermoautotrophicum* were as reported by Risatti *et al.* (1984).

Archaea have been found in a range of environments, *e.g.* soils (Bintrim *et al.*, 1997), settling particulates in upper region ocean waters (Marty, 1993), deep sea waters between 500 and 3000 m (Fuhrman & Davis, 1997), freshwater lake sediments (Hershberger *et al.*, 1996), and marine sediments exceeding 500 m depth below the ocean floor (Parkes *et al.*, 1990, 1993, 1994, 2000). Marty (1993) demonstrated the presence of methanogenic bacteria, principally associated with faecal pellets, in settling particulate matter in the seawater column. The interior of the faecal pellets providing an anaerobic microenvironment in which the methanogens could survive as they pass through oxygenated surface waters. Marty (1993) thus identified enteric methanogenic bacteria as a potential source for the survival of methanogenic bacterial components within surface sediments and for their subsequent burial.

2.2.4. Algae

Two diatomaceous algae: *Skeletonema costatum* and *Haslea ostrearia* were subjected to sequential digestion to investigate the presence of IOM. Diatoms are eukaryotic, unicellular, principally photosynthetic, micro-organisms, whose distinguishing feature is a highly differentiated cell wall usually heavily impregnated with silica (Round *et al.*, 1990). The chemical composition of algae has been shown to vary between species and within species (*e.g.* Parsons *et al.*, 1961). Intraspecies variability in chemical composition has been related to growth phase and environmental conditions (*e.g.* Parsons *et al.*, 1961; Sánchez-Saavedra & Voltolina, 1996; Burkhardt & Riebesell, 1997).

Skeletonema is a filamentous alga that is ubiquitous in coastal waters globally. It can account for periodic blooms, although some oceanic species have been reported (Round *et al.*, 1990).

Haslea ostrearia comprises single cells or cells forming mucilage tubes (Round *et al.*, 1990). Cells are approximately 60 – 100 μm in length, 6 – 10 μm at their central girth and spindle-shaped with acute to rounded ends (Round *et al.*, 1990). *H. ostrearia* is considered fairly widely distributed in the marine environment (Round *et al.*, 1990; Cooke, 1995). In addition, *H. ostrearia* is routinely fed to oysters in parts of France where the blue-green algal pigment, marennine, is imparted to the oysters to produce green colouration in their gills (Cooke, 1995). To date, research associated with *H. ostrearia* has principally focused on the isolation and characterisation of highly branched isoprenoid alkene lipids (Belt *et al.*, 1994, 1996; Cooke, 1995; Wraige *et al.*, 1997, 1998, 1999; Johns *et al.*, 1999, 2000). Their gross biochemical composition has not previously been reported. Samples of *H. ostrearia* used in the current study were cultured under the conditions reported by Wraige *et al.* (1997).

2.3. Experimental procedures

Experimental procedures used for the sequential isolation of IOM from sediments and biota are described in Section 2.3.1 – 2.3.7. Isolation of IOM from Rostherne Mere sediment and *M. jannaschii* was performed in triplicate in order to monitor reproducibility of the digestion procedure. Duplicate digestions were carried out on Kimmeridge Clay and *S. costatum* whilst only one sample of each of *M. thermoautotrophicum*, *D. postgatei* and *H. ostrearia* was sequentially digested. Samples were freeze-dried and weighed prior to digestion and after each stage of the digestion procedure to facilitate mass-balance calculations.

2.3.1. General laboratory procedures

Prior to use, all glassware was soaked in alkaline solution (Decon 90; 5 % v/v; 24 h), rinsed (x 3, hot water; x 5, Milli-Q), oven dried (overnight, 110°C) and pre-rinsed (x3) with the appropriate solvent. Glass fibre wool, anti-bumping granules, cotton wool, Soxhlet thimbles and silica were Soxhlet extracted (dichloromethane, DCM; 24 h).

Before freeze-drying, samples were frozen in Quickfit® (B 24/19) boiling tubes then covered with perforated aluminium foil and Whatman GF filter paper held in place with an elastic band. Covering the samples prevented sample loss when the freeze-dryer vacuum was released. Samples were freeze-dried (-40°C) in an Edwards Modulyo 4K freeze-drier. Freeze-drying was deemed complete when the internal pressure remained static at 10⁻¹ mbar for twenty-four hours.

2.3.2. Extraction of 'aqueous soluble' material

Sediment (*ca* 2 g) was weighed into a glass boiling tube (Quickfit®, B 24/19), water was added (10 ml, Milli-Q) and the contents agitated (15 min, Gallenkamp automatic shaker). The sample was centrifuged (15 min, 2000 rpm) and supernatant decanted to a round-bottom flask. The procedure was repeated once more. Combined supernatant was rotary evaporated (nitrogen cold-finger) to near dryness and transferred to pre-rinsed (3x, DCM), dried and pre-weighed vials, complete with washings. The extract was blow down to dryness (N₂) and re-weighed. Residual sediment was freeze-dried before re-weighing.

2.3.3. Extraction of 'free lipids'

Solvent (10 ml, methanol, MeOH) was added to residual sediment from the 'aqueous soluble' extraction stage and the sample agitated (15 min, Gallenkamp automatic shaker), centrifuged (15 min, 2000 rpm) and supernatant decanted to a round-bottom flask. Extraction was repeated using MeOH (x1; 10 ml); DCM/MeOH (1:1, x1; 10 ml); DCM

(x2; 10 ml); DCM/MeOH (1:1, x4; 10 ml). Supernatants were combined, rotary evaporated (nitrogen cold-finger) to near dryness and transferred to pre-rinsed (3x, DCM), dried and pre-weighed vials complete with washings. The extract was blown down under nitrogen to dryness and re-weighed. Residual sediment was frozen and freeze-dried before re-weighing.

2.3.4. Removal of 'proteins'

Hydrochloric acid (HCl, 10 ml, 6M, AristaR) was added to the residual sediment from the 'free' lipid extraction stage and refluxed (6 x 4 h, 110°C). Following each reflux, the sample was centrifuged (15 min, 2000 rpm) and the supernatant decanted to a round-bottom flask, combining supernatants. After the sixth reflux, water (10 ml, Milli-Q) was added, the sample shaken (15 min, Gallenkamp automatic shaker), centrifuged (15 min, 2000 rpm) and supernatant decanted to the hydrolysate flask. Washing was repeated once more. The extract was rotary evaporated (nitrogen cold-finger, sodium hydroxide, NaOH interceptor) to near dryness then transferred to a measuring flask (50 ml). Potassium hydroxide (KOH, 3M) was added drop-wise to raise the pH to around 5 and made up to the mark with water (Milli-Q) ready for 'protein' determination. Residual sediment was frozen and freeze-dried before re-weighing.

2.3.4.1. 'Protein' determination

A series of standard glycine solutions (0.00, 0.05, 0.20, 0.35, 0.50 mM; BDH 99 % minimum assay) were made up in KOH (0.1M; AnalaR). Acetate/cyanide buffer (0.2 mM NaCN in acetate buffer) was prepared by making 2 ml of stock NaCN solution (0.01 M; 48.9 mg NaCN made up to 100ml in Milli-Q) up to 100 ml with acetate buffer (36.0 g sodium acetate trihydrate with 6.6 ml glacial acetic acid made up to 100 ml with Milli-Q water). An aliquot (1 ml) of each standard was transferred to separate glass test tubes, acetate/cyanide buffer (0.5 ml) and ninhydrin (0.5 ml; 3% w/v in 2-methoxyethanol) were

added, the latter immediately prior to heating in a hot water bath (100°C, 15 min). Immediately after removal from the water bath diluent (10 ml; 1:1, v/v, 2-propanol:Milli-Q) was added before shaking. Absorbance was measured at 570 nm (UV-Visible Chemstation, model 8453) against a water (Milli-Q) blank.

Determination of 'protein' concentration in the hydrolysate was carried out as above but a second aliquot was used to account for indigenous colour by replacing the buffer with KOH (0.5 ml, 0.1M) and substituting the ninhydrin with 2-methoxyethanol (0.5 ml). The latter being subtracted from the former. 'Protein' concentration was calculated from the calibration graph in mmol glycine equivalents using the formula:

$$C = \frac{A - c}{m}$$

where

C	=	concentration of unknown
A	=	absorbance of unknown
c	=	calibration curve regression constant
m	=	X coefficient from calibration curve regression line

2.3.5. Removal of 'carbohydrates'

H₂SO₄ (10 ml, 1M, AnalaR) was added to residual sediment from the 'protein' extraction stage and refluxed (6 x 4 h, 110°C). Following each hydrolysis, samples were centrifuged (15 min, 2000 rpm) and the supernatant decanted to a round-bottom flask, combining supernatants. After the sixth reflux, water (10 ml, Milli-Q) was added, the sample shaken (15 min, Gallenkamp automatic shaker), centrifuged (15 min, 2000 rpm) and supernatant decanted to the combined hydrolysate flask. Washing was repeated once more. Combined supernatants were rotary evaporated to near dryness and transferred to pre-rinsed (3x, DCM), dried and pre-weighed vials complete with washings (Milli-Q). Residual sediment

was frozen and freeze-dried before re-weighing.

2.3.6. Removal of 'bound lipids'

Methanolic KOH (10 ml, 0.5M KOH in MeOH) was added to residual sediment from the 'carbohydrate' extraction stage and refluxed (4 h, 110°C). The sample was acidified to pH 5 with HCl (6M, AristaR) added drop-wise. DCM (10 ml, HPLC grade) was added and the sample centrifuged (15 min, 2000 rpm). The DCM layer was decanted to a round-bottom flask. DCM extraction was repeated four more times adding a little water (Milli-Q) to aid separation as required. Combined supernatants were rotary evaporated (nitrogen cold-finger) to near dryness before transferring to pre-rinsed (3x, DCM), dried and pre-weighed vials complete with washings (DCM). The extract was blown down under nitrogen to dryness and re-weighed. Water (10 ml, Milli-Q) was added to the residual sediment, the sample shaken (15 min, Gallenkamp automatic shaker), centrifuged (15 min, 2000 rpm) and supernatant decanted to a round-bottom flask. Washing was repeated twice more, combining supernatants. The supernatant was rotary evaporated (nitrogen cold-finger) to near dryness before transfer to pre-rinsed (3x, DCM), dried and pre-weighed vials complete with washings (Milli-Q). The extract was blown down under nitrogen to dryness and re-weighed. Residual sediment was frozen and freeze-dried before re-weighing.

2.3.7. Removal of 'minerals'

Concentrated HCl (10 ml, AristaR) was added to residual sediment from the 'bound lipid' extraction stage and stirred cold (24 h) then hot (50°C, 8 h). The sample was centrifuged (15 min, 2000 rpm) and supernatant decanted to a round-bottom flask. Water (10 ml, Milli-Q) was added, sample shaken (15 min, Gallenkamp automatic shaker), centrifuged (15 min, 2000 rpm) and supernatant decanted to a round-bottom flask. Hydrofluoric acid/hydrochloric acid (HF/HCl, 10 ml, 48% HF: conc. HCl, 10% by volume HCl) was added and stirred hot (50°C, 24 h). The solution was neutralised with excess saturated

boric acid and stirred (10 min), centrifuged (15 min, 2000 rpm) and supernatant decanted to waste. Hot water (10 ml, Milli-Q, 50°C) was added, the sample was shaken (15 min, Gallenkamp automatic shaker), centrifuged (15 min, 2000 rpm) and supernatant decanted to a round-bottom flask. Washing was repeated once more. HCl (10 ml, 6M) was added and stirred hot (50°C, 24 h), centrifuged (15 min, 2000 rpm) and supernatant decanted to a round-bottom flask. The residue was washed with hot water (10 ml, 50°C, Milli-Q), shaken (15 min, Gallenkamp automatic shaker), centrifuged (15 min, 2000 rpm) and supernatant decanted to a round-bottom flask. Washing was repeated once more. Excess saturated ammonium carbonate was added, the sample centrifuged (15 min, 2000 rpm) and supernatant decanted to a round-bottom flask. Hot water (10 ml, 50°C, Milli-Q) was added before shaking (15 min, Gallenkamp automatic shaker), centrifuging (15 min, 2000 rpm) and decanting the supernatant to a round-bottom flask. Hot dilute HCl (10 ml, 50°C, 6M) was added, the sample centrifuged (15 min, 2000 rpm) and supernatant decanted to a round-bottom flask. These three steps were repeated a further three times. Residues were washed with hot water (10 ml, 50°C, Milli-Q), shaken (15 min, Gallenkamp automatic shaker), centrifuged (15 min, 2000 rpm) and supernatant decanted to a round-bottom flask. Washing was repeated a further three times. Residual sediment was frozen and freeze-dried before re-weighing.

2.4. Results

2.4.1. Extraction efficiencies of 'aqueous-solubles', 'free lipids' and 'proteins' from Rostherne Mere sediments

Material remaining after each digestion step is operationally defined by the chemical procedure used to obtain that fraction. For example, solvent extraction of 'free lipid' material did not remove all solvent soluble material from the post-aqueous extracted sample. It is recognised that each extraction stage was not entirely exhaustive. However, monitoring of the 'free lipid' and 'protein' extraction procedures showed that fraction

yields markedly decreased as the number of repeated extractions increased. Whilst it is accepted that the true proportion of each fraction is not known, undigested material carried over from one extraction stage to the next is adjudged to comprise only a minor component.

The efficacy of the 'aqueous soluble' and 'free lipid' extraction methods was examined on Rostherne Mere sediment samples (5 – 6 and 95 – 96 cmbswi). Figure 2.4 shows that, gravimetrically, around 60 - 70% of the total 'aqueous soluble' material removed during seven extractions was released during the first two extractions. In order to make results from this work comparable to those of previous studies and in order to save time, the number of aqueous extractions was thereafter limited to two (cf Ripley, 1994).

Around 85% of the total 'free lipid' fraction removed from Rostherne Mere sediments (5 – 6 and 95 – 96 cmbswi; Figure 2.5), measured gravimetrically in the eight stage solvent extraction, was released during the first three extractions.

The protein concentration in 'protein' fractions removed from Rostherne Mere sediments (5 - 6 and 95 - 96 cmbswi) was determined in triplicate using the 'ninhydrin' method (Rosen, 1957; Section 2.1.4.1) and quantified in terms of mmol glycine equivalents g^{-1} dry weight of sediment (Figure 2.6). Over 90 % of the total 'protein' was extracted during the first four extractions.

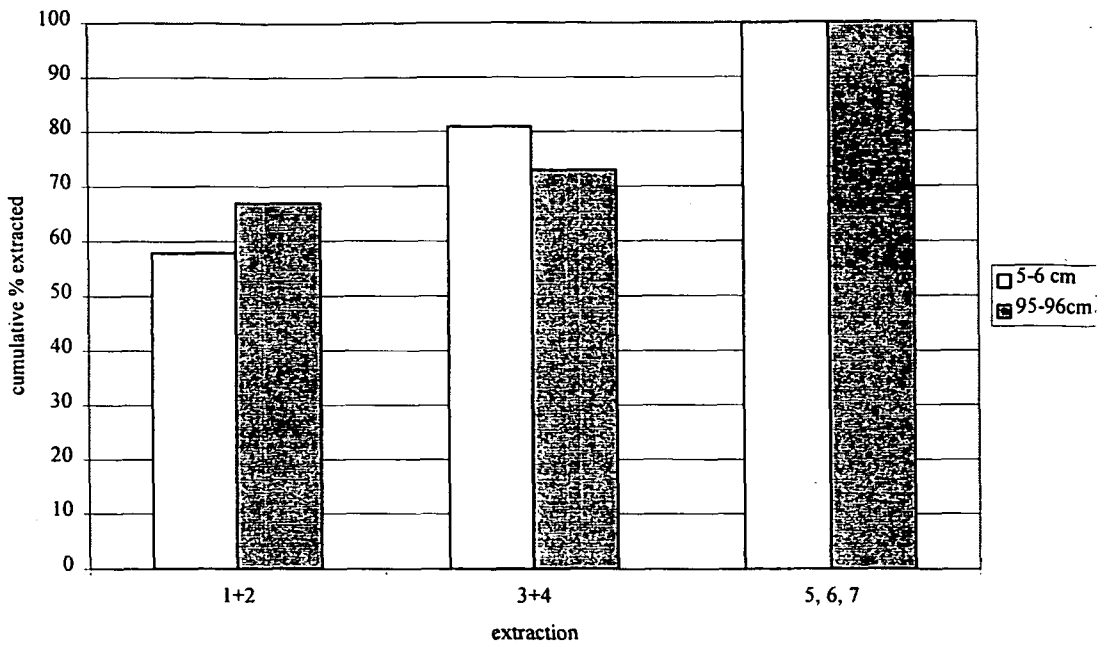


Figure 2.4. Cumulative percentage of 'aqueous soluble' material extracted from Rostherne Mere sediments (5 - 6 cm and 95 - 96 cm).

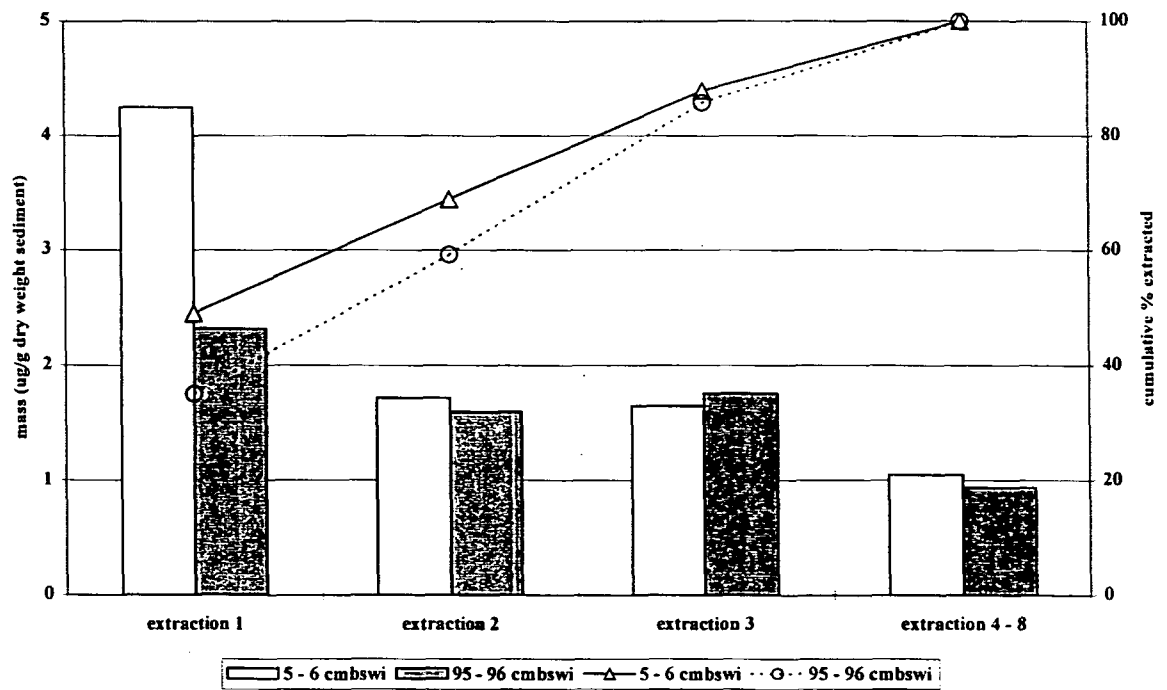


Figure 2.5. Gravimetric results and cumulative percentage of 'free lipids' extracted from Rostherne Mere sediments (5 - 6 cm and 95 - 96 cm).

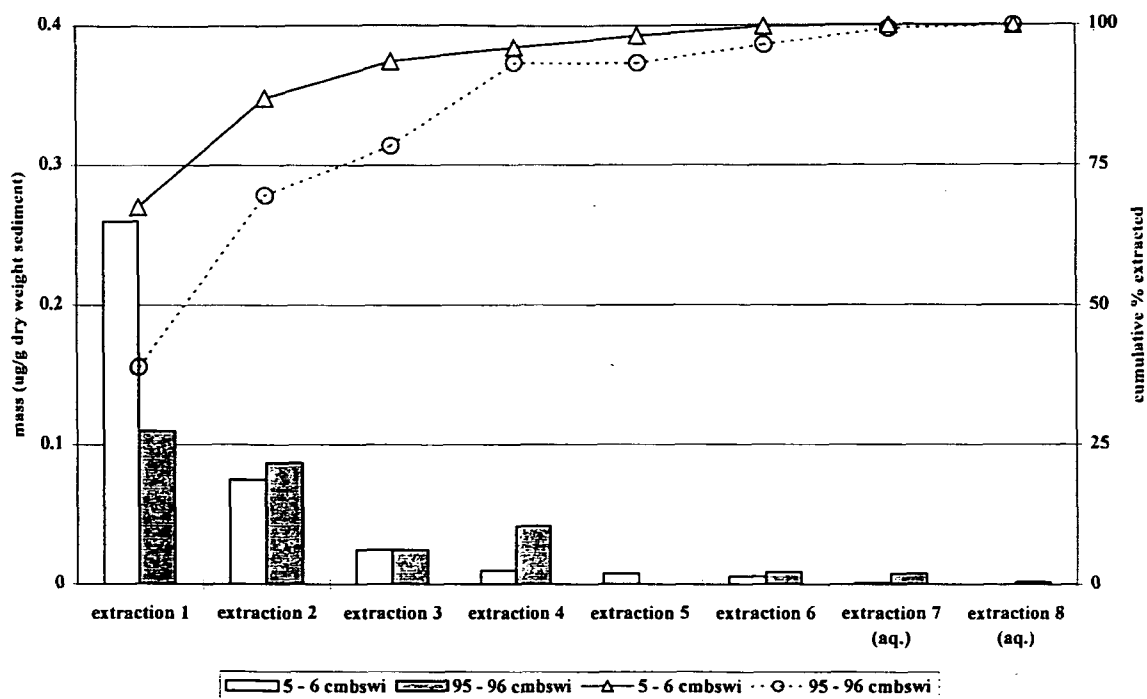


Figure 2.6. Gravimetric results and cumulative percentage of 'proteins' extracted from Rostherne Mere sediments (5 - 6 cm and 95 - 96 cm).

2.4.2. Isolation of IOM from Rostherne Mere sediments

A series of samples from Rostherne Mere sediment were sequentially digested in order to see whether IOM was present in surface sediments and, if present, how the relative proportion of IOM changed with sediment depth. Residual material remaining after each extraction stage and extracts obtained from the sequential digestion procedure was quantified gravimetrically. A number of the samples were sequentially digested in triplicate to check reproducibility. However, replicate samples from the same depths were combined prior to mineral dissolution in order to obtain an adequate amount of IOM for subsequent ionic liquid treatment (Chapter 6). The mass of each operationally defined fraction was calculated as the difference between the mass of freeze-dried sample before each digestion step minus the mass of freeze-dried sample remaining after completion of that digestion step. Each fraction was then normalised and expressed as a percentage of the original sample mass so that relative differences between each sample depth could be

easily identified. One percent of the original sample weight in the experimental determinations represents 10 mg g⁻¹ dry weight original substrate. The major difficulty with determination of the mass balance by difference was that any losses of analyte during isolation (e.g. adhesion to glass fittings) would be attributed to the removed fraction. This overestimates the relative proportion of each removed fraction at the expense of other subsequent fractions. Also, by definition, the operational isolation of each fraction is not completely exhaustive (see Section 2.4.1 for efficiencies), such that a small quantity of each fraction may have been carried over to the subsequent digestion stage.

2.4.2.1. 'Aqueous soluble' fraction

Aqueous extraction has previously been used to isolate 'aqueous soluble' fractions containing volatile fatty acids, amino acids and monosaccharides from Peru Margin sediments (Patience *et al.*, 1990) and salts, carbohydrate material and some amino acids from marine diatomaceous ooze (Klok *et al.*, 1983; Klok *et al.*, 1984). Some gravimetrically determined 'aqueous soluble' fractions isolated in this study contained minute amounts of fine particulates which were visible on the surface meniscus and not removed by prolonged centrifugation. The 'aqueous soluble' fraction of Rostherne Mere sediments accounted for between 1 - 10 % of the original sediment by dry weight (Figure 2.7). There was no statistical correlation ($p < 0.05$) between depth below sediment-water interface and the 'aqueous soluble' content of the sediments. This may have reflected sediment heterogeneity or the relatively small number of samples.

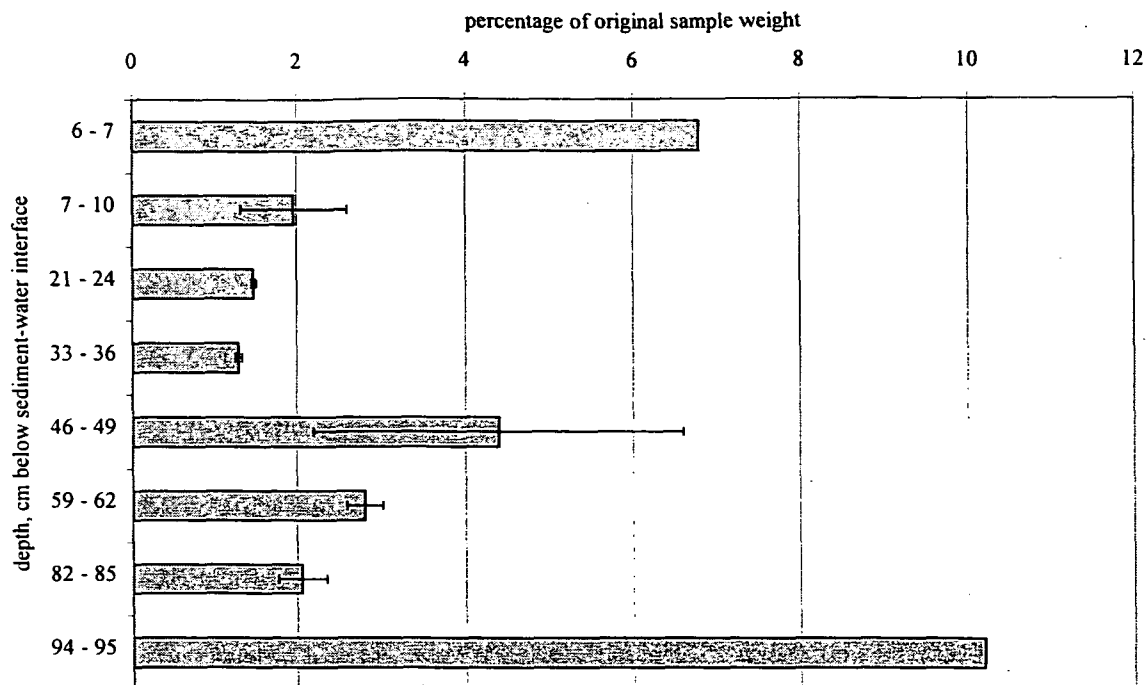


Figure 2.7. 'Aqueous soluble' fractions removed from Rostherne Mere sediments as mean percentages of original sample weight ($n = 3$, except 7 - 10 cm, $n = 2$ where error bars indicate range not standard deviation, and 6 - 7 cm and 94 -95 cm, $n = 1$).

2.4.2.2. 'Free lipid' fraction

Gravimetric determinations of the total 'free lipid' fractions compared favourably to those obtained previously using a non-sequential 'batch' method (Crotty, 1994) for sediments from the same core (Figure 2.8). The 'free lipid' fraction accounted for < 0.5 - 3 % of the original sediment by dry weight (Figure 2.9). There was no statistical correlation ($p < 0.05$) between the depth below sediment-water interface and the 'free lipid' content of the sediments examined in the present study.

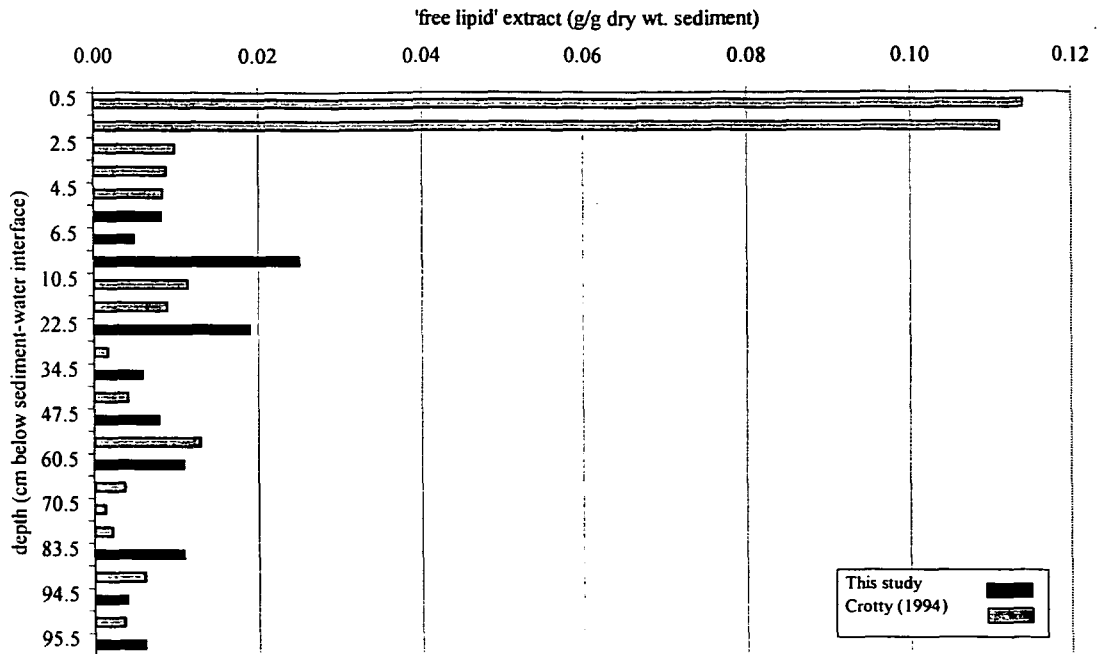


Figure 2.8. Comparison of 'free lipid' concentrations obtained in this study with those obtained by Crotty (1994).

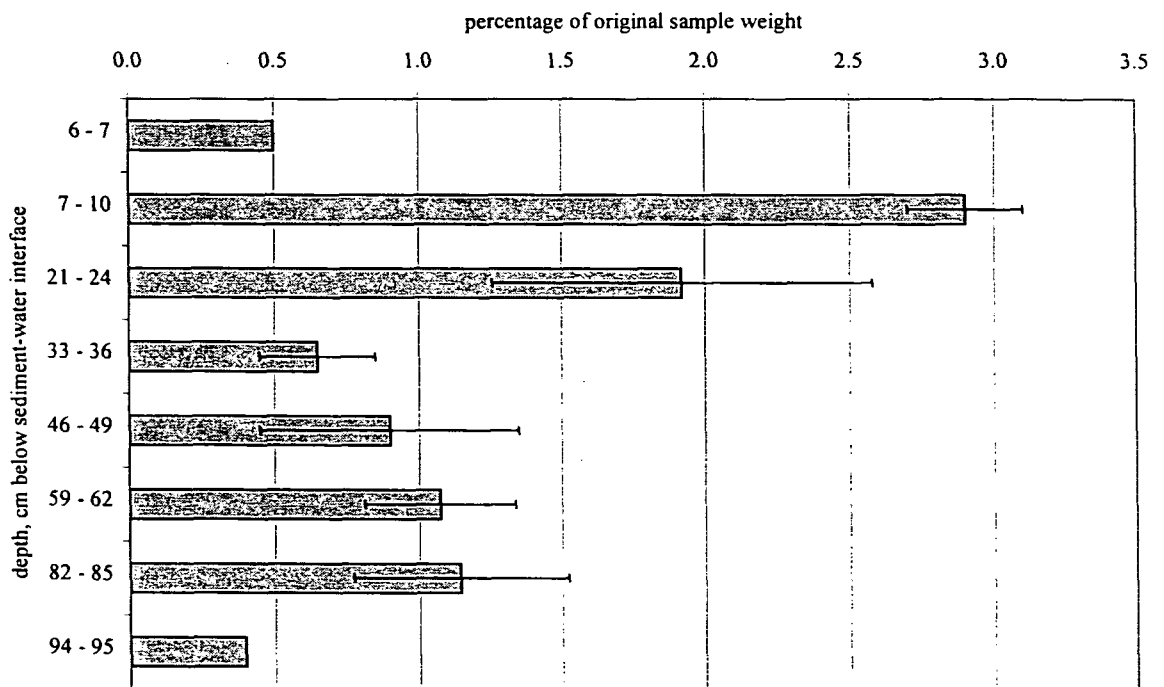


Figure 2.9. 'Free lipid' fractions removed from Rostherne Mere sediments as mean percentages of original sample weight ($n = 3$, except 7 - 10 cm, $n = 2$ where error bars indicate range not standard deviation, and 6 - 7 cm and 94 -95 cm, $n = 1$).

2.4.2.3. 'Protein' fraction

The total protein equivalent concentrations determined in 'protein' extracts from Rostherne Mere sediments (5 - 6 cm and 95 - 96 cm; 0.371 and 0.274 mmol Gly equivalents g⁻¹ dry wt. sediment, respectively) were in good agreement with those previously obtained from the same core using a non-sequential 'batch' method (Crotty, 1994; Figure 2.10). These results indicate that the sequential digestion stages prior to 'protein' removal have had negligible effect on the 'protein' concentrations in the sediments. The 'protein' fraction accounted for 20 - 40 % of the original sample weight (Figure 2.11). Conversion of the 'protein' data from the extracts (mmol Gly equivalents g⁻¹ dry weight sediment) and expressing it in terms of the mass balance (% dry weight sediment), allowed comparison of the mass balance data (obtained by difference) with the 'protein' content of the removed fraction. In this manner, the 'protein' content of removed fractions was calculated at 2 - 3 % of the initial sediment (dry weight), substantially lower than the 20 - 40 % dry weight sediment 'protein' fraction measured by difference. Whilst some amino acids (*e.g.*) are known to be underestimated using the 'ninhydrin' method, it is unlikely that this could explain the entire deficit. A more probable explanation would be the removal of carbonate material during the acid hydrolysis.

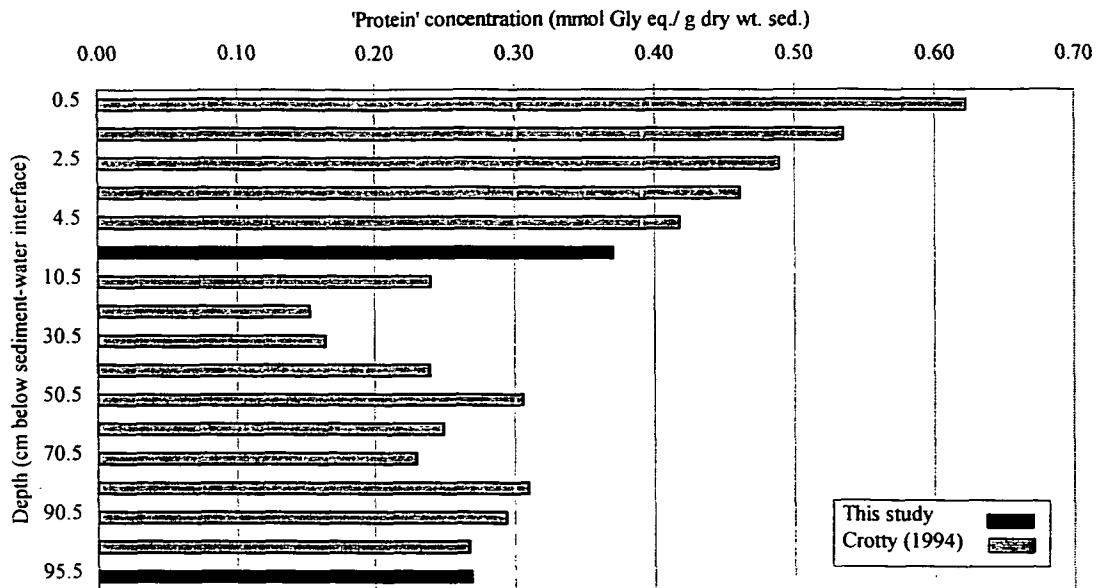


Figure 2.10. Protein equivalent concentrations obtained from 'protein' fractions in this study compared with those obtained by Crotty (1994).

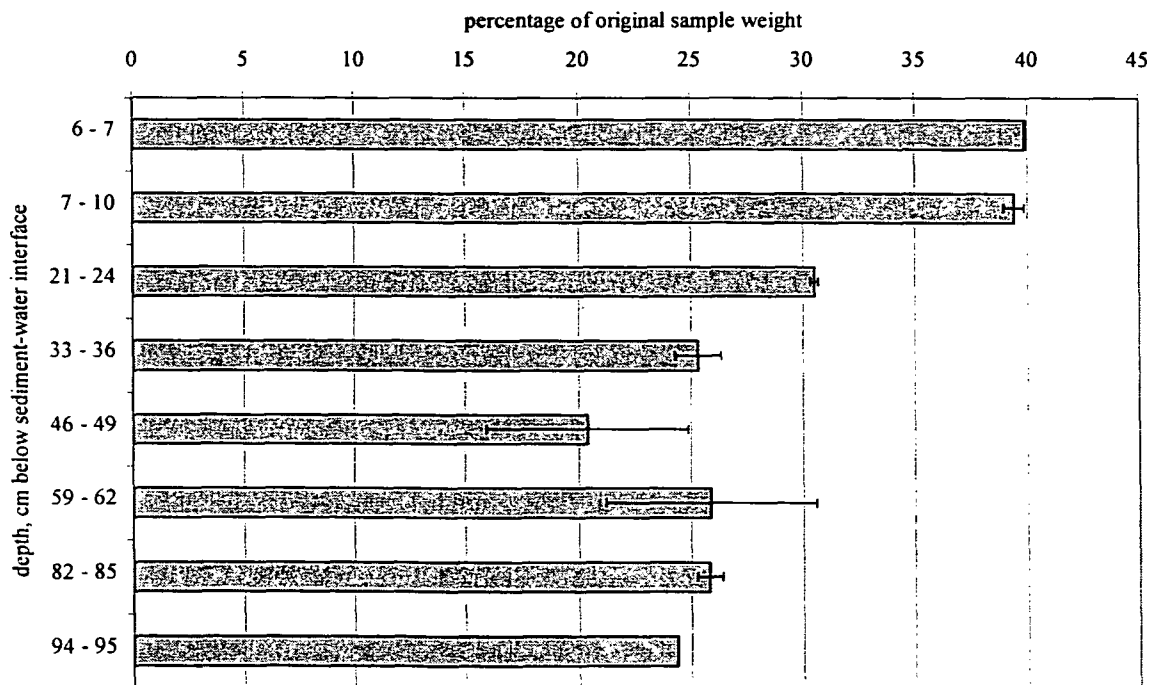


Figure 2.11. 'Protein' fractions removed from Rostherne Mere sediments as mean percentages of original sample weight ($n = 3$, except 7 - 10 cm, $n = 2$ where error bars indicate range not standard deviation, and 6 - 7 cm and 94 - 95 cm, $n = 1$).

2.4.2.4. 'Carbohydrate' fraction

The 'carbohydrate' fraction accounted for 0.4 - 2.7 % of the original sediment mass (Figure 2.12). Incomplete freeze-drying was the most plausible explanation for the mass gain of the 82 - 85 cm sample, although a second freeze-drying still gave a negative 'carbohydrate' yield ($-0.7 \% \pm -0.3$; $n = 3$), *i.e.* a net mass increase of 4 - 10 mg g⁻¹ after removal of the 'carbohydrate' fraction. Removal of residual moisture by freeze-drying following the 'bound lipid' extraction would have served to overestimate the subsequent 'bound lipid' content by up to 1% dry weight sediment.

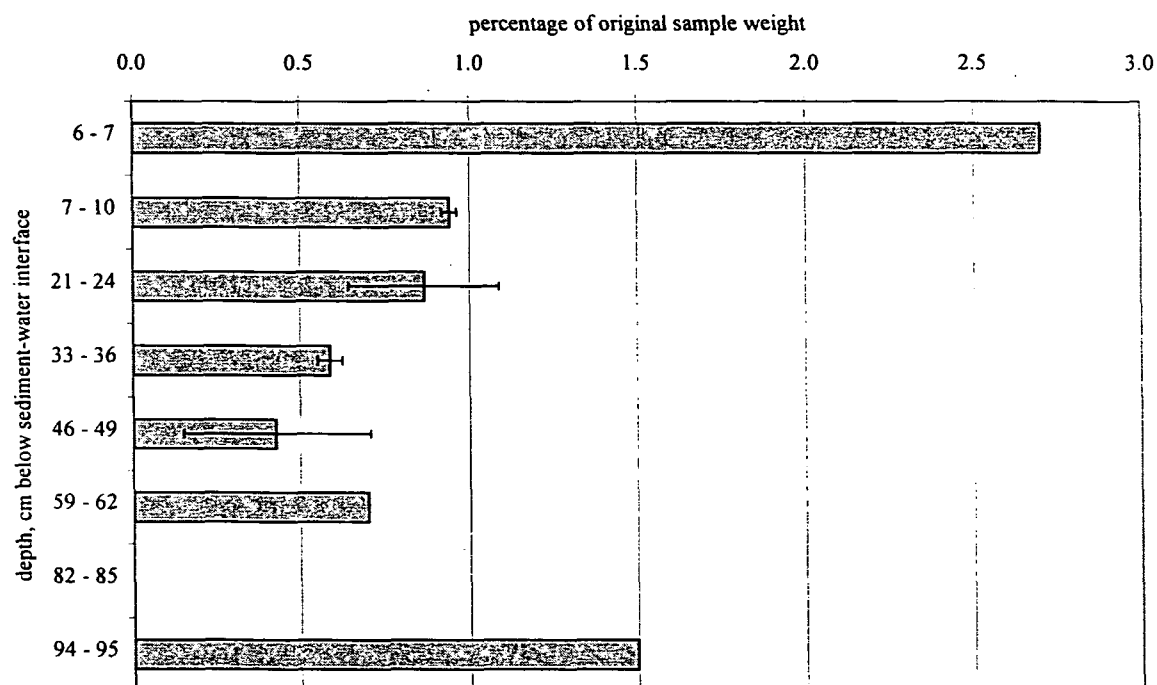


Figure 2.12. 'Carbohydrate' fractions removed from Rostherne Mere sediments as mean percentages of original sample weight ($n = 3$, except 7 - 10 cm, $n = 2$ where error bars indicate range not standard deviation, and 6 - 7, 59 - 62 and 94 - 95 cm, $n = 1$, 82 - 85 cm not determined).

2.4.2.5. 'Bound lipid' fraction

The 'bound lipid' fraction represents the portion of lipids not removed by solvent extraction alone (Section 2.3.3) but which become solvent extractable following

saponification (base hydrolysis). Thus, there is not necessarily any structural difference between 'free' and 'bound' lipids. An operational distinction is made only.

The 'bound lipid' fraction accounted for between 2 and 9.5 % of the original sample mass (Figure 2.13). As discussed in Section 2.4.1, the 'bound lipid' content of the 82 - 85 cm sample may be overestimated. There was no significant correlation between 'bound lipid' content and sediment depth below the sediment-water interface.

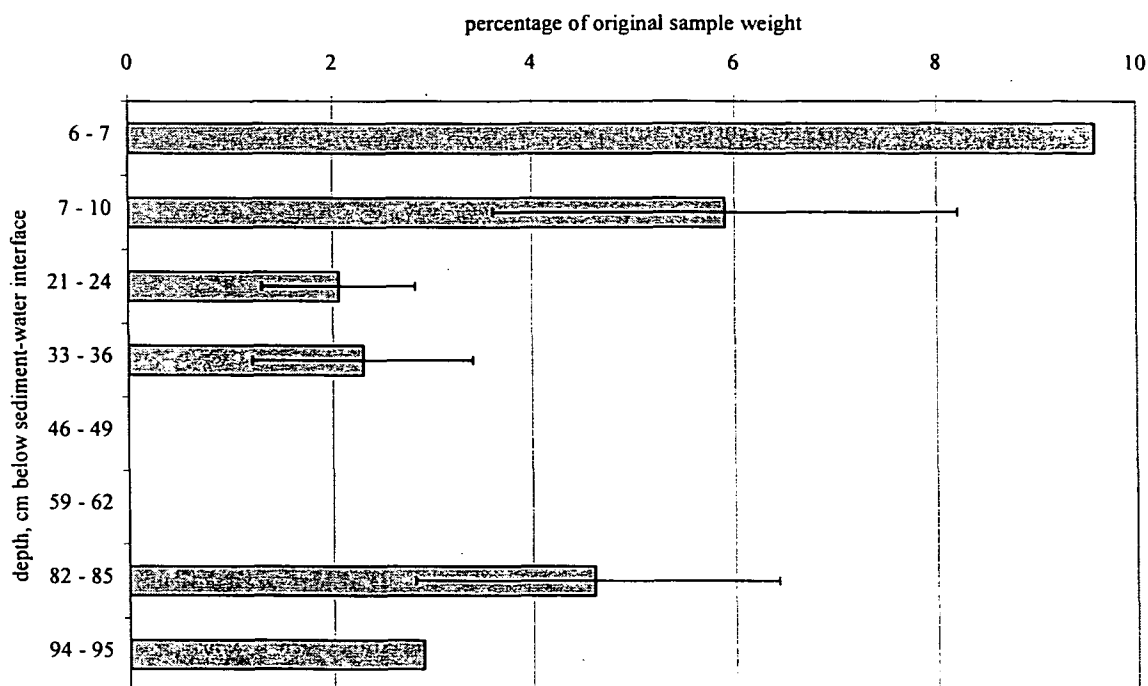


Figure 2.13. 'Bound lipid' fractions removed from Rostherne Mere sediments as mean percentages of original sample weight ($n = 3$, except 7 - 10 cm, $n = 2$ where error bars indicate range not standard deviation, and 6 - 7 cm and 94 - 95 cm, $n = 1$, 46 - 49 cm and 59 - 62 cm not determined).

2.4.2.6. 'Mineral' fraction

Sediment samples were de-mineralised using a hydrofluoric acid/concentrated hydrochloric acid procedure (Section 2.3.7) in order to remove carbonate and silicate

material. Saturated ammonium carbonate was used to prevent the formation of neo-fluorides (e.g. Boucher *et al.*, 1990).

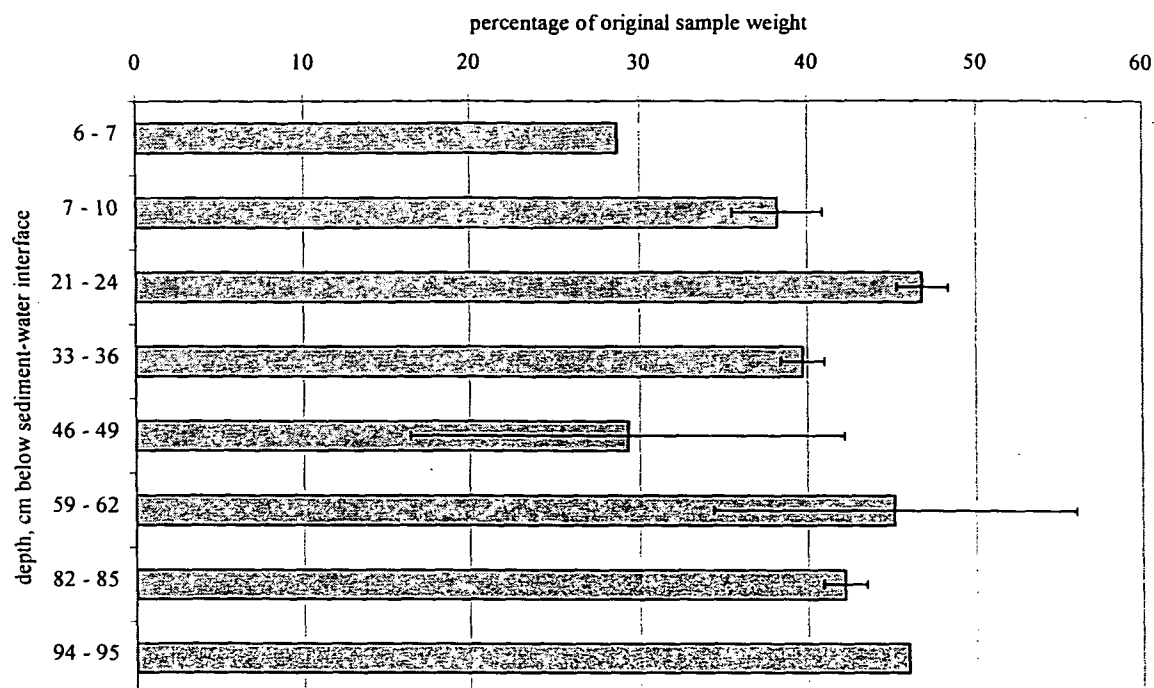


Figure 2.14. 'Mineral' fractions removed from Rostherne Mere sediments as a percentage of original sample weight ($n = 1$; 'error bars' indicate estimated range not standard deviation).

Combination of the post-'bound lipid' residual material from the duplicate analyses prior to de-mineralisation carried an inherent error with it for the quantification of the 'mineral' and IOM fractions. An estimation of the standard deviation associated with quantification of the post-'bound lipid' extracted residue in replicate samples was made in order to estimate maxima and minima mass balance results for the 'mineral' (and IOM) fraction determination (Figure 2.14). The larger range in 'mineral' content for the 46 - 49 and 59 - 62 cmbswi samples reflects experimental losses of analyte from these samples during 'bound lipid' removal. Otherwise, the 'mineral' fraction accounted for between 28 and 47 % of the original sediment. There was no statistical correlation between the 'mineral'

content of the sediment and depth below the sediment-water interface.

2.4.2.7. 'Insoluble organic matter' (IOM)

Material remaining after sequential extraction is operationally defined as 'insoluble organic matter' (IOM). The IOM content of Rostherne Mere sediments was determined gravimetrically (Figure 2.15). The variation associated with determination of the post-'bound lipid' residue in replicate samples was used to estimate the potential variability of the IOM determinations (Figure 2.15). The IOM isolated from Rostherne Mere sediments accounted for 7 - 30 % of the original sample mass. There was no significant correlation between IOM content and depth below the sediment-water interface or between the proportion of IOM and the proportion of any other fractions.

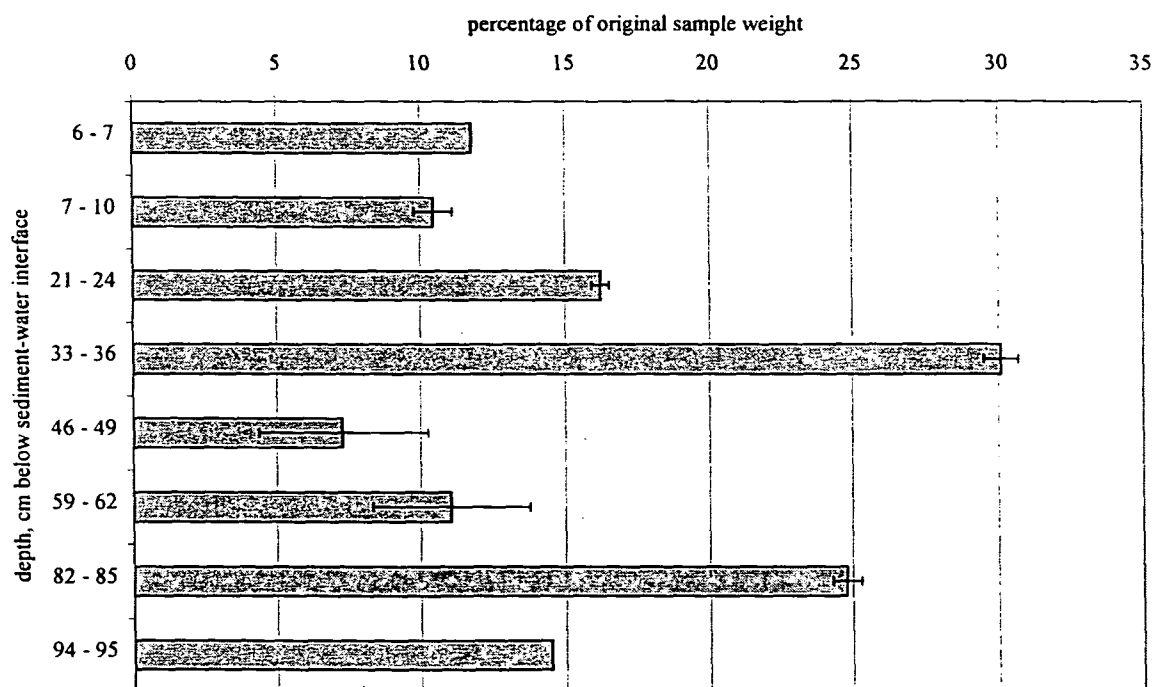


Figure 2.15. IOM fraction isolated from Rostherne Mere sediments as a percentage of original sample weight ($n = 1$; 'error bars' indicate estimated range not standard deviation).

A sample of sedimentary IOM from Rostherne Mere (82 – 85 cmbswi) was extracted with

solvent (DCM) using three techniques, *viz.* reflux (2 x 24 h), sonication (40 min) and accelerated solvent extraction (ASE; 100 °C, 5 min, 1500 psi, Na₂SO₄). Gravimetric determination of the extracts obtained from these experiments demonstrated that the IOM was substantially insoluble in solvent (reflux, < 0.1 %; sonication, 0.4 %; ASE, 0.3 %).

2.4.3. Isolation of IOM from Kimmeridge Clay

The IOM isolation procedure applied to Rostherne Mere sediments was also applied to Kimmeridge Clay sediment. Kimmeridge Clay was found to contain between 11 and 12 % IOM (Figure 2.16) compared to 16 -19 % ($n = 2$) kerogen content determined previously for the same sample using the 'classical' kerogen isolation method (Bertenshaw, 1996) and 16 % reported by Stoneley & Selley (1986). This suggested that the 'classical' method of kerogen isolation, *i.e.* de-mineralisation with HF/HCl and solvent extraction, does not remove readily soluble material as effectively as the sequential digestion procedure used in this study. Furthermore, kerogen isolated using the 'classical' method may contain up to 5 % of the original sample weight as extractable material. Kimmeridge Clay IOM was only sparingly soluble in solvent (DCM, reflux, 2 x 24 h), as the extract obtained comprised <0.1 % of the initial IOM.

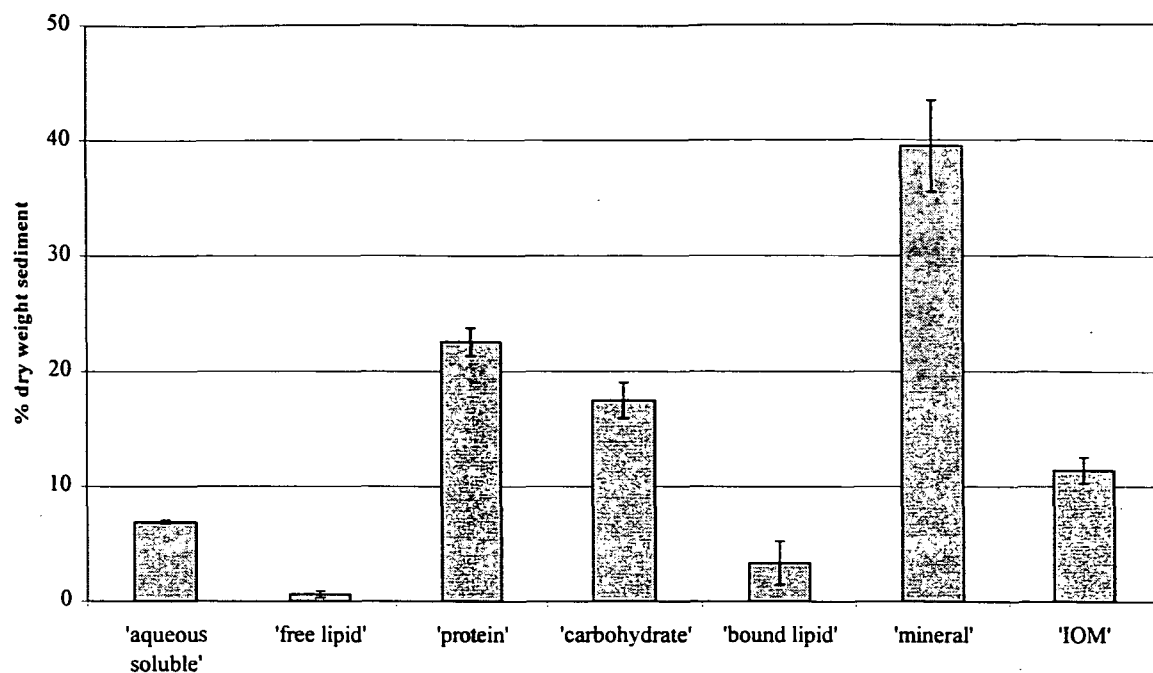


Figure 2.16. Kimmeridge Clay: range of gravimetric results for operationally defined fractions ($n = 2$ for all fractions except 'mineral' and IOM where $n = 1$, error bars represent range for all fractions except 'mineral and IOM where they are an estimate of variability).

2.4.4. Isolation of IOM from bacterial necromass

The two species of methanogenic bacteria (*M. thermoautotrophicum* strain ΔH and *M. jannaschii*) and the sulphate-reducing bacterium, *D. postgatei*, were subject to the same sequential isolation procedure applied to sediments except that the mineral removal stage was omitted. Reproducibility in the operational fractionation of *M. jannaschii* was good with standard deviations below $\pm 1\%$ and residual standard deviations generally below 10% with the exception of the 'carbohydrate' fraction. Two of the three samples of *M. jannaschii* produced negative 'carbohydrate' fractions, *i.e.* a mass gain following 'carbohydrate' removal of -0.7 and -0.2% of the original sample mass. The other sample yielded a 'carbohydrate' fraction +0.7%. The principal operationally defined components of *M. jannaschii* were 'proteins' (60% original dry weight; Figure 2.17) and 'aqueous

soluble' material (28 % original dry weight). *M. jannaschii* was found to contain 2.8 % of the original sample weight as IOM (± 0.3 %; $n = 3$). This IOM was almost insoluble in solvent (DCM, reflux, 2 x 24 h, yield = 0.5 %).

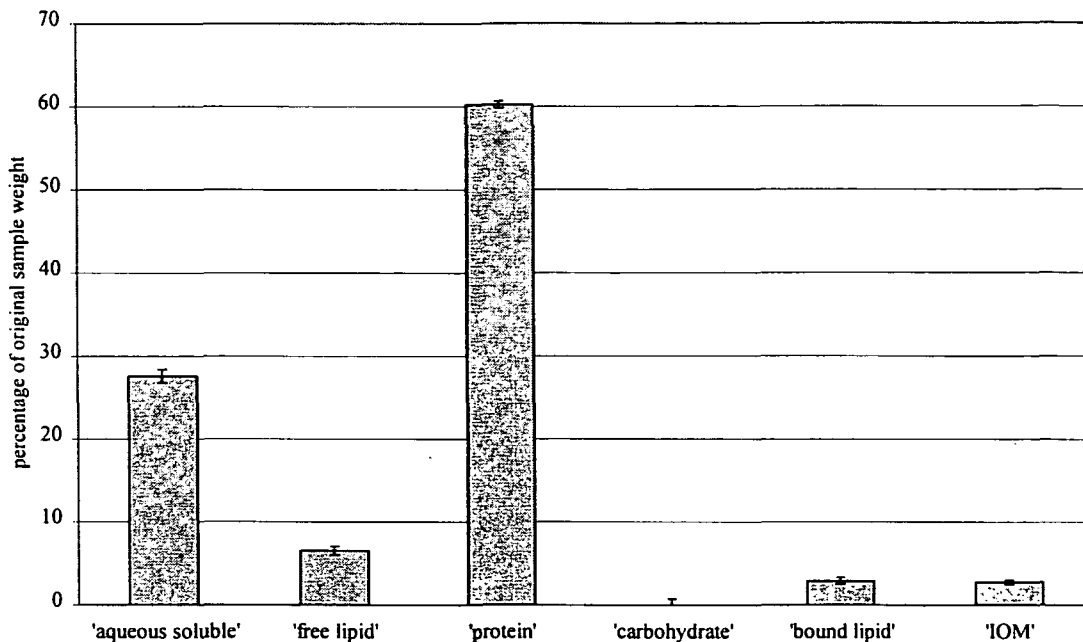


Figure 2.17. *M. jannaschii*: gravimetric results for operationally defined fractions ($n = 3$).

The principal components of *M. thermoautotrophicum* were also 'proteins' (59 %; Figure 2.18) and 'aqueous soluble' material (33 %). 'Free lipids', 'carbohydrates' and 'bound lipids' accounted for 3 %, 3 % and 1 % of the original sample weight, respectively, whilst only 0.1 % of the original sample weight remained as IOM following sequential digestion.

The relative composition of the sulphate-reducing bacterium *Desulfobacter postgatei* (DSM 2034), sequentially digested in the same manner as methanogenic bacteria, is presented in Figure 2.19. Insufficient material for weighing remained after the 'bound lipid' removal stage of the sequential digestion procedure, suggesting that *D. postgatei* contained little or no IOM.

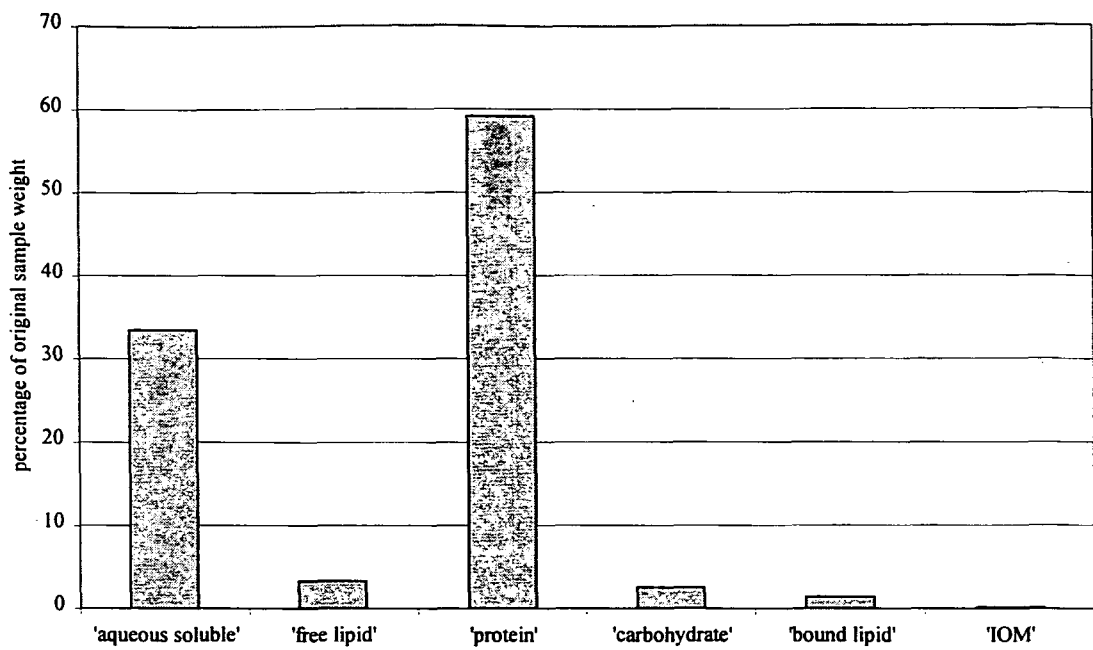


Figure 2.18. *M. thermoautotrophicum*: gravimetric results for operationally defined fractions ($n = 1$).

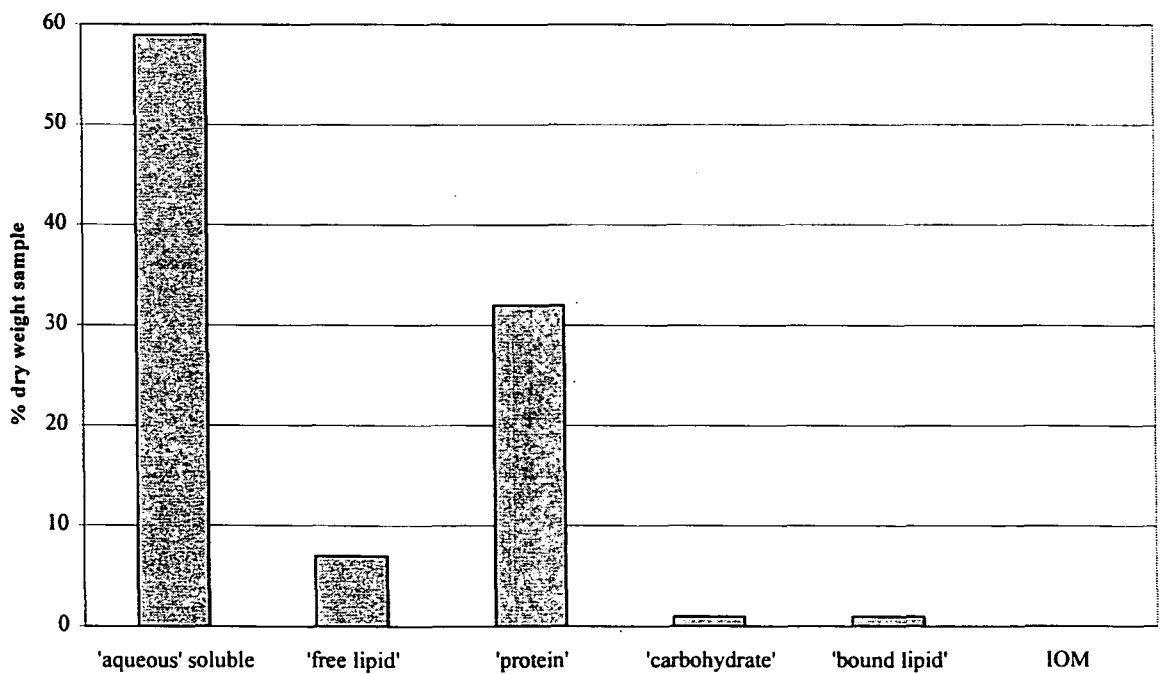


Figure 2.19. *D. postgatei*: gravimetric results for operationally defined fractions ($n = 1$).

2.4.5. Isolation of IOM from algae

The diatomaceous algae *Skeletonema costatum* and *Haslea ostrearia* were fractionated using the sequential digestion procedure (Section 2.1) but were not de-mineralised. Previous studies that have included the gross biochemical composition of *S. costatum* (Table 2.1) have recognised that their cultures were non-axenic but reported that bacterial contributions accounted for less than 1 % of their results (Parsons *et al.*, 1961; Sánchez-Saavedra & Voltolina, 1996). At a maximum, insoluble organic matter, if present, could have accounted for the difference between the total of their isolated fractions (*i.e.* proteins, lipids and carbohydrates) and 100 % (allowing for reproducibility). Therefore, insoluble organic matter may have comprised between 32 – 59 % dry weight of *S. costatum* in these previous studies. However, Parsons *et al.* (1961) found that silicon and phosphorus accounted for 14.3 and 1.7 % of the algal dry mass, respectively. Thus, a more conservative estimate of the potential insoluble organic matter component in these reports would be 16 – 43 % of the dry algal mass. Clearly, the 1 – 3 % dry weight IOM isolated from *S. costatum* in the current work (Figure 2.20) is much lower than that suggested by previous studies and is similar to the amount suggested to arise from bacterial contamination (Parsons *et al.*, 1961; Sánchez-Saavedra & Voltolina, 1996).

The 39 % dry weight IOM isolated from *H. ostrearia* (Figure 2.21) is likely to be an overestimate by up to 14 % since the ‘carbohydrate’ fraction produced a negative yield (-14 % dry weight). This may be explained by either incomplete freeze-drying, or production of chemical artefacts during the ‘carbohydrate’ hydrolysis. Notwithstanding this overestimation of IOM from *H. ostrearia*, the IOM had a distinct morphology when viewed using SEM (Section 3.3.1) characteristic of the untreated alga. Although surface features of the organisms had been removed it appeared that the siliceous ‘skeleton’ remained following the sequential isolation procedure. Therefore, the ‘insoluble’ material isolated from *H. ostrearia* was not considered to be IOM, but principally ‘insoluble’

inorganic matter.

Table 1.6. Gross biochemical composition (% dry weight) of *S. costatum* previously reported

Fraction	Parsons <i>et al.</i> (1961) [†]	Brown (1991) [‡]	Sánchez-Saavedra & Voltolina (1996) [*]	
			Exponential growth phase	Stationary growth phase
Proteins	37	25	39 – 47	39 – 50
Lipids	6.5	11.2	4 – 7	6 – 9
Carbohydrates	20.8	4.6	13 – 24	10 – 18
Ash	39	--	34 – 49	32 – 36
Total	103	40.8	100 - 104	98 - 101

[†] Replicate analyses not reported; protein calculated from Kjeldahl nitrogen x 6.25; lipids includes pigments

[‡] Axenic culture; *n* = 2; lipids includes pigments

^{*} Range included for *n* = 3 under six different experimental conditions

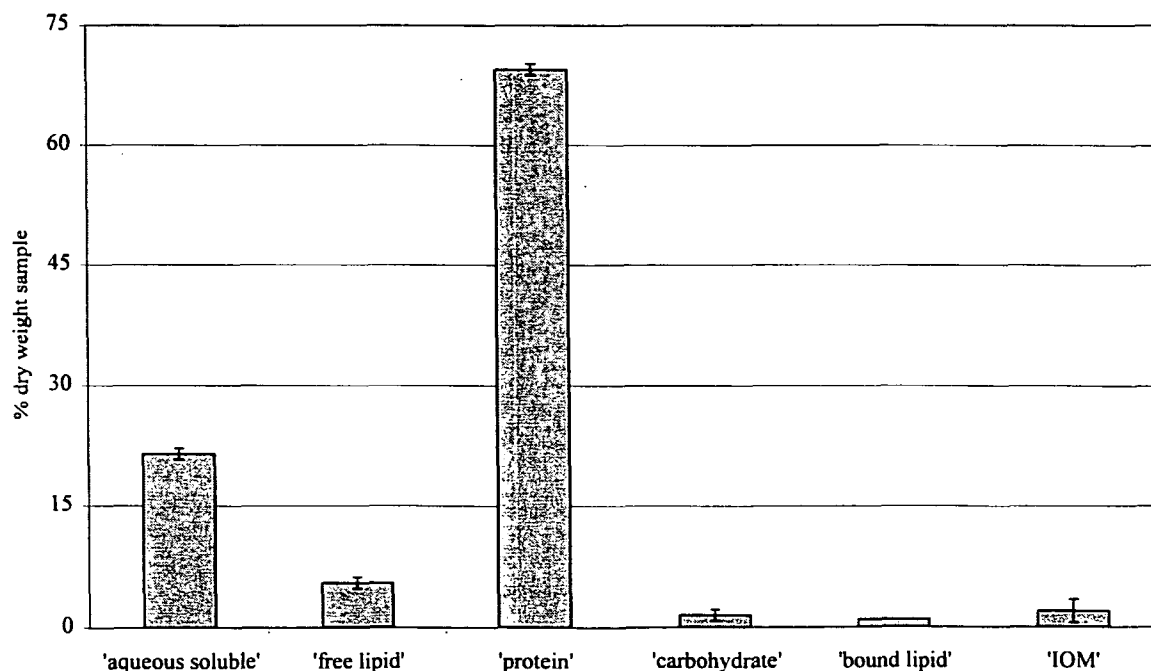


Figure 2.20. *S. costatum*: gravimetric results for operationally defined fractions (*n* = 2; error bars indicate range not standard deviation).

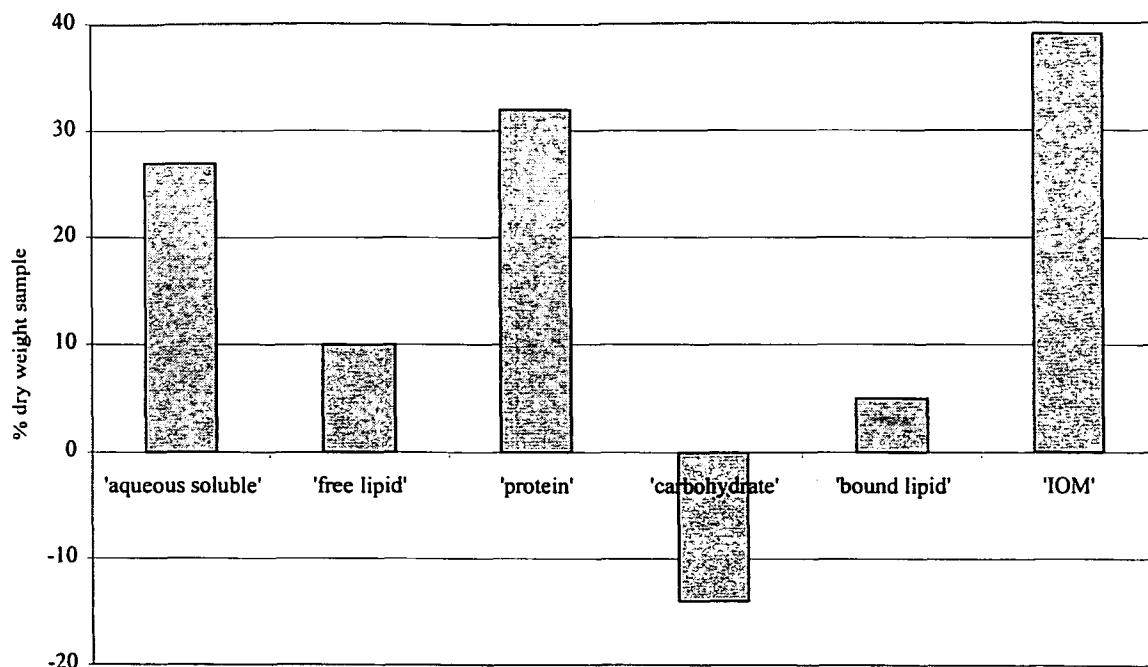


Figure 2.21. *H. ostrearia*: gravimetric results for operationally defined fractions ($n = 1$).

Omission of the 'mineral' removal stage from the sequential isolation procedure applied to algae meant that IOM isolated from *S. costatum* and *H. ostrearia* potentially contained a significant inorganic component. For this reason these samples were not generally analysed further.

2.5. Summary

- IOM was quantitatively isolated from lacustrine Rostherne Mere sediments (7 – 30 %), Kimmeridge Clay (11 – 12 % dry weight) and methanogenic bacteria (*M. jannaschii*, 2.8 % ± 0.3 % dry weight; *M. thermoautotrophicum*, 0.1 % dry weight), Figure 2.22.
- The IOM content of Kimmeridge Clay determined using the sequential isolation procedure (11 – 12 % dry weight) was lower than the kerogen content (16 – 19 % dry weight) previously reported for the same sample using the 'classical' (kerogen) isolation procedure.

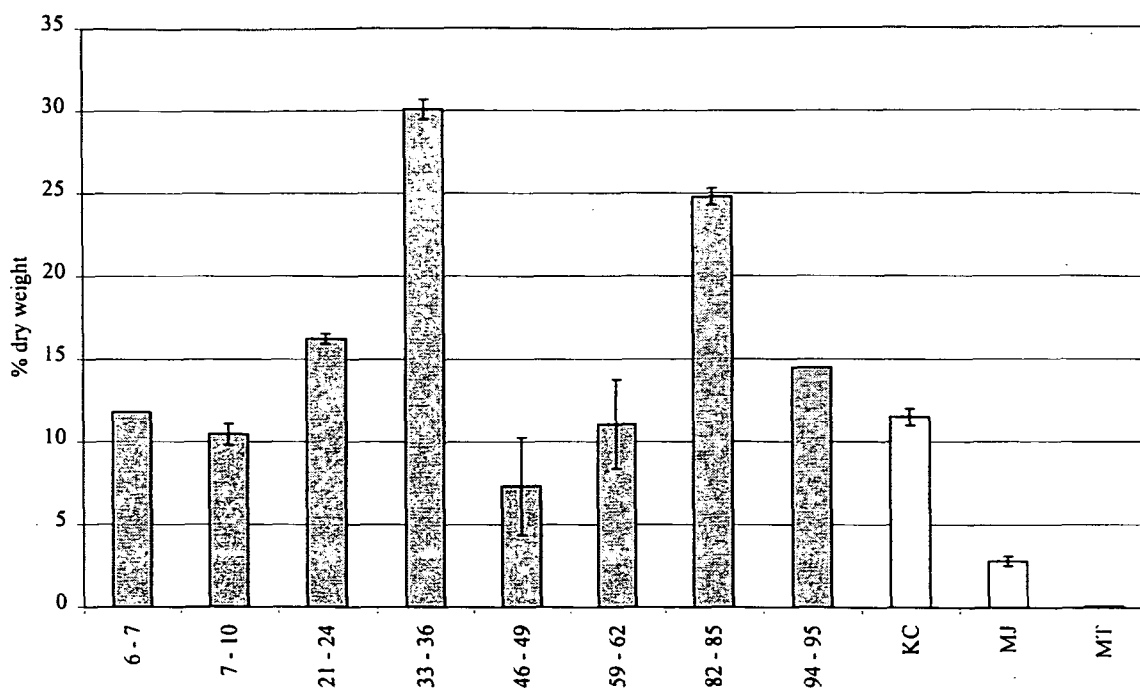


Figure 2.22. Proportion of IOM isolated from lacustrine Rostherne Mere sediments (cmbswi), Kimmeridge Clay (KC), and methanogenic bacteria (*M. jannaschii*: MJ; *M. thermoautotrophicum*: MT). Error bars indicate estimated standard deviation, except *M. jannaschii* where $n = 3$.

- The quantity of IOM isolated from *S. costatum* (1 – 3 % dry weight) was lower than that inferred from previous studies (16 – 43 % dry weight), but comparable to the level previously reported to arise from bacterial contributions in non-axenic cultures (< 1 % dry weight).
- IOM isolated from *H. ostrearia* (39 % dry weight) was overestimated by up to 14 % owing to the negative contribution of the ‘carbohydrate’ fraction (-14 % dry weight) and principally comprised siliceous skeletal remains (*i.e.* inorganic material).
- No IOM was isolated from the sulphate-reducing bacterium *D. postgatei*.

Chapter 3: Instrumental characterisation of IOM from sediments and biota

3.1. Introduction

This chapter describes the bulk characterisation of sediments and biota, and IOM obtained from these substrates following its sequential isolation (Chapter 2), using instrumental techniques routinely applied to geochemical samples, *i.e.* scanning electron microscopy (SEM, Section 3.3.1), elemental analysis (Section 3.3.2), solid-state nuclear magnetic resonance spectroscopy (ss-NMR, Section 3.3.3), and infrared spectroscopy (IR, Section 3.3.4). Untreated sediments and biota and IOM isolated from them were further characterised by molecular instrumental techniques (pyrolysis-gas chromatography-mass spectrometry and time of flight-secondary ion-mass spectrometry, Chapter 4).

3.2. Experimental procedures

General laboratory procedures were as previously described in Section 2.3.1. All samples were freeze-dried prior to instrumental analysis.

3.2.1. Scanning electron microscopy

Freeze-dried samples were mounted on stubs and coated with gold using an Emitech K550 sputter coater before carrying out microscopy using a JEOL JSM-6100 scanning electron microscope operated at 20 kV. Identification of pyritic framboids was made using an ISIS-200 X-ray analyser (Oxford Instruments).

3.2.2. Elemental analysis

Freeze-dried samples were weighed into platinum boats and analysed in triplicate using a CHN analyser.

3.2.3. ^{13}C Solid-state nuclear magnetic resonance spectroscopy (ss-NMR)

Quantitative solid-state ^{13}C nuclear magnetic resonance (ss-NMR) spectra were obtained from Rostherne Mere sediments, and residual sedimentary IOM, using a Bruker MSL 100

spectrometer. Carbon spectra were also obtained for untreated *M. jannaschii* but insufficient material remained following sequential isolation for analysis of the bacterial IOM by ss-NMR. Analysis by ss-NMR used cross-polarisation magic-angle-spinning (CP-MAS) and single pulse excitation (SPE) experiments in order to more accurately estimate aromatic components (Snape, *pers. comm.*).

3.2.4. Infrared Spectroscopy

Solid samples for IR analysis were prepared by adding *ca* 2 mg of freeze-dried sample to *ca* 200 mg of dried potassium bromide (KBr) and grinding in a mortar and pestle. After grinding, the mixture was transferred to a clean dry disc block, attached to a vacuum line and evacuated for two minutes prior to applying pressure (10 tons, 2 min). The resultant disc was placed in a pellet holder, placed in the instrument and allowed to equilibrate for one minute before scanning was commenced. Infrared measurement was controlled *via* OPUS II software. Each sample was determined against a KBr blank that was automatically subtracted from the sample spectrum in order to account for the KBr and any inherent moisture (OH stretching band around 3430 cm⁻¹ and OH bending band at 1630 cm⁻¹). Processing was limited to baseline flattening and peak detection set at peaks > 5 %. All spectra are shown with absorbance on the Y abscissa. No account was taken of the relative absorbance between spectra because the IR analyses were carried out qualitatively and solid samples generally produce relatively broad absorbance bands.

3.3. Results

3.3.1. Scanning electron microscopy

Morphological changes between untreated samples of Rostherne Mere sediments, methanogenic bacteria and algae, and the IOM obtained from these substrates following sequential isolation, were monitored using scanning electron microscopy (SEM). Biogenic material was clearly present in the Rostherne Mere sediments prior to sequential extraction

(Figure 3.1a). For example, higher plant fragments and diatom valves such as those of *Stephanodiscus* spp. could be discerned. The remainder comprised a complex mixture of sedimentary matter. It was apparent from the micrographs that some biological material survived the sequential isolation procedure (Figure 3.1b), albeit apparently somewhat altered. In addition, pyritic framboids were present in the sedimentary IOM.

Under the SEM conditions, untreated *M. jannaschii* appeared as layers of thin leaf-like material with a smooth surface (Figure 3.2a). SEM of the IOM isolated from *M. jannaschii* showed it to have lost its laminar morphology/structure, becoming more blocky with a seemingly rough surface texture (Figure 3.2b).

Freeze-dried but chemically untreated *M. thermoautotrophicum* had a serrated plate-like bulk structure with a generally 'smooth' looking surface texture under SEM conditions (Figure 3.3a). Following sequential isolation this structure was no longer visible and the isolated IOM appeared to be folded but poorly defined with an apparently rough surface texture (Figure 3.3b), not dissimilar to that of *M. jannaschii* IOM (Figure 3.2b).

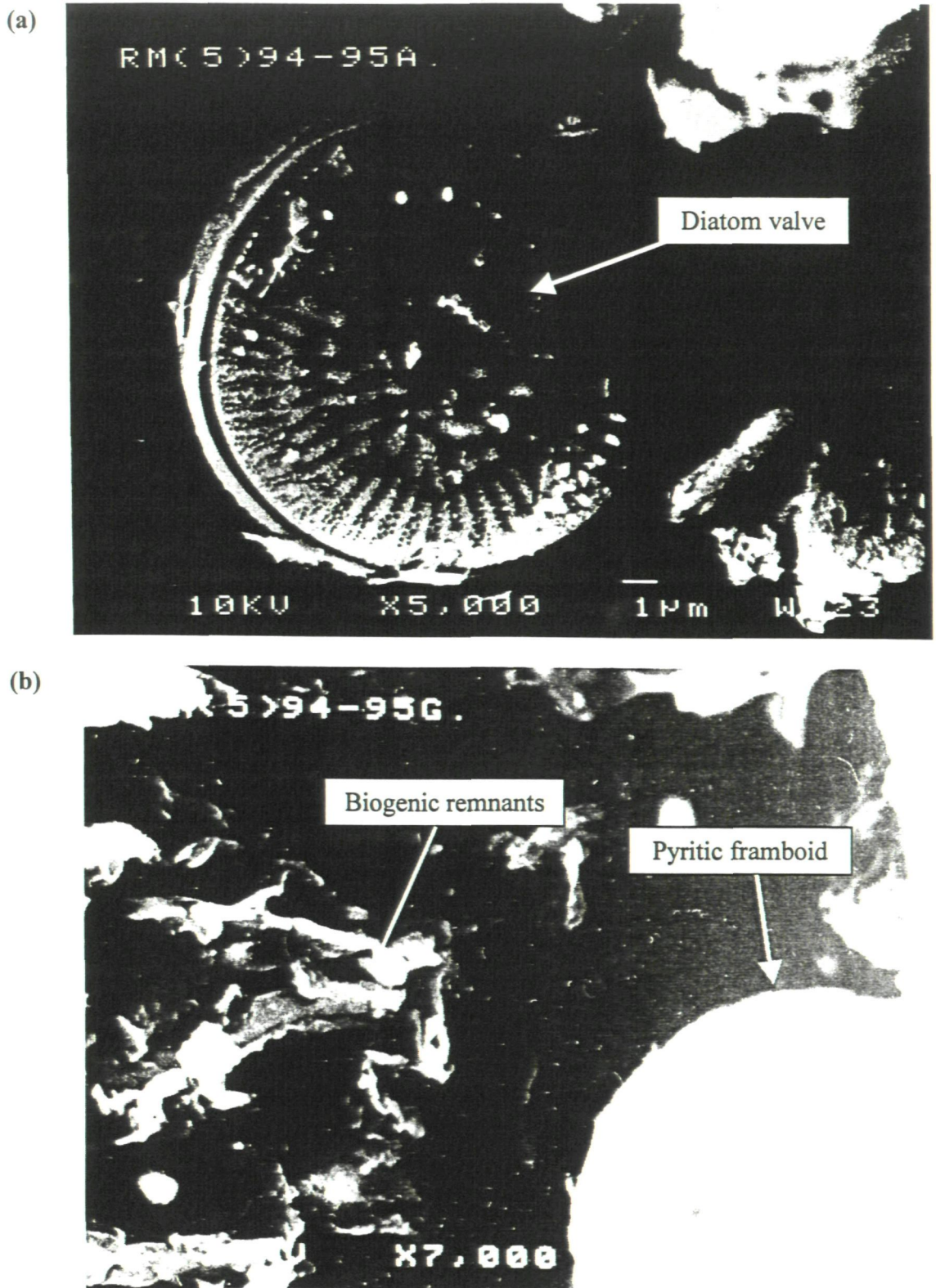


Figure 3.1. SEM micrograph of Rostherne Mere sediment. (a) Untreated (b) IOM.

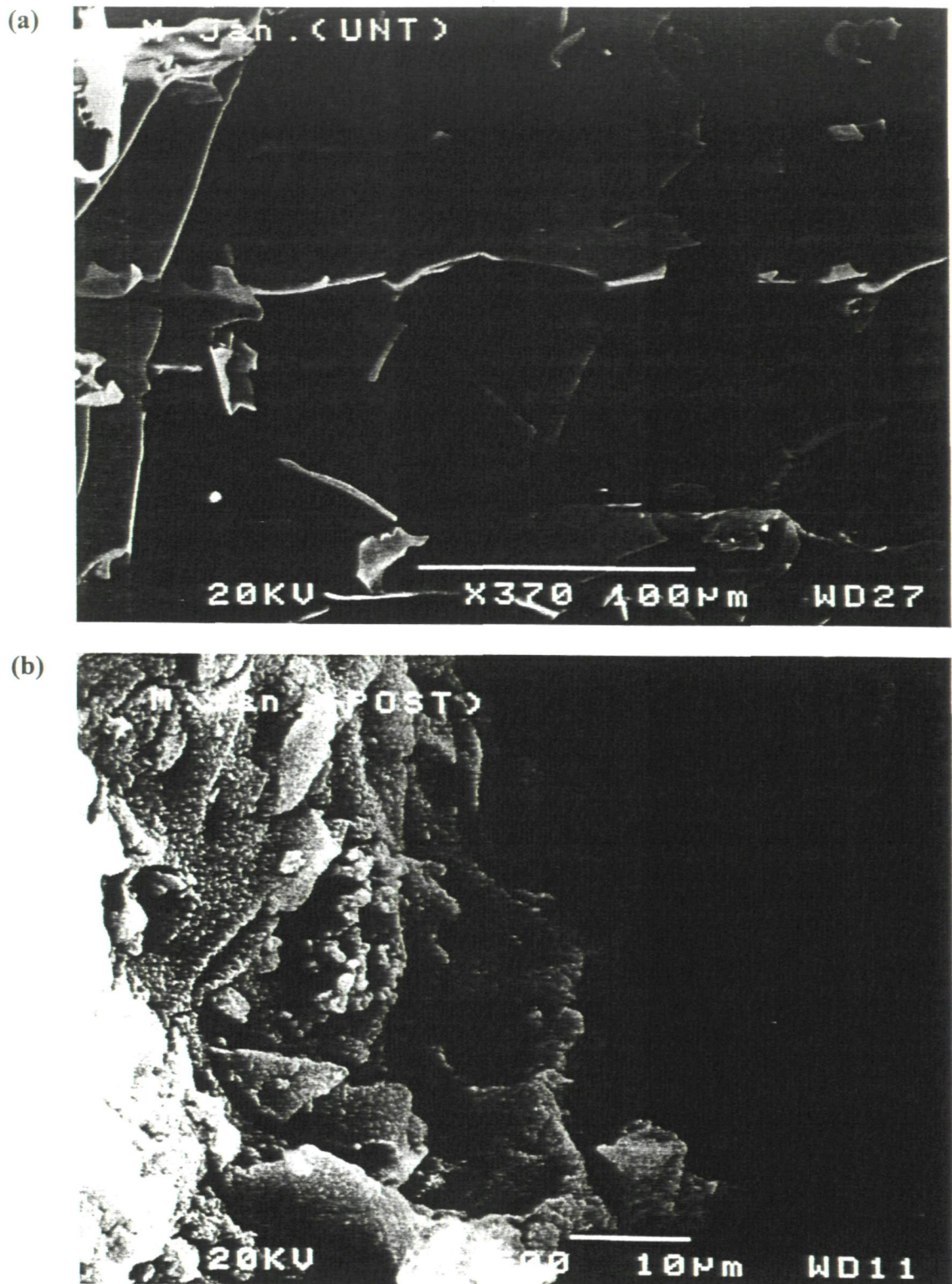
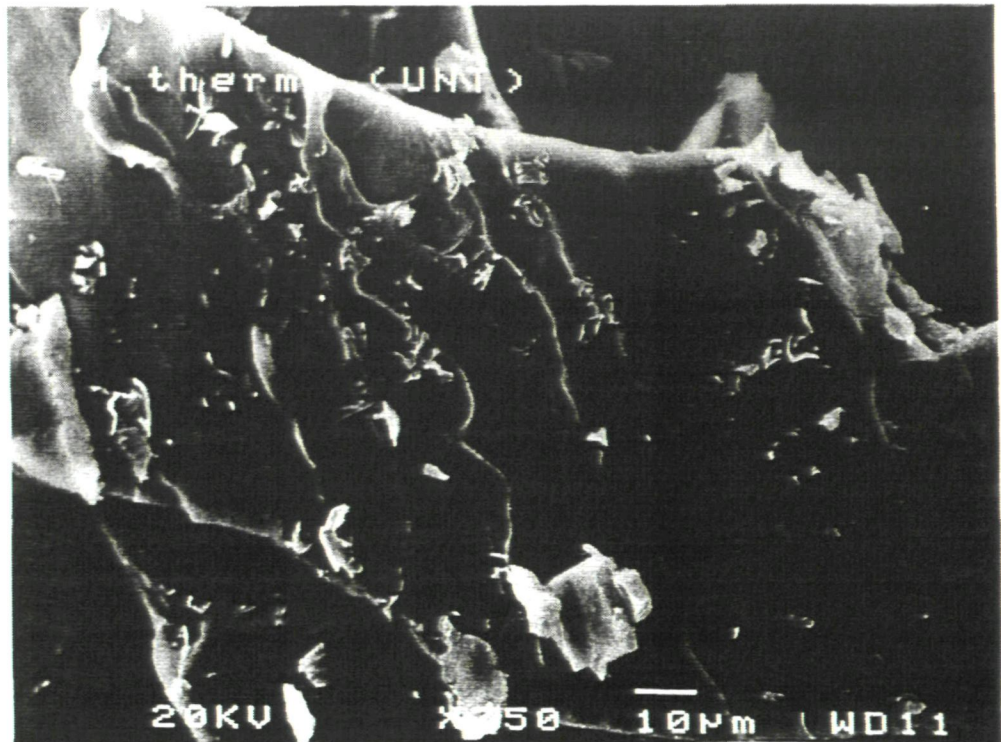


Figure 3.2. SEM micrographs of *M. jannaschii*. (a) Untreated (b) IOM.

(a)



(b)

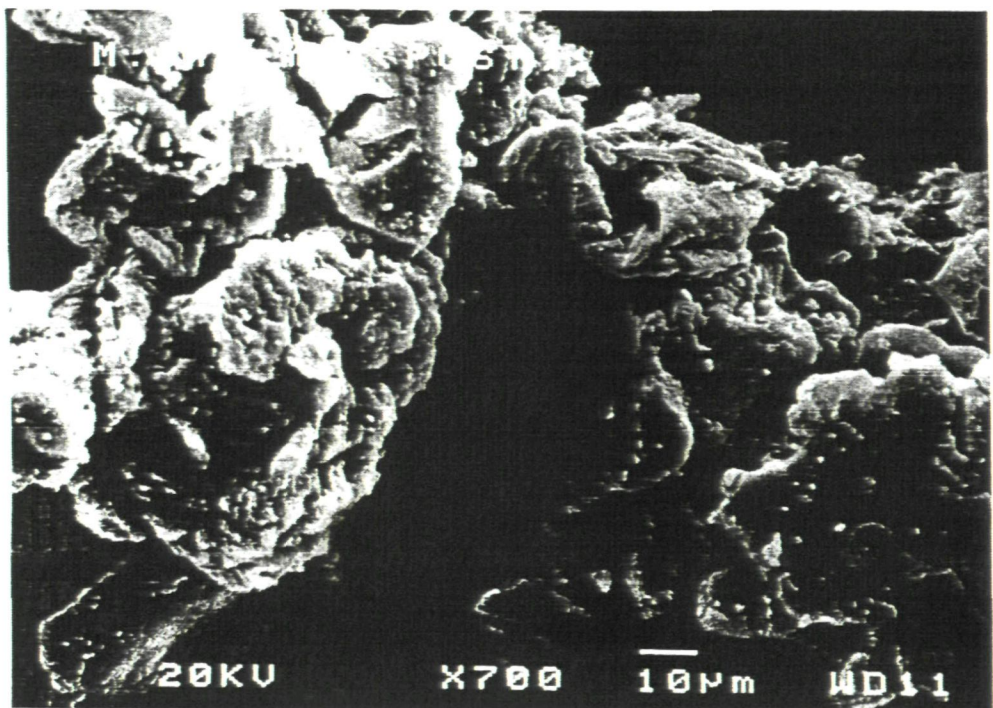
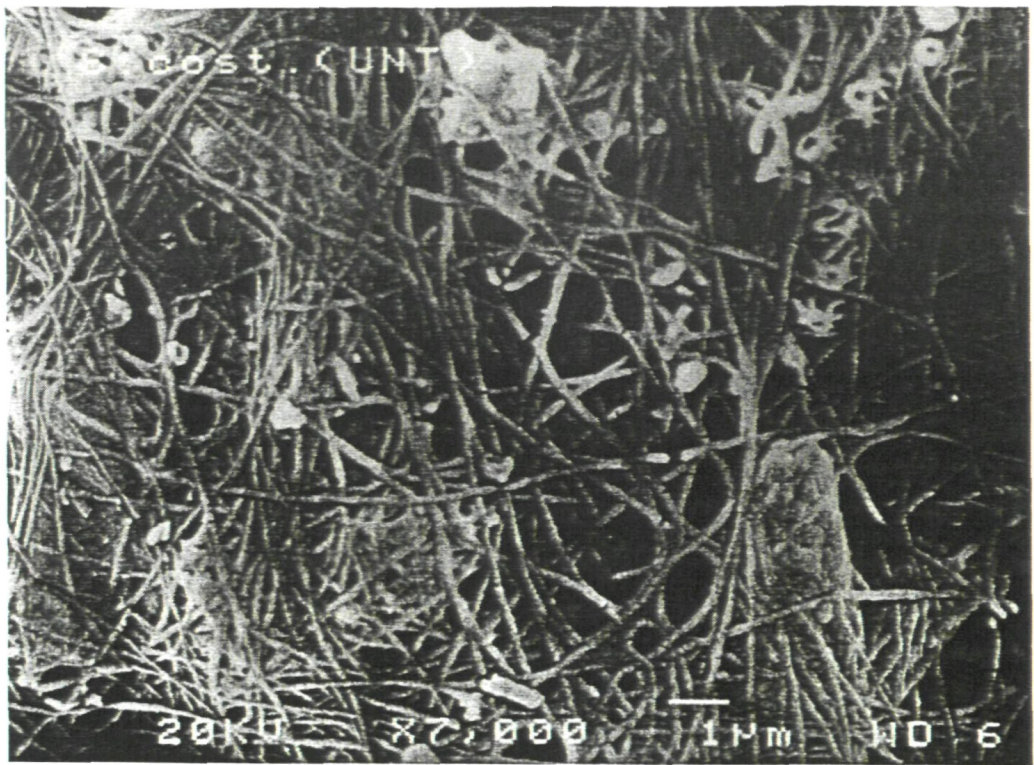


Figure 3.3. SEM micrographs of *M. thermoautotrophicum*. (a) Untreated (b) IOM.

Untreated *Skeletonema costatum* appeared as cross-linked filamentous material when viewed using a SEM (Figure 3.4a). Following sequential isolation, IOM isolated from *S. costatum* (Figure 3.4b) had lost its generally recognisable morphology although some remnants of the original filaments were still evident.

(a)



(b)

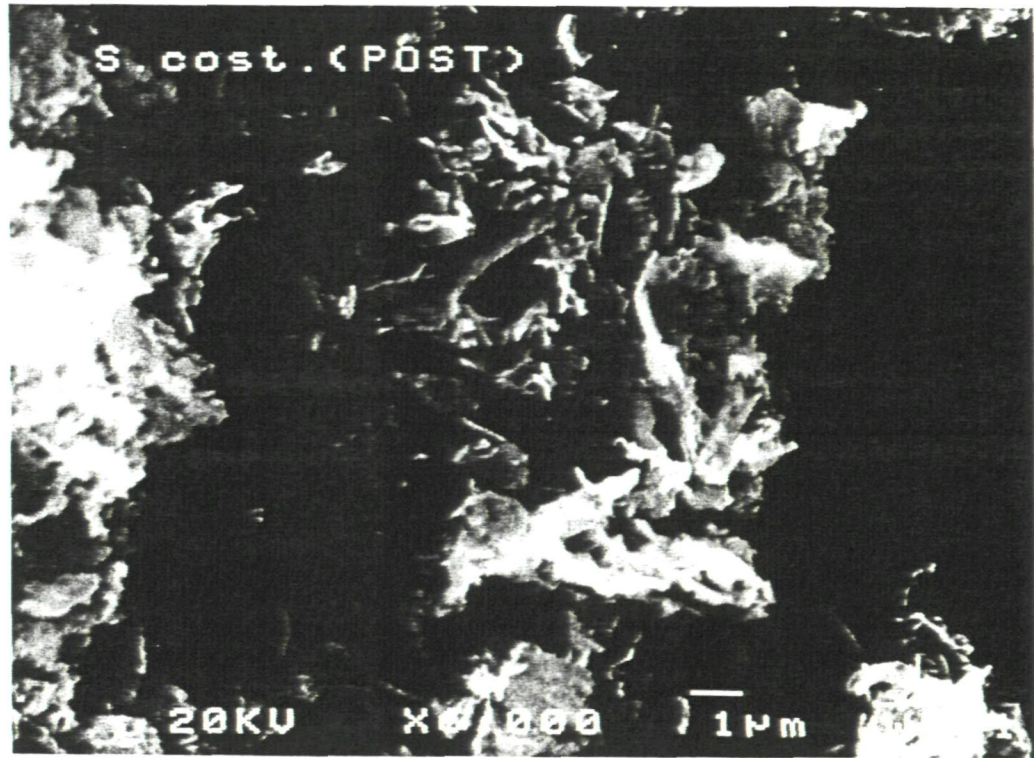


Figure 3.4. SEM micrographs of *S. Costatum*. (a) Untreated (b) IOM.

Individual cells of the large pennate alga could be clearly observed in the untreated sample of *Haslea ostrearia* (Figure 3.5a), typical of this organism (e.g. Round *et al.*, 1990). Obvious remnants of the central ribs of *H. ostrearia* remained after the sequential isolation of IOM from this alga (Figure 3.5b).

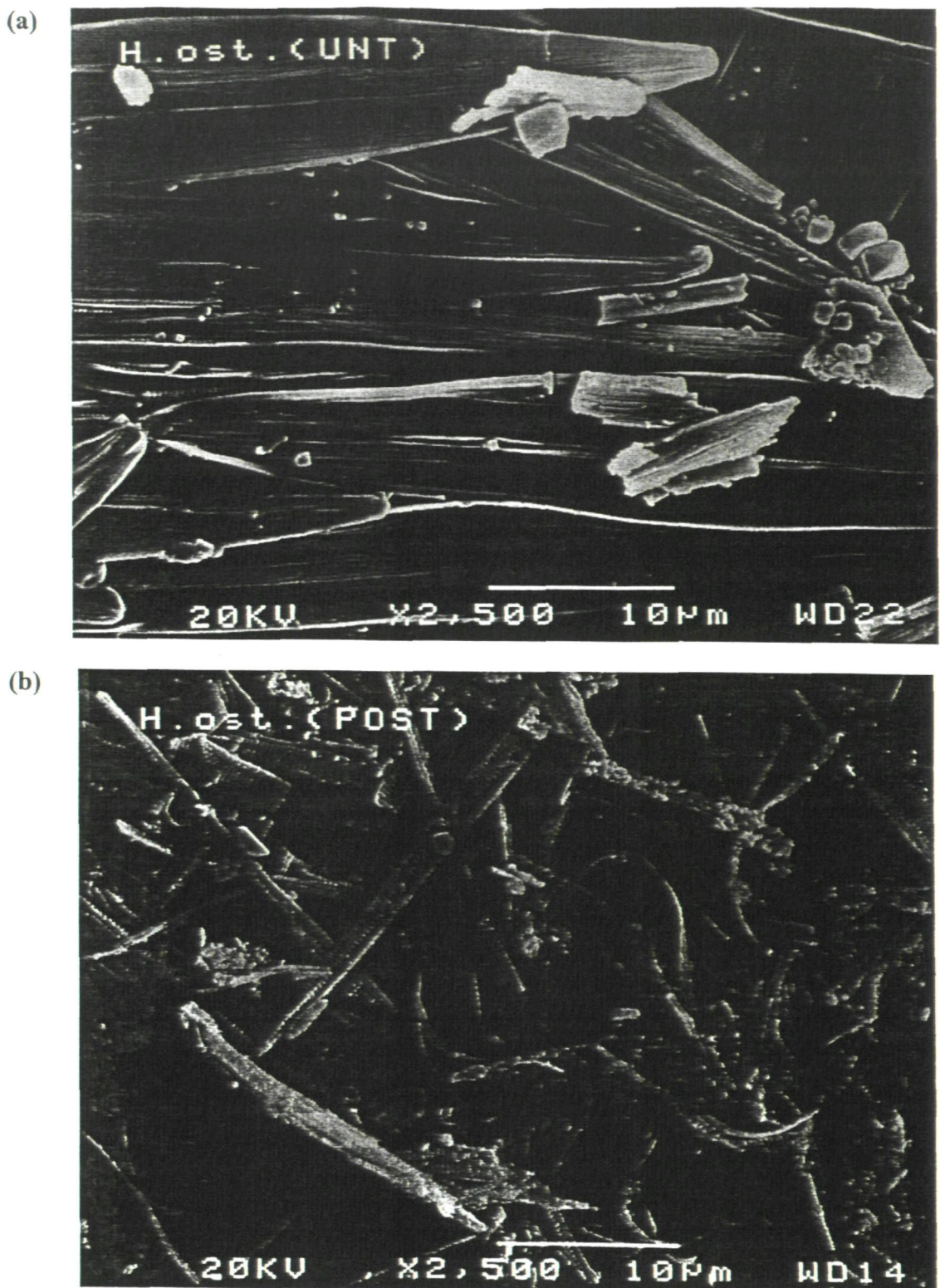


Figure 3.5. SEM micrographs of *H. ostrearia*. (a) Untreated (b) IOM.

The use of SEM has clearly demonstrated that morphological features of all samples were significantly altered during the sequential isolation of IOM. With the exception of IOM isolated from *H. ostrearia*, which comprised well-defined remnants of the untreated alga,

IOM from all other sedimentary and biotic samples appeared somewhat amorphous following its sequential isolation.

3.3.2. Elemental analysis

Carbon, hydrogen and nitrogen content (CHN) was determined in triplicate from untreated sediments from Rostherne Mere and from the respective residual material obtained following each isolation stage (Tables 3.1 and 3.2). Not unexpectedly, the sedimentary IOM was relatively enriched in CHN (49 – 62 % dry weight) compared to the original sample (16 – 19 % dry weight), which contained mineral matter as a major component (28 – 47 % dry weight, Section 2.4.2.6).

Table 3.1. Elemental carbon, hydrogen and nitrogen content of Rostherne Mere sediment (6 - 7 cmbswi) following each stage of the sequential isolation procedure.

Stage in sequential isolation procedure	% C		% H		% N	
	mean	(σ)	mean	(σ)	mean	(σ)
original sample	13.73	(0.36)	1.70	(0.05)	0.99	(0.05)
aqueous extracted	nd	(nd)	nd	(nd)	nd	(nd)
free lipid extracted*	13.58	(0.52)	1.67	(0.06)	0.97	(0.05)
protein extracted	12.41	(0.33)	1.13	(0.04)	0.32	(0.01)
carbohydrate extracted	13.75	(0.75)	1.22	(0.06)	0.33	(0.03)
bound lipid extracted	16.92	(0.60)	1.42	(0.05)	0.42	(0.02)
mineral extracted IOM	44.45	(0.71)	2.98	(0.08)	1.42	(0.03)

* Difference between untreated sample and free lipid extracted residue accounts for 'free lipid' and 'aqueous soluble' extracts; nd - not determined.

Table 3.2. Elemental carbon, hydrogen and nitrogen content of Rostherne Mere sediment (94 - 95 cmbswi) following each stage of the sequential isolation procedure.

Stage in sequential isolation procedure	%C		%H		%N	
	mean	(σ)	mean	(σ)	mean	(σ)
original sample	15.80	(0.17)	2.12	(0.03)	1.05	(0.02)
aqueous extracted	15.64	(0.13)	1.96	(0.09)	0.99	(0.01)
free lipid extracted	14.21	(0.61)	1.91	(0.06)	0.97	(0.04)
protein extracted	13.74	(0.54)	1.52	(0.04)	0.39	(0.01)
carbohydrate extracted	15.44	(0.45)	1.62	(0.03)	0.38	(0.01)
bound lipid extracted	14.57	(0.25)	1.46	(0.04)	0.34	(0.01)
mineral extracted IOM	55.91	(0.38)	4.22	(0.04)	1.79	(0.01)

CHN results were re-calculated to account for mass changes between residues following each stage of the sequential isolation procedure and related back to the respective total elemental contents in the original sample (Figure 3.6). The 'protein' removal stage extracted the largest portion of carbon, hydrogen and nitrogen from both sediment samples.

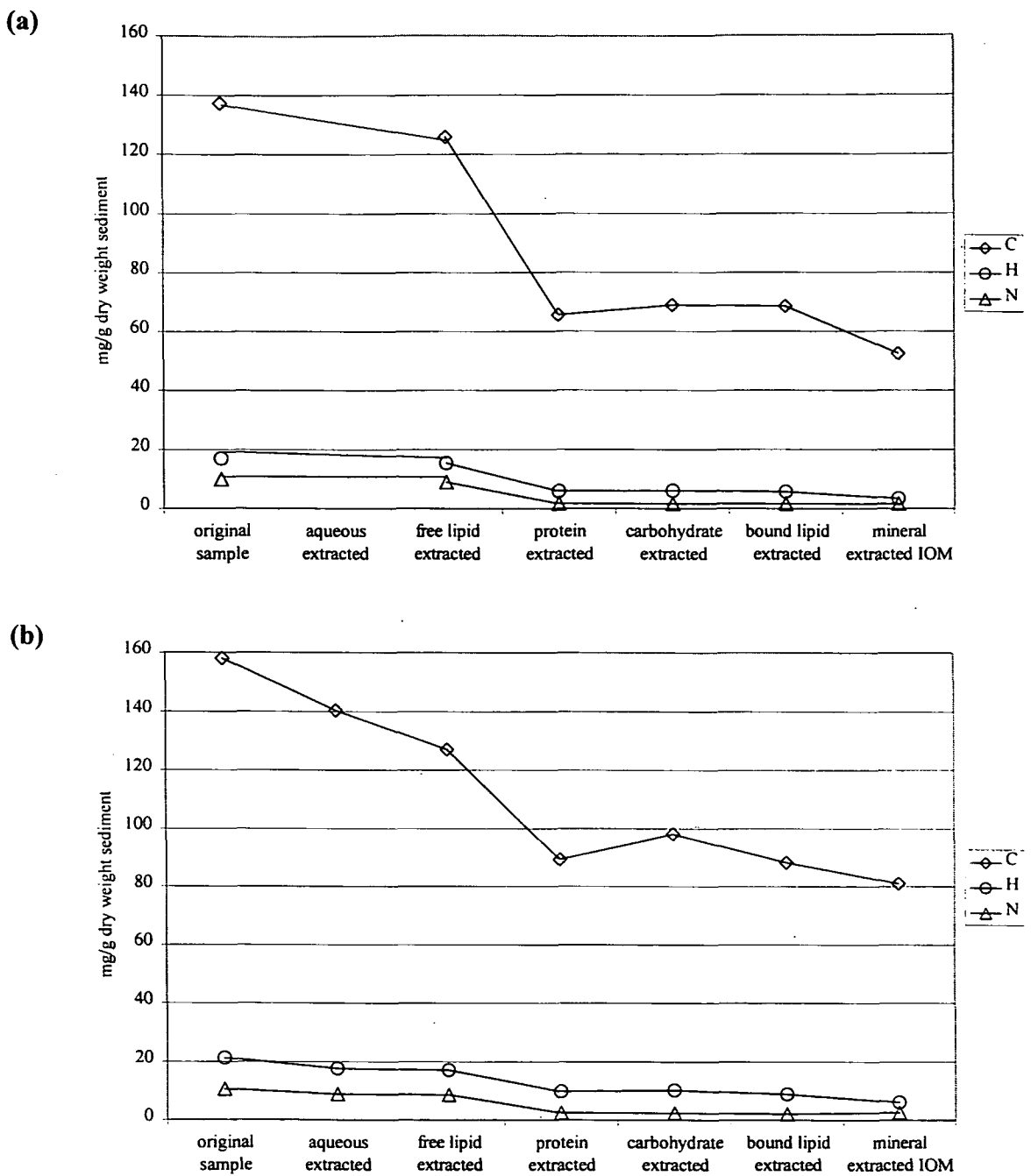


Figure 3.6. Change in CHN content (mg g^{-1} dry weight sediment) in Rostherne Mere sediments following each isolation stage. (a) 6 - 7 cmbswi (b) 94 - 95 cmbswi.

Elemental ratios (H/C, 0.12 and 0.13 and C/N, 14 and 15, for 6 - 7 and 94 - 95 cmbswi, respectively) of the untreated sediments were in general agreement with those reported for the first 0 - 35 cm of sediment from Rostherne Mere by Pratano (1995). The atomic H/C ratios were calculated at 1.5 and 1.6 for the 6 - 7 and 94 - 95 cmbswi untreated sediment samples, respectively (Figure 3.7). Sequential isolation resulted in a decrease of 45 % in

the atomic H/C ratio of both sediments, indicative of increased aromatisation or preferential removal of aliphatic material during the sequential isolation. Atomic N/C ratios decreased from almost 0.06 in the untreated sediments to 0.02 in the 'bound lipid' extracted residue. The slight increase in atomic N/C ratio determined for the IOMs was considered to result from residual nitrogen arising from the use of saturated ammonium borate during the 'mineral' dissolution stage of the sequential isolation procedure.

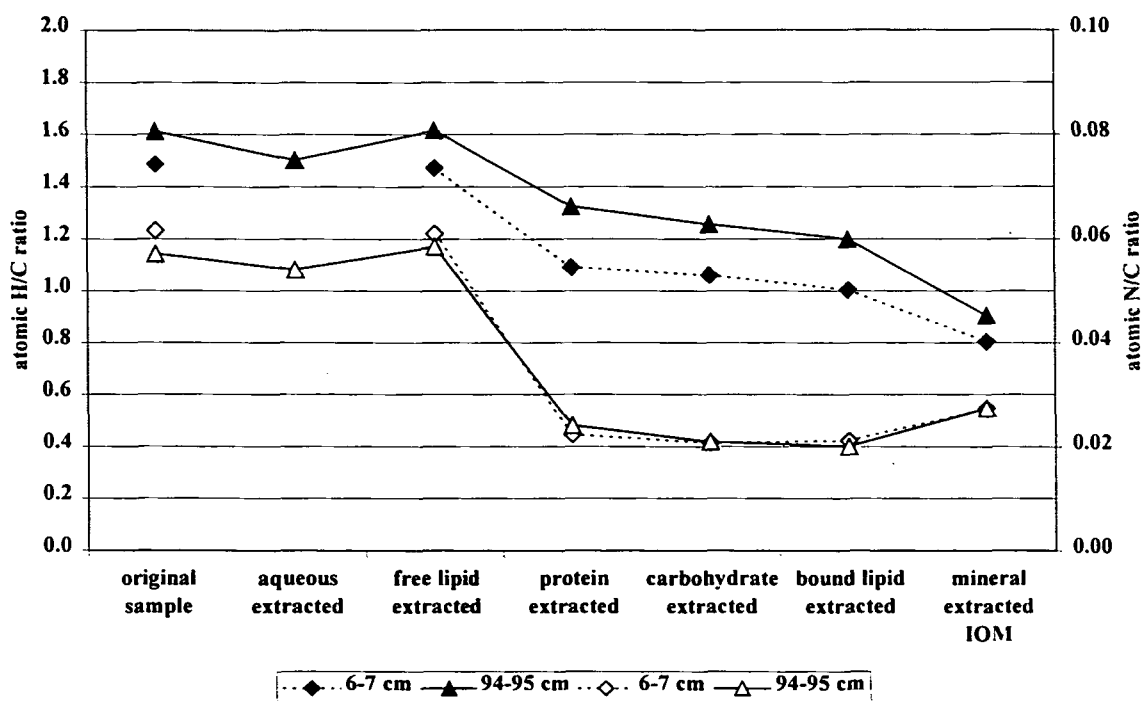


Figure 3.7. Change in sedimentary atomic H/C and N/C ratios after each sequential isolation stage (closed symbols H/C ratio, open symbols N/C ratio).

3.3.3. ¹³C Solid-state nuclear magnetic resonance spectroscopy (ss-NMR)

Quantitative solid-state ¹³C nuclear magnetic resonance (ss-NMR) spectra were obtained of the organic matter in untreated Rostherne sediments from 6 - 7 and 94 - 95 cmbswi and residual sedimentary IOM (Figures 2.23 and 2.24). Cross-polarisation magic-angle-spinning (CP-MAS) ¹³C NMR underestimated aromatic components by around 8 mole % (Snape, *pers. comm.*) so a single pulse excitation (SPE) experiment was carried out to allow for this difference in the IOM isolated from 94 - 95 cmbswi. Whilst there was little difference in the qualitative appearance of the spectra for untreated samples from both

depths (6 - 7 and 94 - 95 cm below sediment-water interface) and between IOM isolated from these samples, there were significant differences between untreated samples and IOM (Figures 3.8 - 3.10). The principal carbon types in untreated sediments resulted from cellulosic (60 - 100 ppm), aliphatic (lipid; 0 - 50 ppm) and aromatic (110- 167 ppm) carbons with lesser contributions from methoxy (50 - 60 ppm), carboxyl (167 - 190 ppm) and carbonyl (190 - 220 ppm) carbon (Table 2.6). In contrast, IOM obtained from these sediments was dominated by aromatic and aliphatic resonances whilst resonances owing to cellulosic material were virtually absent.

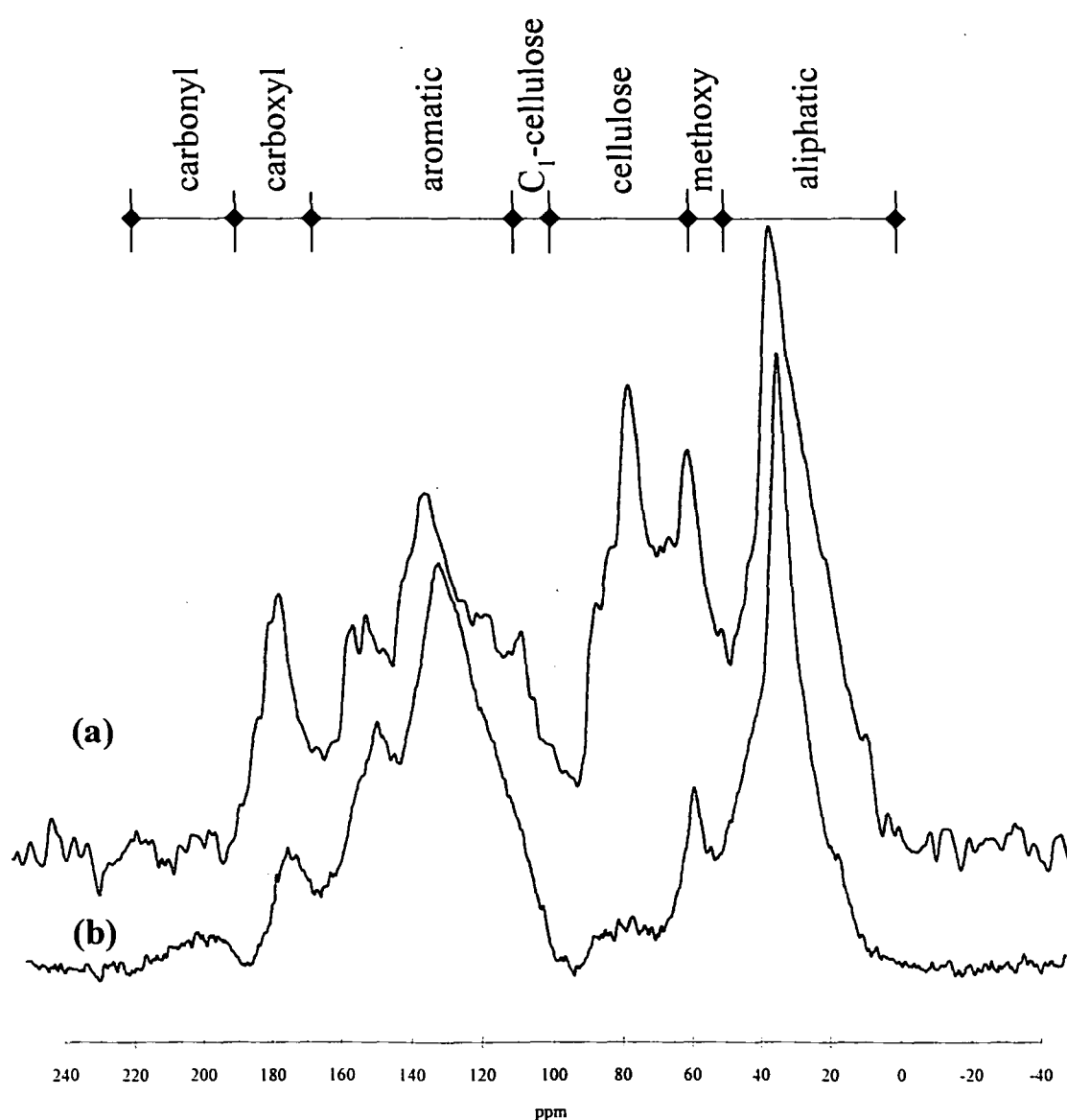


Figure 3.8. Solid-state CP-MAS ^{13}C NMR spectra of Rostherne Mere sediment from 6 - 7 cm below sediment-water interface. (a) Untreated (b) IOM.

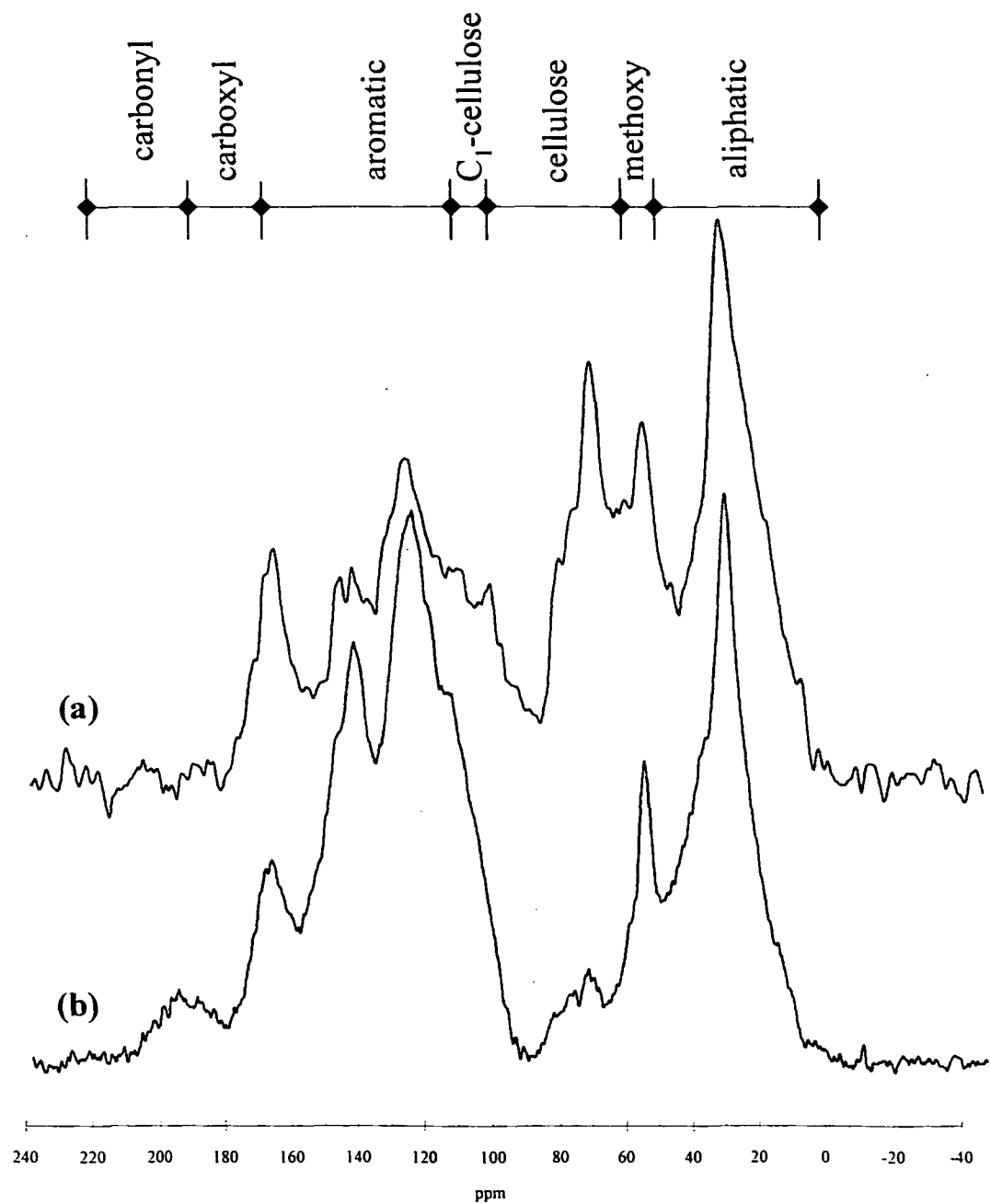


Figure 3.9. Solid-state CP-MAS ^{13}C NMR spectra of Rostherne Mere sediment from 94 - 95 cm below sediment-water interface. (a) Untreated (b) IOM.

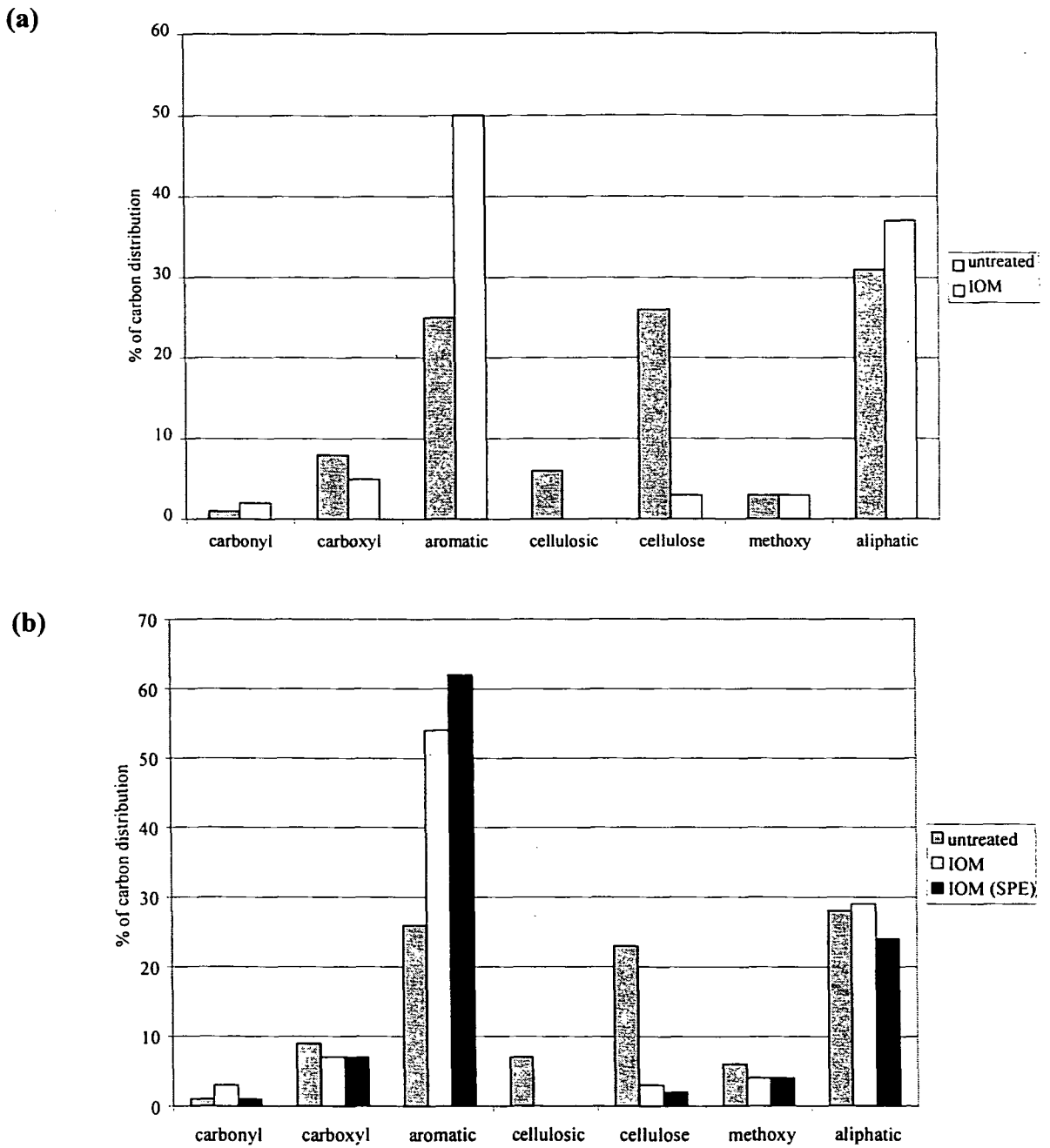


Figure 3.10. Summary of carbon distributions (%) from the CP-MAS and SPE ss-NMR ^{13}C spectra of Rostherne Mere sediments (a) 6 - 7 cmbswi and (b) 94 - 95 cmbswi.

The mass of carbon in each carbon environment in the untreated sediments was calculated using the elemental data (Section 3.32) and by equating the ss-NMR response to the total carbon present in the untreated samples. Similarly, the ss-NMR response for the IOMs was equated to the adjusted carbon content (Figure 3.11) and the differences between untreated samples and IOMs expressed as a percentage (Figure 3.12). The sequential isolation procedure appeared to have removed almost all of the cellulosic carbon and around half of the aliphatic, carboxyl and methoxy carbon.

Almost 25 % of the aromatic carbon was apparently removed from the 6 - 7 cm sample during the sequential isolation (Figure 3.12) whilst there was a net increase of between 7 % (CP-MAS) and 22 % (SPE) in aromatic carbon after sequential isolation of IOM from the 94 - 95 cm sample. Although CP-MAS probably underestimated the aromatic carbon component by around 8 %, this would not have affected comparison between CP-MAS data. In addition, the loss of aromaticity from the 6 - 7 cm IOM sample was not consistent with the decreased atomic H/C ratio reported in Section 3.3.2. The net increase in aromaticity for the 94 - 95 cm IOM sample may have been indicative of aromatisation during isolation, perhaps *via* artefactual melanoidin-type production. Changes in the relative proportion of each carbon environment in terms of the total carbon (TC) between the untreated samples and the IOM (Figure 3.12) revealed that the following were removed during the sequential isolation procedure; aliphatic (47 - 54 %), methoxy (62 - 66 %), rest of cellulose (93 - 96 %), C-1 cellulose (100%) and carboxyl (60 - 76 %). The apparent contradiction in results for carbonyl compounds for the 94 - 95 cm sample (54 % gain using CP-MAS compared to 49 % loss using SPE) sample may be due to difficulties in integrating the carbonyl fraction which only comprised 1% of the TC of the untreated sample. Because the relative distribution of carbon environments has been equated to the sum of the spectral peaks, minor variations may be induced in other carbon classes between the results from CP-MAS and SPE experiments.

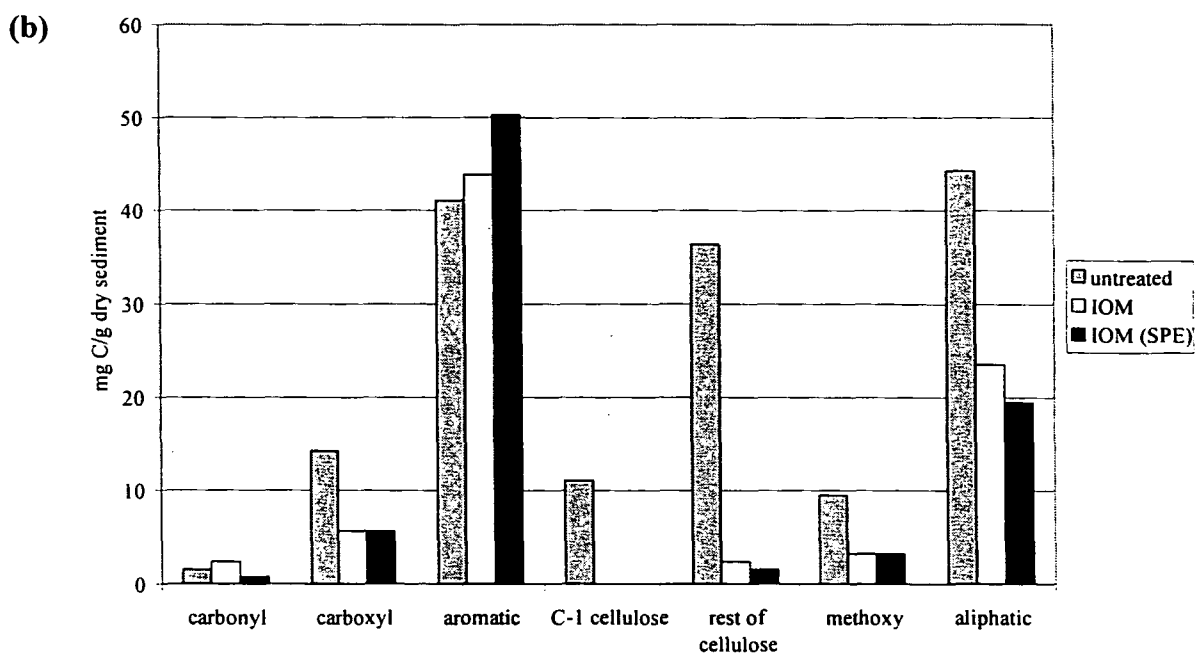
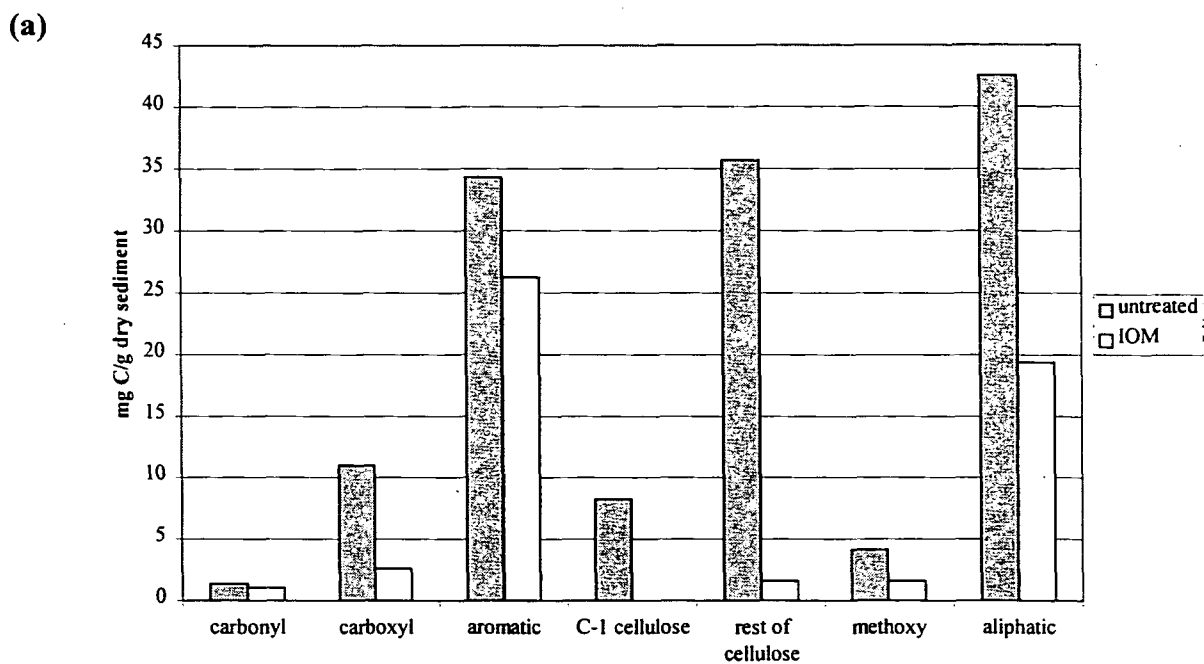


Figure 3.11. Change in carbon fractions following sequential isolation (mg C g^{-1} dry sediment). (a) 6 - 7 cm (b) 94 - 95 cm.

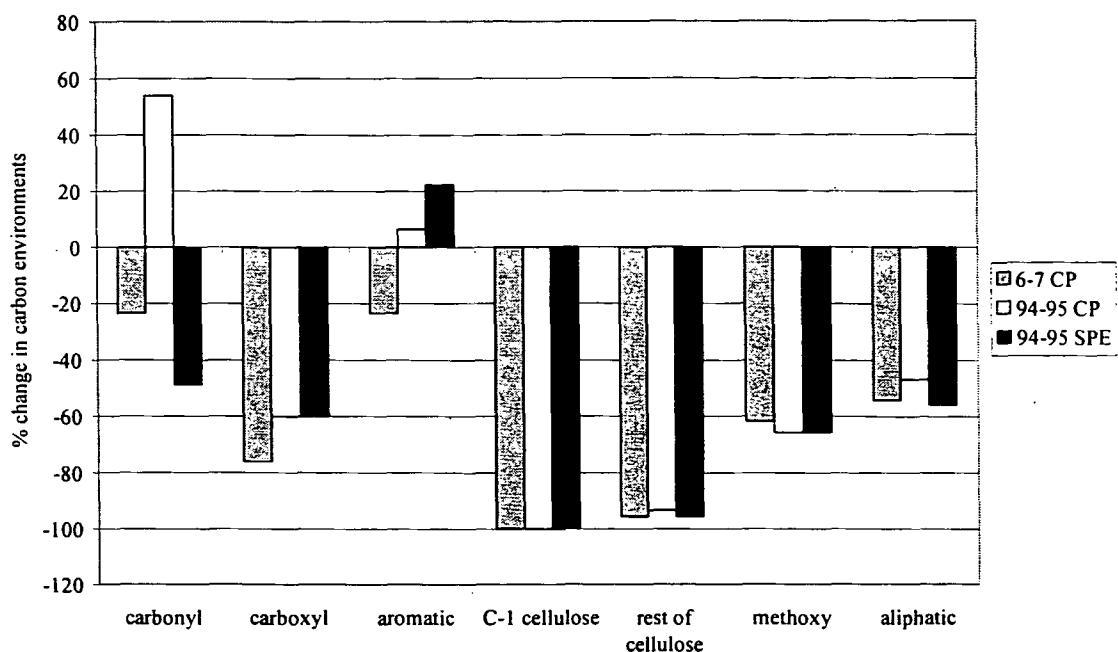


Figure 3.12. Percentage change in calculated mass of carbon environments between untreated Rostherne Mere sediments (6 - 7 and 94 - 95 cmbswi) and respective IOMs using ss-NMR CP-MAS and SPE experiments.

Solid-state ^{13}C NMR of freeze-dried untreated bacterium *M. jannaschii* (Figure 3.13) showed that the bulk of the carbon was present in aliphatic (methyl, 0 - 50 ppm and methylenic, 50 - 60 ppm), cellulose (60 - 95 ppm) and carboxyl (167 - 190 ppm) environments. There were minor contributions from C-1 cellulose (95 - 110 ppm) and aromatic (110 - 167 ppm) carbons. Insufficient IOM material was available for ^{13}C ss-NMR analysis.

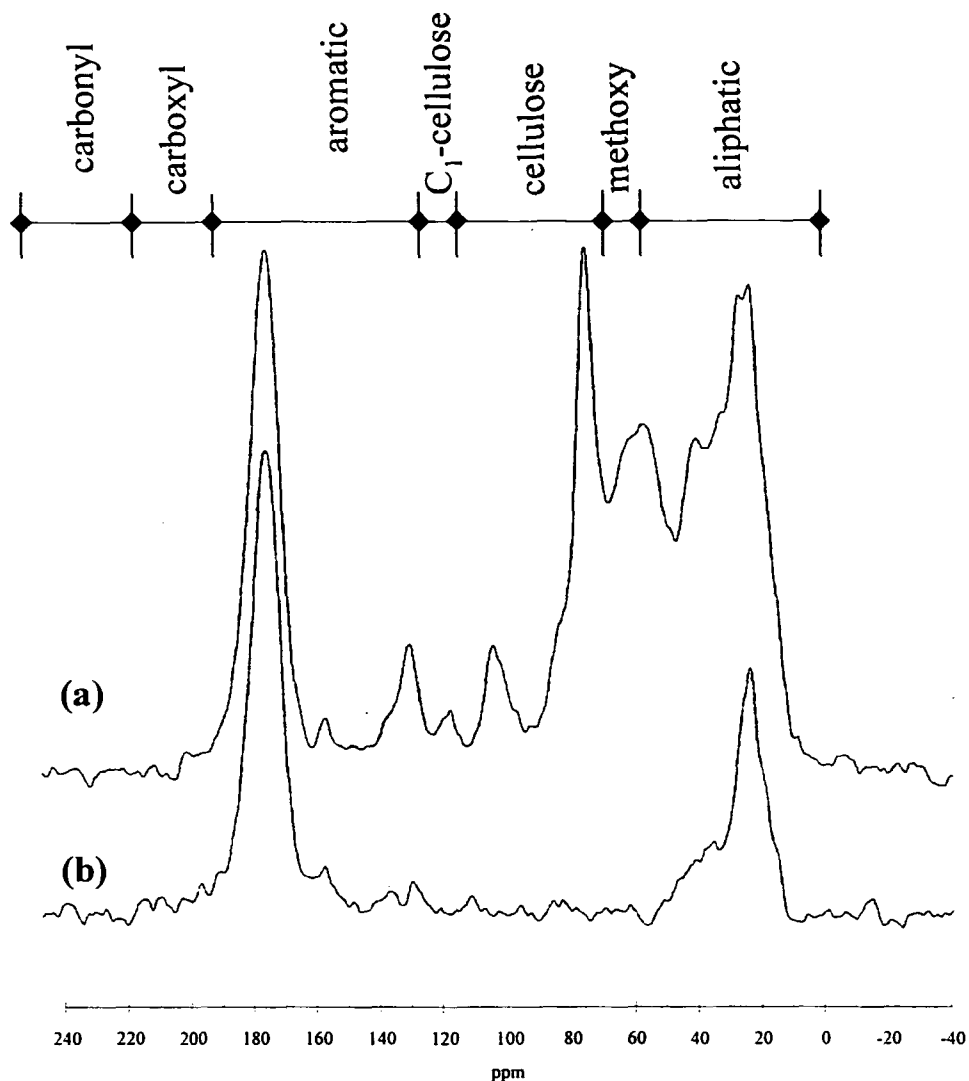


Figure 3.13. Solid-state NMR spectra of untreated *M. jannaschii* bacterial necromass.
(a) CP 3 ms (c) CPDD 3 ms.

3.3.4. Infrared Spectroscopy

There were marked similarities between the IR spectra of untreated Rostherne Mere sediments (6 – 7 and 94 – 95 cmbswi, Figures 3.14a and 3.15a, respectively) and between the IR spectra of IOM isolated from the same sediments (6 – 7 and 94 – 95 cmbswi, Figures 3.14b and 3.15b, respectively). In contrast, the IR spectra of untreated sediments were distinctly different to those of isolated IOM. Untreated sediment spectra were dominated by a broad absorption band with a maximum at around 3420 cm^{-1} and a strong band between 1100 and 1000 cm^{-1} . The former is indicative of OH stretching vibrations and the latter due to alcohol OH stretching. A strong broad absorbance peak in the

shallower sediment centred at 1425 cm^{-1} was the main difference between the spectra of the untreated sediments. It is unlikely that this absorbance peak is due to ionic carbonate (CO_3^-) because it is also present in both spectra of the IOM obtained after mineral dissolution. Another minor difference was that the maxima of the broad peak between $1100 - 1000\text{ cm}^{-1}$ shifted from 1033 cm^{-1} in the shallower sediment to 1094 cm^{-1} in the deeper sediment. In addition, a sharp band at 873 cm^{-1} , possibly due to the out-of-plane isolated aromatic CH deformation vibration, was present in the 6 – 7 cmbswi sample.

IR spectra of IOM isolated from Rostherne Mere sediments (6 – 7 and 94 – 95 cmbswi, Figures 3.14b and 3.15b, respectively) were characterised by a very broad OH stretching band centred around $3300 - 3000\text{ cm}^{-1}$, a C=O (carbonyl and/or carboxyl) stretching band at 1706 cm^{-1} , alkyl CH_2 stretching bands at 2925 and 2853 cm^{-1} , C=O (quinone bonded to acidic OH) or C=C (olefin or aromatic ring) stretching band at 1610 cm^{-1} , unidentified bands at 1506 and 1423 cm^{-1} , strong bands centred around 1210 cm^{-1} , a broad weak unidentified band at 625 cm^{-1} , and a sharp band around 425 cm^{-1} which is probably due to the presence of pyrite. As shown by solid-state ^{13}C NMR spectroscopy, the IOM from these substrates was relatively enriched in aromatic carbon (Section 3.3.3). The strong band at 1610 cm^{-1} is more likely to be due to aromatic carbon-carbon double bonds than quinones linked to acidic OH or olefinic double bonds. The broad absorbance ‘hump’ between 3600 and 2000 cm^{-1} is somewhat better resolved in the deeper sediment. Aside from this broad ‘hump’ the IOM spectra exhibit a marked similarity between 1800 and 500 cm^{-1} .

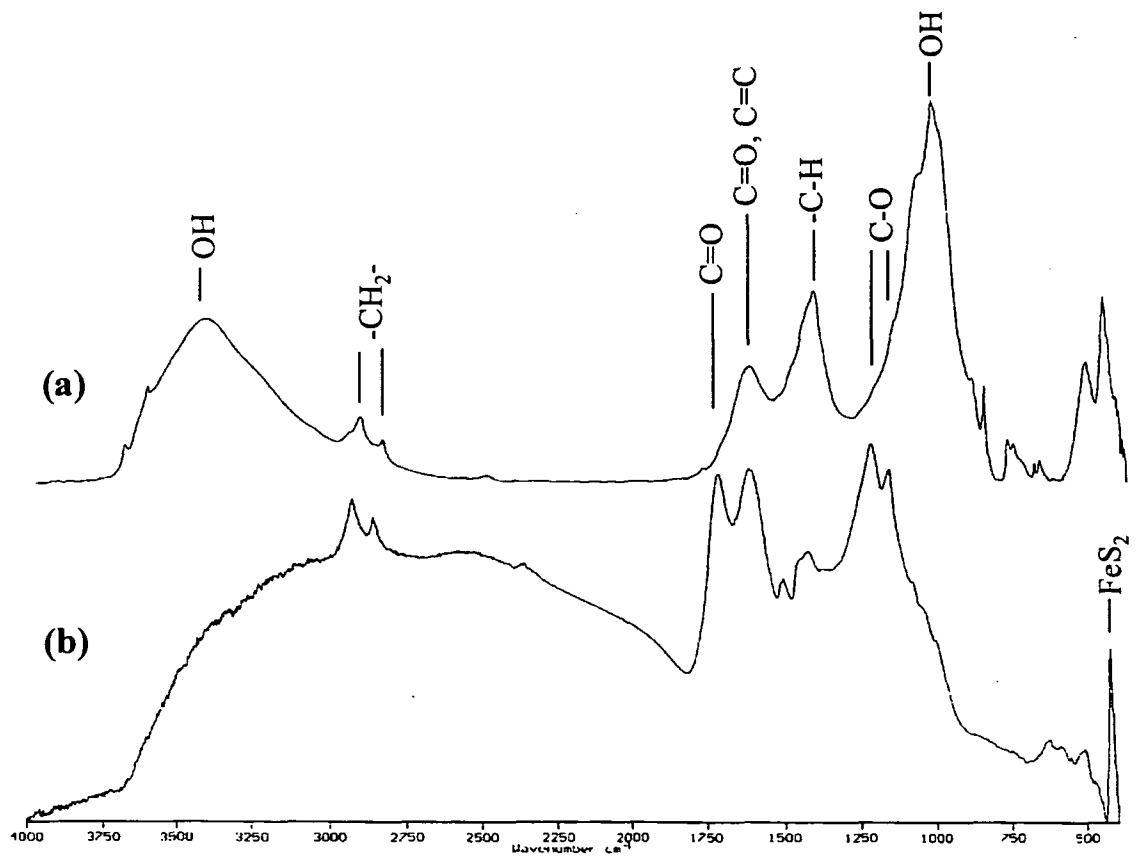


Figure 3.14. Infrared absorbance spectra of Rostherne Mere sediment, 6 – 7 cmbswi. (a) Untreated (b) IOM.

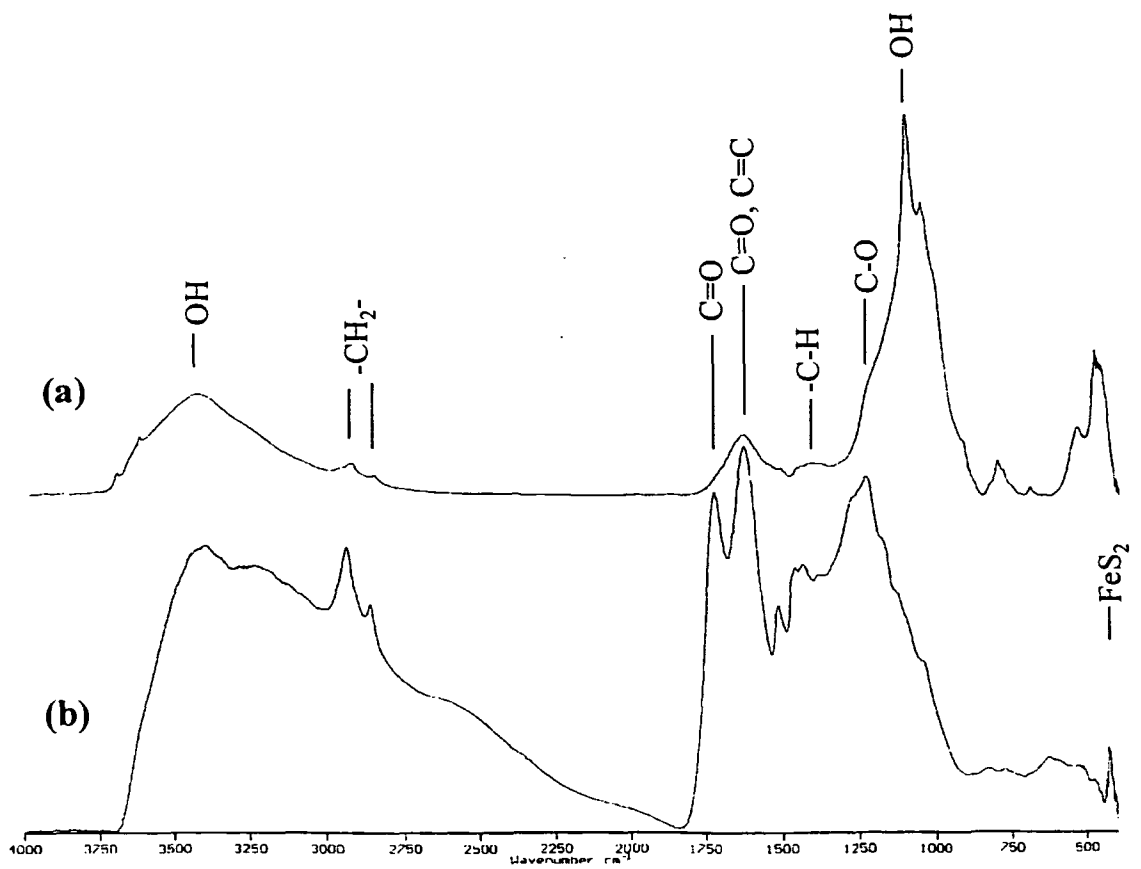


Figure 3.15. Infrared absorbance spectra of Rostherne Mere sediment, 94 – 95 cmbswi. (a) Untreated (b) IOM.

IOM isolated from Rostherne Mere sediment (5 – 6 cmbswi) was extracted with solvent (3 x 10 ml, DCM) in order to assess whether any solvent extractable material remained following the sequential isolation procedure and IR spectra were recorded before and after the extraction (Figure 3.16). There was little difference between the general shape of the spectra. Assignments were the same for both spectra [broad band with maxima at 3406 cm^{-1} , OH stretching vibration; broad maxima at 3200 cm^{-1} ; broadening below 3000 cm^{-1} , carboxylic acids; 2922 and 2851 cm^{-1} , alkyl CH_2 asymmetric and symmetric stretching; 1709 cm^{-1} , C=O stretching of carbonyl (aldehyde/ketone) and/or carboxyl (acid/ester) groups; 1620 cm^{-1} , C=O stretching of quinones bridged to acidic hydroxyls or C=C stretching of olefins, aromatic rings or polyaromatic layers; $1461 - 1415\text{ cm}^{-1}$, CH_2 and/or CH_3 asymmetric bending; 1212 and 1154 cm^{-1} , C-C aliphatic and/or aromatic skeletal vibrations, C-O stretching of ether and/or alcohol groups and/or C-OH deformation of alcohol groups; 627 , 555 and 504 cm^{-1} , unassigned; 421 cm^{-1} , pyrite].

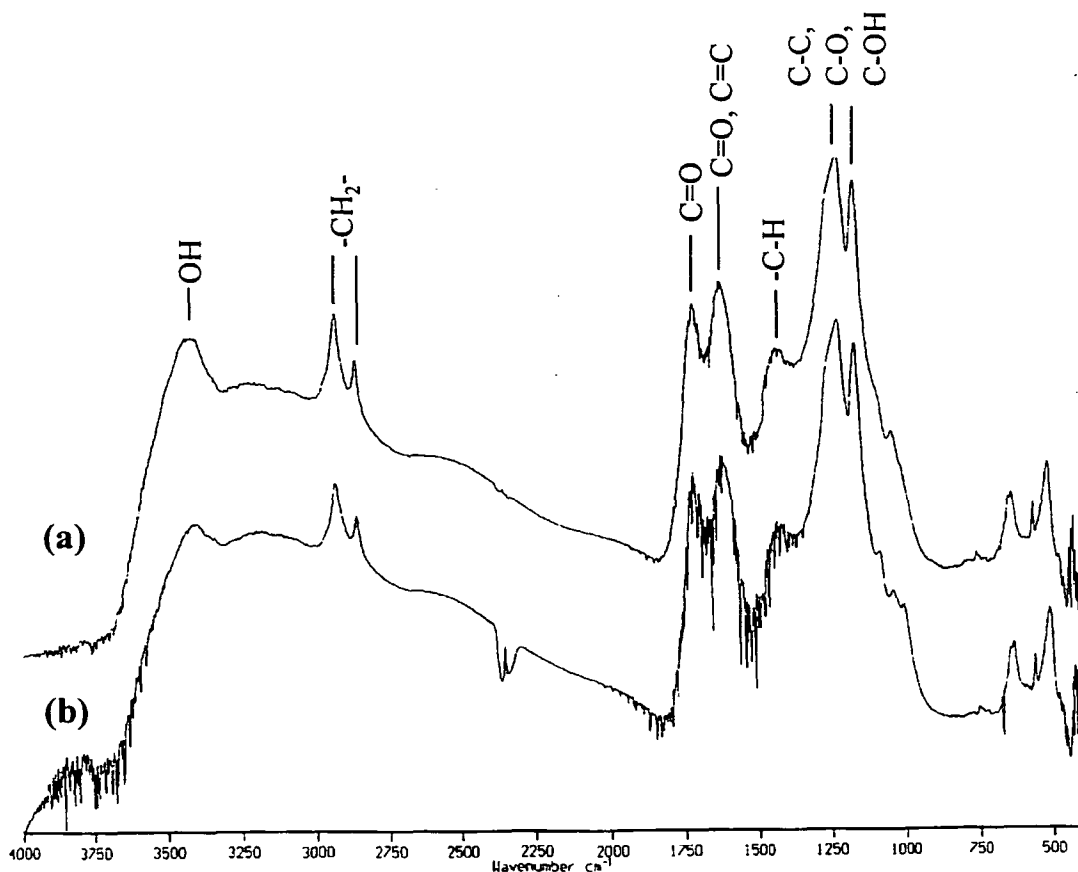


Figure 3.16. Infrared absorbance spectra of Rostherne Mere sediment (5 – 6 cmbswi). (a) IOM (b) DCM extracted IOM.

The IR spectrum of the untreated Kimmeridge Clay (Figure 3.17a) was dominated by a shouldered strong absorbance at 1031 cm^{-1} typical of alcohol OH, alkyl CH_2 and/or methyl asymmetric bending absorption at 1457 cm^{-1} , a weak alkyl CH_2 stretching band at 2926 cm^{-1} , a broad OH stretching band centred at 3421 cm^{-1} , a sharp band at 874 cm^{-1} possibly owing to aromatic CH out-of-plane deformation vibration. In addition, there were unassigned absorbance peaks at 3620 , 798 , 537 and 470 cm^{-1} . The IR spectrum of IOM isolated from Kimmeridge Clay (Figure 3.17b) had a similar shape to that of the untreated material although the centre of the strong absorbance at 1031 cm^{-1} in the untreated sample had shifted to 1093 cm^{-1} in the IOM (present as a shoulder in the untreated sample). Furthermore, the relative absorbance intensity of the different peaks had also changed. The alkyl CH_2 stretching bands at 2925 and 2853 cm^{-1} had become more intense, as had the $\text{C}=\text{O}$ stretching band at 1709 cm^{-1} , the $\text{C}=\text{C}$ stretching band at 1620 cm^{-1} and the two unassigned bands at 798 cm^{-1} .

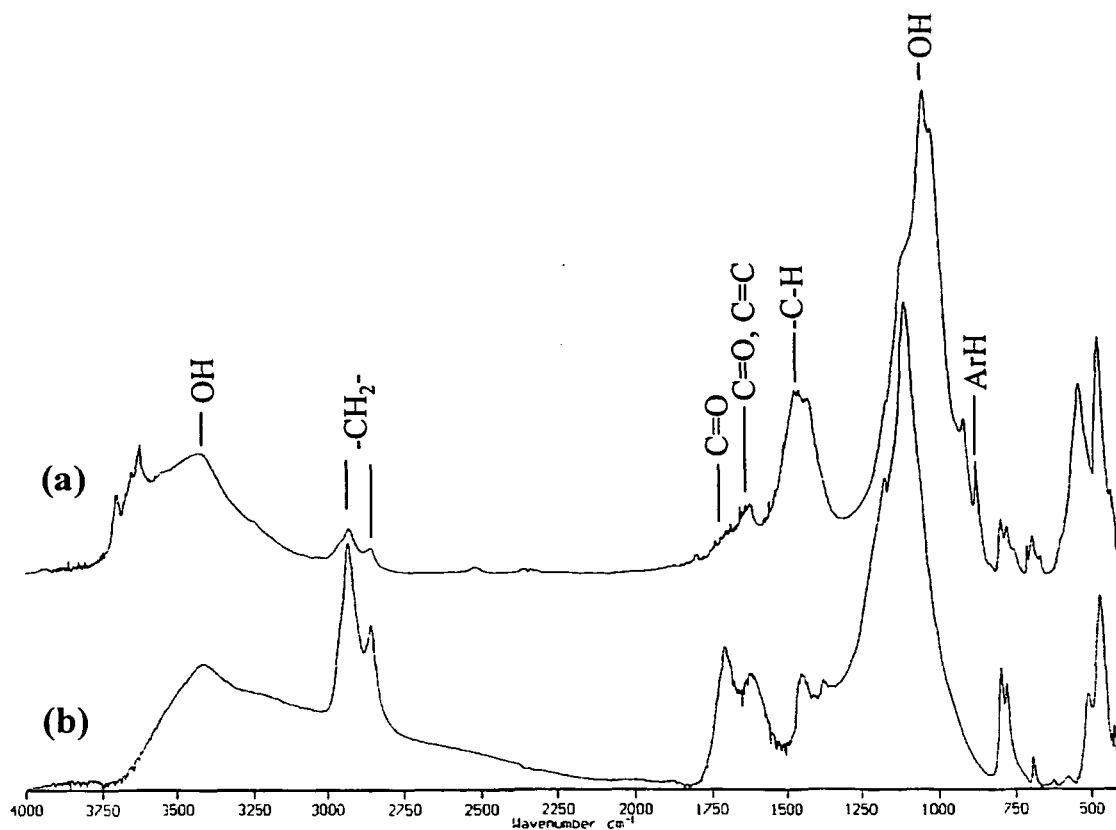


Figure 3.17. Infrared spectra of Kimmeridge Clay. (a) Untreated (b) IOM.

A broad OH stretching band centred at 3319 cm^{-1} was evident in the IR spectrum of untreated *M. jannaschii* (Figure 3.18a). In addition, there were poorly resolved alkyl CH_3 and CH_2 stretching absorbance bands at 2962 and 2928 cm^{-1} , respectively, and $\text{C}=\text{O}$ and/or $\text{C}=\text{C}$ stretching at 1656 cm^{-1} , CH deformation of di- or tri- methyl groups at 1397 cm^{-1} , and four absorption bands between 1240 and 1036 cm^{-1} that may be attributable to single bonded carbon linked to carbon, nitrogen or oxygen. The strong band at 1542 cm^{-1} , the weak absorbance bands at 2360 and 2340 cm^{-1} , and the broad but relatively weak 'hump' between 750 and 500 cm^{-1} were not assigned. The IR spectrum of IOM isolated from *M. jannaschii* (Figure 3.18b) was similar to that of the untreated material and featured a strong reasonably well resolved OH stretching band at 3422 cm^{-1} , alkyl stretching bands (CH_3 and CH_2 at 2962 and 2928 cm^{-1} , respectively), unassigned bands at 2360 and 2340 cm^{-1} , and a broad poorly resolved region between 750 and 500 cm^{-1} . Between 1800 and 1000 cm^{-1} absorption bands were less well resolved in the IOM spectrum with the most intense absorption occurring at 1620 , 1377 and 1219 cm^{-1} . The band at 1620 cm^{-1} may be ascribable to aromatic or olefinic $\text{C}=\text{C}$ stretching whilst that at 1377 cm^{-1} may be due to symmetric bending of methyl groups. A weak but sharp band at 667 cm^{-1} was present in both the untreated bacteria and the IOM but remains unassigned.

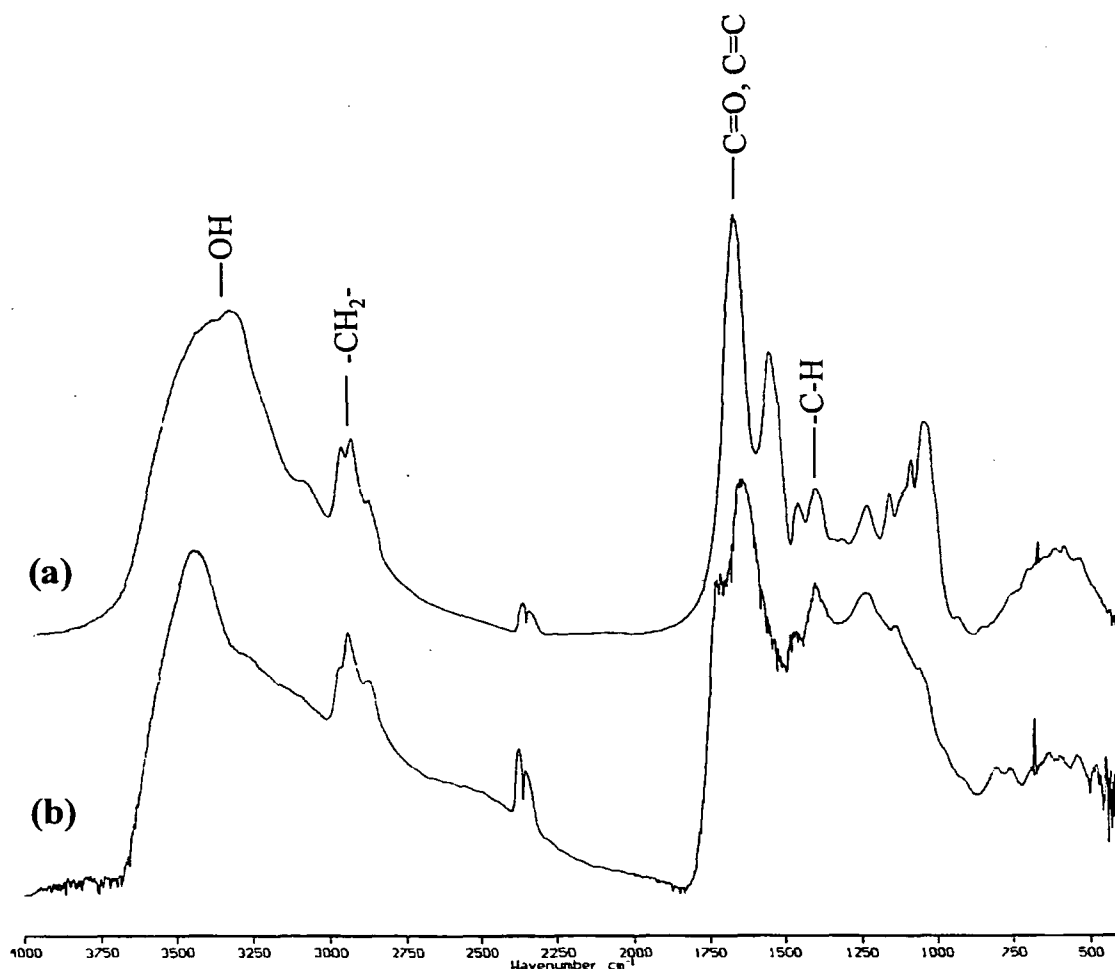


Figure 3.18. Infrared spectra of *M. jannaschii*. (a) Untreated (b) IOM.

The IR spectrum of untreated *M. thermoautotrophicum* (Figure 3.19a) was comparable to that of untreated *M. jannaschii* (Figure 2.31a) and the same assignments apply. Similarly, the IR spectrum of IOM isolated from *M. thermoautotrophicum* (Figure 3.19b) was principally the same as that of IOM isolated from *M. jannaschii* (Figure 3.18b).

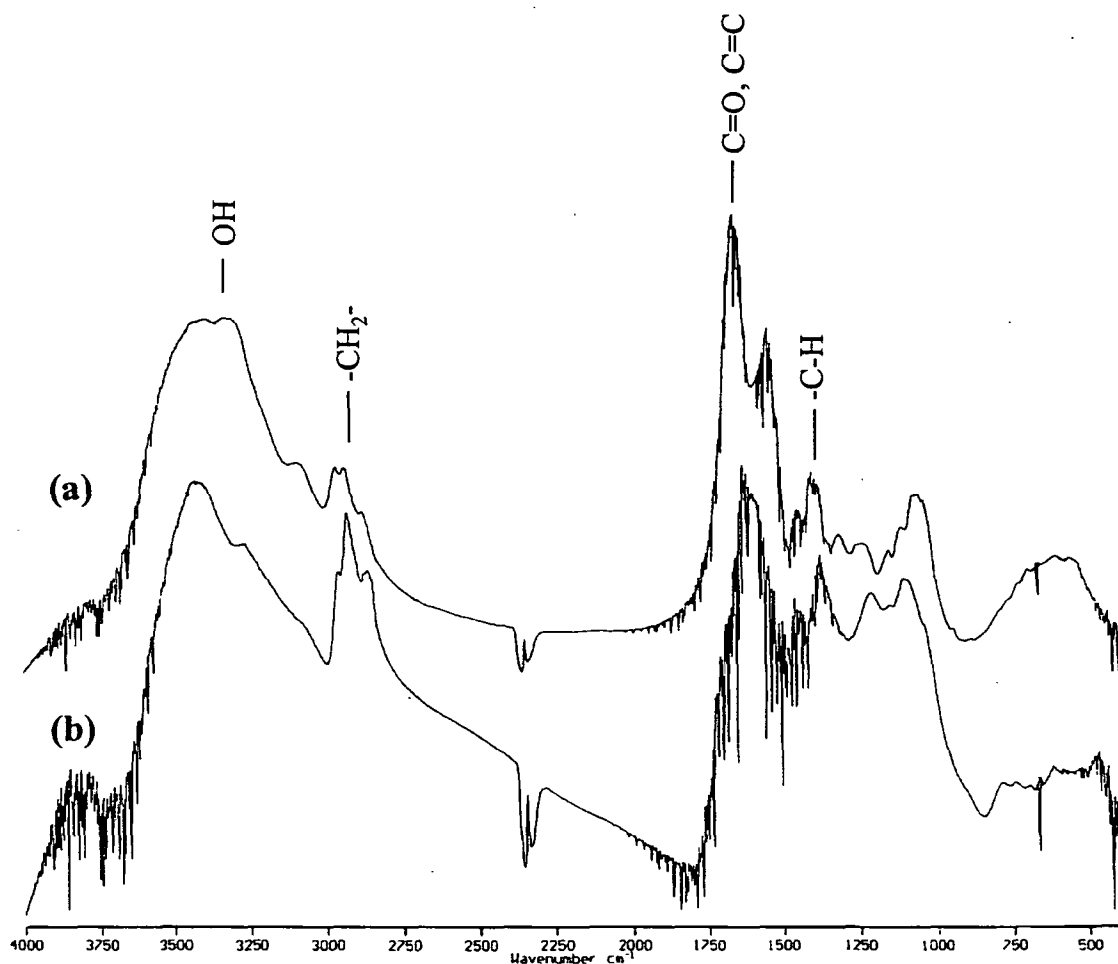


Figure 3.19. Infrared spectra of *M. thermoautotrophicum*. (a) Untreated (b) IOM.

The IR spectrum of untreated *S. costatum* (Figure 3.20a) was characterised by a broad OH stretching absorption band centred at 3427 cm^{-1} , methylene stretching bands at 2925 and 2859 cm^{-1} , an unassigned band at 2521 cm^{-1} , a weak absorption band at 1789 cm^{-1} (unassigned), a broad band at 1477 cm^{-1} (possibly CH_2 or CH_3 bending) with a shoulder at 1632 cm^{-1} (aromatic or olefinic $\text{C}=\text{C}$, or acidic OH bonded $\text{C}=\text{O}$), a band at 1080 cm^{-1} (possibly alcohol OH stretching or C-C, C-N or C-O groups), a strong sharp band at 855 cm^{-1} (possibly due to aromatic CH deformation), a narrow band at 708 cm^{-1} and a weak broad band centred at 596 cm^{-1} (unassigned). IOM isolated from *S. costatum* had a distinctly different IR spectrum (Figure 3.20b) to that of the untreated alga, dominated by a strong broad absorption band centred at 1088 cm^{-1} whilst the broad methyl/methylene band observed in the untreated sample was absent from the IOM spectrum. Other absorption

bands seen in the IOM spectrum were the broad OH stretching band at 3436 cm^{-1} , weak alkyl bands around 2929 cm^{-1} and unassigned absorption bands at 960 and 798 cm^{-1} .

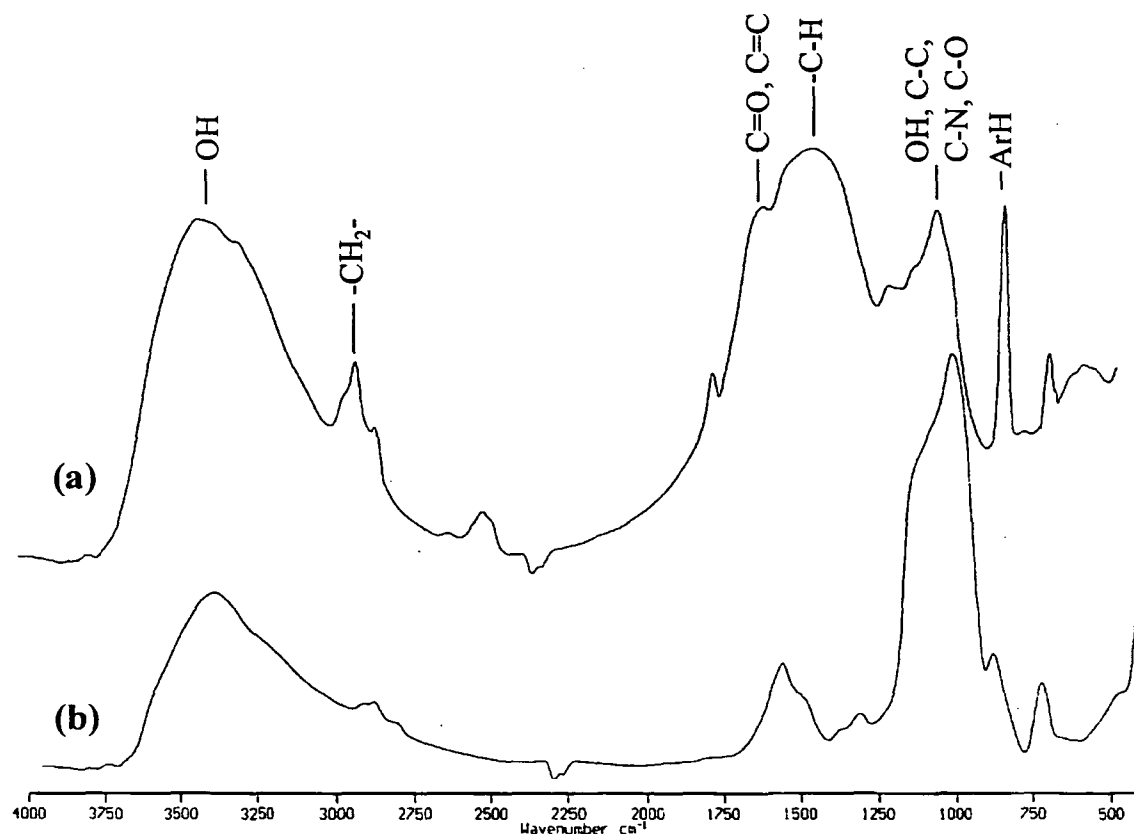


Figure 3.20. Infrared absorbance spectra of *S. Costatum*. (a) Untreated (b) IOM.

The IR spectrum of untreated *H. ostrearia* (Figure 3.21a) contained a broad OH stretching band centred at 3398 cm^{-1} , alkyl CH_2 and CH_3 stretching bands around 2928 cm^{-1} , an olefinic $\text{C}=\text{C}$ stretching band at 1658 cm^{-1} , broad poorly resolved bands around 1385 cm^{-1} (possibly CH deformation of di- and tri-methyl substituted carbons), a strong absorbance band at 1090 cm^{-1} (OH stretching or absorption by C-C, C-N or C-O groups) with a broad shoulder to 1300 cm^{-1} (unassigned), and unassigned absorption bands at 798 and 463 cm^{-1} . In contrast, the spectrum of IOM obtained from *H. ostrearia* (Figure 3.21b) was dominated by an intense band at around 1093 cm^{-1} with poorly resolved shoulders at higher and lower wave numbers. Otherwise, the IOM spectrum contained the same absorption bands as the untreated alga, albeit at relatively lower intensities, with the exception of the band at 1547 cm^{-1} which was absent from the IOM spectrum.

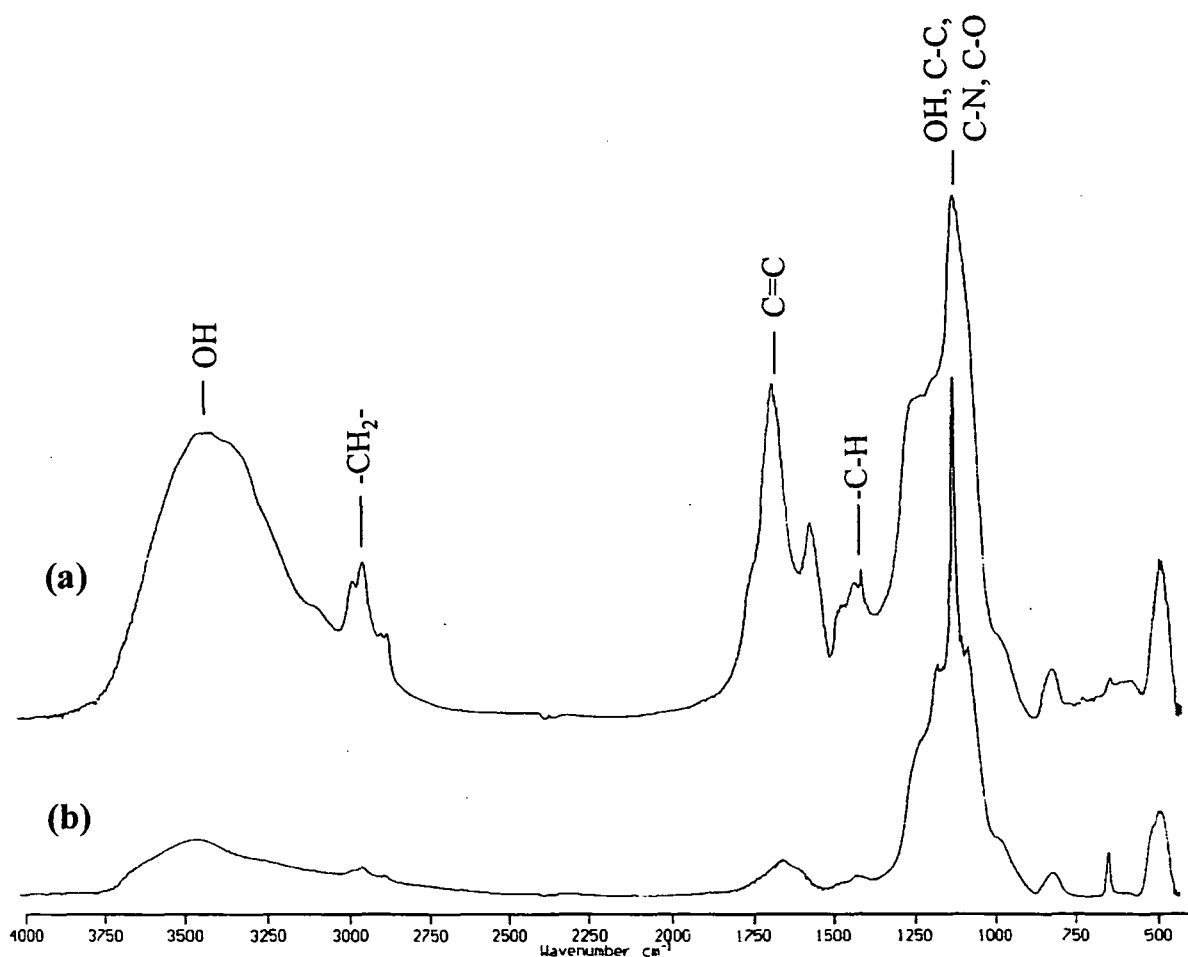


Figure 3.21. Infrared spectra of *H. ostrearia*. (a) Untreated (b) IOM.

3.4. Summary

- Characterisation of untreated Rostherne Mere sediments using SEM showed them to contain identifiable organisms and biogenic material, following isolation of IOM some altered organic matter was still apparent as was the presence of pyritic framboids whilst other material was amorphous.
- Instrumental and analytical characterisation of untreated Rostherne Mere sediments revealed elemental concentrations of 14 – 16 % C, 2 % H and 1 % N (dry weight) and atomic ratios of H/C 1.5 and N/C 0.06, with the carbon almost equally distributed between aliphatic, aromatic and cellulosic forms as determined by ¹³C ss-NMR.
- IOM isolated from Rostherne Mere sediments contained 45 % of the original total carbon and was relatively enriched in aromatics compared to the untreated sediment,

owing to the preferential removal of aliphatic, methoxy, carboxyl (50 % of each) and cellulosic (>90 %) components.

- IOM isolated from the methanogenic bacteria *M. jannaschii* and *M. thermoautotrophicum* appeared amorphous when viewed using SEM compared to the more well-defined structures of the parent materials.
- SEM analysis of the IOM isolated from the diatomaceous algae *S. costatum* and *H. ostrearia* indicated that a substantial portion of the IOM comprised siliceous 'skeletal' remains.
- Although infrared spectra of untreated samples and IOMs generally contained broad absorbance bands that hindered unambiguous assignments, all samples produced aromatic, aliphatic and oxygen-functionalised absorbances, with differences between untreated samples and IOMs generally limited to differences in absorbance intensity.

Chapter 4: Monitoring the sequential isolation of ‘insoluble organic matter’ (IOM) using pyrolysis-gas chromatography-mass spectrometry (Py-GC-MS) and time of flight-secondary ion mass spectrometry (ToF-SIMS)

4.1. Introduction

This chapter describes the monitoring of the sequential isolation procedure (Chapter 2) applied to Rostherne Mere sediments, Kimmeridge Clay and *M. jannaschii* using pyrolysis-gas chromatography-mass spectrometry (Py-GC-MS) and time of flight-secondary ion mass spectrometry (ToF-SIMS). Results from the relatively routine Py-GC-MS technique used in organic geochemistry are compared with those obtained from the newer surface-sensitive ToF-SIMS technique.

The following is a brief review of the techniques used in the current study viz Py-GC-MS (Section 4.1.1) and ToF-SIMS (Section 4.1.2). Rather than provide an extensive overview of previous applications of these techniques to different substrates, the intention here is to identify shortcomings of these techniques when applied to complex solid samples. The idea being to emphasise how crucial it would be to develop a dissolution protocol for such insoluble substrates that would allow their subsequent analysis using solution instrumental techniques that are not generally subject to the same level of interfering factors as analytical techniques applied to solids.

3.1.1. Pyrolysis-gas chromatography-mass spectrometry (Py-GC-MS) applied to insoluble organic matter

Pyrolysis techniques involve the preferential thermolytic cleavage of relatively weak bonds (e.g. C — O or C — S) in organic molecules which releases smaller organic fragments for subsequent determination (Lewis, 1997). Available pyrolysis methods and coupled systems applied to geochemistry research have been widely reviewed (Larter & Douglas, 1982; Eglinton *et al.*, 1991; Larter & Horfield, 1993). Whilst these reviews have generally focused on the utility of pyrolysis methods in typing kerogens and source rocks, and the identification of specific components such as biomarkers, they have also recognised some of the limitations associated with pyrolysis techniques. Such limitations will now be

discussed more fully with particular regard to the technique used in the current study, Py-GC-MS.

Non-pyrolysable refractory organic matter is not volatilised during pyrolysis and therefore not recorded on the pyrolysis chromatogram (Larter & Horsfield, 1993). Similarly, pyrolysable but non-GC-amenable material is also not recorded. This suggests that results from Py-GC-MS analyses will always provide underestimates of the total organic content of a sample. Thermolytic cleavage of organic molecules during pyrolysis is intimately associated with fragmentation of the initial matrix and proceeds with the formation of radical cations which may then undergo secondary reactions with other cleaved moieties in the pyrolysis chamber. Even when the primary fragmentation products can be identified using GC-MS they do not provide specific evidence of how the fragments were bound in the original matrix (Rullkötter & Michaelis, 1990), and the original position of secondary reaction products in the parent architecture is even more difficult to establish.

Although evidence indicates that the presence of inorganic minerals influences the composition of some pyrolysates, by inhibiting the volatilisation and subsequent recording of higher molecular weight ($>C_{15}$) material, Larter & Douglas (1982) noted that this was not a universal phenomenon and was more likely to be problematic when source-rocks were pyrolysed. Pyrolysis chromatograms of GC-amenable material obtained from the pyrolysis of kerogens and source-rocks generally contain three fundamental characteristic features, (1) a volatiles peak, (2) chromatographically resolved components, and (3) chromatographically unresolved components often referred to as the unresolved complex mixture (UCM or 'hump'). Resolved components can usually be unambiguously identified from their mass spectra but often only account for a minor portion of the entire chromatographic response. Although the volatiles peak can comprise a quantitatively important portion of the chromatogram, the mass spectrum of the volatiles peak is of little

diagnostic value and provides little information regarding how its components were bound in the original sample. The UCM can account for a major portion of the chromatographic response but can not be unambiguously identified because mass spectra of the UCM are complicated by interfering ions from adjacent unresolved compounds.

Larter & Horsfield (1993) point out that the aromatic portion of kerogens as represented by Py-GC data have been shown to be similar to those obtained by ^{13}C NMR and thereby adequately represent the kerogen matrix. This is based on the presumption that ^{13}C NMR accurately represents aromaticity within the kerogen, which it may not (Wilson, 1987; Whelan & Thompson-Rizer, 1993). Many pyrolysis studies have lacked the use of an internal standard which makes it difficult to accurately quantify pyrolysis products, other than in terms of mass difference between pyrolysis substrate and residue or relative chromatographic response, and relate them back to the original sample mass (*e.g.* Zegouagh *et al.*, 1999). In order to address this point and attempt to reveal the quantitative relationship between pyrolysis products, an internal standard, poly-*tert*-butylstyrene (PtBS) was added to samples before pyrolysis in the current work. PtBS pyrolyses to form predominantly *tert*-butylstyrene ($m/z = 145, 160$; Eglinton *et al.*, 1991) whose peak area may then be related to the peak area of other components. Whilst the major drawback of this procedure is that the relative response factors of other materials in relation to PtBS are not known, it does at least provide semi-quantitative data on the amount of pyrolysable material in a sample.

Mass spectrometers used in many pyrolysis studies of kerogens are operated over a limited mass range, typically between around 40 and 600 mass units. As the average mass of kerogen has been estimated at between 10000 and 25000 amu (Faulon *et al.*, 1990; Behar & Vandenbroucke, 1987) it is possible that some GC-amenable fragments released during pyrolysis will have a mass exceeding the capabilities of the mass spectrometer. In such

cases the masses of these components are likely to be underestimated.

In summary, analysis of insoluble organic matter (kerogen) using Py-GC-MS is complicated by a number of factors. These are primarily, the very nature of kerogen as a complex organic matrix intimately associated with mineral matter, its non-quantitative volatilisation and potential for undergoing secondary reactions during pyrolysis, non-quantitative transfer of volatile products to the chromatographic column, and difficulties associated with the identification and quantification of GC-amenable components.

4.1.2. Time of flight-secondary ion mass spectrometry (ToF-SIMS) techniques

The ejection of atomic and molecular ions from a surface under bombardment from heavy particles provides the basis for secondary ion mass spectrometry (SIMS; Benninghoven *et al.*, 1987). SIMS is fundamentally a surface-sensitive technique that induces changes in the uppermost monolayer of the bombarded surface and the concurrent sputtering of surface material as secondary ions (Figure 4.1). Charged secondary ions released in this manner are then separated, and recorded using a mass analyser.

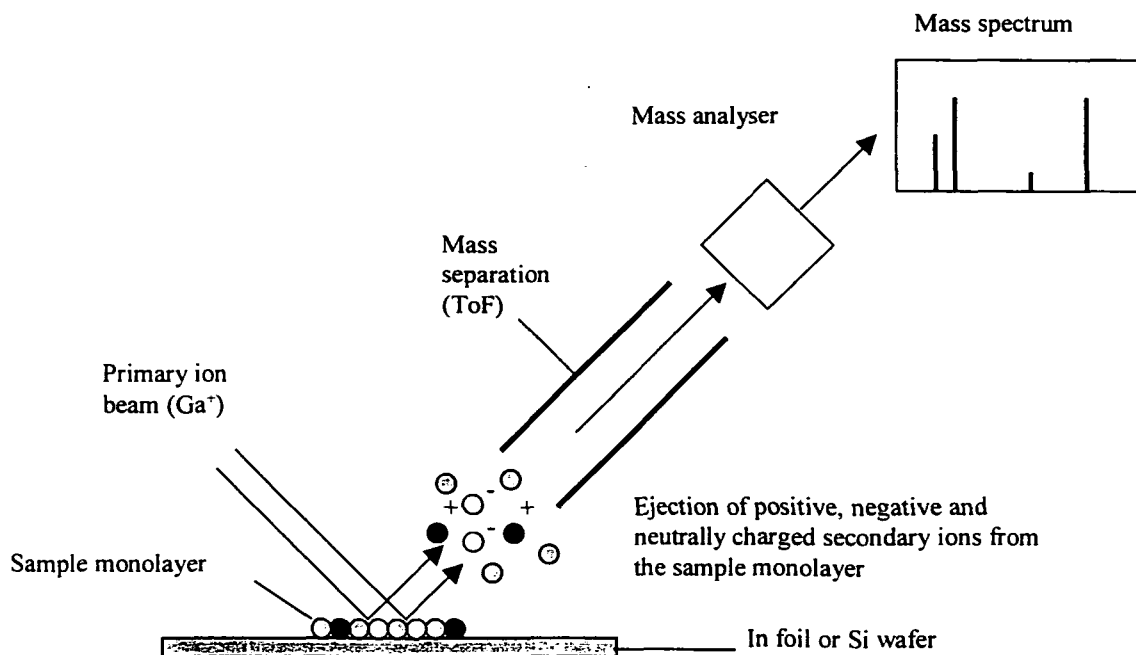


Figure 4.1. Schematic layout of the ToF-SIMS instrumentation.

This brief review will concentrate on the ToF-SIMS technique used in the current study. Two modes of SIMS analysis are recognised based on the different erosion processes occurring at the sample surface (Benninghoven *et al.*, 1987). Static SIMS uses a very low primary ion current density to eject secondary ions from the surface monolayer whilst dynamic SIMS utilises a high primary ion current density to rapidly erode material from the sample surface and provide depth-profile information on the target. Although the precise mechanisms involved in secondary ion formation from organic molecules have not yet been elucidated, Benninghoven (1982, cited in Benninghoven *et al.*, 1987) provided a model that fitted SIMS observations of organic molecules. The four assumptions of his model were:

1. A precursor (of same composition and charge sign) of the emitted secondary ion exists on the substrate surface.
2. Rapid transfer of a small amount of energy to the precursor promotes a high probability of it being ejected as an unfragmented parent-like secondary ion.
3. The charge sign of the precursor is conserved during separation from the surface and transformation into the emitted secondary ion.
4. Fragmentation results from transfer of high energy to a surface molecule with direct fragmentation of the molecule or decomposition of molecular ions in an excited state.

The most commonly observed charged parent-like secondary ions observed in SIMS analysis of organic molecules are summarised in Table 4.1. In addition, positive and negative fragment ions of the general composition $(M - C)^{\pm}$, where C represents small stable complexes such as COOH, CO₂, H₂O *etc.*, are also emitted during SIMS analysis.

Table 4.1. Summary of parent-like positive and negative secondary ion species observed in mass spectra from the SIMS analysis of organic substrates (from Benninghoven *et al.*, 1987; Me = metal, *e.g.* Ga).

Positive ions	Negative ions
Protonated: $(M + H)^+$	Deprotonated: $(M - H)^-$
Cationised: $(M + Me)^+$	Anionised: $(M + Cl)^-$, $(M + Au)^-$
Cationised deprotonated: $(M + 2Me - H)^+$	
Dimerised protonated: $(2M + H)^+$, $(2M + Me)^+$	Dimerised deprotonated: $(2M - H)^-$

The potential for very complex organic mass spectra obtained from mixtures of compounds, *i.e.* $m/z = n(M_n \pm X [-H])^{\pm}$ in positive ion mode where M_n = number of compounds present and X = stable complex, H, or $Me_{(n)}$, has so far hampered the routine application of ToF-SIMS to organic geochemical substrates. To date, the application of ToF-SIMS to organic matrices has typically been restricted to pure compounds, *e.g.* polymers (Briggs *et al.*, 1989; Delcorte *et al.*, 1997; Wien, 1997; and review by Van Vaeck *et al.*, 1999), proteins, peptides and oligosaccharides (reviewed in Benninghoven, 1987), surfactants (Briggs & Hearn, 1988), and immunosuppressive agents (Muddiman *et al.*, 1994). Recently however, ToF-SIMS has started to be used more widely for applications in organic geochemistry such as studies of coal macerals (Hou *et al.*, 1995) and the distribution of bacterial biomarker precursors (Steele *et al.*, in preparation).

4.2. Experimental procedures

4.2.1. Pyrolysis-gas chromatography-mass spectrometry (Py-GC-MS)

A procedural blank was run before each sample. This comprised a solvent rinsed (DCM) quartz capillary tube containing two plugs of pre-extracted (DCM, 2 x 24 h) glass fibre wool inserted into the coil of the pyrolysis probe and pyrolysed in air ($600 \text{ }^\circ\text{C} \pm 5 \text{ }^\circ\text{C}$, 1 min). The probe was inserted into the injector and the procedural blank pyrolysed

(590 °C ± 5 °C, 1 min) and pre-run on an accelerated GC programme (40 – 300 °C at 10 °C min⁻¹). Where the gas chromatogram of the pre-run procedural blank was free of peaks the procedural blank was re-run under the GC conditions used for analysis of samples (-10 – 300 °C at 5 °C min⁻¹). Glass fibre wool from the procedural blank was used for trapping the sample in the subsequent sample analysis. Sample (*ca.* 0.2 mg) was weighed into the capillary tube, pre-plugged at one end, and the second plug of glass fibre wool inserted to trap the sample. An internal standard, poly-*tert*-butylstyrene (PtBS; 0.5 µl, 0.2 mg ml⁻¹ stock solution in DCM), was injected onto the glass wool and the capillary tube fitted into a CDS 120 pyroprobe. The pyroprobe was then inserted into the pyrolysis unit.

4.2.1.1. Instrumental details

Samples were pyrolysed at 590 °C ± 5 °C for 1 minute before injection at 230 °C through a modified packed column injector onto an Rtx-5 column (nominal length 30 m; 0.32 mm ID; 0.25 µm film of cross-bonded: 95 % dimethyl, 5 % diphenyl polysiloxane) fitted in a high resolution Carlo Erba Mega 6100 GC unit with helium carrier gas at 0.45 kg cm⁻² head pressure. The gas chromatograph temperature programme was raised from -10 to 300 °C at 5 °C min⁻¹ and held at 300 °C for 10 minutes. Cryo-cooling was achieved using a Cryo 520 Carlo Erba cryo-cooling unit with liquid CO₂ as coolant. Mass spectra were measured using a Kratos MS25 double-focusing mass spectrometer (source temperature, 230 °C; ionising potential, 40 eV; emission current, 600 – 1000 µA; nominal mass range, 40 – 576 amu; magnet control, field control).

4.2.1.2. Data collection

Gas chromatographic and mass spectral data were recorded using Kratos DS90 software. Initially, data processing was carried out using Kratos DS90 software, subsequently linked through an EMU-TEK emulation programme to a PC. Later, data processing was

undertaken using a windows based data processing programme, WSearch (<http://minyos.its.rmit.edu.au>), after file transfer from the Kratos DS90 using the Kermit file transfer protocol. Chromatographic peak identifications were based on comparisons with retention data of standards, previously reported retention data from the same instrument, and comparisons of mass spectra with library spectra (NBS, NIST) and spectra reported in the literature.

4.2.1.3. Quality control and quantification

A pyrolysis blank (capillary tube plus glass wool) was run before each sample and blanks containing the P_tBS standard were run intermittently. Quantification of unknown compounds was calculated relative to the mass of the P_tBS internal standard using the formula:

$$\text{mass of unknown } (\mu\text{g}) = \frac{\text{mass of P}_{t}\text{BS } (\mu\text{g}) \times \text{peak area of unknown}}{\text{peak area P}_{t}\text{BS}}$$

Summation of the mass of resolved components, and total response, on each pyrogram was then related back to the mass of initial substrate subjected to pyrolysis using:

$$\% \text{ Pyrolysable material} = \frac{\text{Total mass of resolved components } (\mu\text{g}) \times 100}{\text{Mass of initial substrate } (\mu\text{g})}$$

The reproducibility of the P_tBS injection technique was monitored chronologically by recording the peak area of the internal standard on each pyrolysis run. Samples were repeated where the peak area of the internal standard was greater than $\pm 3\sigma$ from the mean. A number of samples were run in triplicate to monitor reproducibility in weighing out.

4.2.2. Time of flight-secondary ion mass spectrometry (ToF-SIMS)

ToF-SIMS analysis was conducted using a Phi Evans T-2000 TRIFT instrument with a spot size of approximately 0.3 – 0.5 μm . A 15 kV gallium ion source (average current

of 2 pA) was used with a 156 ps pulse width and 10 kHz repetition rate, which corresponded to 5.7×10^{13} ions cm^{-2} static SIMS ion dosage after 240 seconds acquisition time. Samples were pressed on to gold coated indium foil or silicon wafers under lamina flow conditions using a pre-cleaned (ultrasonication, 30 s; methanol; hexane; acetone; ethanol) stainless steel needle before immediately placing the samples into the instrument. Masses were recorded between 1 – 1000 amu. Blanks comprised pre-extracted gold coated indium foil and silicon wafers. Controls comprised ultrasonically cleaned (30 s; methanol; hexane; acetone; ethanol) blank gold-coated indium foil and silicon wafers left exposed within the lamina flow cabinet prior to analysis, and foil and wafers exposed to fingerprints, and dust and air from outside the lamina flow cabinet.

4.3. Results

4.3.1. Py-GC-MS reproducibility

Reproducibility in the addition of the P_tBS to the sample being pyrolysed was monitored by determining the peak area of the internal standard from each chromatogram and plotting these chronologically (Figure 4.2). There was a significant difference ($p < 0.05$) between the mean chromatographic response recorded for the 0.1 μg P_tBS administered before November 1997 and after April 1998 (pre-November 1997, mean = 14460000, $\pm\sigma$ 30 %; post-April 1998, mean = 6006000, $\pm\sigma$ 20 %). On average, internal standard addition after April 1998 resulted in chromatographic peak areas 40 % less than those obtained previously, albeit with reduced variability. Build-up of non-pyrolysable material in the pre-column and/or increased residue on the ion source were the most likely explanations for the decreased response experienced between the two periods of pyrolysis analyses.

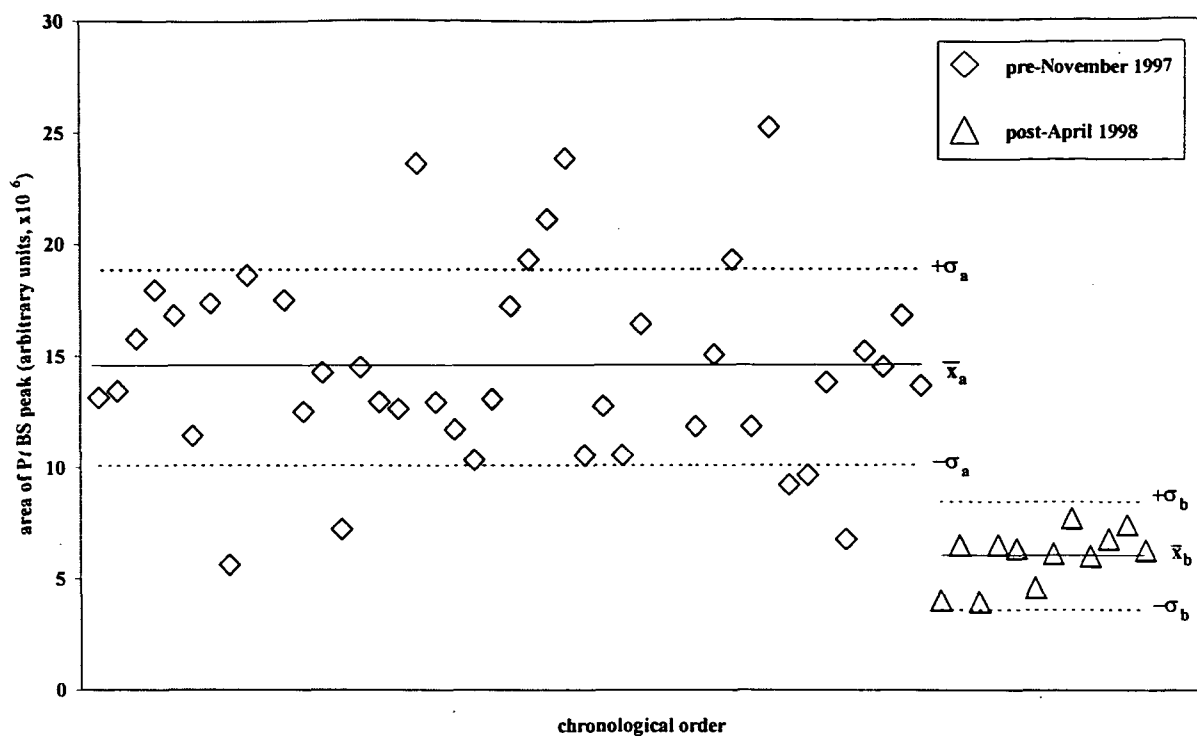


Figure 4.2. Chronological variability in chromatographic response (peak area) of P/BS internal standard used in Py-GC-MS analyses

The reproducibility of the pyrolysis method used in this work was examined by analysing two sediment samples (5 – 6 cmbswi untreated and IOM) in replicate. In each case the resolved peak areas and the total areas (including the unresolved area below the baseline) were integrated and quantified in terms of the original mass of sample loaded into the pyrolysis tube. Resolved components, including the volatiles peak, accounted for less than 2 % of the original mass of sample (5 – 6 cmbswi untreated, mean = 0.5 ± 0.5 %, $n = 4$; 5 – 6 cmbswi IOM, mean = 1.3 ± 0.5 %, $n = 4$). The chromatographically unresolved fraction (area below the baseline) obtained from these samples accounted for up to 60 % of the total chromatographic response. However, this was likely to have been an over-estimate because it included a contribution from the area below the baseline during the static temperature phase of the GC programme (> 52 min). Nevertheless, quantification of the total chromatographic response (resolved plus unresolved) still only accounted for less than 2.5 % of the original pyrolysed sample mass (5 – 6 cmbswi untreated, mean = 1.0 ± 0.8 %, $n =$

4; 5 – 6 cmbswi IOM, mean = 2.3 ± 0.8 %, $n = 4$). Sample/internal standard (PtBS) interactions have previously been reported to interfere with quantitative determinations in Py-GC studies where mineral matter was present in whole-rock samples (Eglinton *et al.*, 1991). A reduction in the response from the PtBS internal standard in the current work would have resulted in an overestimate of the mass of pyrolysed material unless this was accompanied by even greater reduction in the response from pyrolysable components. Reproducibility was poorer for the untreated sediment samples (resolved components, 93 % rsd; total response, 86 % rsd) than for the IOM (resolved components, 35 % rsd; total response, 29 % rsd). These differences were thought to reflect the more heterogeneous nature of the untreated sediment, which contained a large (*ca.* 50 %) mineral fraction and relatively labile biochemicals (*e.g.* proteins). Quantification of the total chromatographic response from other sedimentary and bacterial samples analysed using Py-GC-MS generally accounted for only a minor portion of the mass of sample subjected to pyrolysis (Table 4.2).

Table 4.2. Chromatographic response quantified as a percentage of the sample mass subjected to Py-GC-MS (resolved includes peaks above the baseline; total includes unresolved area below the baseline)

	untreated		IOM	
	resolved	total	resolved	total
Rostherne Mere sediments	0.5 ± 0.5 $(n = 4)$	1.0 ± 0.8 $(n = 4)$	1.3 ± 0.5 $(n = 4)$	2.3 ± 0.8 $(n = 4)$
<i>M. jannaschii</i>	< 1	4	< 0.1	< 0.1
Kimmeridge Clay	2	6	7	9

The resolved peaks in pyrograms from standard compounds analysed using Py-GC-MS accounted for a greater portion of the original pyrolysis sample mass than for

environmental substrates (anthracene, 106 – 109 %; phenanthrene, 86 – 90 %; G₁P-[6]-Obn, 20 %, G₂P-[12]-Obn, 95 %; Chapter 5). This suggests that some of the environmental matrices examined in this study contained material that was significantly resistant to pyrolysis and/or contained, or produced upon pyrolysis, non-GC amenable compounds. The production of aromatic residual involatile material from kerogens has been recognised in previous Py-GC and Py-GC-MS studies (Larter & Douglas, 1982, and references therein). However, production of involatile material during pyrolysis has since been suggested to have minimal impact on how representative the pyrolysis data is of the kerogen matrix (Larter & Horsfield, 1993).

4.3.2. Monitoring sequential isolation of IOM from Rostherne Mere sediments

The effects of each stage of the sequential isolation procedure (Chapter 2) were monitored for a sediment sample from Rostherne Mere (5 – 6 cmbswi) using Py-GC-MS. Pyrograms obtained from these analyses were normalised to the toluene or C_{23:1} *n*-alkene peak to aid clarity of display and are presented in Figure 4.3 i - iii. A number of compounds were identified as common components in each of the pyrograms; *n*-alkanes; *n*-alk-1-enes; branched alkanes/alkenes; prist-1-ene; benzene (peak not shown), methyl-, dimethyl-, trimethyl- and tetramethylbenzenes; C₃-alkylated benzenes; phenol, cresol and dimethylphenols; indene; naphthalene, methyl-, dimethyl- and trimethylnaphthalenes; methyldibenzofurans; phenanthrene; anthracene and methylanthracenes; and fluorene. Unexpectedly, however, few qualitative changes were detected between the constituents found in the pyrograms obtained from material after each isolation stage. Given that the isolated IOM represented around 15 % of the original sample mass and 50 % of the total carbon, a more pronounced reflection of the removal of major chemical classes had been expected from these Py-GC-MS analyses. For example, analysis of the 'protein' extracted fraction ('protein' accounted for around 25 % of the original sample mass; Figure 4.3d) was expected to be characterised by a loss in nitrogen-containing species such as nitriles,

pyrroles, pyridines and imidazoles, but this was not observed. The most striking changes occurred in the pyrogram of the 'demineralised IOM' (Figure 4.3g) where the chain length of *n*-alkanes and *n*-alk-1-enes was seen to increase. Extension of the *n*-alkane/*n*-alk-1-ene series in the untreated sediment (C₆/C_{6:1} – C₂₄/C_{24:1}) to that in the IOM (C₆/C_{6:1} – C₃₀/C_{30:1}) was consistent with that reported by Gormly & Mukhopadhyay (1983) for whole-rock and related kerogen isolates analysed using Py-GC. Mineral removal may have had a two-fold effect. Firstly, a relative concentration of the OM, promoting signal enhancement may have occurred, and second, adsorption of OM to mineral surfaces in the pyrolyser may have been reduced. Peaks marked with triangles (Figure 4.3 iii) were identified as triterpenoids (*m/z* = 191). These survived the sequential isolation procedure suggesting that they were intrinsically bound into the 'insoluble' matrix. A series of compounds whose mass spectra (Figure 4.4) were consistent with those of fluorinated alkanes/alkenes were identified in the IOM pyrogram but were absent from the pyrogram of the material prior to HF treatment. This series was differentiated from the *n*-alkane/alkene series by plotting the ion chromatograms (Figure 4.5). Ion chromatograms showed that the suspected fluorinated compounds eluted between and consecutively with the *n*-alkane series but were not present beyond the C₂₂ alkane. The most likely source of these fluorinated alkanes/alkenes was from the Teflon® beakers and/or stirring bars used during the HF digestion. Teflon® used in the manufacture of the beakers was Teflon® PFA 440 HP grade (D. Clarke, Techmate Ltd., *Pers. Comm.*) which comprises a copolymer mix of tetrafluoroethylene (CF₂=CF₂) with perfluoroalkyl vinyl ether [F(CF₂)_xCF₂OCF=CF₂] (<http://www.bibby-sterilin.com/cat/azlon/pfa.htm>, 2000; Figure 4.6), whilst stirrer bars were made from polytetrafluoroethylene (PTFE). A previous study into the mechanisms of pyrolysis of fluoropolymers (Lonfei *et al.*, 1986) showed that a tetrafluoroethylene-perfluoromethyl vinyl ether copolymer fragmented during pyrolysis producing series of fluorinated alkanes, alkenes and ethers. The typical mass spectrum found in the current study (Figure 4.4) was comparable to the Py-MS spectrum reported by these workers, with characteristic ions at

$m/z = 69, 119, 169$ ($C_nF^{+}_{2n+1}$; $n = 0 - 2$), $81, 131, 181, 231, 281$ ($C_nF^{+}_{2n-1}$; $n = 1 - 5$), and $100, 81$ (C_2F_4). Whilst Lonfei *et al.* (1986) did not report the presence of ions at $m/z = 51, 101, 151, 201$ and 251 , these ions are consistent with fragments with the general formula $C_nF_{2n}H^+$ ($n = 1 - 5$). Although Teflon® is generally considered inert to chemical attack under the reaction conditions employed it is apparent that either some leaching occurred or that material was mechanically dislodged during the mineral dissolution.

Three peaks from the pyrogram of the 'aqueous soluble' extracted residue (marked with asterisks in Figure 4.3 iib) were identified as phthalate plasticisers associated with bleed from PVC (Middleditch, 1989). The source of these contaminants was thought to be plastic tubing attached to the Milli-Q water dispenser, Subsequently, water was obtained from the feeder tank after removal of the tubing, after which phthlates were not observed in the pyrograms of aqueous extracted fractions.

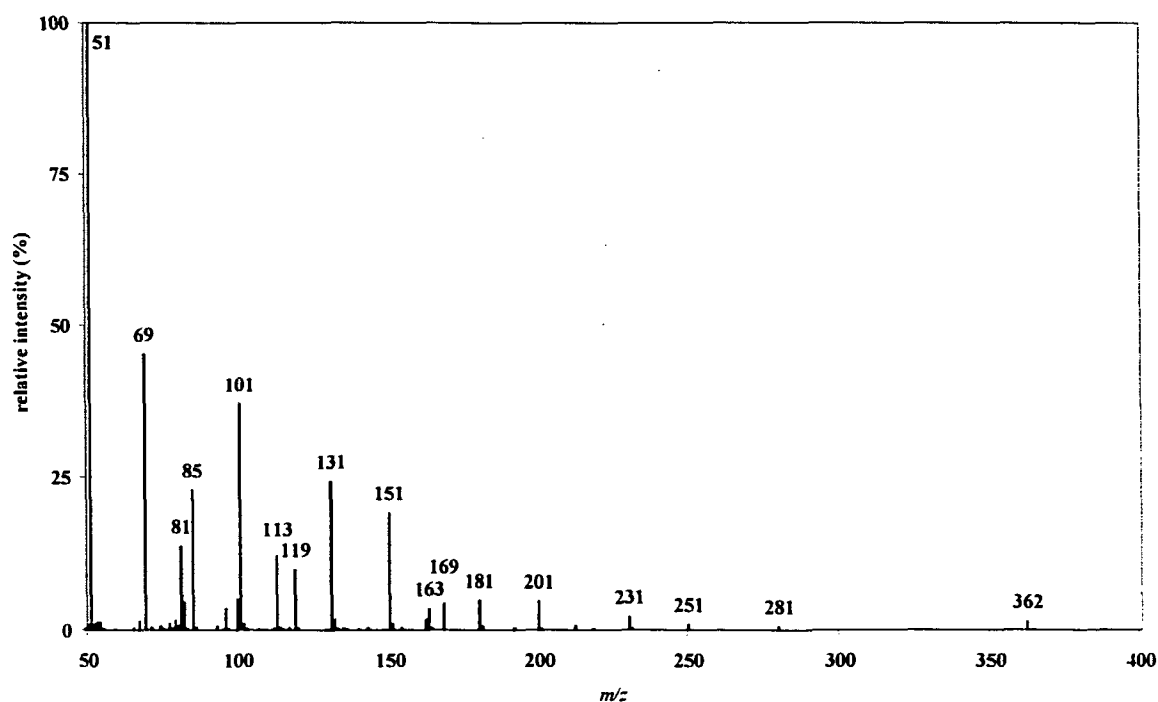


Figure 4.4. Typical mass spectrum (RT = 6:03 min) from the series of fluorinated compounds identified in the Py-GC-MS chromatogram of IOM isolated from Rostherne Mere sediment (5 – 6 cmbswi).

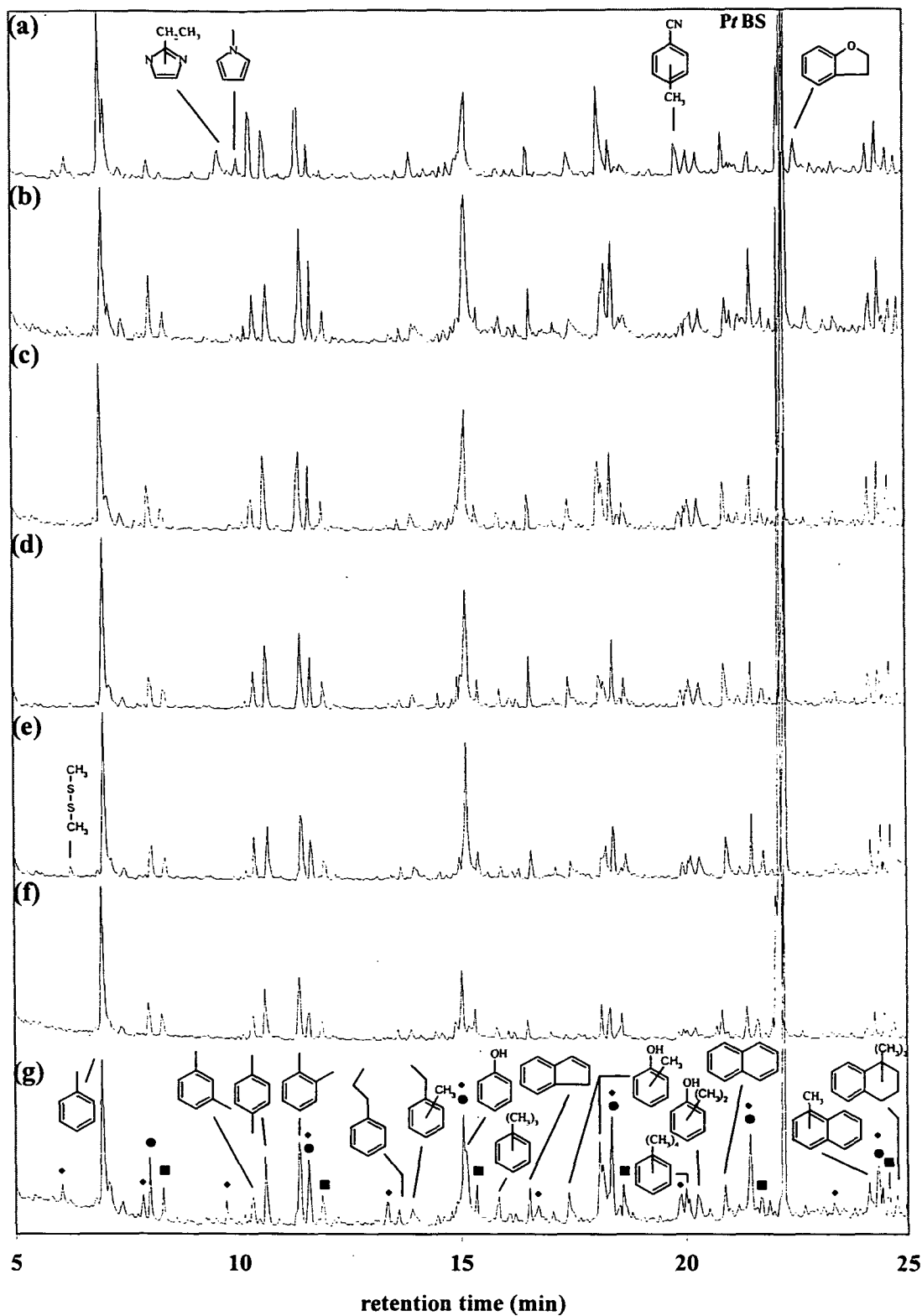


Figure 4.3 i. Reconstructed total ion chromatograms (5 – 25 min) from the Py-GC-MS of Rostherne Mere sediment (5 – 6 cmbswi) following each stage of the sequential isolation procedure normalised to toluene. (a) Untreated (b) ‘aqueous soluble’ extracted (c) ‘free lipid’ extracted (d) ‘protein’ extracted (e) ‘carbohydrate’ extracted (f) ‘bound lipid’ extracted (g) ‘demineralised IOM’ (● *n*-alk-1-ene; ■ *n*-alkane; ♦ fluorinated alkanes/alkenes).

cont. overleaf

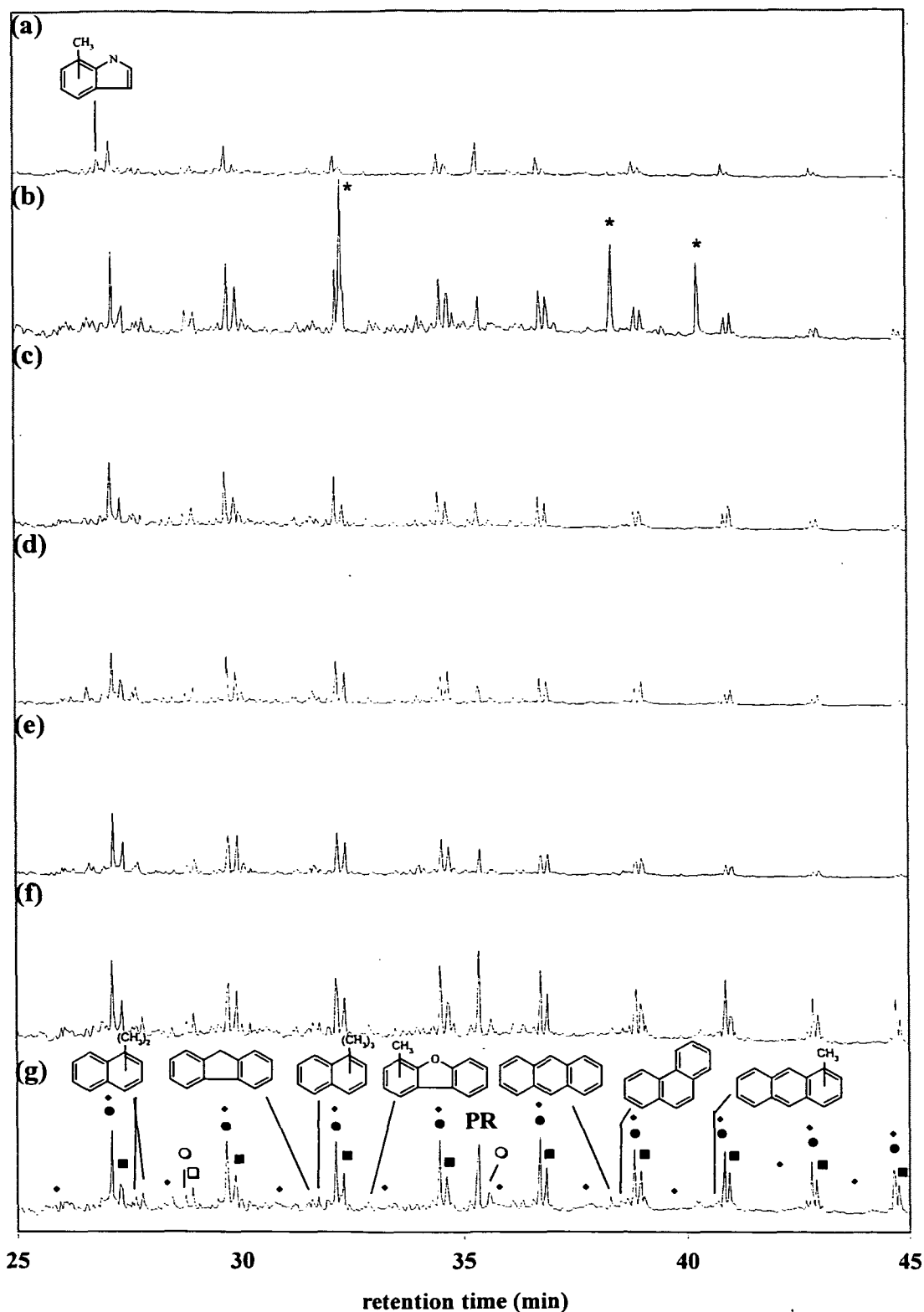


Figure 4.3 ii. Reconstructed total ion chromatograms (25 – 45 min) from the Py-GC-MS of Rostherne Mere sediment (5 – 6 cmbswi) following each stage of the sequential isolation procedure normalised to toluene. (a) Untreated (b) ‘aqueous soluble’ extracted (c) ‘free lipid’ extracted (d) ‘protein’ extracted (e) ‘carbohydrate’ extracted (f) ‘bound lipid’ extracted (g) ‘demineralised IOM’ (● *n*-alk-1-ene; ○ alkene; ■ *n*-alkane; □ alkane; PR = prist-1-ene; ♦ fluorinated alkanes/alkenes; * phthalate plasticiser).

cont. overleaf

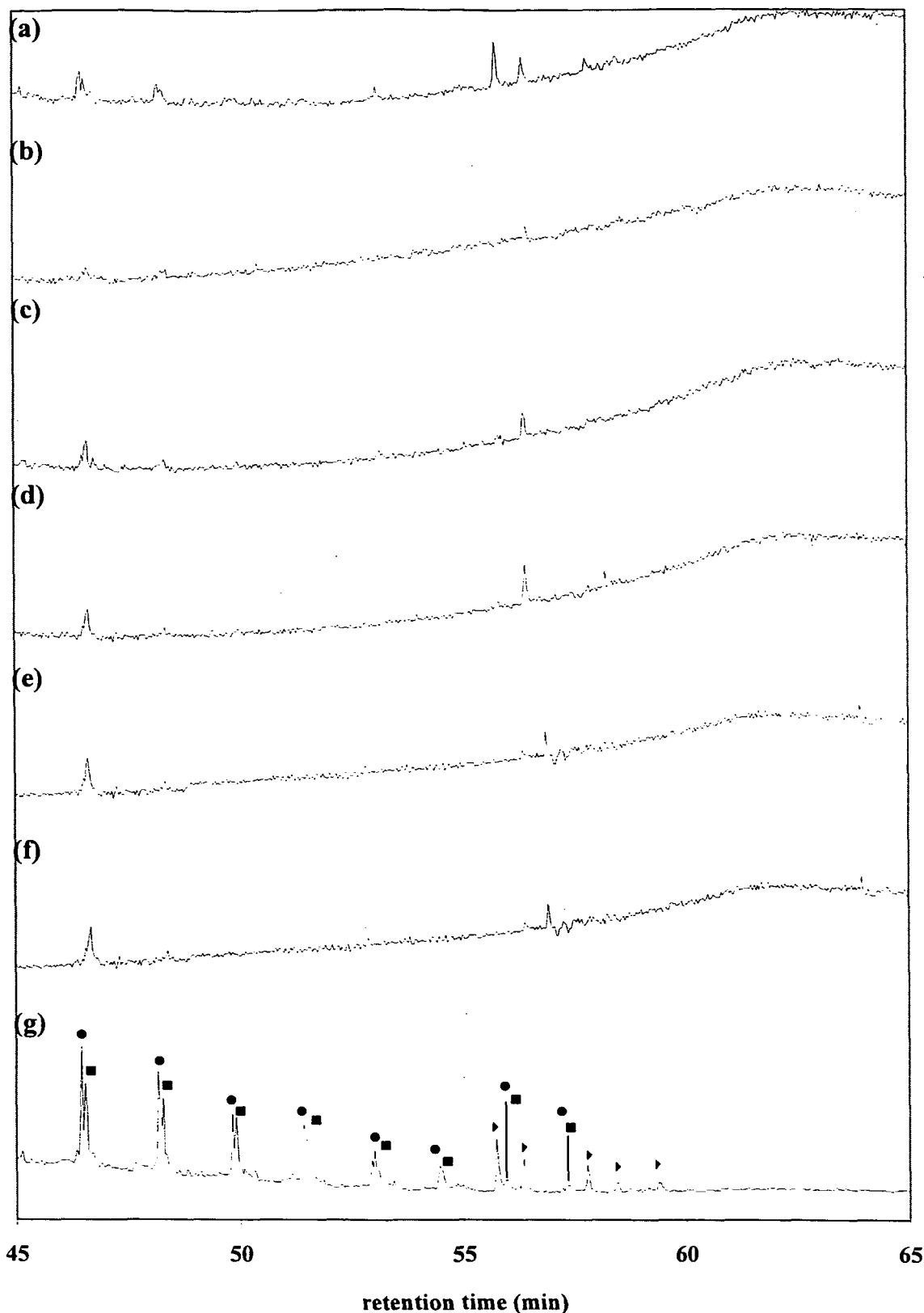


Figure 4.3 iii. Reconstructed total ion chromatograms (45 – 65 min) from the Py-GC-MS of Rostherne Mere sediment (5 – 6 cmbswi) following each stage of the sequential isolation procedure normalised to toluene. (a) Untreated (b) ‘aqueous soluble’ extracted (c) ‘free lipid’ extracted (d) ‘protein’ extracted (e) ‘carbohydrate’ extracted (f) ‘bound lipid’ extracted (g) ‘demineralised IOM’. (● *n*-alk-1-ene; ■ *n*-alkane; ◆ fluorinated alkanes/alkenes; ▴ triterpenoids).

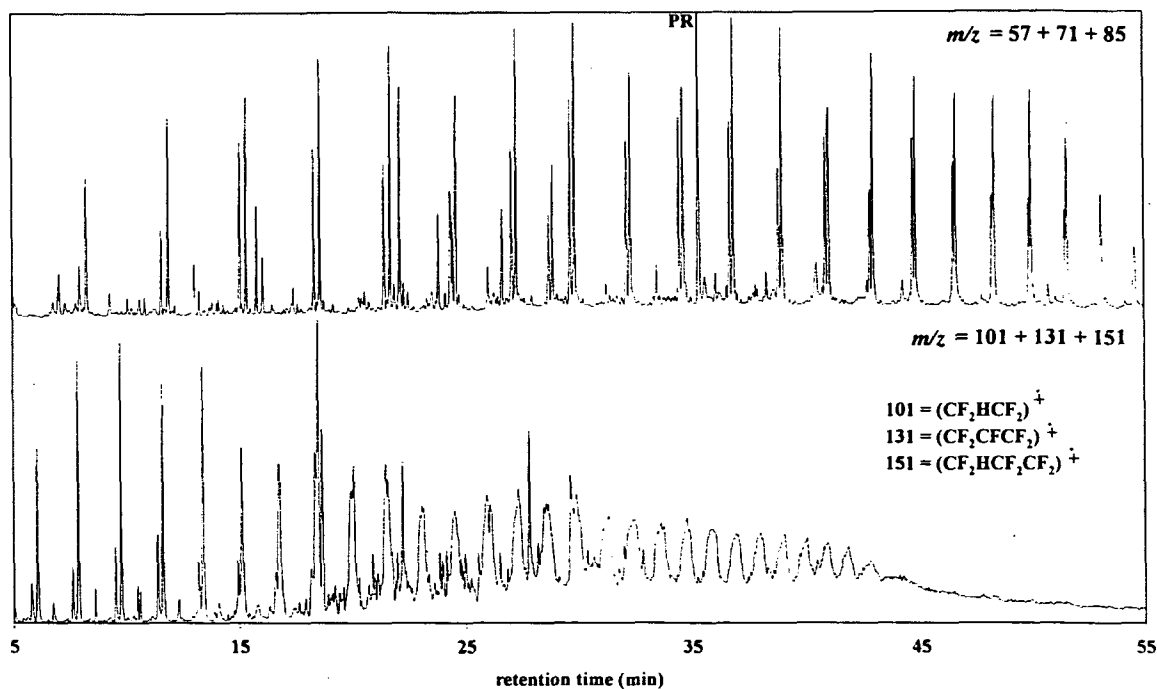


Figure 4.5. Ion chromatograms from the Py-GC-MS of IOM isolated from Rostherne Mere sediment (5 – 6 cmbswi) differentiating the series of fluorinated compounds (lower) from the *n*-alkane/alk-1-ene series (upper)

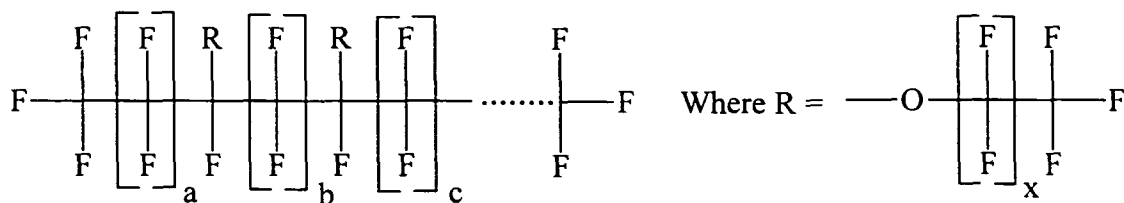


Figure 4.6. Generic structure of Teflon® PFA

Averaged mass spectra of the chromatographic response between 3 – 60 minutes were obtained to allow rapid identification of changes in the bulk composition between the untreated sediment and the isolated IOM (Figure 4.7). The difference in signal intensity between the two spectra probably reflects the relative enrichment of organic carbon in the IOM (*ca.* 50 %) compared to the untreated sediment (*ca.* 14 %) whilst ions at $m/z = 145$ and 160 were characteristic of the P ν BS internal standard. Overall, there was an apparent reduction in signal intensity from some lower molecular weight ions (*e.g.* $m/z = 67, 79, 94, 107, 117$) in the IOM averaged spectrum. This was accompanied by a relative increase in the alkane/alkene signal intensity ($m/z = 57, 71, 85$ and $55, 69, 83$, respectively) with respect to the aromatic ion ($m/z = 91$). Ions at $m/z = 131, 181, 231; 151, 201; 169, 219, 269, 319$ in the IOM spectrum were consistent with the fragmentation of fluoropolymers whilst $m/z = 191$ indicated the presence of triterpanes.

Because the use of Py-GC-MS failed to elucidate subtle changes in the composition of residual material following each isolation stage its use was subsequently limited to the analysis of untreated samples and the IOM isolated from them.

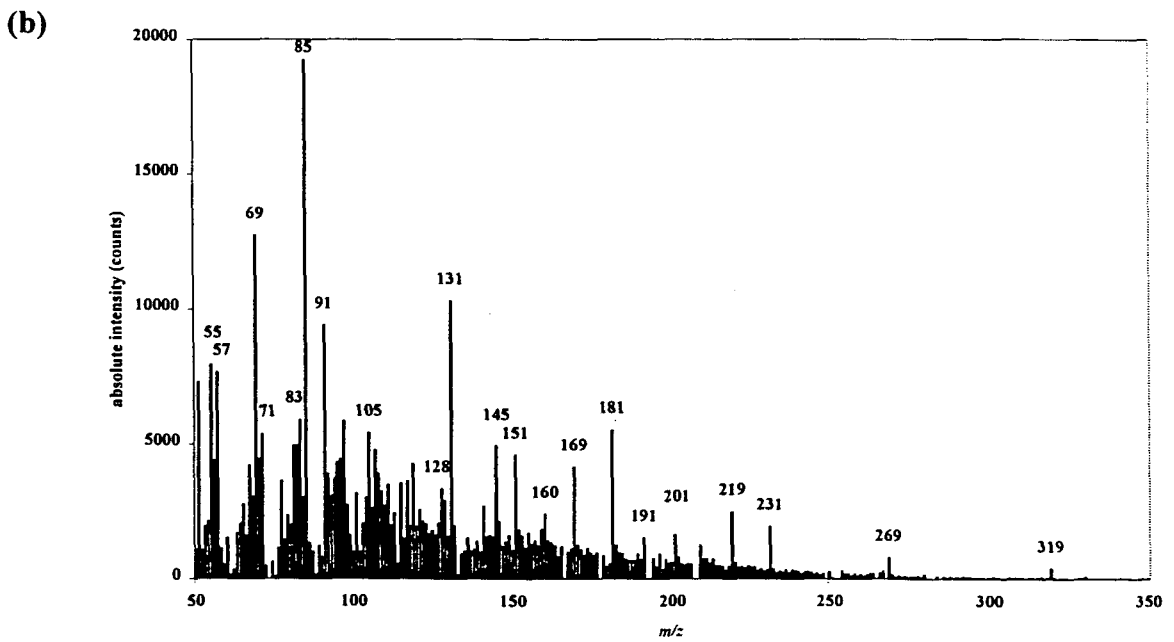
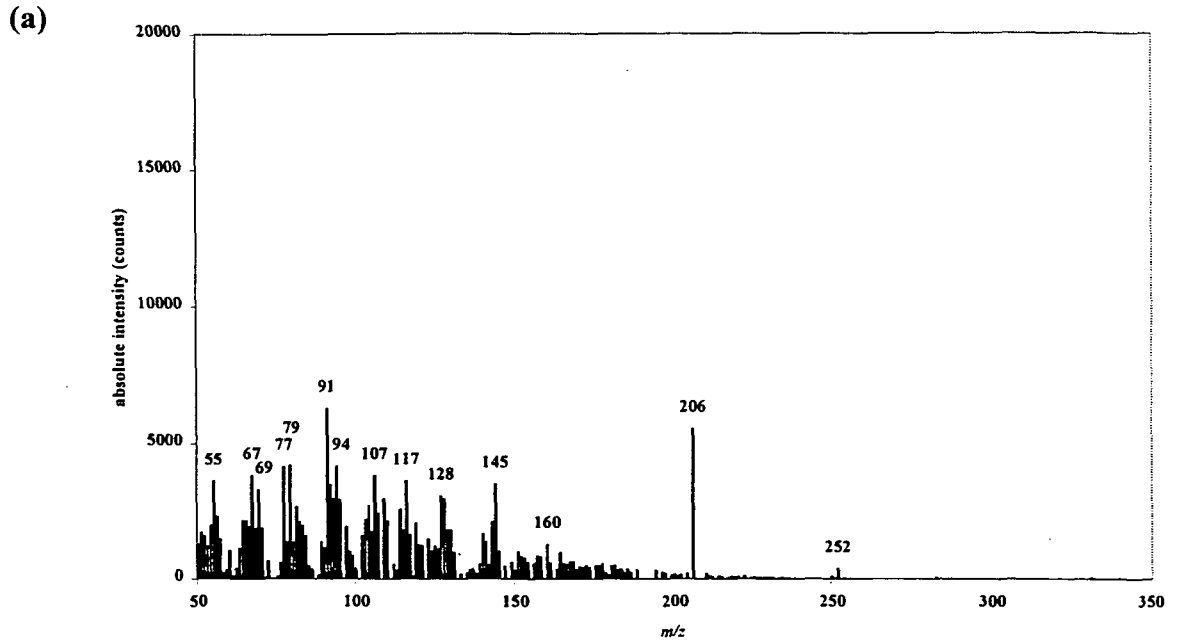
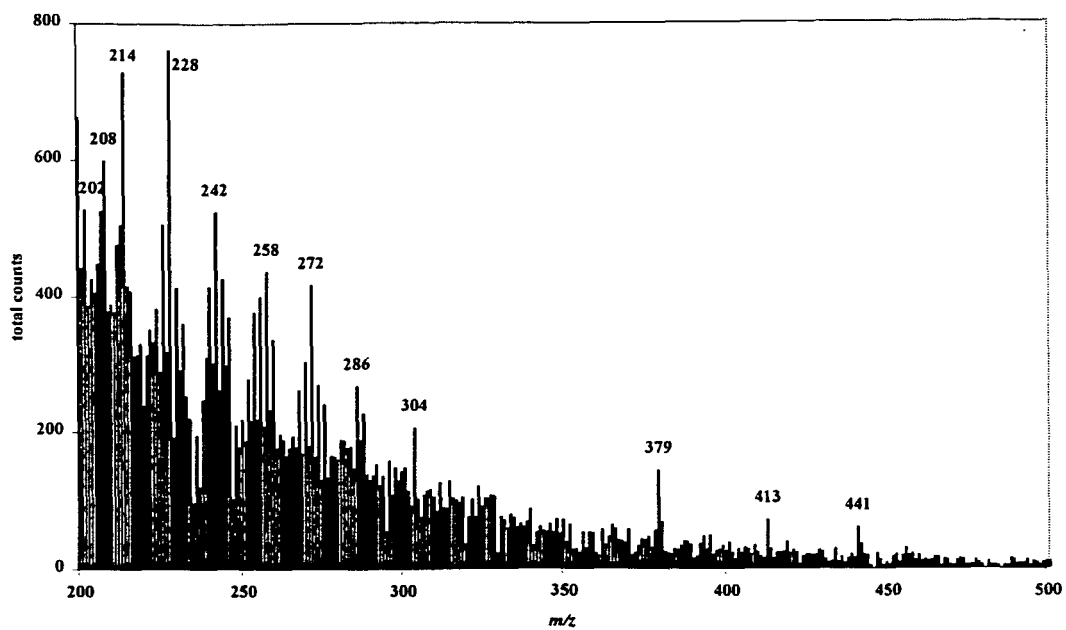


Figure 4.7. Averaged mass spectra (3 – 60 min) from the Py-GC-MS analyses of 0.4 mg of Rostherne Mere sediment, 5 – 6 cmbswi. (a) Untreated (b) IOM.

Four samples of untreated sediment from Rostherne Mere (7 – 10, 21 – 24, 59 – 62, and 82 – 85 cmbswi) and IOM isolated from the same sediments were subjected to analysis using ToF-SIMS. In each case, most of the response from ToF-SIMS analysis was attributable to components of molecular mass < 500 amu and signals between 500 – 1000 amu were weak and intermittent. One of the prominent features of the positive ion mass spectra obtained from analyses of the untreated sediments (Figure 4.8) was the presence of ion clusters at fourteen mass unit intervals each comprising four or five apparent homologous series separated from each other by two mass units. The masses of each series did not correspond with those of the *n*-alkanes or *n*-alk-1-enes (e.g. ToF-SIMS ions, $m/z = 254, 256, 258, 260$; $C_{19:0}$, RMM = 268; $C_{19:1}$, RMM = 266) found from the Py-GC-MS analyses of the same samples. At higher mass resolution, the unidentified series had comparable masses (M^{+}) to those of alkenes with four to eight unsaturations (e.g. ToF-SIMS ion, $m/z = 258.2260$ and 252.1298 ; $C_{19:4}$ and $C_{19:8}$, calculated RMM = 258.2350 and 252.1878, respectively) and oxygen-containing *n*-alkanes/alkenes (e.g. ToF-SIMS ions, $m/z = 260.2362$ and 258.2260 ; $C_{15}H_{32}O_3$ and $C_{15}H_{30}O_3$, calculated RMM = 260.2351 and 258.2195, respectively) but were isotopically heavier than possible aromatic species. If the alkyl chains had been ether-cross linked, similar to those reported for algaenans (e.g. Largeau *et al.*, 1984; Gelin *et al.*, 1994), then pyrolytic ether cleavage accompanied by subsequent loss of oxygen during pyrolysis could be more readily reconciled with ToF-SIMS data where perhaps only simple ether cleavage occurs.

(a)



(b)

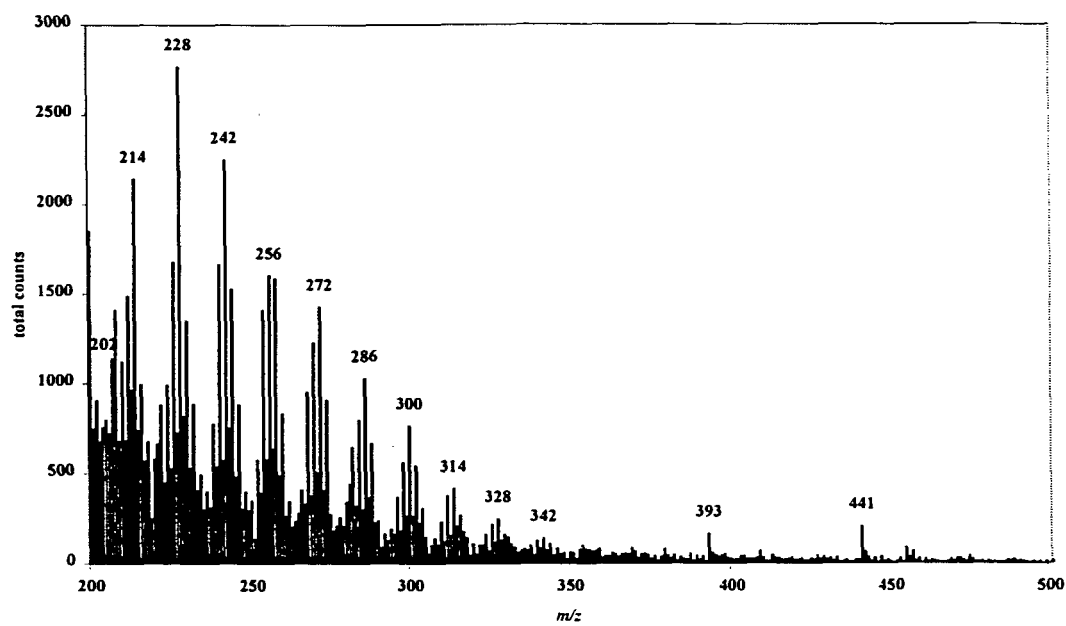


Figure 4.8. *cont. overleaf*

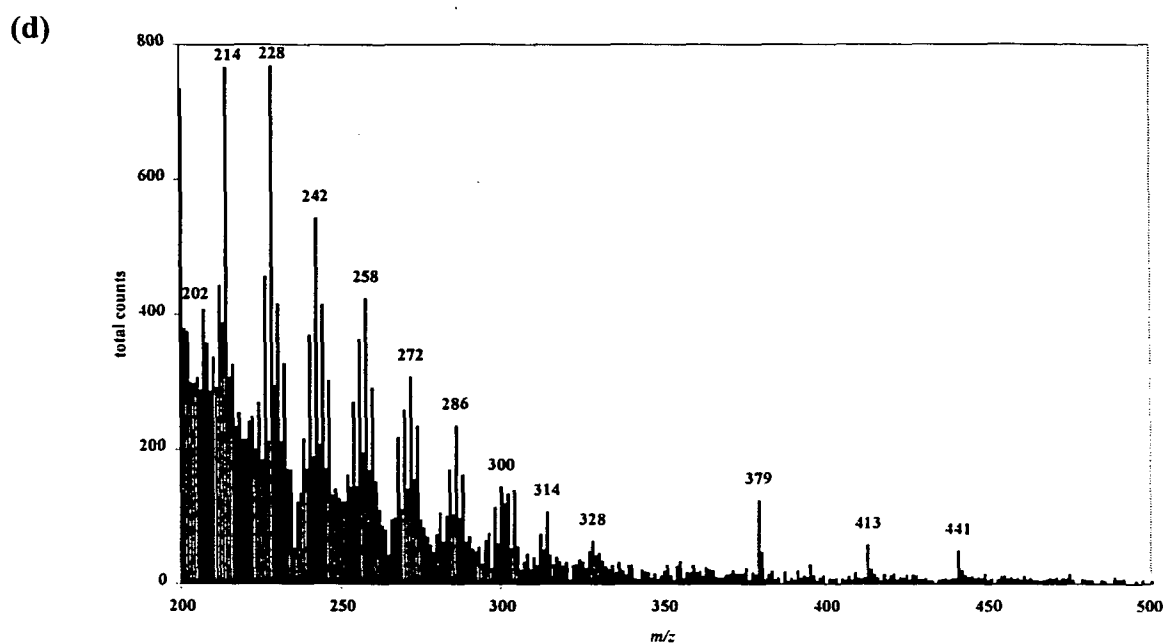
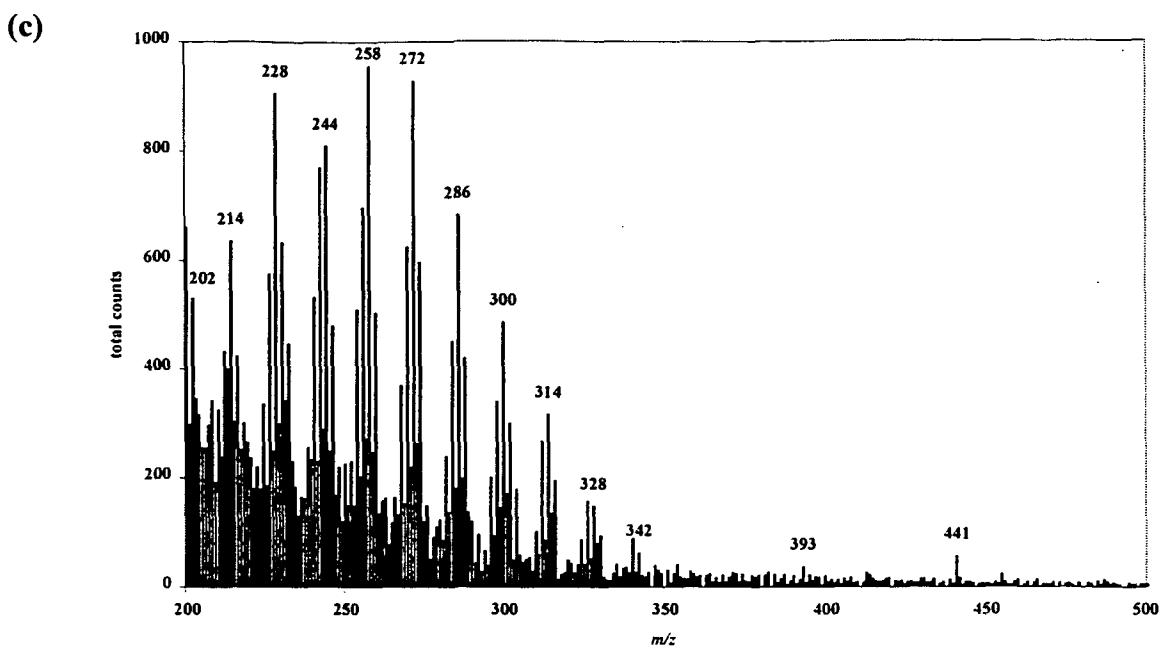


Figure 4.8. Partial ToF-SIMS positive ion mass spectra (200 – 500 amu) of untreated Rostherne Mere sediments. (a) 7 – 10, (b) 21 – 24, (c) 59 – 62, (d) 82 – 85 cmbswi.

The ToF-SIMS positive ion mass spectra recorded for IOM isolated from Rostherne Mere sediments (Figure 4.9) were similar to those of the corresponding untreated sediments. This supported the Py-GC-MS data and suggested that the sequential isolation procedure did not significantly alter the intrinsically insoluble organic matter. However, ions at $m/z = 231, 281, 331, 381$ and 431 in the mass spectrum of IOM from 21 – 24 cmbswi may have

been indicative of fluorinated alkanes. A prominent ion found in all four untreated samples ($m/z = 441$) survived the sequential isolation procedure in two of the four IOM samples. Although the source of this ion has yet to be identified it has also been observed in the ToF-SIMS mass spectra of a range of sedimentary, bacterial and meteoritic samples (Steele, *pers. comm.*, 2000).

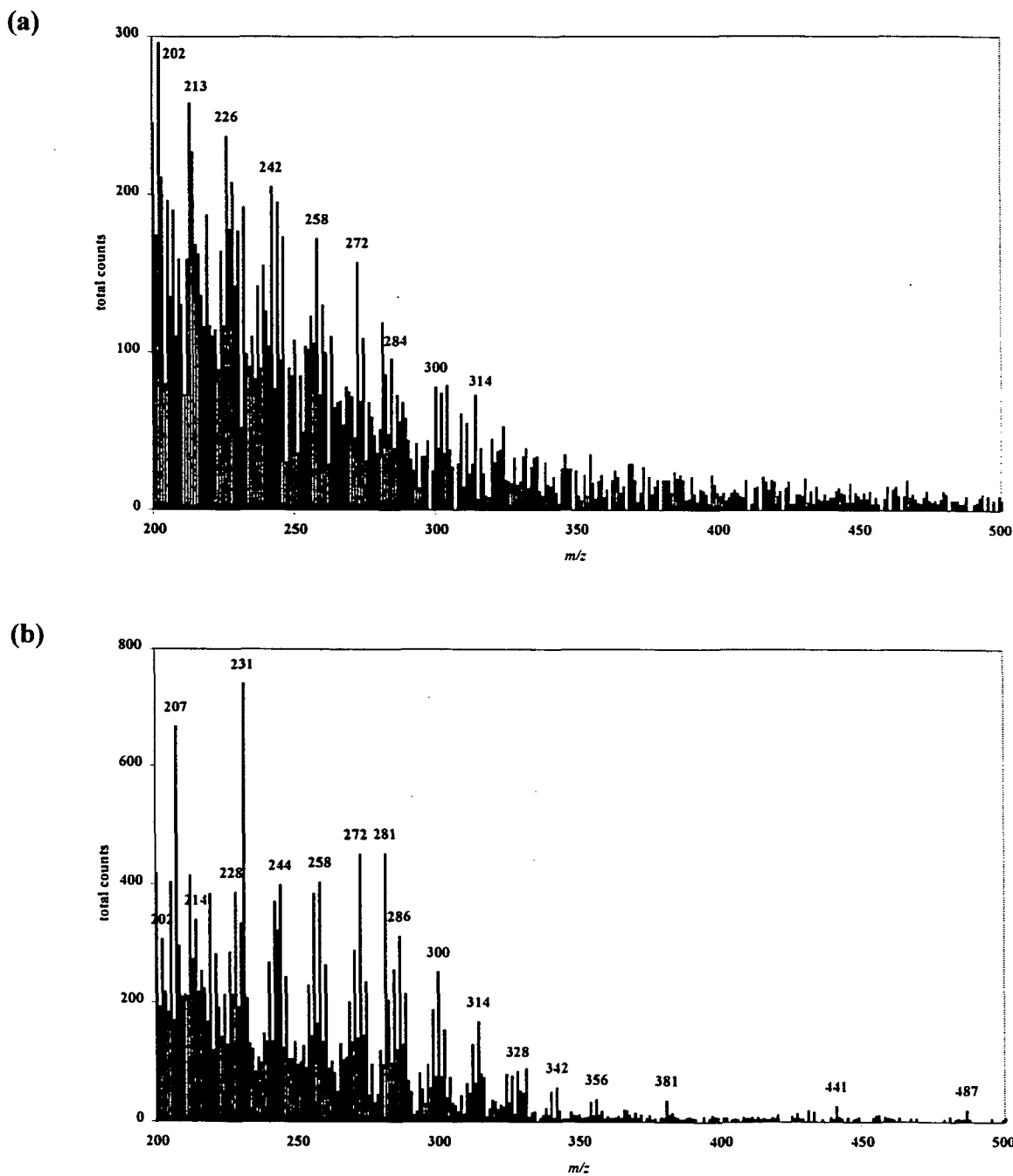


Figure 4.9. *cont. overleaf*

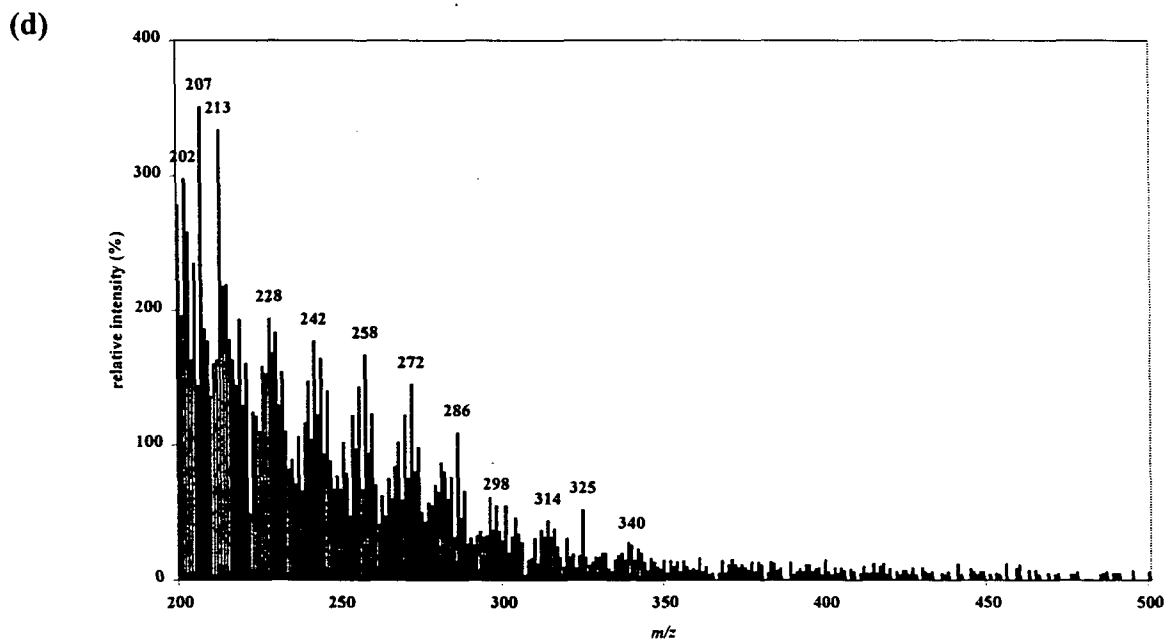
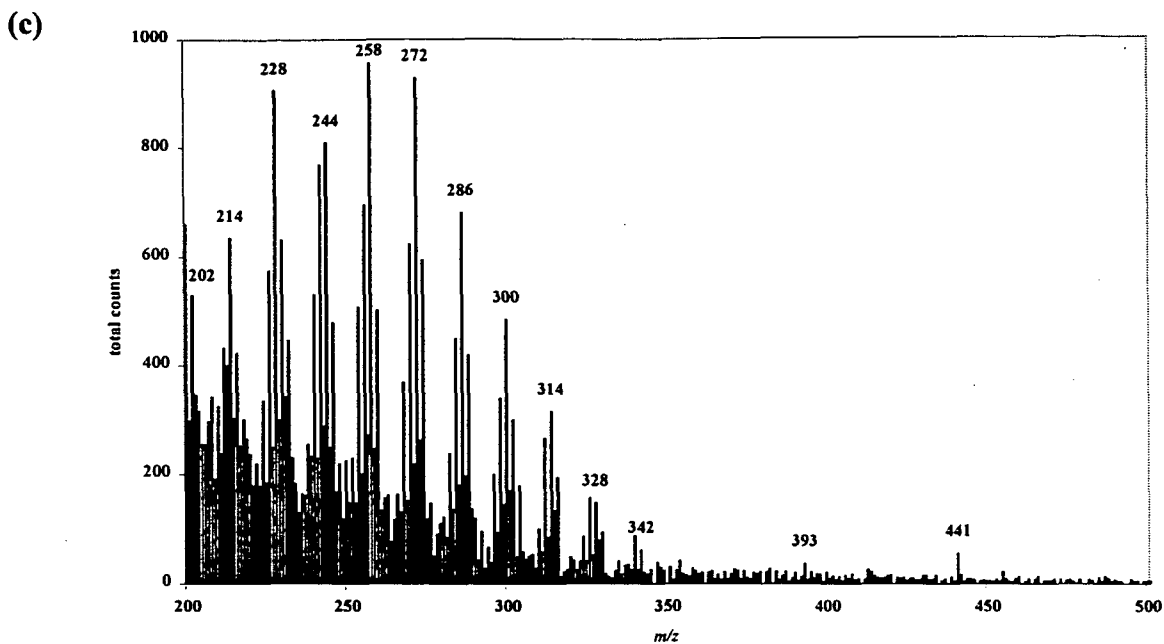


Figure 4.9. Partial ToF-SIMS positive ion mass spectra (200 – 500 amu) of IOM isolated from Rostherne Mere sediments. (a) 7 – 10, (b) 21 – 24, (c) 59 – 62, (d) 82 – 85 cmbswi.

4.3.3. Monitoring the isolation of IOM from Kimmeridge Clay

Pyrograms from the Py-GC-MS analysis of untreated Kimmeridge Clay and IOM isolated from the same substrate are presented in Figure 4.10 i-iii. The untreated Kimmeridge Clay and IOM both contained homologous series of *n*-alkanes and *n*-alk-1-enes with chain

lengths extending from C₇ – C₂₆ in the untreated sample and to C₇ – C₃₂ in the IOM. In the latter instance, this range was similar to the C₄ – C₃₀ range reported by Boucher *et al.* (1990) for kerogen obtained from Dorset Kimmeridge Clay and typical of an immature Type II kerogen. Other prominent components of both pyrograms were benzenes (methylated, C₁ – C₄ and alkylated, C₂ – C₃), naphthalenes (dihydromethyl-, and mono-, di- and trimethyl-), thiophenes (methylated, C₁ – C₃; alkylated C₂ – C₃; and methylbenzo- and dibenzo-), indenes and fluorene. Few differences between the minor components of the untreated material and IOM could be unambiguously identified, principally owing to the relatively large unresolved fraction below the baseline. The unresolved region was observed to become more pronounced in the IOM pyrogram with maxima eluting later than observed for the untreated sediment. This indicated that either lower molecular weight material had been removed during the sequential isolation with a concomitant relative increase in the unresolved component or that artefactual material (*e.g.* melanoidin-like) had been produced.

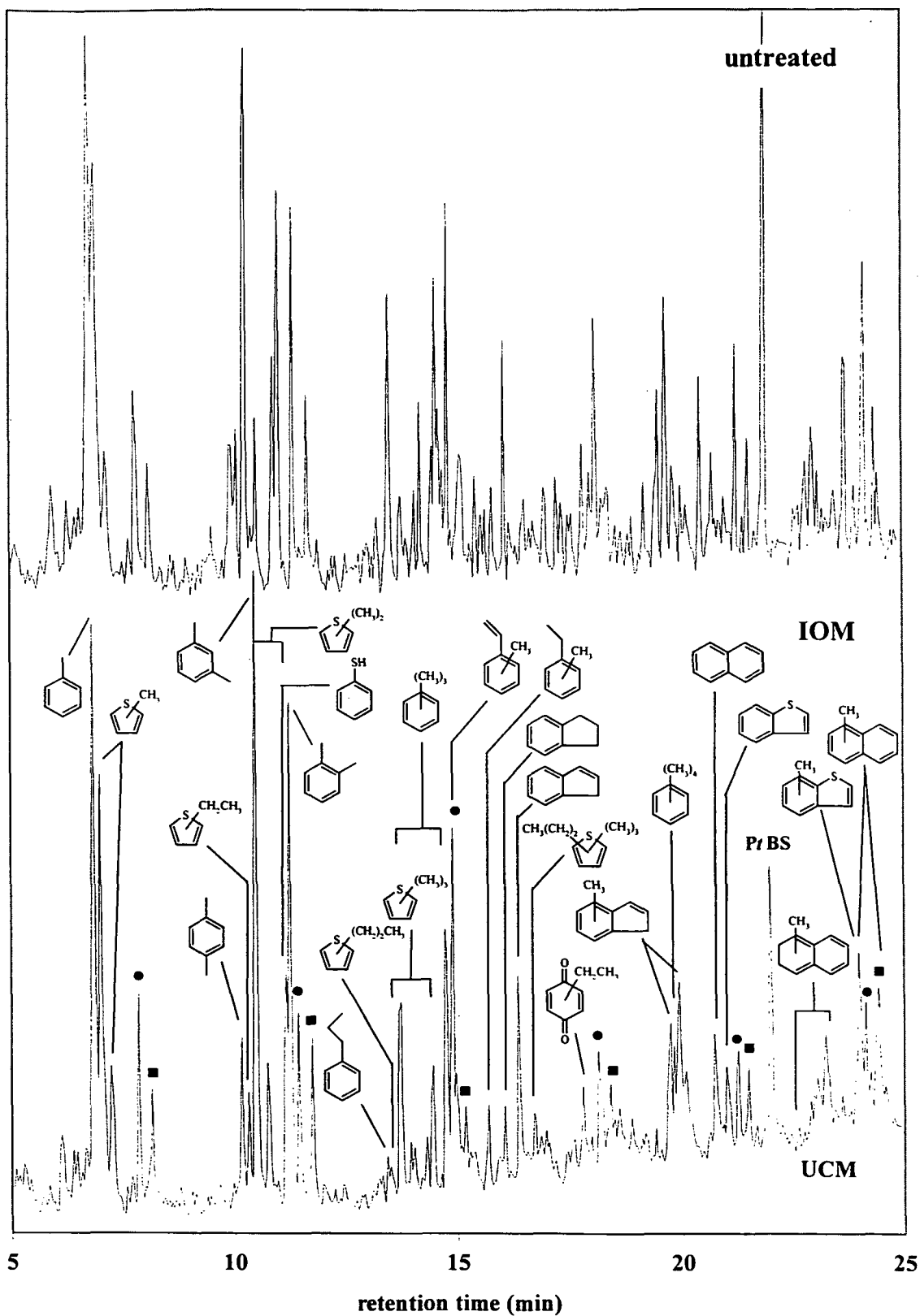


Figure 4.10 i. Reconstructed total ion chromatograms (5 – 25 min) from the Py-GC-MS of untreated Kimmeridge Clay (upper) and 'IOM' isolated from the same sample (lower) normalised to toluene (● *n*-alk-1-ene; ■ *n*-alkane).

cont. overleaf

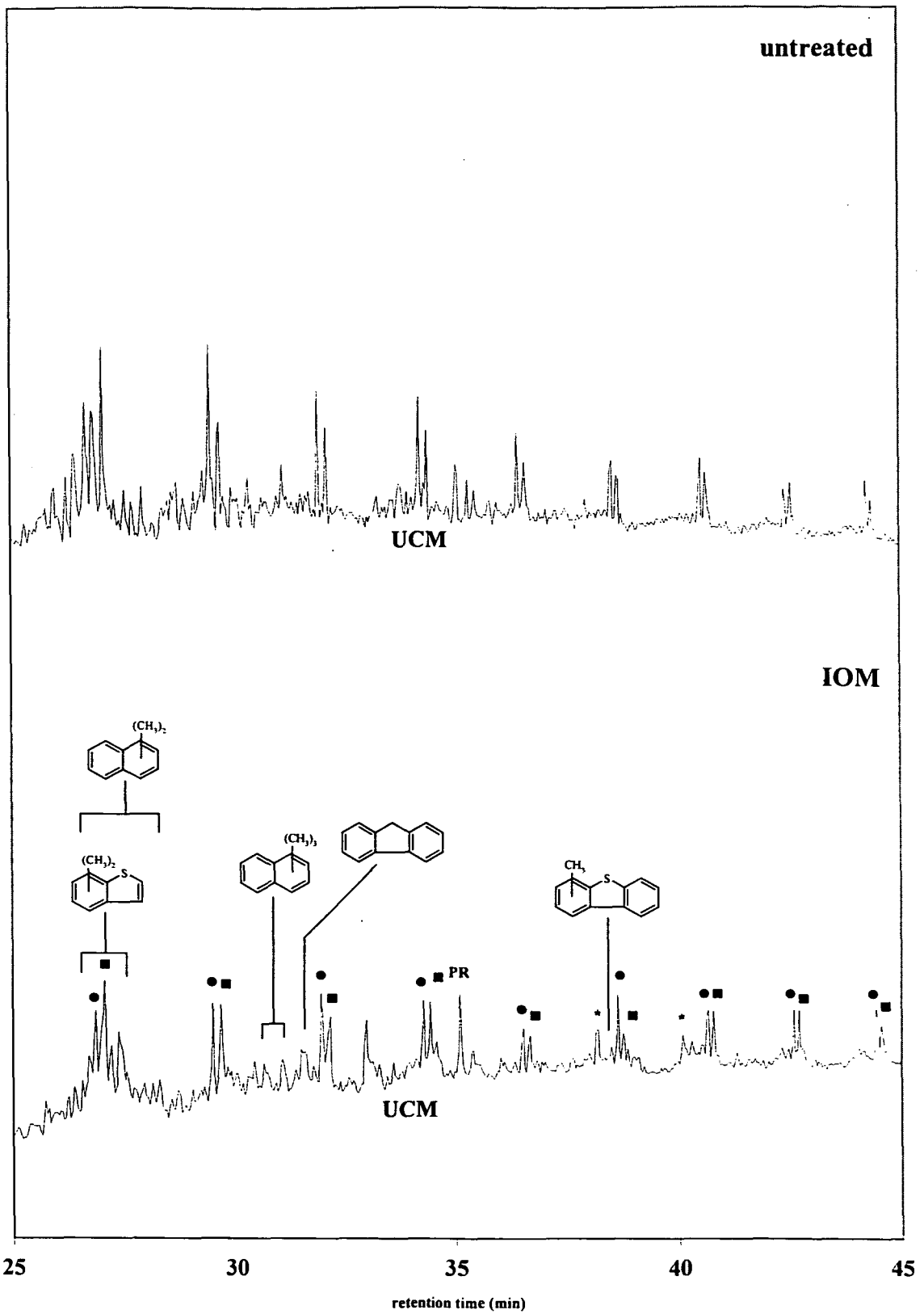


Figure 4.10 ii. Reconstructed total ion chromatograms (25 – 45 min) from the Py-GC-MS of untreated Kimmeridge Clay (upper) and 'IOM' isolated from the same sample (lower) normalised to toluene (● *n*-alk-1-ene; ■ *n*-alkane; PR prist-1-ene; * phthalate).

cont. overleaf

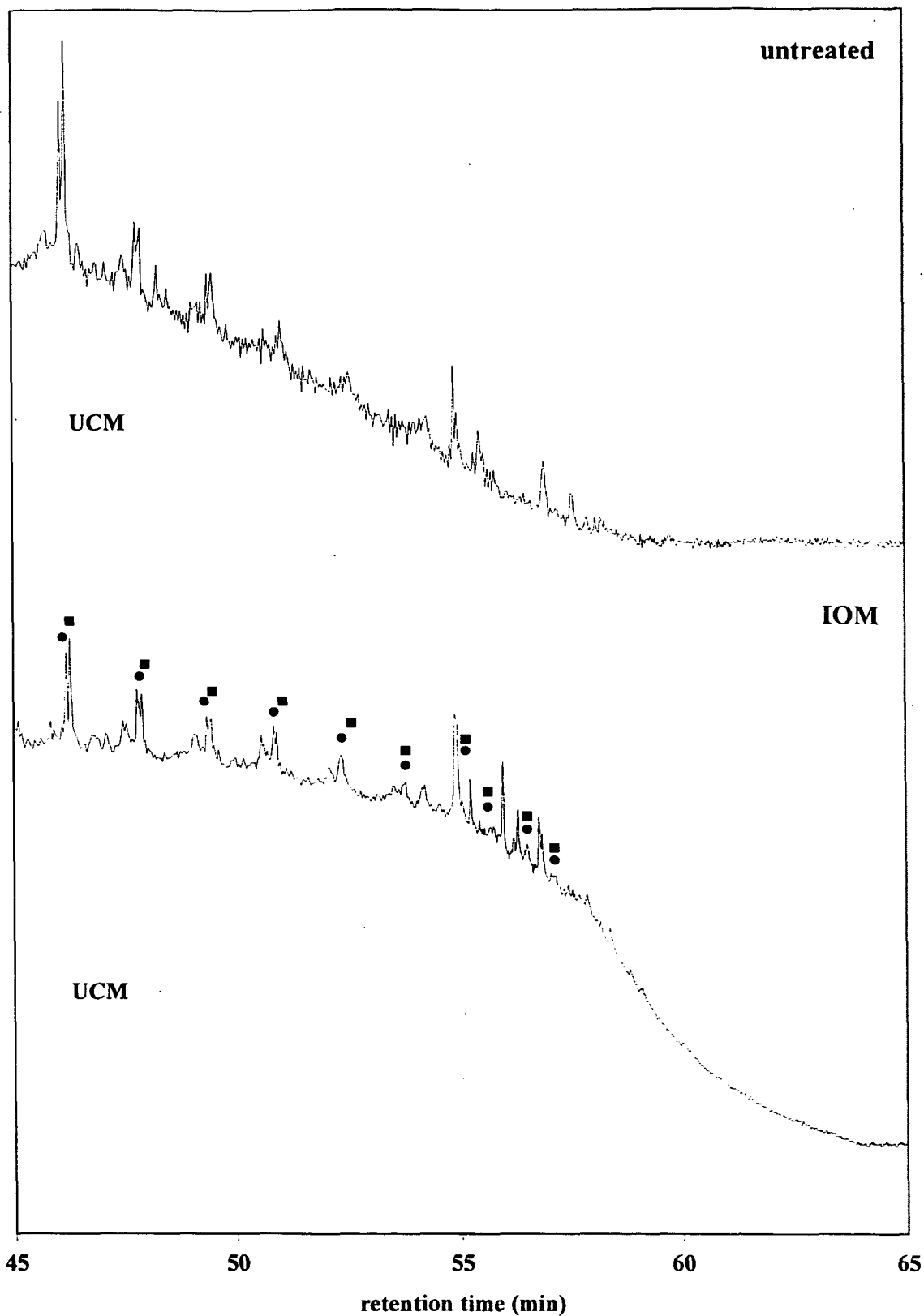


Figure 4.10 iii. Reconstructed total ion chromatograms (45 – 65 min) from the Py-GC-MS of untreated Kimmeridge Clay (upper) and 'IOM' isolated from the same sample (lower) normalised to *n*-tricosane (● *n*-alk-1-ene; ■ *n*-alkane).

Background-subtracted averaged mass spectra (3 – 65 min; Figure 4.11) from the pyrograms of untreated Kimmeridge Clay and the isolated IOM clearly demonstrated the general increase in molecular weight associated with the IOM. Two clusters of ions centred around $m/z = 331$ and 341 in the averaged spectrum of the IOM were absent from the spectrum of the untreated sediment. This may have been indicative of the formation of higher molecular weight material than was present in the untreated sample (*i.e.* artefacts) or merely reflect an alternative fragmentation pathway of the IOM during pyrolysis.

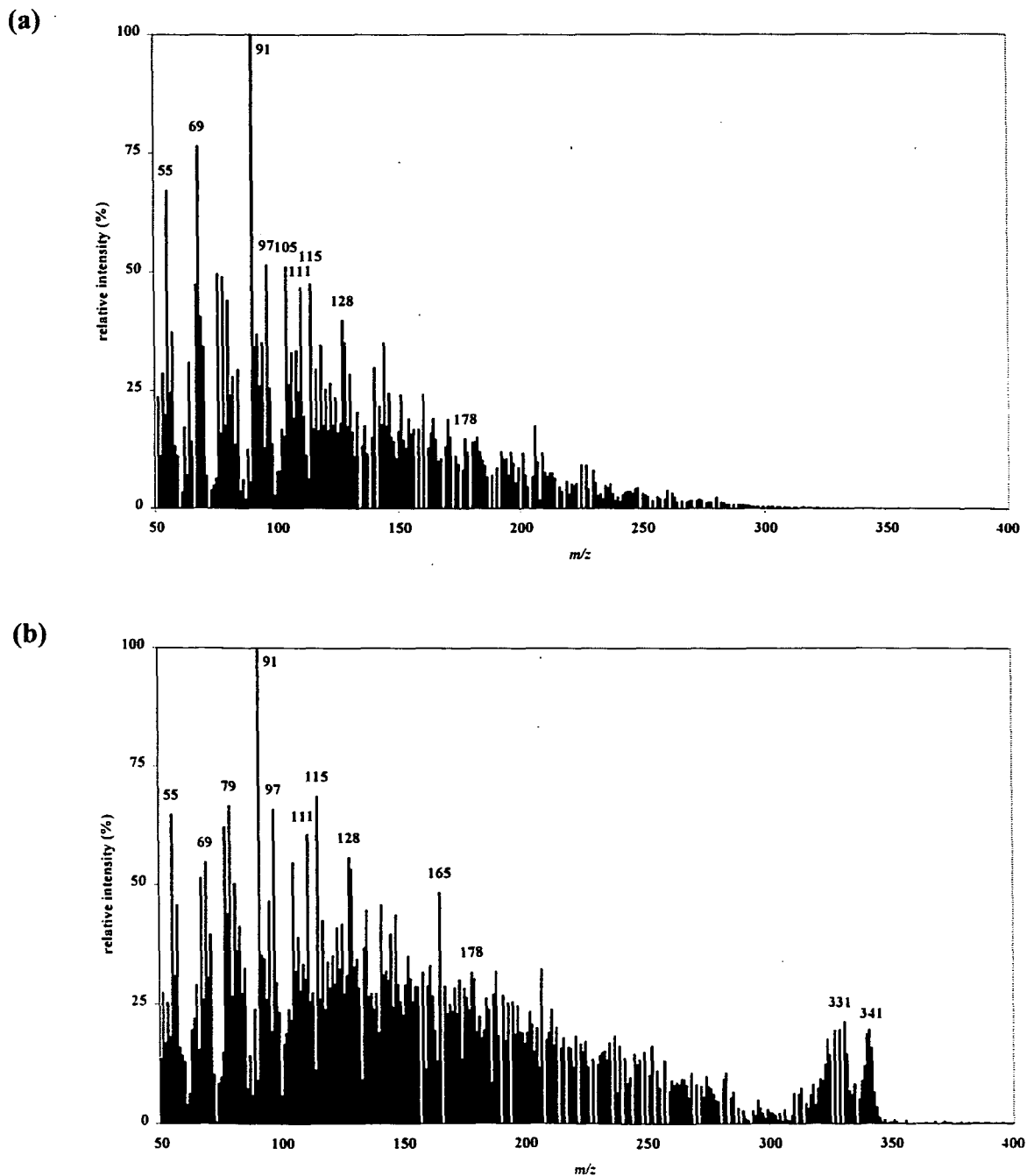


Figure 4.11. Background subtracted averaged mass spectra (5 – 65 min) of pyrograms obtained from the Py-GC-MS of (a) untreated Kimmeridge clay and (b) 'IOM'.

The ToF-SIMS positive ion mass spectrum of untreated Kimmeridge Clay (Figure 4.12a) was similar to those of untreated Rostherne Mere sediments with most of the response attributable to material with molecular mass < 500 amu, little signal between 500 – 1000 amu, and clusters of an apparently homologous series between $m/z = 200 - 314$. Ions at $m/z = 379, 393, 413,$ and 441 were common to the untreated material from both locations (Figures 4.8 and 4.12a) but, as yet, remain unidentified. The clusters of homologues were less well defined in the spectrum of the Kimmeridge Clay IOM (Figure 4.12b), although still apparent, whilst the other ions noted between $m/z = 379$ and 441 were absent from the spectrum of the IOM. Ions at $m/z = 331$ and 431 from the averaged Py-GC-MS spectrum of Kimmeridge Clay IOM were not obvious features of the ToF-SIMS spectrum. This suggested that the appearance of higher molecular weight material in the averaged mass spectrum of the pyrolysis experiment resulted from an alternative fragmentation pathway rather than artefact formation.

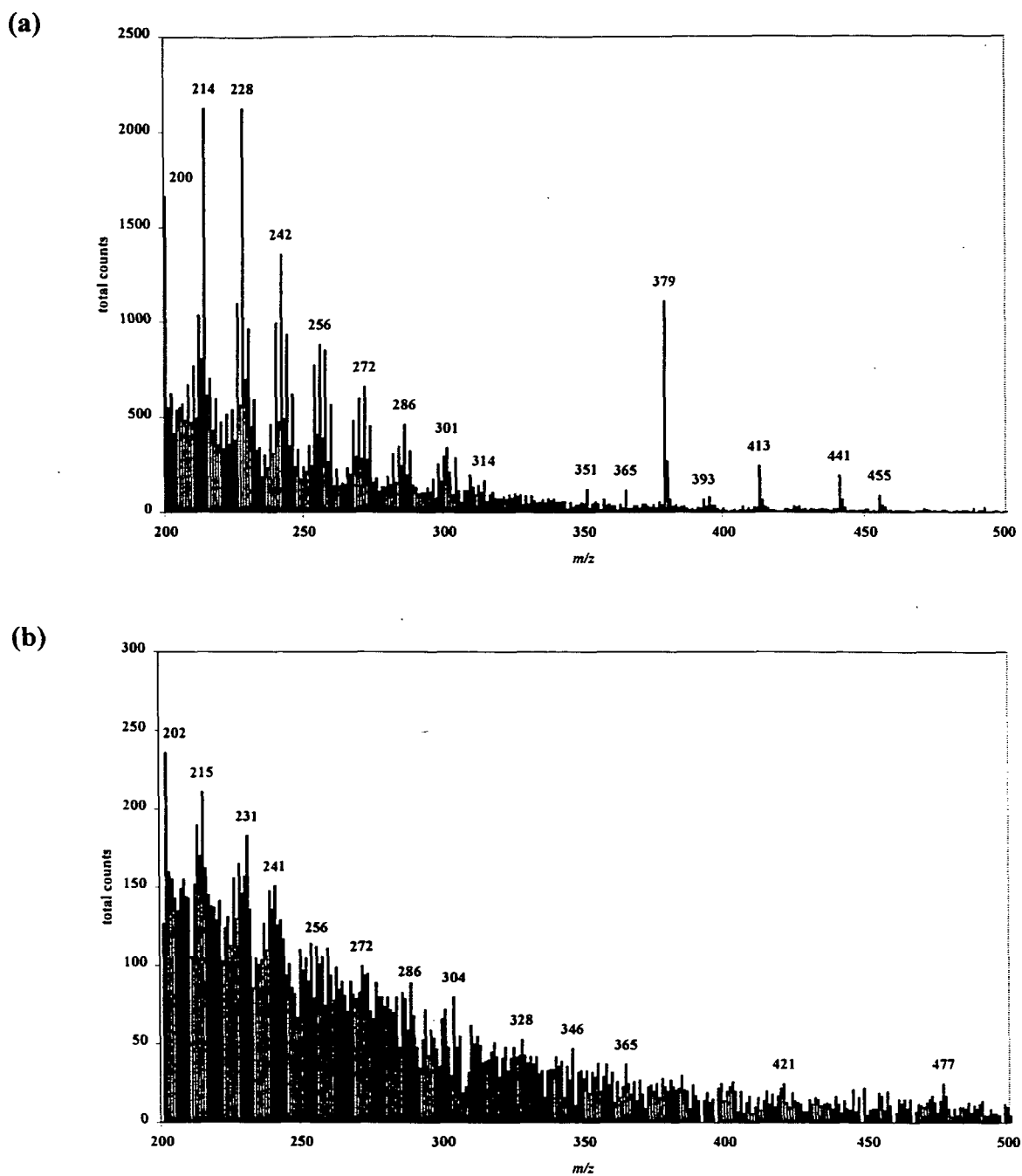


Figure 4.12. Partial ToF-SIMS positive ion mass spectra ($m/z = 200 - 500$) of (a) untreated Kimmeridge Clay and (b) IOM isolated from the same material.

4.3.4. Monitoring the isolation of IOM from *M. jannaschii*

Pyrograms obtained from the Py-GC-MS analysis of untreated *M. jannaschii* and bacterial IOM isolated from the same sample are presented in Figure 4.13. A number of components were common to both pyrograms. These principally comprised methyl and alkyl benzenes, methylnaphthalenes, cyclic and aromatic alcohols, and short-chain branched alkenes.

Alkanes and alkenes were also present in the untreated *M. Jannaschii* and the bacterial IOM but not as homologous *n*-alkane/*n*-alk-1-ene doublets (Figure 4.14). *n*-alkanes from C₁₅ – C₁₈ and prist-1-ene could be distinguished in the *M. jannaschii* IOM pyrogram but not unambiguously identified in the untreated material. Two distinct peaks (RT = 42:27 and 42:33 min) from the untreated sample had similar mass spectra, characterised by alkane/alkene signatures ($m/z = 57, 71, 85$ and $55, 69, 83$), prominent ions at $m/z = 236$, and possible molecular ions at $m/z = 280$ and 321 . Three later eluting peaks (RT = 52:47 – 53:40 min) had a similar mass spectral alkane/alkene signature but contained prominent ions at $m/z = 281$ (typical siloxane ion) and possible molecular ions at $m/z = 419, 417$ and 415 . The most obvious consequence of the sequential isolation was the removal of nitrogen-containing species, *i.e.* pyrroles, pyridines and nitriles, indicative of proteinaceous material, which accounted for 60 % of the original bacterial mass. Other compounds removed during the isolation included precursors of alkylated (C₃ and C_{4:1}) benzenes, indenenes and ethenyl-*bis*-benzene. Although few compounds could be unambiguously identified in either pyrogram beyond 25 minutes, the unresolved region below the baseline was less prominent in the isolated IOM than the untreated bacteria. This was accompanied by a reduction in 'noise'.

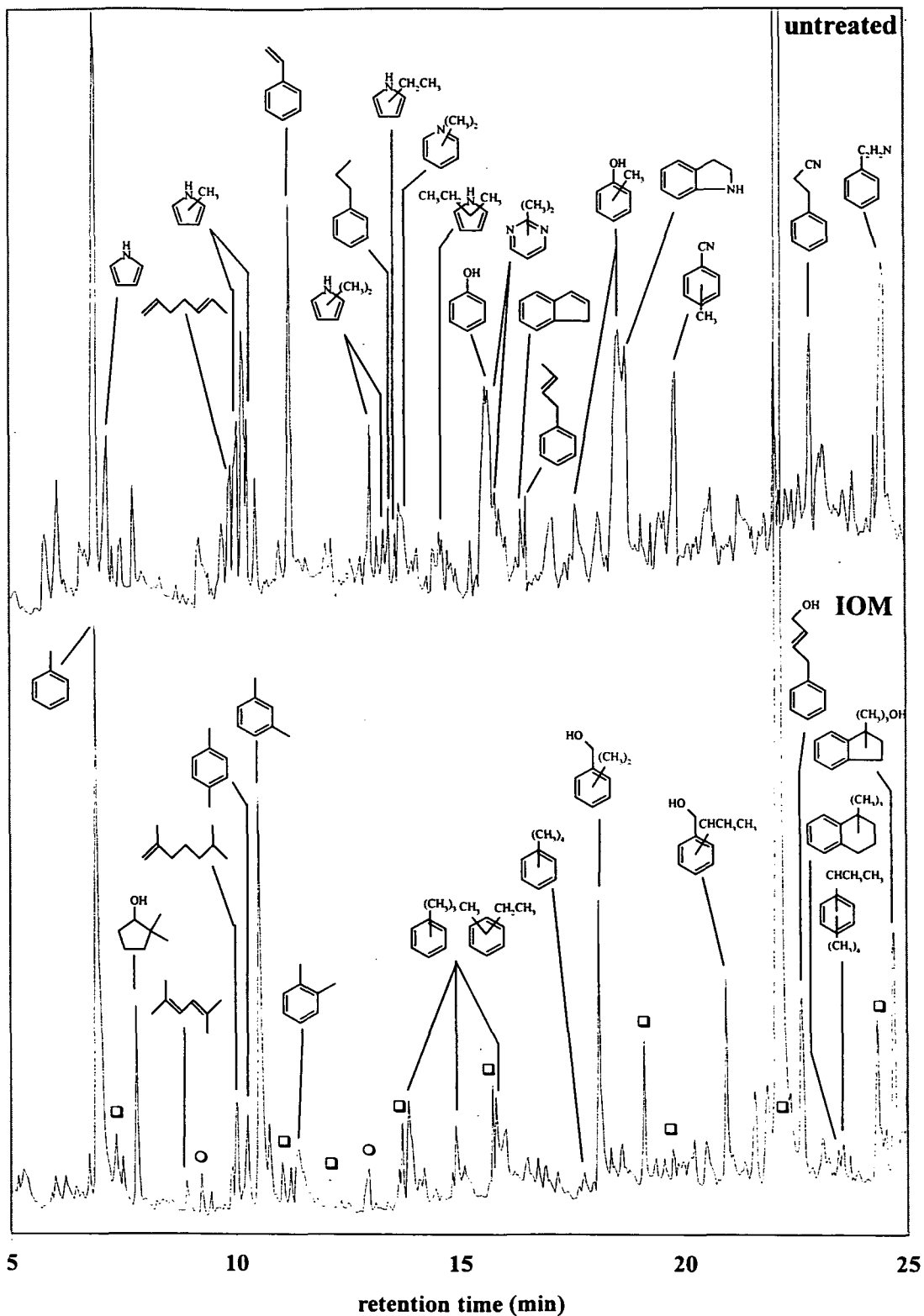


Figure 4.13 i. Reconstructed total ion chromatogram (5 – 25 min) from the Py-GC-MS of untreated *M. jannaschii* (upper) and 'IOM' isolated from the same sample (lower) normalised to toluene (○ alkene; □ alkane).

cont. overleaf

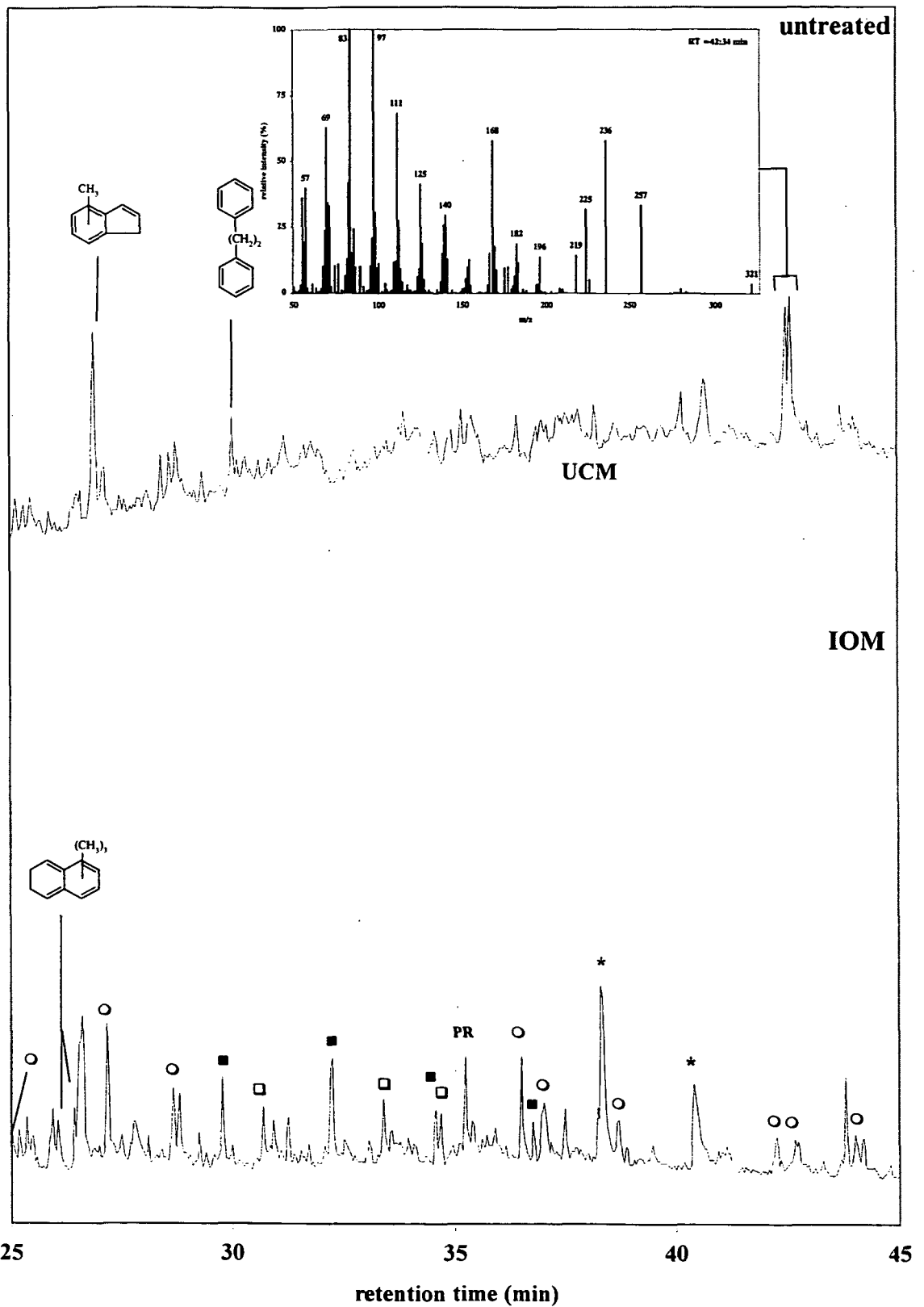


Figure 4.13 ii. Reconstructed total ion chromatogram (25 – 45 min) from the Py-GC-MS of untreated *M. jannaschii* (upper) and 'IOM' isolated from the same sample (lower) normalised to toluene (○ alkene; ■ *n*-alkane; □ alkane; PR = prist-1-ene; * phthalate).

cont. overleaf

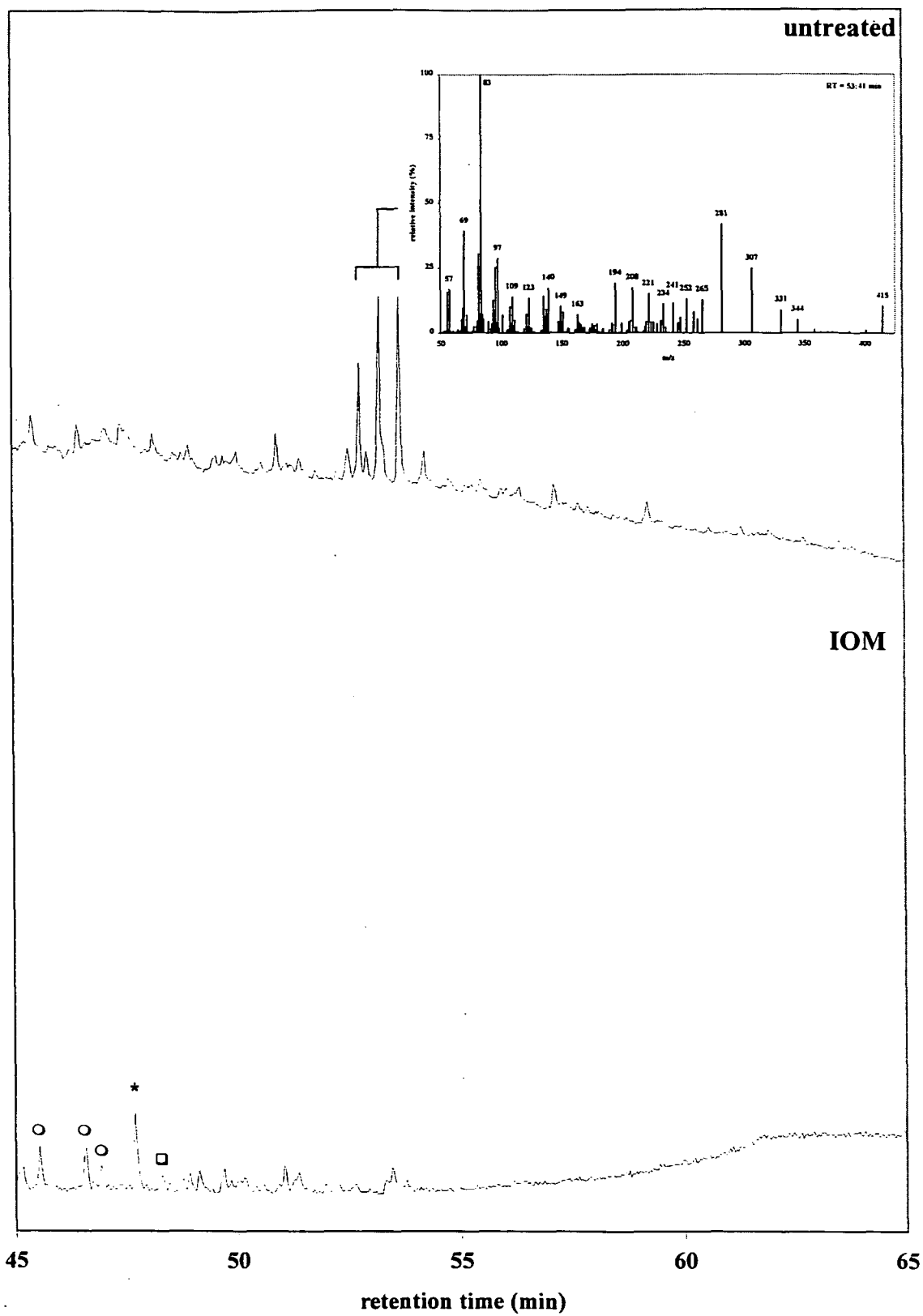


Figure 4.13 iii. Reconstructed total ion chromatogram (45 – 65 min) from the Py-GC-MS of untreated *M. jannaschii* (upper) and 'IOM' isolated from the same sample (lower) normalised to toluene (○ alkene; ◻ alkane; * phthalate).

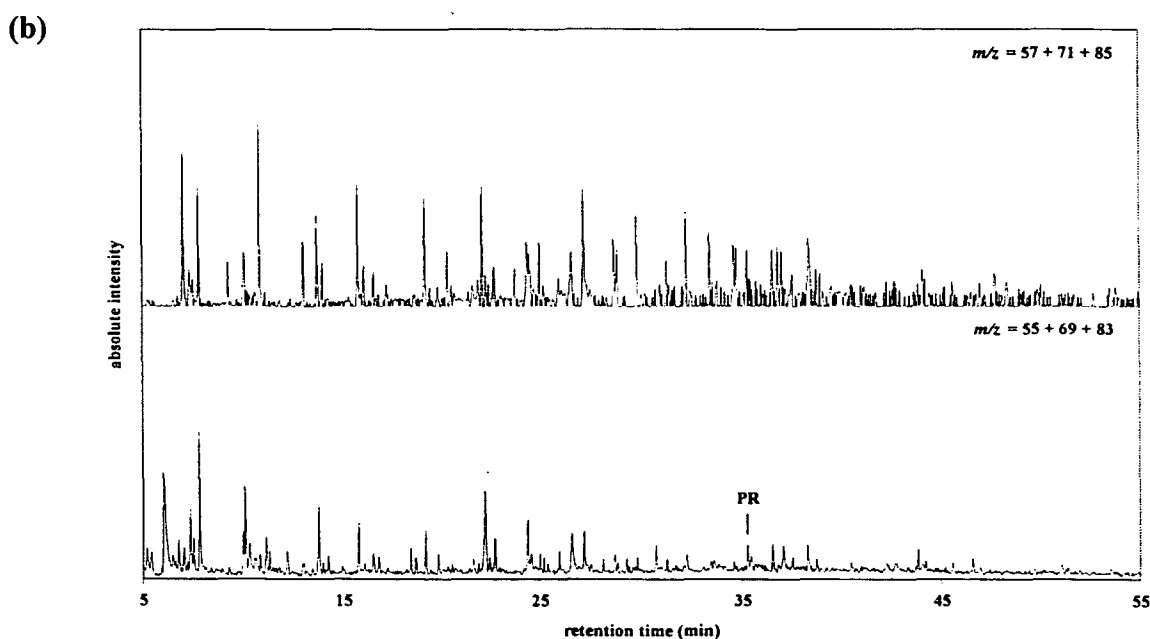
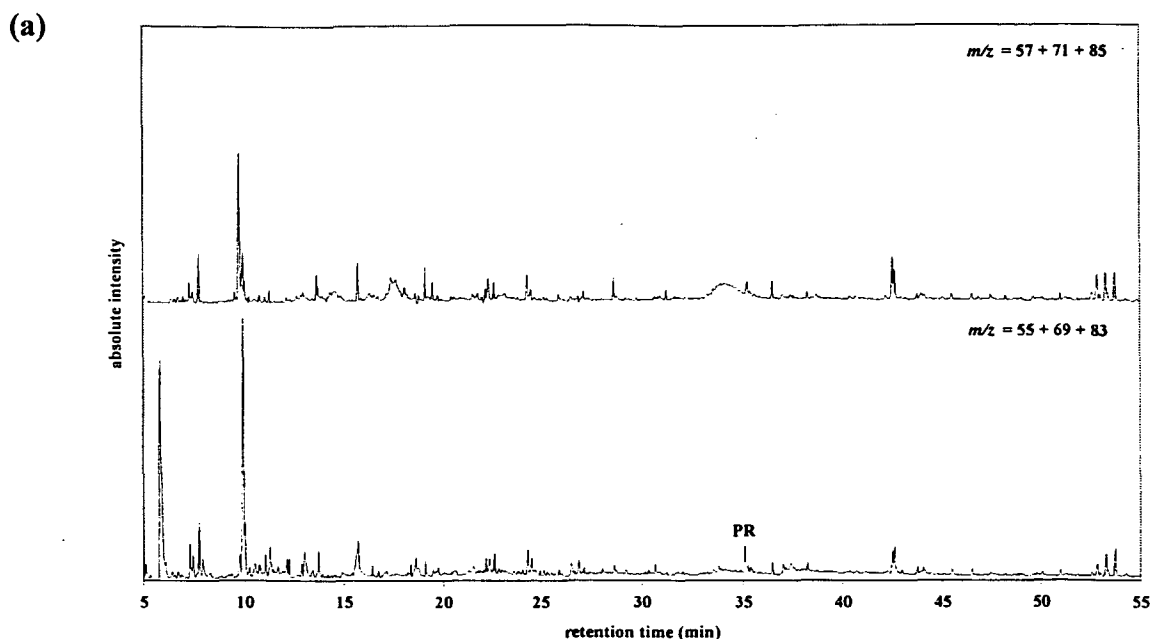


Figure 4.14. Alkane and alk-1-ene ion chromatograms from (a) the Py-GC-MS analysis of untreated *M. Jannaschii* (each vertical scale 1×10^6 counts) and (b) IOM isolated from the sample (each vertical scale 1×10^5 counts). PR = prist-1-ene.

Background subtracted averaged mass spectra from the Py-GC-MS analysis of untreated *M. jannaschii* and the isolated IOM are presented in Figure 4.15. The removal of the major portion of the unresolved fraction during sequential isolation is graphically illustrated by the decreased ion density in the IOM spectrum compared to that of the untreated material.

This inferred that much of the unresolved material comprised compounds with molecular weight < 320 amu. However, *M. jannaschii* is known to contain compounds whose mass exceeded the capabilities of the mass spectrometer used herein (e.g. macrocyclic ether lipids, > 650 amu; Koga *et al.*, 1993) although these are likely to have been fragmented during pyrolysis.

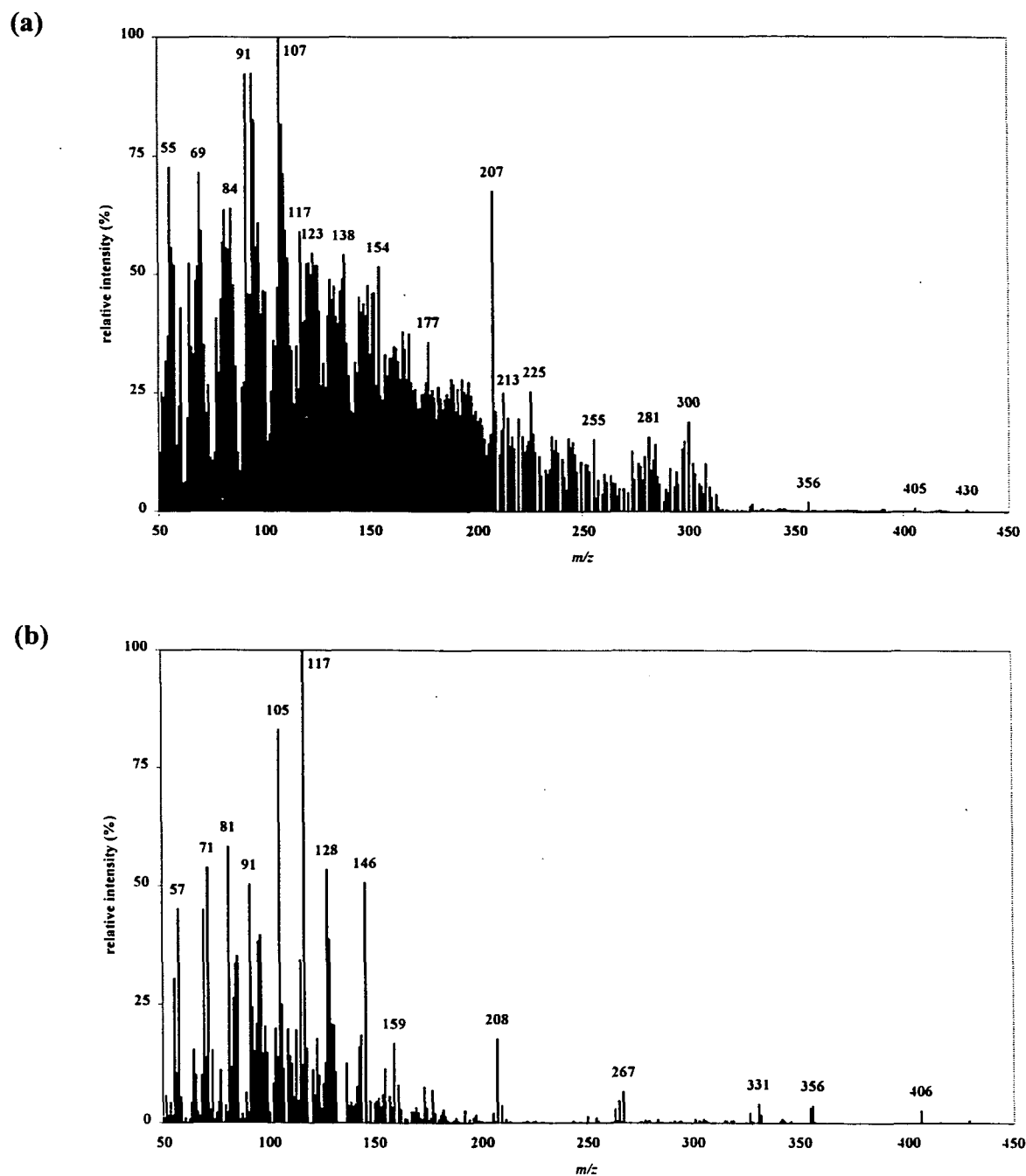


Figure 4.15. Background subtracted averaged mass spectra (5 – 65 min) from the Py-GC-MS of (a) untreated *M. jannaschii* and (b) IOM isolated from the same sample.

The positive ion ToF-SIMS mass spectrum of untreated *M. jannaschii* (Figure 4.16) was characterised by ions between $m/z = 674$ and 981 . These masses did not correspond with those of the structures of macrocyclic archaeol-containing polar lipids previously reported to account for the bulk of lipidic material in *M. jannaschii* (Sprott *et al.*, 1991; Koga *et al.*, 1993) and may therefore represent other lipids or proteins. If these ions at $m/z > 600$ were molecular ions they would not have been detected during Py-GC-MS analysis, whilst if they fragmented sufficiently to be detected using Py-GC-MS the association between the fragmented components would not have been obvious. The ToF-SIMS mass spectrum of IOM isolated from *M. jannaschii* differed substantially to that of the untreated material. Ions at $m/z > 600$ were no longer present indicating the removal of this material during the sequential isolation. However, the appearance of new ions between $m/z = 397$ and 515 suggested that artefactual material may have been formed during the isolation procedure or merely reflected chemical degradation of higher mass components. With such limited information it was difficult to establish any relationship between these ions and those observed in the untreated bacteria. Of the $m/z 200 - 400$ region, three ions centred on $m/z = 261$ in the IOM mass spectrum were two mass units apart, indicative of homologous unsaturations. This cluster was 15.967 mass units less than the next adjacent cluster of four ions around $m/z = 277$, suggesting the loss of an oxygen atom. Similarly ions at $m/z = 413$ and 429 , and at 441 and 457 were each separated by 15.96 mass units. The presence of oxygen-containing species was consistent with aromatic alcohol fragments identified from the Py-GC-MS analysis of the IOM.

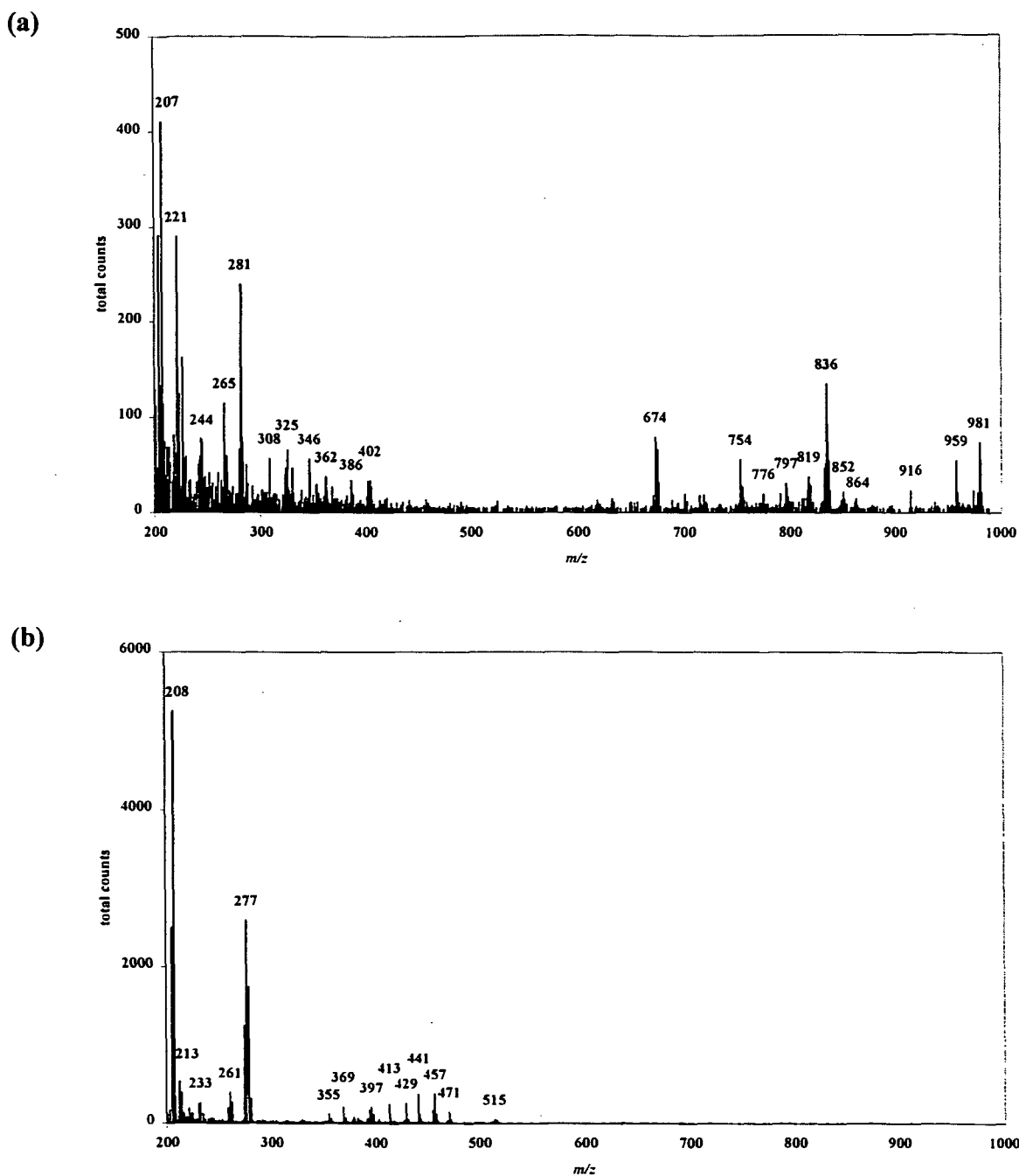


Figure 4.16. Partial ToF-SIMS positive ion mass spectra ($m/z = 200 - 1000$) of (a) untreated *M. jannaschii* and (b) IOM isolated from the same material.

4.4. Summary

- Quantification of resolved and total chromatographic responses obtained from the Py-GC-MS analysis of sediments and bacteria and the IOM isolated from them demonstrated that less than 10% of these substrates were amenable to analysis using this technique.

- Sequential removal of major classes of biochemicals from Rostherne Mere sediment was not substantially reflected in qualitative changes in pyrograms from the Py-GC-MS analysis of sediment samples obtained after each isolation stage.
- The averaged mass spectra of pyrolysis chromatograms and ToF-SIMS spectra provided little evidence for the formation of higher molecular weight material (artefacts) during the sequential isolation of IOM.
- Demineralisation of sedimentary samples elicited the most striking changes in Py-GC-MS pyrograms, principally, an extension of the carbon number range of homologous series of *n*-alkanes and alk-1-enes.
- Background subtracted averaged mass spectra of pyrograms allowed rapid identification of changes in the bulk composition of samples.
- Recent and ancient sediments and the IOM isolated from them produced a number of common pyrolysis products, *n*-alkane and alk-1-ene series, phenols, methyl and alkylbenzenes, indenes, naphthalenes and fluorene. Pyrroles and furans in the untreated Rostherne Mere sediments were not observed in the untreated Kimmeridge Clay indicative of their different maturities or source inputs. Thiophenes were a prominent constituent of the Kimmeridge Clay IOM.
- ToF-SIMS analysis of untreated sediments and sedimentary IOM provided little evidence of the presence of material with molecular weight exceeding 500 amu. Furthermore, ToF-SIMS analysis indicated that the alkane/alkene series determined using Py-GC-MS may have been ether linked in the sediment matrix.

- IOM isolated from the methanogenic bacterium *M. jannschii* produced mainly methyl and alkyl benzenes, phenols and naphthalenes upon pyrolysis. ToF-SIMS analysis indicated that components of *M. jannschii* IOM generally had molecular weights of < 500 amu whereas the untreated bacterium contained components having a molecular weight of at least up to 980 amu, judging from literature reports.

Chapter 5: Synthesis and characterisation of insoluble melanoidins

5.1. Introduction

This chapter describes the quantitative preparation of insoluble melanoidins from mixtures of amino acids and glucose in aqueous and acidic media. The melanoidins were reused for dissolution experiments using ionic liquid, [emim]Cl-AlCl₃ {X(AlCl₃), X = 0.65} (Chapter 6). Melanoidin syntheses were carried out under these conditions to reflect chemical conditions used in the sequential isolation procedures used to obtain IOM from biota and recent and ancient sediments (Chapter 2), and also to assess their potential contribution to the production of artefactual material during the isolation procedure as inferred by Allard *et al.* (1997). Synthesised insoluble melanoidins were characterised using Py-GC-MS and IR spectroscopy to provide a comparison with the IOM isolated from sediments and biota.

Melanoidins comprise a group of ill-defined complex high molecular weight (*e.g.* 10000 – 30000 amu; Rubinsztain *et al.*, 1984) macromolecules formed from the condensation of sugars with amino acids, *via* the Maillard reaction (Maillard, 1913). Polymeric materials formed in this way generally comprise soluble and insoluble polymers, the latter of which form the focus of this review. The geochemical importance of melanoidins lies in their reported chemical, spectroscopic (¹³C solid-state NMR and IR) and pyrolytic (*e.g.* Py-GC-MS) similarity to organic residues found in soils (Wershaw *et al.*, 1990; Saiz-Jimenez, 1992) and sediments (Larter *et al.*, 1983; Engel *et al.*, 1986; Suzuki & Philp, 1990; Wershaw *et al.*, 1990; Saiz-Jimenez, 1992; Almendros *et al.*, 1997). These similarities have been used to support the suggestion that naturally occurring Maillard-type reactions are responsible for the formation of organic geopolymers in these media. Conversely, the formation of artefactual melanoidin-like material during the isolation of insoluble organic matter from bacteria has been reported to account for the bulk of the insoluble residue (Allard *et al.*, 1997). The term pseudomelanoidin has been used to describe melanoidin-like polymers produced from sugars alone under the same reaction conditions used for melanoidin synthesis (Rubinsztain *et al.*, 1984).

Many researchers have synthesised and analysed melanoidins (e.g. Larter *et al.*, 1983; Rubinsztain *et al.*, 1984; Engel *et al.*, 1985; Hayase *et al.*, 1986; Rubinsztain *et al.*, 1986; Suzuki & Philp, 1990; Wedzicha & Kaputo, 1992; Cämmerer & Kroh, 1995; Alemendros *et al.*, 1997). Some authors have considered that the chemistries of melanoidin products arising from these experiments are dependent upon the initial reactants and reaction conditions (Ikan *et al.*, 1996), whilst others maintained that they are not (Wedzicha & Kaputo, 1992; Cämmerer & Kroh, 1995). Only a few workers have reported the quantitative isolation or characterisation of the insoluble residues associated with melanoidin synthesis. Larter *et al.* (1983), for example, reported that 20 – 30 % of the starting material formed an insoluble residue (*i.e.* not aqueous or solvent extractable) after the alkaline condensation (pH 8, 100 °C, 350 h) of glucose with amino acids and lipid (phytol). In many other cases, soluble products of melanoidin synthesis have been deemed analogous to humic and fulvic acid fractions, dried and examined as if they were insoluble solids (Rubinsztein *et al.*, 1986; Milić, 1987; Cämmerer & Kroh, 1995; Almendros, 1997). In fact, insoluble melanoidins are likely to account only for part of the products formed *via* the Maillard reaction of carbohydrates and amino acids present in a sediment or biological substrate.

Melanoidins have previously been synthesised under various acidic (Hayase *et al.*, 1986; Wedzicha & Kaputo, 1992; Cämmerer & Kroh, 1995; Alemendros *et al.*, 1997), basic (Ioselis *et al.*, 1983; Larter *et al.*, 1983; Engel *et al.*, 1986; Rubinsztain *et al.*, 1986; Milić, 1987), or neutral conditions (Suzuki & Philp, 1990). These procedures were carried out by combining the reactants dissolved in aqueous solution.

The IOM isolation procedure applied to sediments and biota in the current study (Chapter 2) included an aqueous extraction stage designed to remove aqueous soluble saccharides,

amino acids (*e.g.* sucrose, glycine) and other water-soluble products. Likewise, proteinaceous material should have been removed as amino acids during the acid hydrolysis of ‘proteins’ prior to the alkaline ‘bound lipid’ removal stage. Nevertheless, conceding that the sequential digestion procedure was not entirely exhaustive, it can be speculated that some carbohydrate and amino acid material remained following ‘carbohydrate’ removal (Section 2.3.5) providing the potential for melanoidin formation. However, poor yields reported for insoluble melanoidins (4 – 30 %; Larter *et al.*, 1983; Rubinsztain *et al.*, 1984) produced *via* alkaline synthesis, exacerbated by the relatively small amounts of starting materials and the limited treatment period used in the present study, suggest that this would provide only a minor contribution to the isolated IOM during this extraction stage. Therefore, the greatest potential for melanoidin production during the sequential digestion procedure existed at the ‘protein’ digestion stage (Section 2.3.4) prior to the removal of the reactants necessary for melanoidin formation. For this reason a series of melanoidins was synthesised under acidic conditions in order to test whether insoluble melanoidin-like artefacts could be formed during the ‘protein’ removal stage of the digestion procedure. The products from these experiments were extracted with water and solvent, and insoluble residues analysed by Py-GCMS and subjected to ionic liquid treatment (Sections 4.2.1 and Chapter 6, respectively).

5.2. Experimental procedures

General laboratory procedures were as previously described in Section 2.3.1. Amino acids: glycine (Gly); histidine (His); lysine (Lys); and arginine (Arg), used in the synthesis of melanoidins were Sigma Ultra titration grade (> 99 %). D-(+) glucose (Glu) was Sigma Ultra HPLC grade (> 99.5 %). These compounds were used as supplied.

5.2.1. Aqueous synthesis of insoluble melanoidins

A series of mixtures of amino acids and glucose, a mixture of several amino acids with glucose, and a glucose procedural blank (Table 5.1) were made up in water (Milli-Q) and the pH recorded before reflux (100 °C, 150 h). After cooling, the products were frozen and freeze-dried before weighing.

Table 5.1. Composition and pH of mixtures of amino acids and glucose used in the attempted aqueous synthesis of insoluble melanoidins

Reactants	Mole ratio	pH
Glu	1 M	7
Gly/Glu	1 : 1	8
His/Glu	1 : 1	14
Lys/Glu	1 : 1	14
Arg/Glu	1 : 1	7
Gly/His/Lys/Arg/Glu	1 : 1 : 1 : 1 : 4	12

Approximately 2 g of residual material obtained from each mixture was weighed into a boiling tube and water added (Milli-Q, 20 ml). Samples were shaken (15 min, Gallenkamp autosshaker) and centrifuged (15 min, 2000 rpm) prior to removing the supernatant by decanting (Gly/Glu) or vacuum filtration through a sintered glass filter (all other samples). Residual material remaining after aqueous extraction was frozen and freeze-dried, and reweighed. Freeze-dried residual material from aqueous extracted Gly/Glu and His/Glu mixtures (other combinations of amino acids and glucose did not yield insoluble products) was extracted with solvent (MeOH, MeOH/DCM, DCM, 3 x 10 ml) by shaking (15 min, Gallenkamp autosshaker), centrifugation (15 min, 2000 rpm) and decanting the supernatant. Residual material was oven dried (50 °C, overnight) before reweighing.

5.2.2. Acidic synthesis of insoluble melanoidins

Acid (50 ml, HCl, 6M) was added to equimolar mixtures of Gly/Glu and His/Glu weighed into round bottom flasks and refluxed for 44 h (110 °C). After reflux, the mixtures were vacuum filtered through sintered glass filters and washed with water (Milli-Q) until the filtrate ran clear. Residual material was frozen and freeze-dried before reweighing. Aqueous extracted material was weighed into a boiling tube and refluxed with solvent (*ca* 15 ml, DCM, 2 x 24 h). After solvent extraction the supernatant was decanted to a round-bottom flask, rotary evaporated to near dryness and transferred to a pre-weighed vial, complete with washings. The extract was blown down to dryness (N₂) and re-weighed.

5.2.3. Pyrolysis-gas chromatography-mass spectrometry

Insoluble melanoidins were analysed using Py-GC-MS. Instrumental details, operating conditions and sample preparation details were as described in Section 4.2.1.

5.2.4. Infrared spectroscopy

Infrared spectroscopic analysis of solid melanoidin samples was carried out as detailed in Section 3.2.4.

5.3. Results

5.3.1. Insoluble melanoidins synthesised in water

All of the mixtures of amino acids and glucose turned dark brown within twelve hours of the commencement of heating, whilst the glucose procedural blank changed from clear to pale yellow. This 'browning' is typical of Maillard-type reactions involving the condensation of sugars and amino acids (*e.g.* Rubinsztain *et al.*, 1984). The product yields following the aqueous reflux of amino acids with glucose and their subsequent aqueous and solvent extraction are presented in Table 5.2. Whilst the yield of material produced by the aqueous reflux of amino acid and glucose mixtures ranged from 65 – 81 % of the initial

mass of reactants, with the exception of Gly/Glu and His/Glu mixtures, this material was entirely aqueous soluble. Pseudo-melanoidins, possibly produced during the reflux of glucose alone, were entirely soluble. Material remaining after the aqueous extraction of Gly/Glu and His/Glu reflux products was poorly soluble in solvent, such that 22 % of the original mass of Gly/Glu and 14 % of the His/Glu reactants could be considered as insoluble. Previously Rubinsztain *et al.* (1984) reported yields of 4 to 14 % for various reactant ratios of Gly/Glu melanoidins synthesised under alkaline conditions, whilst Larter *et al.* (1983) reported yields of 20 – 30 % of acid-insoluble melanoidins from the alkaline heating of mixtures of glucose, protein and lipid.

Table 5.2. Product yields of melanoidins synthesised in aqueous solution

Composition	Product yield (% of initial mass of reactants)		
	Post reflux	Post aqueous extraction	Post solvent extraction
Glu	117	--	--
Gly/Glu	65	26	22
His/Glu	76	15	14
Lys/Glu	74	--	--
Arg/Glu	81	--	--
Gly/His/Lys/Arg/Glu	65	--	--

5.3.2. Melanoidins synthesised in acid

Both mixtures of amino acid and glucose subject to acid reflux changed from clear to dark brown solutions within thirty minutes of commencement of heating, a change typical of the Maillard reaction. Material remaining after aqueous washing of the reflux products comprised 13 % and 10 % of the Gly/Glu and His/Glu starting materials, respectively. Solvent extraction failed to solubilise any of this residue which was a fine dark-brown

powder in both cases. Product yields of Gly/Glu and His/Glu melanoidins are presented in Table 5.3.

Table 5.3. Product yields of melanoidins synthesised in acid solution

Composition	Product yield (% of initial mass of reactants)	
	Post acid reflux and aqueous extraction	Post solvent extraction
Gly/Glu	13	13
His/Glu	10	10

Insoluble melanoidins produced *via* acid synthesis were adjudged to provide a better reflection of the potential formation of artefactual material during the sequential digestion procedure. This was because the aqueous extraction used in the sequential digestion was fairly rapid (2 x 15 min) and did not involve sample heating, whilst the protein extraction stage involved extensive reflux under acid conditions (6 x 4 hr, 6 M HCl). For these reasons the acid-synthesised insoluble melanoidins were analysed further rather than those synthesised in water.

The potential for melanoidin-like material to be formed during the sequential digestion procedure was estimated by multiplying the percentage mass of material remaining after the 'protein' removal stage by the greatest melanoidin yield. As the 'protein' fraction of Rostherne Mere sediments accounted for 20 – 40 % of the initial dry sediment weight, residual material remaining after this stage accounted for 60 – 80 %. Therefore, 8 – 10 % of post-'protein' extracted material may have comprised melanoidin-like compounds. However, Py-GC-MS analysis of material before and after the 'protein' removal stage (Section 4.3.2) provided little evidence to support such a pessimistic estimate.

5.3.3. Analysis of amino acids, glucose and melanoidins using pyrolysis-gas chromatography-mass spectrometry

Unreacted amino acids (glycine and histidine) and glucose were analysed using Py-GC-MS (Figures 5.1 – 5.3). Pyrolysis chromatograms from these analyses generally contained relatively few peaks. Many of these peaks were poorly resolved, indicating the presence of polar functional groups, *i.e.* carboxylic acids (RCOOH), aldehydes (RCOH) and ketones (RCOR). The entire chromatographic response, including the area below the baseline, accounted for 3 – 7 % of the pyrolysed sample masses. In each case around half of the total chromatographic response was attributable to (partially) resolved components.

The pyrogram of glycine (Figure 5.1) was characterised by the presence of nitriles, pyrrole, glycyglycine and 2,5-diketopiperazine. Three other components (peaks A1 – A3) could not be unambiguously identified from their mass spectra. The mass spectrum of peak A1 had an ion at $m/z = 70$, but no obvious parent ion above this mass, and therefore could not be rationalised with the structure of glycine. Similarly, the mass spectrum of peak A2 provided little structural information other than an intense ion at $m/z = 42$, indicative of a more volatile compound than suggested by the retention time. The mass spectrum of peak A3 had an intense ion at $m/z = 128$ and fragment ions characteristic of an alkyl substituted compound ($m/z = 57, 71, 85$), possibly an alkyl substituted naphthalene. Previously, Chiavari & Galletti (1992) using a similar Py-GC-MS method but operated at 70 eV found that glycine produced only rapidly eluting volatile fragments that were of little diagnostic value. However, the presence of 2,5-diketopiperazine is consistent with their proposed general fragmentation pathway of an initial decarboxylation of two glycine units, followed by a double dehydration and subsequent combination of the two fragments (Chiavari & Galletti, 1992). These workers also reported the formation of hydrocarbons and/or substituted hydrocarbons *via* the homolysis of the amino acid aliphatic chain, which is not inconsistent with the mass spectrum of peak A3.

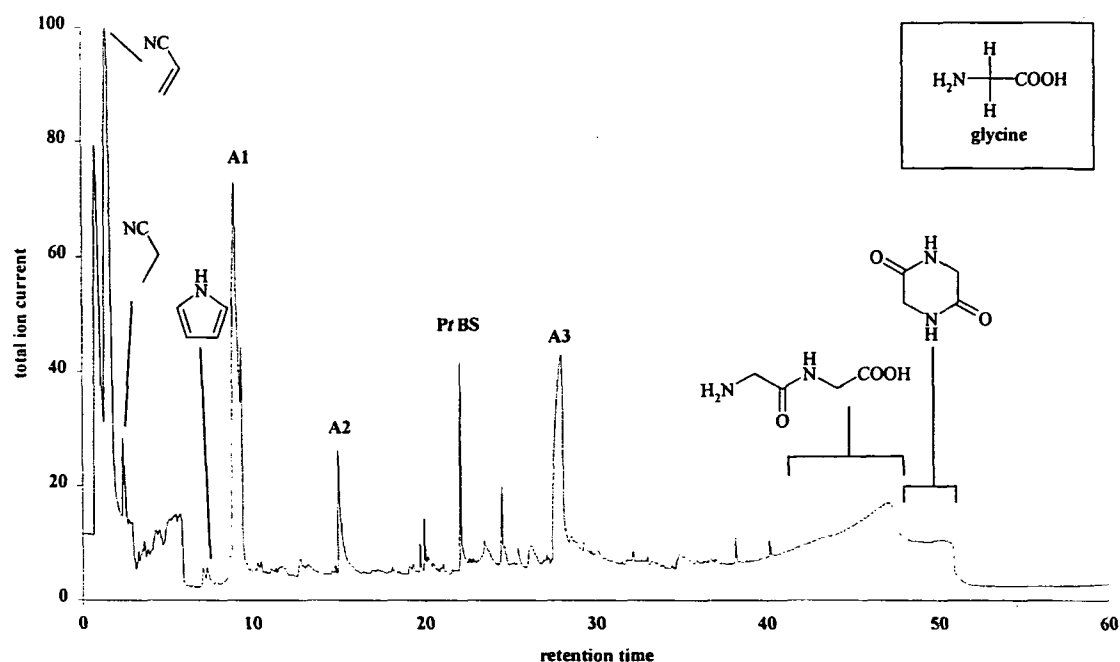


Figure 5.1. Py-GC-MS TIC of glycine (pyrolysis at $595\text{ }^{\circ}\text{C} \pm 5\text{ }^{\circ}\text{C}$, 1 min; GC programme, -10 to $300\text{ }^{\circ}\text{C}$ at $5\text{ }^{\circ}\text{C min}^{-1}$, hold at $300\text{ }^{\circ}\text{C}$ for 10 min; Rtx-5 column; MS operated at 40 eV).

Amongst the compounds identified in the pyrogram from the Py-GC-MS analysis of histidine (Figure 5.2) were nitriles, pyrrole and imidazoles. The single most important peak was assigned as methylimidazole rather than methylpyrazole, which has a comparable mass spectrum, because it could be more readily reconciled with fragmentation of histidine *via* β -scission during pyrolysis. A number of peaks could not be readily identified from their mass spectra. Peak B1 was probably due to a doubly dehydrated form of histidine with a molecular ion at $m/z = 119$ and ions characteristic of imidazole at $m/z = 65$ and 81 , although the base peak was at $m/z = 94$. Peaks B2 and B3 had mass spectra with ions at $m/z = 65, 79, 93, 106$ and 133 . The apparent molecular ion at $m/z = 133$ suggested that this compound was a pyrolysis rearrangement product of histidine because the difference between the apparent molecular ion and the mass of histidine could not be reconciled. Mass spectra of a number of poorly resolved peaks (B3) contained apparent molecular ions

at $m/z > 155$, indicative of addition products formed during pyrolysis. These results contrast with the findings of Chiavari & Galletti (1992) who used a similar method, but recorded their mass spectra at 70 eV, and reported that histidine did not yield any significant pyrolysis products.

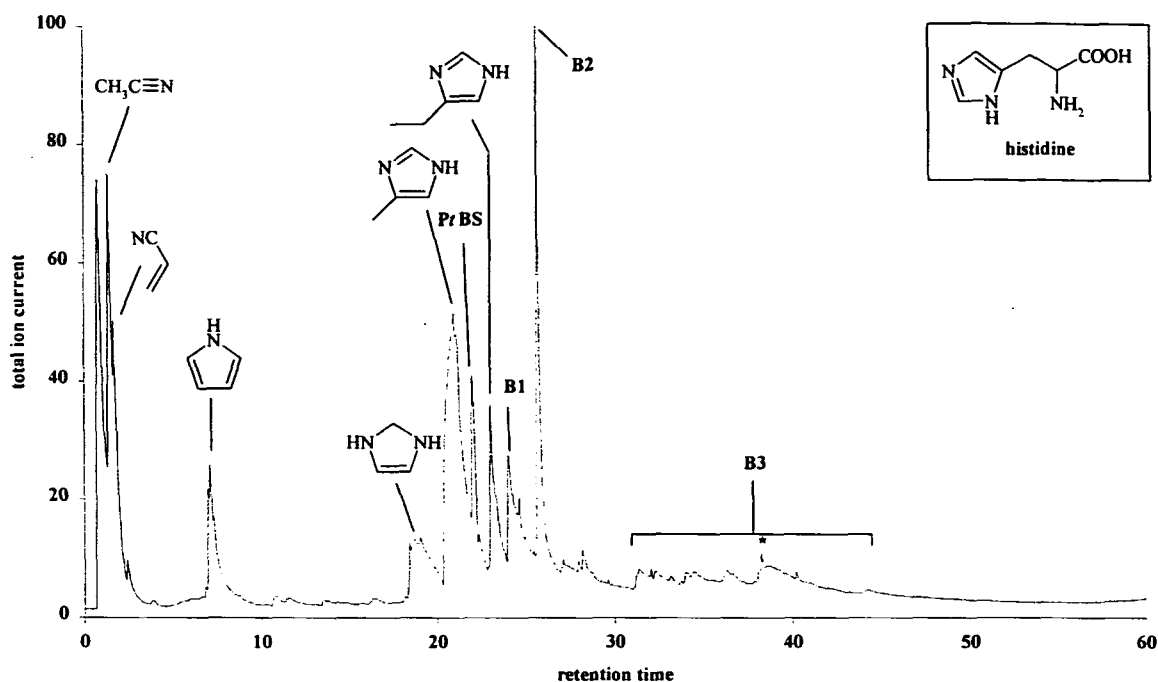


Figure 5.2. Py-GC-MS TIC of histidine (pyrolysis at $595\text{ }^{\circ}\text{C} \pm 5\text{ }^{\circ}\text{C}$, 1 min; GC programme, -10 to $300\text{ }^{\circ}\text{C}$ at $5\text{ }^{\circ}\text{C min}^{-1}$, hold at $300\text{ }^{\circ}\text{C}$ for 10 min; Rtx-5 column; MS operated at 40 eV).

The pyrolysis chromatogram of glucose (Figure 5.3) was dominated by two poorly resolved peaks (RT = 31:40 – 35:00 and 36:10 – 38:10 min) which accounted for 37 and 27 % of the total chromatographic response. Although mass spectra from these two products could not be unambiguously identified, they may have been dehydrated forms of glucose, *e.g.* glucopyranose-type or levoglucosan-type compounds (Meuzelaar, *et al.*, 1982; Almendros *et al.*, 1997). Other products, more commonly characteristic of the pyrolysis of saccharides (Irwin, 1982; Meuzelaar, *et al.*, 1982; Almendros *et al.*, 1997), included unsaturated species, *e.g.* pentenyne and pentene, aromatics including substituted

derivatives (e.g. benzene, naphthalene, toluene and xylene), and oxygen-containing species (e.g. substituted furans, phenol and aldehydes).

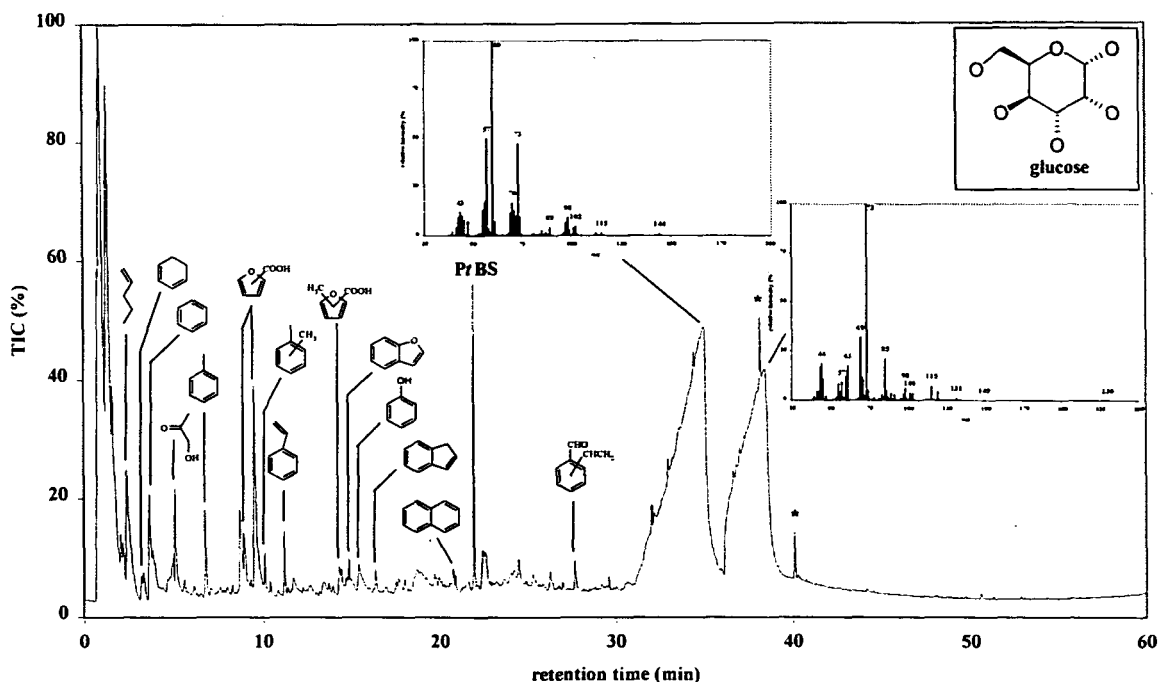


Figure 5.3. Py-GC-MS TIC of glucose (pyrolysis at $595 \text{ }^\circ\text{C} \pm 5 \text{ }^\circ\text{C}$, 1 min; GC programme, -10 to $300 \text{ }^\circ\text{C}$ at $5 \text{ }^\circ\text{C min}^{-1}$, hold at $300 \text{ }^\circ\text{C}$ for 10 min; Rtx-5 column; MS operated at 40 eV).

Chromatograms from the Py-GC-MS analysis of acid synthesised Gly/Glu and His/Glu melanoidins are presented in Figures 5.4 and 5.5, respectively. Both chromatograms were characterised by numerous peaks (> 70) and a distinct unresolved component below the baseline which accounted for 42 % (Gly/Glu) and 76 % (His/Glu) of the total chromatographic response.

A number of peaks in the pyrogram from the Gly/Glu melanoidin (Figure 5.4) were common to those identified in the pyrogram from glucose (i.e. methylfuran, cyclohexadiene, xylene, benzofuran, indene and naphthalene) suggesting that glucose was preserved to some degree in the melanoidin structure. This is consistent with the findings of Rubinsztain *et al.* (1984) that the sugar moiety of melanoidin polymers has a general

formula *ca* C₆H₆O₃. Nitrogen-containing species observed in the glycine pyrogram (Figure 5.1) were noticeably absent from the Gly/Glu pyrogram, although pyrazoles were present. This suggests that either two glycine molecules reacted before becoming incorporated into the melanoidin structure, or that two peripheral melanoidin nitrogen-containing moieties are released upon pyrolysis and subsequently formed pyrazoles in the pyrolysis chamber. Little of the higher molecular weight material could be readily identified. However, much of this material produced similar mass spectra characterised by three to six intense ions separated by 13 – 15 mass units and potential molecular ions from around $m/z = 240 - 330$ at 14 or 16 mass units higher than that of the next highest mass ion. The averaged mass spectrum of this region of the pyrogram (inset Figure 5.4) illustrates the relative intensity of the higher mass ions. This material may have represented the pyrolysis products of high molecular weight, *i.e.* $M_r > 10000$, previously reported to have been formed from the acid and aqueous/solvent syntheses of Gly/Glu melanoidins (Wedzicha & Kaputo, 1992; Yaylayan & Kaminsky, 1998, respectively).

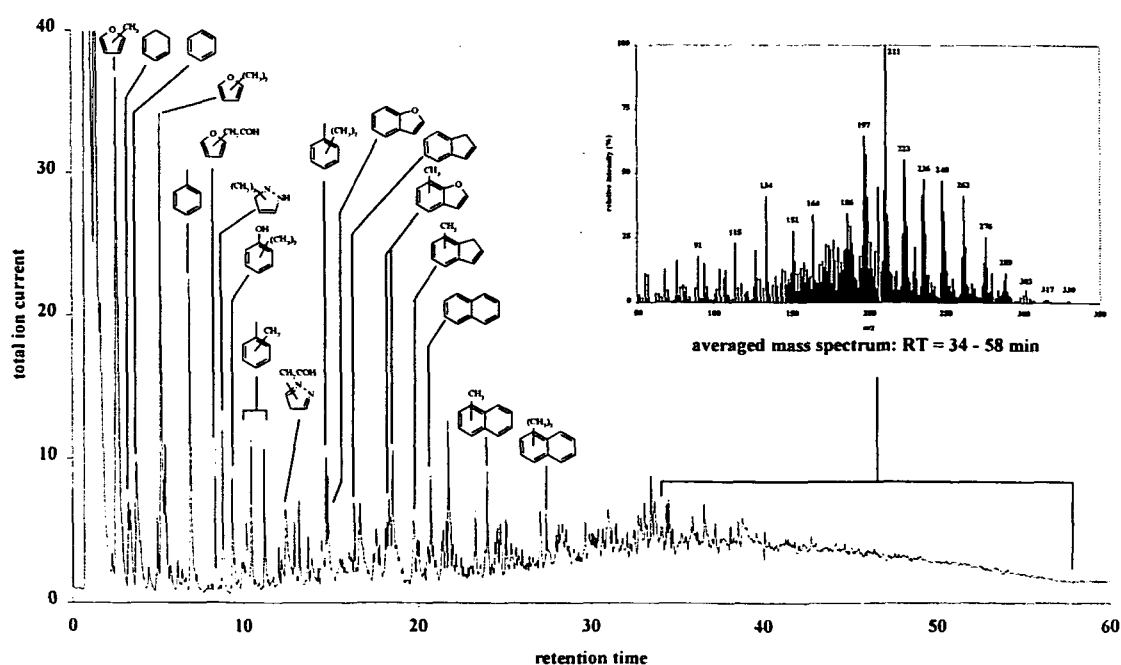


Figure 5.4. Py-GC-MS TIC of acid synthesised Gly/Glu melanoidin (pyrolysis at 595 °C \pm 5 °C; GC programme –10 to 300 °C at 5 °C min⁻¹, hold at 300 °C for 10 min, Rtx-5 column; MS operated at 40 eV).

Resolved components from the pyrogram of the His/Glu melanoidin (Figure 5.5), identified by comparison with library spectra, were similar to those found in the Gly/Glu melanoidin pyrogram. These principally comprised furans, benzenes, naphthalenes, indenenes and phenols. The apparent absence of imidazoles suggested that the imidazole moiety of histidine had not been preserved during melanoidin synthesis although it is conceivable that this moiety rearranged to form pyrazoles, which were present in the His/Glu pyrogram. Alternatively, this may have indicated that amino acids were degraded during melanoidin formation and subsequently bound into higher molecular weight material. This higher molecular weight material was present as a distinctive 'hump' which eluted until the end of the GC programme. The averaged mass spectrum of the high molecular weight material (inset Figure 5.5) was less well defined than that from the corresponding region of the Gly/Glu pyrogram (inset Figure 5.4), although it had a similar maximum ($m/z = 200$) and range (up to $m/z = 340$). Mass spectra from this region were not as apparently contiguous as those from the Gly/Glu pyrogram and tended to be less dominated by higher mass ions ($m/z = > 200$). This implied that the range of products from His/Glu melanoidin synthesis was more complex than that from Gly/Glu synthesis.

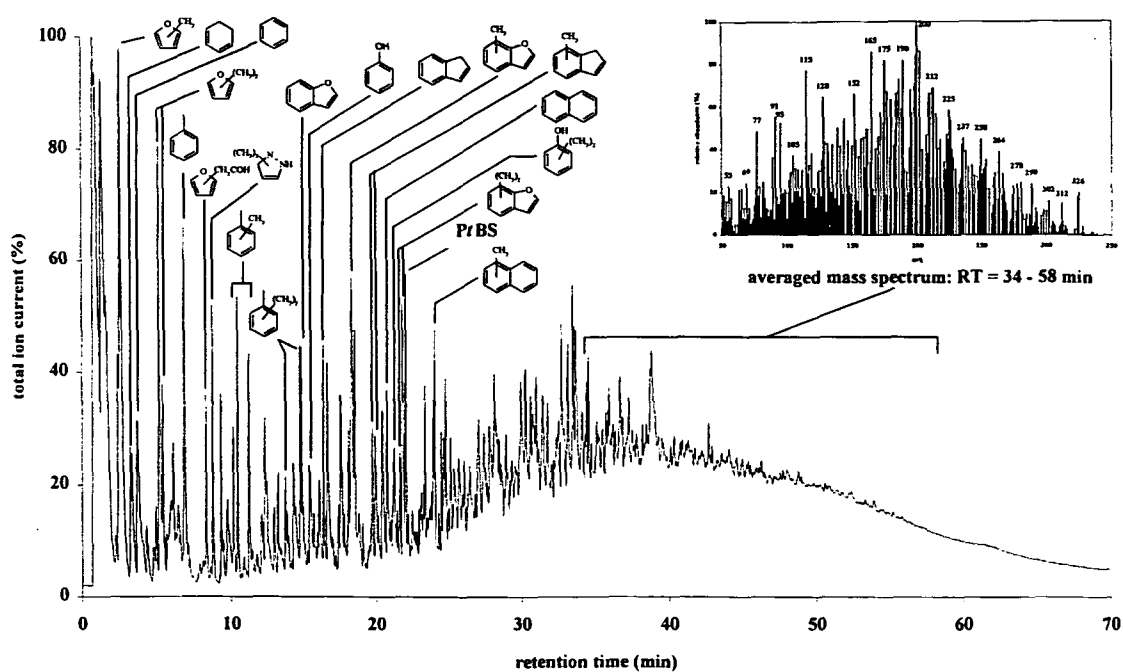


Figure 5.5. Py-GC-MS TIC of acid synthesised His/Glu melanoidin (pyrolysis at 595 °C \pm 5 °C; GC programme -10 to 300 °C at 5 °C min⁻¹, hold at 300 °C for 10 min, Rtx-5 column; MS operated at 40 eV).

A number of characteristics of the melanoidin pyrograms, *e.g.* benzenes and naphthalenes, as well as the unresolved ‘hump’, were also common features of those observed in sedimentary IOM pyrograms (Chapter 4). However, these were of little diagnostic value in assessing whether melanoidins were formed during the digestion procedure because they were present in samples from all stages of the sequential isolation. Conversely, the absence of furans and nitrogen-containing species in the sediment pyrograms strongly indicates that melanoidins did not provide a substantial contribution to the isolated sedimentary IOM. This is supported by a general lack of bias towards ions at $m/z > 200$ in the 34 – 58 minute region of the sedimentary IOM pyrograms as seen in the melanoidin pyrograms.

5.3.4. Analysis of melanoidins using infrared spectroscopy

The IR spectra of acid synthesised Gly/Glu and His/Glu melanoidins were practically identical (Figure 5.6) with the exception of a less intense absorbance band at 3123 cm⁻¹ in

the Gly/Glu spectrum. Absorbance band assignments were: 3425 cm^{-1} , -O-H and/or -N-H stretching; 3123 cm^{-1} , -C-H phenyl; 2970 and 2926 cm^{-1} , aliphatic -C-H stretch; 1706 cm^{-1} , -C=O stretch; 1618, 968 and 803 cm^{-1} , alkene or benzyl -C=C-; 1511 cm^{-1} , tentatively assigned as R-NO₂ nitro groups; 1380 cm^{-1} , -O-H deformation; 1200 cm^{-1} , -C-O- and/or -C-N- stretch; and 1050 cm^{-1} , -C-O-, -C-N-, -C-C- stretch. The broad poorly resolved bands between 1400 – 1200 cm^{-1} may be confirmatory bands for either -C-O- (stretch), -O-H (bend) or R-NO₂ nitro groups. These assignments were consistent with those reported by Cämmerer & Kroh (1995) for Gly/Glu melanoidins formed in aqueous and solvent-free systems and similar to those reported by Yaylayan & Kaminsky (1998) for water-methanol synthesised Gly/Glu melanoidins. This similarity in IR data for Gly/Glu melanoidins manufactured using different methods may be explained by the relative insensitivity of melanoidin composition to changes in reaction conditions, *e.g.* temperature, reactant ratios and heating periods (Wedzicha & Kaputo, 1992; Cämmerer & Kroh, 1995). Furthermore, the similarity between the IR spectra of Gly/Glu and His/Glu melanoidins was inconsistent with their dissimilar pyrograms, supporting the contention that identical bulk functional composition does not necessarily imply identical molecular conformation.

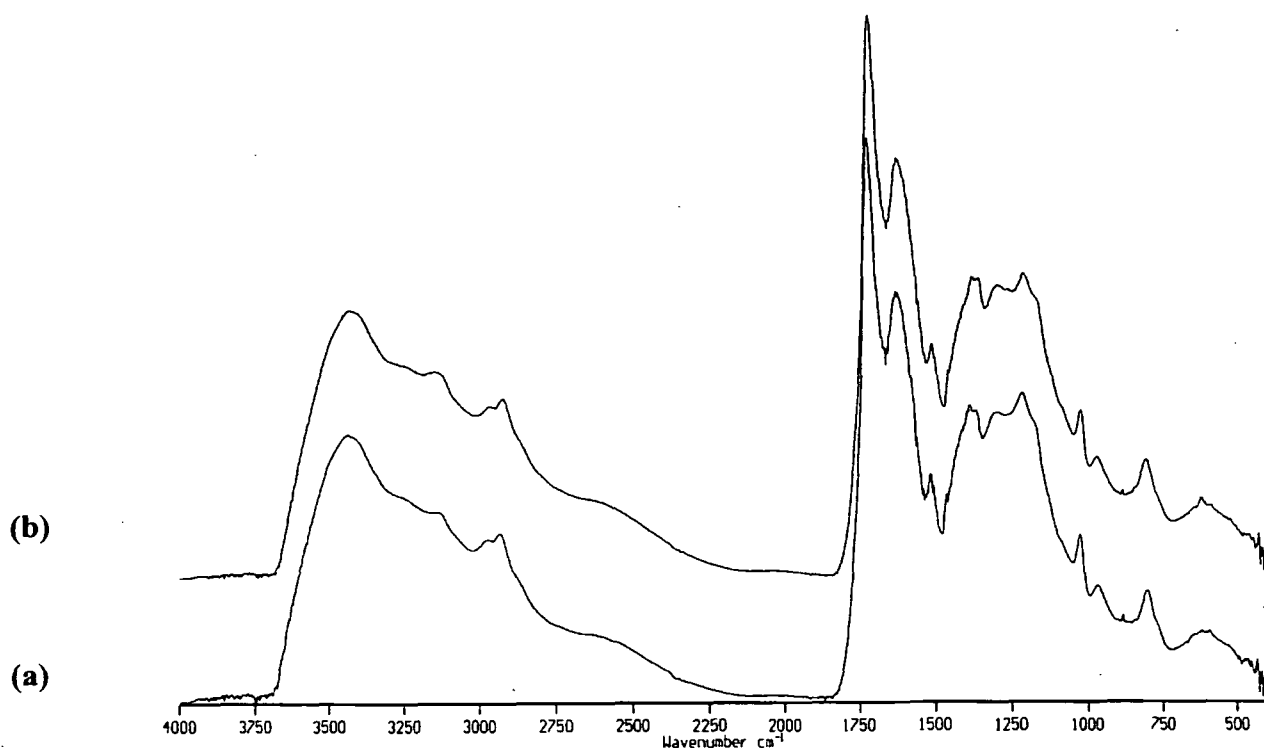


Figure 5.6. Infrared absorbance spectra of acid synthesised melanoidins. (a) Gly/Glu, (b) His/Glu.

The IR spectra of acid-synthesised melanoidins were similar to those recorded from sedimentary and bacterial IOM (Section 3.3.4), in particular absorbance bands at 3425 (–OH stretch), 2970 and 2926 (–CH stretch), 1706 (–C=O stretch), 1618 (olefinic or benzyl –C=C–) and 1200 cm^{-1} (probably –C–O– stretch) were common to the IOMs from different sources. However, given the molecular fragment evidence from Py-GC-MS analyses, IR bands were generally too broad to allow unambiguous differentiations and precise conclusions to be made.

5.4. Summary

- 10 – 22 % yields of insoluble melanoidins were obtained from the aqueous and acid synthesis of simple mixtures of amino acids with glucose.
- Py-GC-MS analysis of simple amino acids and glucose each produced relatively complex pyrograms.

- Unresolved components accounted for most of the chromatographic response from both Gly/Glu and His/Glu melanoidins.
- Resolved components in melanoidin pyrograms were dominated by glucose pyrolysis fragmentation products whilst amino acid signatures were noticeably absent.
- Averaged mass spectra of the higher molecular weight regions of Gly/Glu and His/Glu pyrograms indicated more complex pyrolysis products from the latter.
- Gly/Glu and His/Glu melanoidins gave almost identical spectra when examined using IR spectroscopy.
- Comparison of melanoidin pyrograms with those of sediments subject to sequential digestion provided little evidence for the formation of artefactual material during IOM isolation, although IR absorbances recorded for melanoidins were also present in the IR spectra of sedimentary and bacterial IOM.

Chapter 6: Attempted dissolution of 'insoluble organic matter' (IOM) using the ionic liquid 1-ethyl-3-methylimidazolium chloride/ aluminium (III) chloride

6.1. Introduction

This chapter describes the effects of treating simple organic substrates, more complex dendrimer molecules containing similar functional groups to those observed in many kerogens, and isolated IOM from sediments and biota (Chapter 2) with the acidic ionic liquid 1-ethyl-3-methylimidazolium chloride/aluminium (III) chloride, [emim]Cl-AlCl₃ {X(AlCl₃), X = 0.65}. In addition, the ionic liquid treatment of acid-synthesised Gly/Glu and His/Glu insoluble melanoidins (Chapter 5) is described, in order to determine whether they react in a similar fashion to sedimentary and bacterial IOM.

Recent advances in molten salt chemistry have resulted in the development of new ionic liquid solvents that contain both organic and inorganic moieties. In order to appreciate the potential effects of treating complex organic substrates with an ionic liquid it is first necessary to understand what ionic liquids are, and how they have been utilised previously in studies on simple organic compounds. Therefore necessarily, with the wider range of organic compounds present in IOM (Chapter 4), much of the following review focuses on the use of ionic liquids in organic syntheses.

The development of dendritic molecules provides a source of relatively high molecular weight (> 1000 amu) compounds with highly specific architecture and composition which have the potential to be used as instrumental standards or substrate analogues in geochemical analyses. Incorporation of functional groups similar to those identified in more complex geochemical matrices is likely to promote a better understanding of how these functionalities are perceived using routine geochemical analytical techniques. For these reasons, and because two dendrimers were used in the present study, an overview of dendrimer chemistry is provided.

6.1.1. Review of ionic liquids

Ionic liquids are liquids comprised entirely of ionic species. For example, sodium chloride would be an ionic liquid if raised to a temperature of around 800 °C. In the literature these mixtures are sometimes referred to as molten salts (*e.g.* Pagni, 1987; Koch *et al.*, 1976; Smith *et al.*, 1989), melts (*e.g.* Zawodzinski, Jr., *et al.*, 1988; Carper *et al.*, 1996; Surette *et al.*, 1996) or neoteric solvents (Seddon, 1996, 1997). However, as Seddon (1996, 1997) suggests, the first two descriptions invoke connotations of high-temperature, corrosive, viscous media whilst the latter would include supercritical fluids which are not ionic liquids.

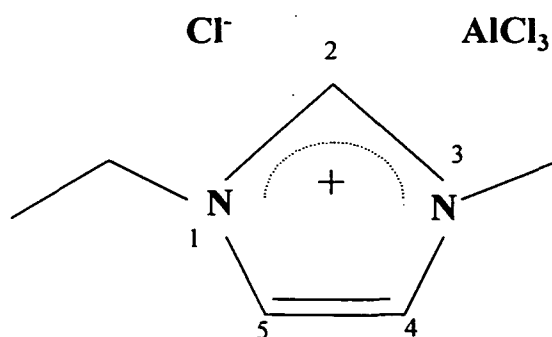
The advantages of newly developed ionic liquids (Seddon, 1997) are that they;

- Remain liquid over a large temperature range and can be used at room temperature.
- Suppress conventional solvation and solvolysis phenomena
- Suppress dissociation, disproportionation and degradation reactions at ambient temperature
- Can extend the lifetime of species which are unstable in conventional solvents

Ionic liquids are synthesised by combining two or more ionic species. Whilst early work centred on the combination of inorganic species which required elevated temperatures to remain in a liquid state (>100 °C; Jones & Osteryoung, 1975) the liquidus range was greatly extended (-96 °C to 200 °C) with the synthesis of ionic liquids containing inorganic and organic species, *e.g.* 1-ethyl-3-methylimidazolium chloride/aluminium (III) chloride (Wilkes *et al.*, 1982). The latter ionic liquid was used in two preliminary studies of the effects of ionic liquids on kerogens (Patell, 1994; Dutta, 1994). These qualitative experiments suggested that Types I – III kerogens could be effectively solubilised by treatment with 1-ethyl-3-methylimidazolium chloride/aluminium (III) chloride. The aim of the present study was to verify (or otherwise) these preliminary findings and

also to examine whether IOM from recent sediments and biota could be similarly 'dissolved'. Although most of the literature relating to the use of acidic [emim]Cl-AlCl₃ ionic liquid is principally concerned with its use in organic syntheses, this is reviewed here to provide an insight into the scope and nature of organic reactions that have been shown to occur in this medium.

1-Ethyl-3-methylimidazolium chloride/aluminium (III) chloride (**I**) is an anhydrous binary mixture produced by stirring together purified solid 1-ethyl-3-methylimidazolium chloride and solid aluminium (III) chloride under dry-box conditions (Wilkes *et al.*, 1982). This ionic liquid is referred to variously in the literature as [emim]Cl-AlCl₃ (Abdul-Sada *et al.*, 1993; Avent *et al.*, 1994; Elaiwi *et al.*, 1995; Seddon, 1997), [MeEtim]Cl/AlCl₃, MeEtImCl-AlCl₃ or MEICl-AlCl₃ (Appleby *et al.*, 1986; Boon *et al.*, 1986; Carper *et al.*, 1996), ImCl + AlCl₃ or ImCl-AlCl₃ (Zawodzinski *et al.*, 1988), AlCl₃-EMIC or EMIC/AlCl₃ (Smith *et al.*, 1989; Hondrogiannis *et al.*, 1993; Lee *et al.*, 1996). The abbreviation [emim]Cl-AlCl₃ will be used throughout this text when referring to the ionic liquid used in this work and when citing works using fundamentally the same mixture.



Acidity of the ionic liquid is governed by the relative proportion of reactants, $X[\text{emim}]\text{Cl}$ and $X(\text{AlCl}_3)$. Where the mole fraction (X) of aluminium (III) chloride, $X(\text{AlCl}_3)$ exceeds 0.5, the ionic liquid is termed acidic. The term basic is used when $X(\text{AlCl}_3) < 0.5$ and

neutral when $X(\text{AlCl}_3)$ equals 0.5. The phase diagram (Figure 6.1) shows that $[\text{emim}]\text{Cl}-\text{AlCl}_3$ is liquid at room-temperature throughout basic $\{X(\text{AlCl}_3), X = 0.3\}$ to acidic compositions $\{X(\text{AlCl}_3), X = 0.65\}$.

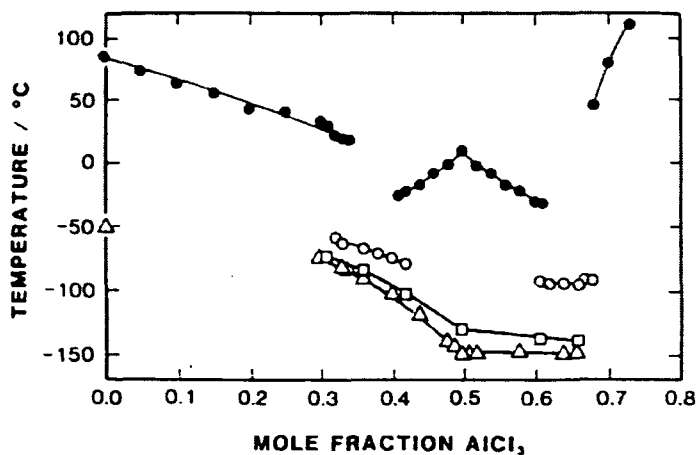


Figure 6.1. Phase diagram for $[\text{emim}]\text{Cl}-\text{AlCl}_3$ (Fannin *et al.*, 1984; (●) melting and freezing points; (○) experimental glass transitions; (□) T_0 's from absolute viscosity experiments; (Δ) T_0 's from equivalent conductivity experiments).

Traditional concepts of acidity, *e.g.* Arrhenius or Brønsted and Lowry, are not appropriate for ionic liquids which, like $[\text{emim}]\text{Cl}-\text{AlCl}_3$ are aprotic. Arrhenius' definition of an acid as a chemical which forms hydrogen ions (H^+) or hydronium ions (H_3O^+) in aqueous solution and a base as a species which forms hydroxide ions in aqueous solution is patently not applicable to a non-aqueous system. Similarly, Brønsted and Lowry's definition of acids as proton donors and bases as proton acceptors does not allow for the concept of acidity in systems that do not contain protic sources. Although the Lewis concept of acidity, *i.e.* acid as an electron-pair acceptor and base as an electron-pair donor, allows for acids and bases in non-protic systems and has commonly been used to describe the acid-base chemistry of ionic liquids (Boon *et al.*, 1986; Smith *et al.*, 1989; Goldenberg & Osteryoung, 1994; Carper *et al.*, 1996), Seddon (1997) states that acid-base terms used in relation to ionic liquids are those defined in the Franklin solvent-system concept (Franklin, 1905). However, as the total removal of protic impurities and/or adventitious moisture appears to

be an inherent problem in the synthesis of ionic liquids it is not unreasonable to presume that their acidity is adequately described by Lewis acid-base behaviour.

In Pagni's (1987) review of reactions in molten salts, at around the time of the development of [emim]Cl-AlCl₃ systems, he identified the principal reactions which occur in chloroaluminate ionic liquids as Friedel-Crafts reactions (*e.g.* electrophilic aromatic substitutions; Figure 6.2), acid catalysed isomerisations and rearrangements (*e.g.* Fries rearrangement; Figure 6.3), and the Scholl reaction (Figure 6.4). Friedel-Crafts and acid catalysed reactions in ionic liquids were considered to occur similarly to those using aluminium chloride in conventional solvents but more rapidly and often with better yields. The Scholl reaction, which involves coupling of two aromatic substrates promoted by treatment with a Lewis acid and protic acid or Lewis acid alone, also occurred with better yields (*i.e.* >10 %) in an ionic liquid (Pagni, 1987). Whilst most of the work reviewed by Pagni involving chloroaluminate ionic liquids centred on inorganic systems like AlCl₃-NaCl, AlCl₃-NaCl-KCl and AlCl₃-NH₄Cl, in each case the aluminium chloride moiety was considered to be the reaction-promoting centre. Notwithstanding this, the presence of protic impurities associated with the reagents was also cited as a possible reaction-initiation source.

(a)



(b)



Figure 6.2. Schematic of electrophilic aromatic substitution, Friedel-Crafts (a) alkylation, (b) acylation.

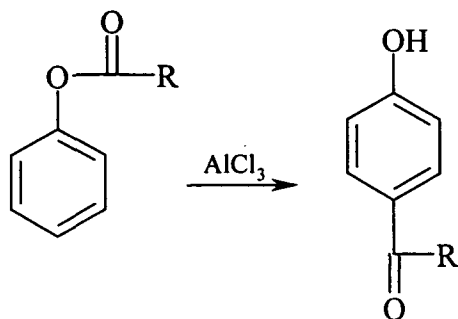
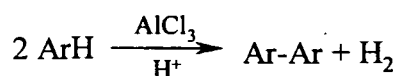


Figure 6.3. Schematic of the Fries rearrangement

(a)



(b)

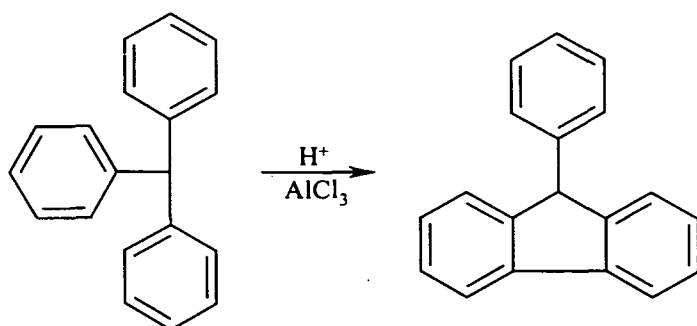


Figure 6.4. Schematic of the Scholl reaction, (a) intermolecular, (b) intramolecular

Secondary ion mass spectrometry (SIMS) work by Franzen *et al.* (1986) identified the presence of the ions [Cl]⁻ and [AlCl₄]⁻ in acidic [emim]Cl-AlCl₃ and the possibility of [Al₃Cl₁₀]⁻ and [Al₂Cl₇(Al(OH)₃)_n]⁻ (*n* = 1, 2 or 3). The existence of [Al₃Cl₁₀]⁻ was later confirmed by the IR spectroscopic studies of Dymek *et al.* (1988) and negative-ion fast-atom-bombardment work by Abdul-Sada *et al.* (1989). Abdul-Sada *et al.*, (1993) reported the presence of numerous ionic species (Table 6.1) in purified [emim]Cl-AlCl₃ {*X*(AlCl₃), *X* = 0.67} using fast atom bombardment mass spectrometry, the principal anions being [Al₂Cl₇]⁻ and [Al₃Cl₁₀]⁻. Small amounts of oxide-containing species were attributed to

the initial hydrolysis products of $[\text{Al}_3\text{Cl}_{10}]^-$, demonstrating the extremely hygroscopic nature of the ionic liquid. The two oxide species found by Abdul-Sada *et al.* (1993) contrast with the three oxide species (one hydroxochloaluminate and two oxygen-bridged oxochloroaluminate species) previously reported by Zawodzinski & Osteryoung (1987, 1990) for acidic $[\text{emim}]\text{Cl}-\text{AlCl}_3$. Upon extended hydrolysis by contact with atmospheric moisture, a number of oxide and hydroxide species were formed (Table 6.1). Clearly, the presence of oxide and/or hydroxide species owing to partial hydrolysis of AlCl_3 , or the presence of protic impurities, has implications for the acid-base behaviour of the ionic liquid when in contact with a substrate. Additionally, neither research group excluded the possibility of hydrolysis product formation during sample introduction into their instrumentation.

Table 6.1. Ionic species present in purified and hydrolysed $[\text{emim}]\text{Cl}-\text{AlCl}_3$ { $\text{X}(\text{AlCl}_3)$, $\text{X} = 0.65$ } (Franzen *et al.*, 1986; Dymek *et al.*, 1988; Abdul-Sada *et al.*, 1989; 1993).

Anions		Cations
Pure $[\text{emim}]\text{Cl}-\text{AlCl}_3$	Hydrolysed $[\text{emim}]\text{Cl}-\text{AlCl}_3$	Pure $[\text{emim}]\text{Cl}-\text{AlCl}_3$
$[\text{Al}_3\text{Cl}_{10}]^-$, $[\text{Al}_3\text{Cl}_8\text{O}]^-$, $[\text{Al}_3\text{Cl}_8]^-$, $[\text{Al}_2\text{Cl}_7]^-$, $[\text{Al}_2\text{Cl}_5\text{O}]^-$, $[\text{AlCl}_4]^-$, $[\text{Cl}_2]^-$, $[\text{Cl}]^-$	$[\text{Al}_4\text{Cl}_9\text{O}_2]^-$, $[\text{Al}_3\text{Cl}_8\text{O}]^-$, $[\text{Al}_3\text{Cl}_7\text{O}(\text{OH})]^-$, $[\text{Al}_3\text{Cl}_6\text{O}_2]^-$, $[\text{Al}_2\text{Cl}_7]^-$, $[\text{Al}_2\text{Cl}_6(\text{OH})]^-$, $[\text{Al}_2\text{Cl}_5\text{O}]^-$, $[\text{AlCl}_4]^-$, $[\text{Cl}_2]^-$, $[\text{Cl}]^-$	$[(\text{emim})_2(\text{AlCl}_4)]^+$, $[(\text{emim})_2\text{Cl}]^+$, $[\text{emim}]^+$

The presence of protic impurities in $[\text{emim}]\text{Cl}-\text{AlCl}_3$ has profound implications for the acid-base behaviour of the ionic liquid and its ability to mediate in organic reactions. Some of the literature pertaining to organic reactions carried out in $[\text{emim}]\text{Cl}-\text{AlCl}_3$ contains references to the presence of such protic impurities and to speculation of their part in

initiating protonation of organic substrates (*e.g.* Carlin *et al.*, 1992; Hondrogiannis *et al.*, 1993). Truelove & Osteryoung (1992) found the only proton-containing species present in oxide-free acidic [emim]Cl-AlCl₃ to be HCl, whilst in oxide-containing acidic [emim]Cl-AlCl₃ a single hydroxychloroaluminate species exists. Besides protic impurities, oxide impurities are also ubiquitous contaminants of [emim]Cl-AlCl₃ (Abdul-Sada *et al.*, 1993) but may be removed by treatment of the ionic liquid with phosgene gas (Abdul-Sada *et al.*, 1993a). Removal of oxide-contaminants from the [emim]Cl-AlCl₃ used in this study was not undertaken.

Since Pagni's (1987) early review detailing organic reactions in ionic liquids the principal reactions reported between acidic [emim]Cl-AlCl₃ and organic substrates have included Friedel-Crafts reactions (Pagni, 1987; Boon *et al.*, 1986; Adams *et al.*, 1998), the Scholl reaction (Pagni, 1987), and polymerisation reactions (Goldenberg and Osteryoung, 1994). Boon *et al.* (1986) reported the acidic [emim]Cl-AlCl₃ catalysed Friedel-Crafts alkylation of benzene with a number of chlorinated alkylating agents (methyl-, ethyl-, *n*-propyl-, *n*-butyl-, cyclohexyl-, and benzyl- chloride) at room-temperature or at the reflux temperature of the alkyl chloride, whilst basic [emim]Cl-AlCl₃ did not catalyse these reactions. Products were extracted with ether from the aqueous mixture after quenching the reaction with water. These authors reported relative yields of mono-, di-, tri-, tetra-, penta- and hexa-alkylated products but did not quantify the products in terms of the initial reactants. In addition to the alkylation of benzene, toluene and chlorobenzene could be alkylated in this medium, but nitrobenzene could not. Boon *et al.*, (1986) further demonstrated the Friedel-Crafts acylation of benzene with acetyl chloride (AcCl) with the reaction rate determined by the acidity (*i.e.* $X(\text{AlCl}_3)$) of the ionic liquid. These experiments suggested that [Al₂Cl₇]⁻ acted as the catalyst, although the later work of Abdul-Sada *et al.* (1993) indicated that [Al₃Cl₁₀]⁻ present in acidic [emim]Cl-AlCl₃ may also have had catalytic effect.

Adams *et al.* (1998) carried out Friedel-Crafts acetylations using AcCl in acidic [emim]Cl-AlCl₃ { $X(\text{AlCl}_3)$, $X = 0.67$ } with a variety of aromatic (Ar) substrates (naphthalene, toluene, chlorobenzene, anisole, 1,1,2,6-tetramethyl-3-isopropylindane, anthracene, phenanthrene and pyrene). With the exception of anthracene, phenanthrene and pyrene, the reactions worked efficiently producing the stereoelectronically favoured products (Table 6.2). Production of the thermodynamically unfavoured 1-acetylnaphthalene was explained as consequence of the free acylium ion acting as the acetylating agent in the ionic liquid. This allowed attack at the more sterically hindered 1-position rather than the common 2-position attack in more conventional solvents, *e.g.* by the larger AcCl-AlCl₃-nitrobenzene complex where the solvent is nitrobenzene. The acetylation of anthracene, phenanthrene and pyrene in acidic [emim]Cl-AlCl₃ { $X(\text{AlCl}_3)$, $X = 0.67$ } behaved differently to those of the simpler arenes. For anthracene, dependent upon reaction conditions, a variety of mono- and diacetylated anthracene products were formed as well as unreacted or reversibly formed anthracene (Table 6.3). Adams *et al.*, (1998) proposed the scheme shown in Figure 6.5 to account for the acetylation reactions of anthracene. The reversible formation of 9-acetylanthracene was accounted for by a proton-catalysed mechanism *via* the addition of water to the ionic liquid, which acts as a protic source in the formation of HCl and confers superacidity (Smith *et al.*, 1989) to the ionic liquid. Acetylation of pyrene (20 °C, 2 h, 1.2 AcCl/equiv.) resulted in the formation 1,6- and 1,8-diacetylpirene (55 %) and 1-acetylpirene (13 %) whilst acetylation of phenanthrene (-10 °C, 5 min, 1.5 AcCl/equiv.) yielded primarily monacetylated products 9- (55 %), 1- (30 %) and 2-acethylphenanthrene (<5 %), but little diacetylated product.

Table 6.2. Yields and reaction conditions for the Friedel-Crafts acetylation of aromatic compounds in [emim]Cl-AlCl₃ {X(AlCl₃), X = 0.67} (Adams *et al.*, 1998)

Compound	T (°C)	t (h)	Products (% yield)
Naphthalene	0	1	1-AcAr (89), 2-AcAr (2)
Toluene	20	1	4-AcAr (98), 2-AcAr (1)
Chlorobenzene	20	24	4-AcAr (97), 2-AcAr (2)
Anisole	-10	0.25	4-AcAr (99)
1,1,2,6-tetramethyl-3-isopropylindane	0	1	5-AcAr (99)

Table 6.3. Yields and reaction conditions for the Friedel-Crafts acetylation of anthracene at 0 °C in [emim]Cl-AlCl₃ {X(AlCl₃), X = 0.67} (Adams *et al.*, 1998)

t	AcCl/equiv.	Composition (%)			
		II	III	IV	V
5 min	1.1	23	69	0	0
24 h	1.1	34	0	32	24
5 min	1.5	15	73	3	1
24 h	1.5	25	0	42	33
5 min	2.1	13	69	5	3
24 h	2.1	1	1	57	42

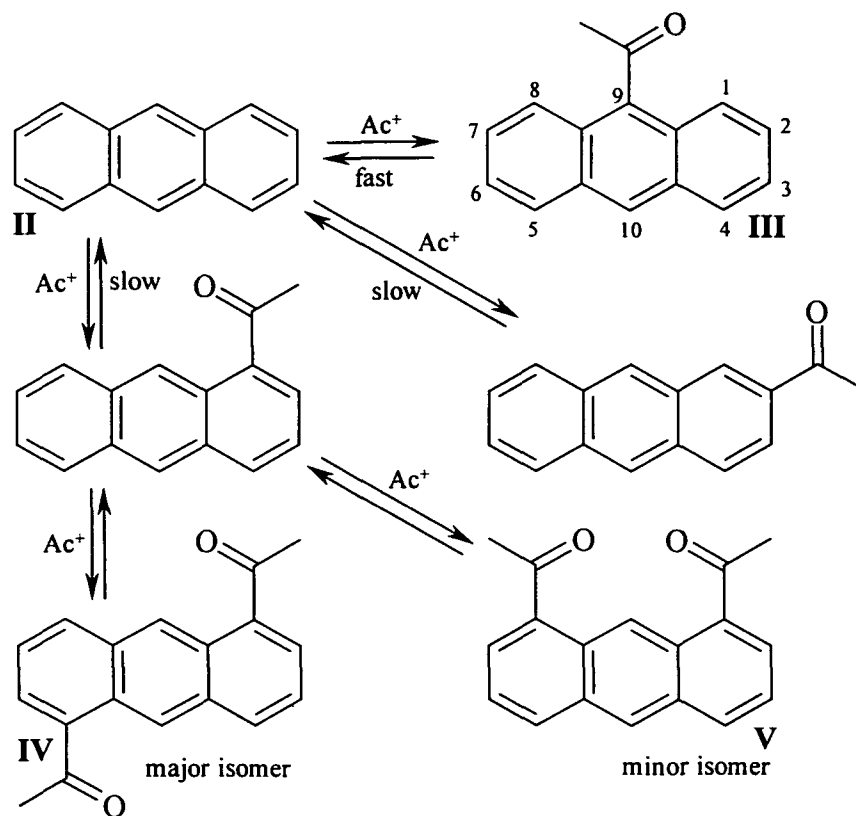


Figure 6.5. Proposed reaction scheme for the acetylation of anthracene (Adams *et al.*, 1998)

Smith *et al.*, (1989) reported the semi-quantitative protonation of arenes in slightly acidic $[\text{emim}]\text{Cl}-\text{AlCl}_3 \{X(\text{AlCl}_3), X = 0.55\}$ ionic liquid containing HCl. Although these workers did not hydrolyse the mixture and extract the resulting solution to examine the products, they did demonstrate the ability of proton-containing $[\text{emim}]\text{Cl}-\text{AlCl}_3$ to protonate aromatic compounds (Table 6.4). Their work suggests that when water is added to $[\text{emim}]\text{Cl}-\text{AlCl}_3$ containing mixtures, the potential exists for superacidic protonation of arenes before the ionic liquid is fully hydrolysed. The oxidation of anthracene in proton free acidic $[\text{emim}]\text{Cl}-\text{AlCl}_3 \{X(\text{AlCl}_3), X = 0.6\}$ was reported by Carlin *et al.* (1992) to occur in two, one-electron oxidation steps. First the production of a radical cation, then the formation of a dication. They speculated that even in their proton-free ionic liquid, trace protic impurities might have initiated the reaction. Furthermore, they noted the reversible but non-quantitative protonation of anthracene, forming the anthracenium ion (VI^+), in

superacidic [emim]Cl-AlCl₃ {X(AlCl₃, X = 0.6} with [emim]HCl₂ as the proton source. The equilibrium reaction for this latter reaction is shown below (Figure 6.6).

Table 6.4. Degree of protonation of arenes in the superacidic HCl-containing [emim]Cl-AlCl₃ ionic liquid (Smith *et al.*, 1989).

Compound	Degree of protonation
Biphenyl	None
Naphthalene	Slight
9H-fluorene	10 – 20 %
Chrysene	10 – 20 %
2-Methylnaphthalene	75 – 90 %
Mesitylene	almost complete
Pentamethylbenzene	almost complete
Hexamethylbenzene	almost complete
Anthracene	complete
9,10-Dimethylantracene	complete

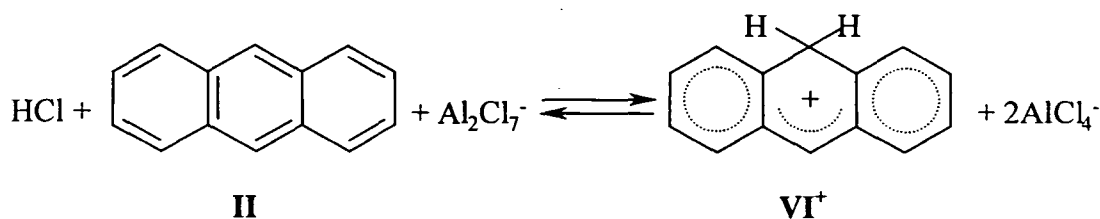
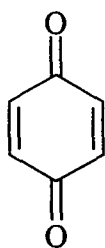


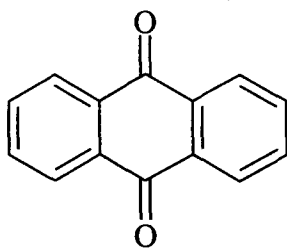
Figure 6.6. Reaction equilibrium for the protonation of anthracene in superacidic [emim]Cl-AlCl₃ with [emim]HCl₂ as the proton source (Carlin *et al.*, 1992).

1,4-Benzoquinone (VII) was reported to react with acidic [emim]Cl-AlCl₃ {X(AlCl₃), X = 0.6} (Uribe & Osteryoung, 1988) with loss of the carbonyl groups. Although the reaction products were not determined, this behaviour contrasted with that of anthraquinone (VIII)

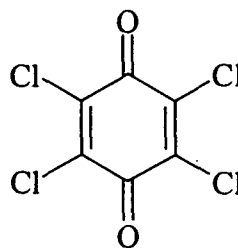
or chloranil (XIV) which did not react in acidic [emim]Cl-AlCl₃ (Cheek & Osteryoung, 1982, 1982a).



VII

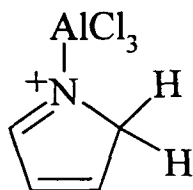


VIII



XIV

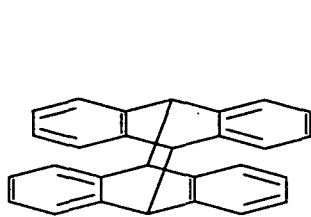
Zawodzinski *et al.* (1988) were unable to polymerise pyrrole in basic or acidic [emim]Cl-AlCl₃ ionic liquids. They found that pyrrole did not react in the basic ionic liquid whilst the reversible formation of an adduct (X) between pyrrole and AlCl₃ at the nitrogen position prevented polymerisation in the acidic ionic liquid by removing electron density from the ring. Upon hydrolysis of pyrrole in acidic ionic liquid, an insoluble black product was formed which the authors speculate may have been polymeric 'pyrrole black'. In contrast, Goldenberg and Osteryoung (1994) reported that electropolymerisation of benzene occurred in [emim]Cl-AlCl₃ ionic liquid regardless of the acidity or introduction of a protic source into the mixture.



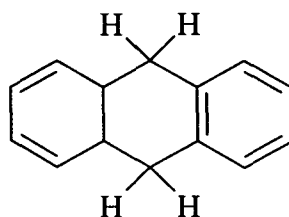
X

The photochemistry of anthracene (II) in basic and acidic [emim]Cl-AlCl₃ {X(AlCl₃), X = 0.45 and 0.55, respectively} has been investigated by Hondrogiannis *et al.* (1993). In the basic ionic liquid, photolysis of anthracene yielded exclusively 9,9',10,10'-bianthracene

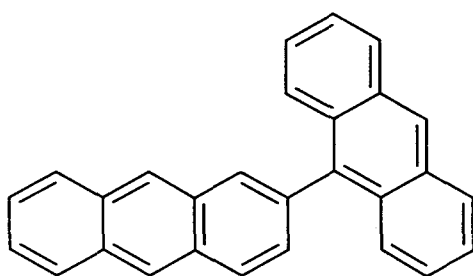
(XI), whilst in the acidic ionic liquid at least 16 products were formed, the major ones of which (XI, XII, XIII, XIV, XV, XVI) are shown below. As photolysis in the acidic ionic liquid continued, the yields of XI and XVI increased whilst the mass balance decreased. The authors suggested that the formation of oligomeric and polymeric compounds at longer reaction times might account for the product deficit. Furthermore, they explained this novel photochemistry by the formation of the anthracenium ion (VI⁺) by protonation of anthracene by trace amounts of HCl impurities in the ionic liquid (Eqs. 1 – 3).



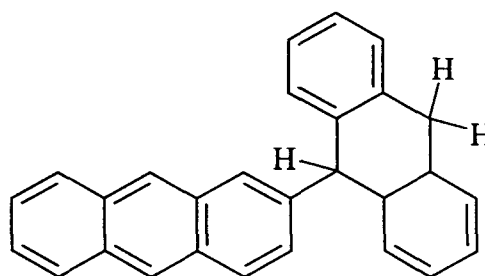
XI



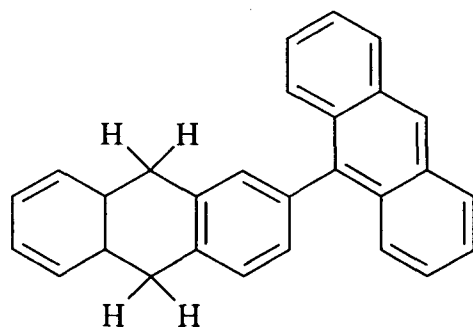
XII



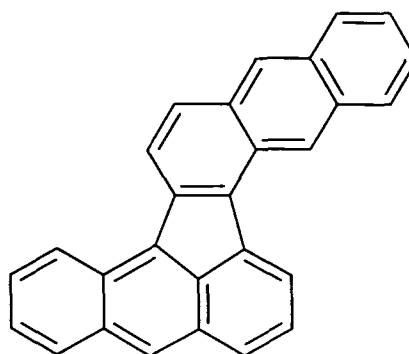
XIII



XIV



XV



XVI



(Eq. 1)



Patell (1994) and Dutta (1994) investigated the dissolution of kerogens and coal using the same acidic [emim]Cl-AlCl₃ {X(AlCl₃), X = 0.65} ionic liquid used in the current study. Their experimental procedure is outlined in Figure 6.7. Following experiments into the effects of different kerogen/solvent systems (no solvent, MeOH, and DMSO), different ionic liquid compositions ({X(AlCl₃), X = 0.4 and 0.65}), and heating systems (conventional oven *versus* microwave oven) for kerogen/[emim]Cl-AlCl₃ mixtures, they used a microwave heating stage in their protocol to heat the ionic liquid/substrate mixtures in Carius tubes under vacuum in order to promote 'dissolution'. Microwave heating had no apparent effect on kerogen concentrates when solvents were not present, whereas the introduction of conventional solvents combined with the use of a Parr bomb led to partial dissolution (MeOH, 0.5 %; DMSO, 8 – 10 %). Acidic ionic liquid {X(AlCl₃), X = 0.65} was reported to dissolve Type I (95 %), II (98 %) and III (65 %) kerogens when microwave heating was used, whilst basic ionic liquid {X(AlCl₃), X = 0.40} dissolved 0 % (Type I), 5 – 8 % (Type II) and 10 – 12 % (Type III). Microwave heating was reported to be a superior means of promoting 'dissolution' than conventional oven heating with 98 % dissolution of Kimmeridge Clay kerogen reported to occur compared to 29 % dissolution when heated in a conventional oven at 100 °C.

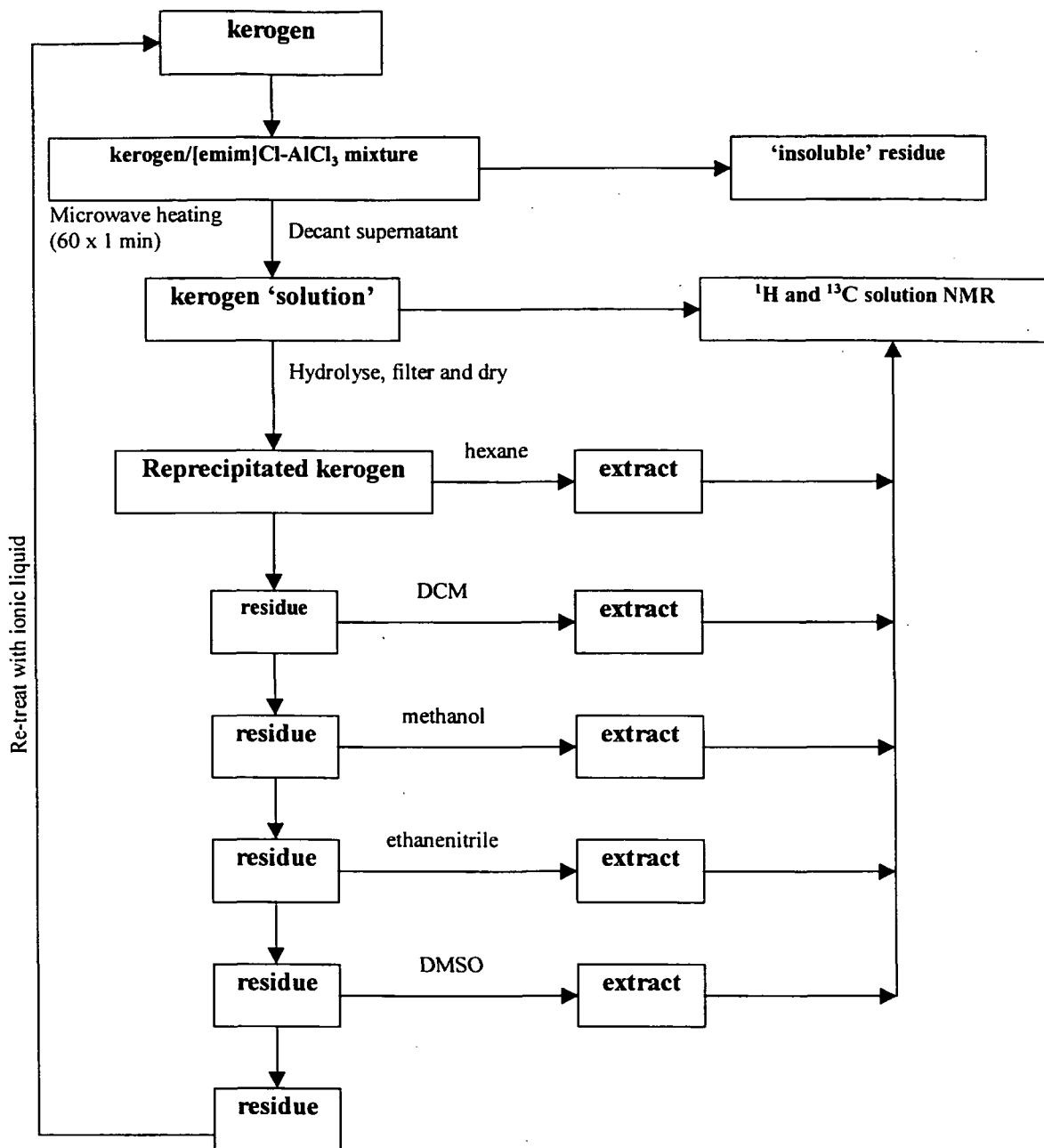


Figure 6.7. Flow chart of ionic liquid 'dissolution' procedure used by Patell (1994) and Dutta (1994)

The attempted $[emim]Cl-AlCl_3$ $\{X(AlCl_3), X = 0.65\}$ dissolution of Type I (Green River Shale) and Type II (Kimmeridge Clay and Liassic Shale) kerogens, and a Northumberland coal equivalent to Type III kerogen, was carried out by Patell (1994) and Dutta (1994). Their studies were primarily focused on the qualitative bulk characterisation of material that became solvent soluble following ionic liquid treatment and provided little quantitative data regarding the proportion of material that was solubilised by ionic liquid

treatment or that was solvent-soluble after ionic liquid treatment. In addition, it appears that their claims for up to 98 % dissolution of kerogens were based on calculating the proportion of material extracted from the reprecipitated kerogen rather than quantifying the solvent-soluble material as a percentage of the initial amount of kerogen subject to ionic liquid treatment. For example, for Liassic Shale kerogen, Dutta (1994) reported the yield of reprecipitated material as 1.18 g from an initial mass of 15 g kerogen, *i.e.* 8 %, of which 0.83 g was solvent-soluble, *i.e.* 70 % of the reprecipitated material but only 5.5 % of the original mass of kerogen. Solution ^1H NMR studies indicated that sequential solvent extracts (hexane, benzene, dichloromethane, methanol, ethanenitrile, and dimethylsulphoxide) from ionic liquid treated but re-precipitated (*via* aqueous hydrolysis) Type I and II kerogens were dominated (>80 %) by aliphatic signals (Tables 6.5 and 6.6). The solvent soluble portion of these reprecipitated kerogens analysed by ^1H solution NMR was more aliphatic than the reprecipitated material after ionic liquid treatment but prior to solvent extraction or the original sample (Table 6.7; Patell, 1994). Possible reasons for this may have been that: (1) ionic liquid treatment allowed subsequent preferential release of aliphatic components from the 'solubilised' matrix, (2) aromatic constituents were more strongly bound to the kerogen matrix, (3) aromatic components were refractory, or (4) ^{13}C CPMAS NMR overestimated the aromatic component of the original kerogen, or (5) ionic liquid treatment promoted the formation of poorly soluble aromatic compounds. The relative chemical composition of the 'solubilised', re-precipitated, ionic liquid-treated kerogen samples, as determined by ^{13}C solid-state NMR (Tables 6.7 and 6.8), appeared to be substantially different from that of the original Type I and II kerogen samples, *i.e.* increased aromaticity, decreased aliphaticity. ^{13}C CPMAS NMR analysis of the residue not 'dissolved' by ionic liquid treatment (Dutta, 1994; Table 6.8) indicated that the chemical character of this material was more akin to that of the original sample than that of the re-precipitated material. Whilst Patell (1994) and Dutta (1994) concentrated on attempting the total dissolution of the reprecipitated fraction of ionic liquid-treated kerogens they did not

attempt to 'redissolve' the residue that did not 'dissolve' in the ionic liquid after the first attempt. Based on the available literature, reviewed above, which focuses on the use of [emim]Cl-AlCl₃ {X(AlCl₃), X = 0.65} for organic synthetic reactions, it is the present author's contention that ionic liquid-treatment of kerogens may have resulted in Friedel-Crafts-type reactions that promoted oligo- and polymerisation of aromatic components such that they were difficult to extract with normal solvents. As a consequence of these reactions alkanes and alkyl substituents were cleaved from the kerogen matrix. This would explain the high aliphatic and low aromatic yields obtained by Patell (1994) and Dutta (1994) in their solvent extracts.

Table. 6.5. Relative proportion (%) of compound classes released during each stage of the sequential extraction of reprecipitated Green River Shale kerogen (Type I) after treatment with [emim]Cl-AlCl₃ {X(AlCl₃), X = 0.65} (Patell, 1994). nd – not detected.

Extract	Aliphatic	Aromatic	Ketonic
Hexane	94	6	nd
Benzene	92	8	nd
Dichloromethane	92	8	nd
Methanol	91	9	nd
Ethanenitrile	94	6	nd
Dimethylsulphoxide	76	17	7

Table. 6.6. Relative proportion (%) of compound classes released during each stage of the sequential extraction of reprecipitated Kimmeridge Clay kerogen (Type II) after treatment with [emim]Cl-AlCl₃ {X(AlCl₃), X = 0.65} (Patell, 1994). nd – not detected.

Extract	Aliphatic	Aromatic	Ketonic
Hexane	93	7	nd
Benzene	85	15	nd
Dichloromethane	88	12	nd
Methanol	85	15	nd
Ethanenitrile	88	13	nd
Dimethylsulphoxide	59	31	10

Table 6.7. Relative proportion of carbon environments in Type I and II kerogens before and after treatment with [emim]Cl-AlCl₃ {X(AlCl₃), X = 0.65} determined by ¹³C CPMAS NMR (Patell, 1994). *Re-precipitated sample after ionic liquid-treatment.

		Original sample	Precipitate*
Green River kerogen (Type I)	aliphatic	76	51
	aromatic	21	44
	>C=O/-C(O)OR	3	5
Kimmeridge Clay kerogen (Type II)	aliphatic	66	50
	aromatic	30	47
	>C=O/-C(O)OR	4	3

Table 6.8. Relative proportion of carbon environments in Type II and Northumberland coal before and after treatment with [emim]Cl-AlCl₃ {X(AlCl₃), X = 0.65} determined by ¹³C CPMAS NMR (Dutta, 1994). *Reprecipitated sample after ionic liquid-treatment.

		Original sample	Precipitate*	'Insoluble' residue
Liassic kerogen (Type II)	aliphatic	57	52	59
	aromatic	37	44	34
	>C=O/-C(O)OR	7	3	6
Northumberland coal (Type III)	aliphatic	30	36	26
	aromatic	67	63	69
	>C=O/-C(O)OR	3	1	5

6.1.2. Review of dendrimer compounds

Over the past twenty years, advances in the field of dendrimer (Greek *dendro-*, tree-like) chemistry have resulted in the synthesis of a multitude of novel organic and organo-metallic compounds. Dendrimers (sometimes referred to as cascade polymers) are compounds synthesised by the iterative step-wise extension of repeating units to form assemblages that are generally, polyfunctional, macromolecular, and have well defined chemical composition. Their well-defined composition differentiates them from traditional polymers, *e.g.* polystyrene, that tend to have a relatively broad mass range (Figure 6.8). Dendrimers were selected to investigate the action of the ionic liquid, rather than more traditional polymeric materials, primarily because of their high mass and purity, but also because the available functionalities reflect those found in many kerogens (*e.g.* benzyl and ester groups, and ether linkages; Rouxhet *et al.*, 1980).

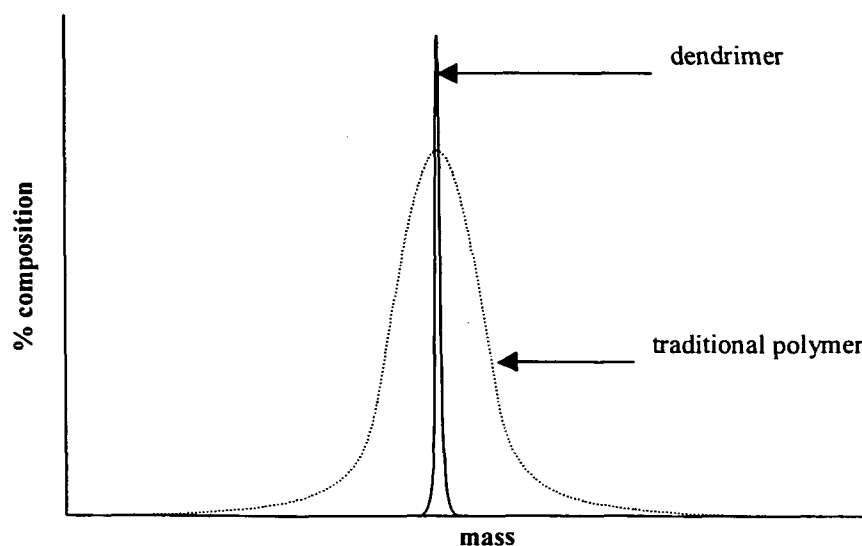


Figure 6.8. Mass distribution of traditional polymers and dendrimers

Dendrimers are synthesised using either divergent or convergent methods. Divergent synthesis involves the repetitive addition of fragments to an initiator core (G_0) that has one or more attachment sites (Figure 6.9a). The increased number of available attachment sites

after the first addition (G_1) allows a greater number of fragments to be subsequently attached ($\dots G_n$). This process can be repeated until steric controls prevent further additions, the so-called de Gennes limit (de Gennes & Hervet, 1983). Fragment addition is often controlled by the chemical protection and de-protection of end terminal (or surface) groups. Convergent synthesis, as the name implies, involves the iterative addition of fragments to surface groups prior to conjunction with a core molecule (Figure 6.9b).

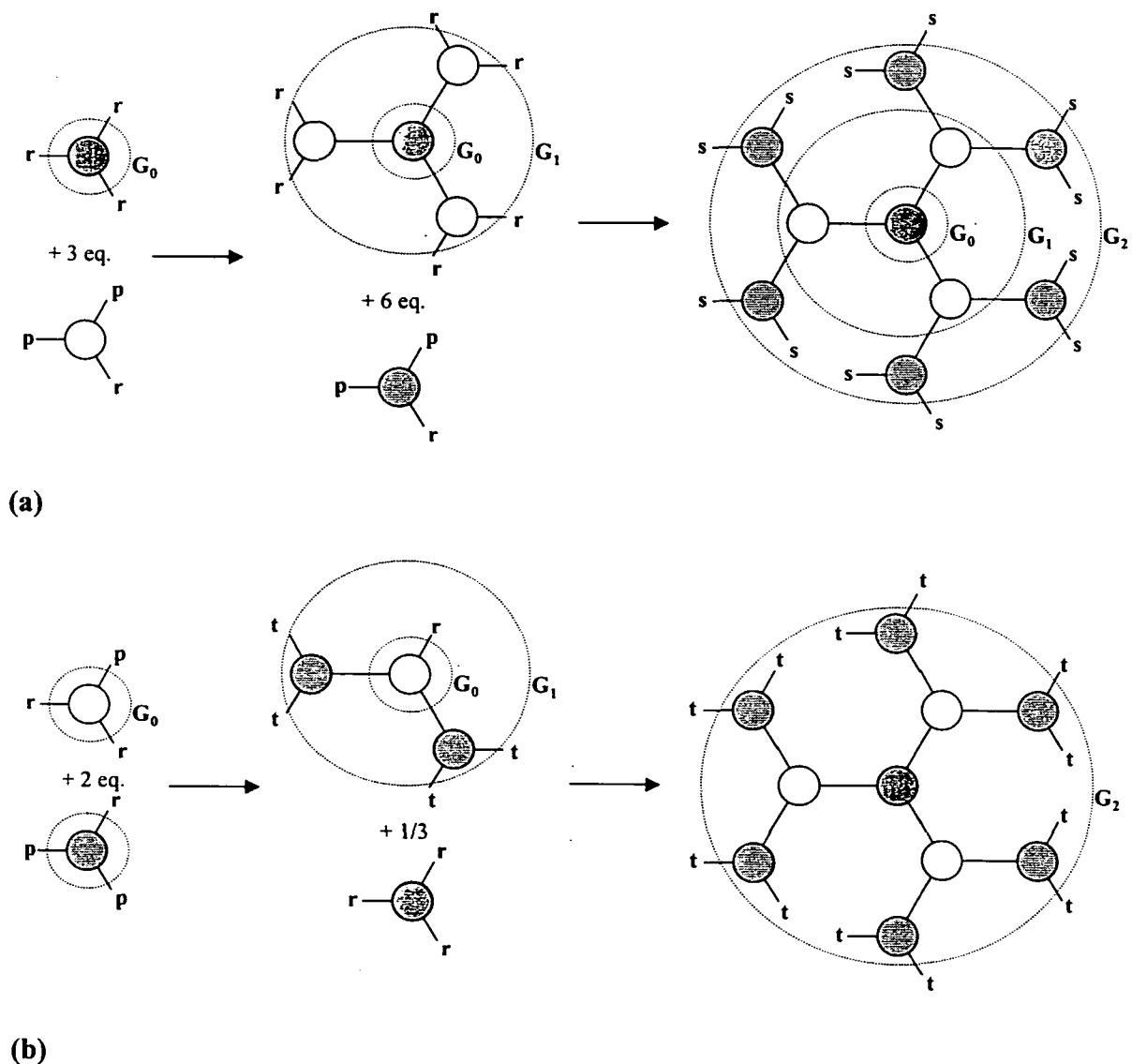


Figure 6.9. Simplified dendrimer synthesis: (a) divergent (b) convergent. G_0 , G_1 , G_2 , G_n , - generation number; r - reactive attachment site; p - protected site; t - terminal group; s - site of possible further attachment.

The often large and complex molecules produced by iterative synthesis have been

recognised to be problematic in terms of naming using either the *IUPAC* system or *Chemical Abstracts* nomenclature (Newkome *et al.*, 1993, 1996). These customary nomenclature systems fail to readily identify surface groups, branching multiplicity or the initiator core, whereas trivial names used by some researchers did not include chemical information (*e.g.* Starburst™ dendrimers; Tomalia, 1994, 1995). Although two new nomenclature systems (cascade and fractal) which overcome these shortcomings have been proposed, at present neither has been universally adopted. Because the two dendrimers used in this work were obtained from the same research group their trivial nomenclature system (Haddleton *et al.*, 1996), which is adequately descriptive, will be used herein. The first letter and subscripted number denote the generation, *e.g.* G₁ = generation one, G₂ = generation two, *etc.*, the second letter identifies the initiator core, *e.g.* P = phloroglucinol. These dendritic aryl esters were synthesised *via* the divergent extension of a phloroglucinol (1,3,5-trihydroxybenzene) core using benzyl protected 3,5-dihydroxybenzoic acid in dicyclohexylcarbodiimide, deprotection by catalytic hydrogenation and subsequent repetition of the esterification process (Haddleton *et al.*, 1996). Matrix-assisted laser desorption-time of flight-mass spectrometry (MALDI-TOF-MS) was used to confirm the calculated relative molecular mass of both dendrimers as 1075 amu and 2454 amu for G₁P-[6]-Obn and G₂P-[12]-Obn, respectively (Sahota *et al.*, 1994; Figures 6.10 and 6.11, respectively).

6.2. Experimental work

6.2.1. Preparation of [emim]Cl-AlCl₃ {X(AlCl₃), X = 0.65}

Acidic [emim]Cl-AlCl₃ {X(AlCl₃), X = 0.65} (I) was prepared using the method of Wilkes *et al.* (1982). Principally, this involved stirring together purified 1-ethyl-3-methylimidazolium chloride (X = 0.35) and solid aluminium (III) chloride (X = 0.65) under nitrogen dry-box conditions (< 5 ppm H₂O). Owing to the anhydrous nature of the binary mixture, all subsequent work was carried out under dry-box conditions.

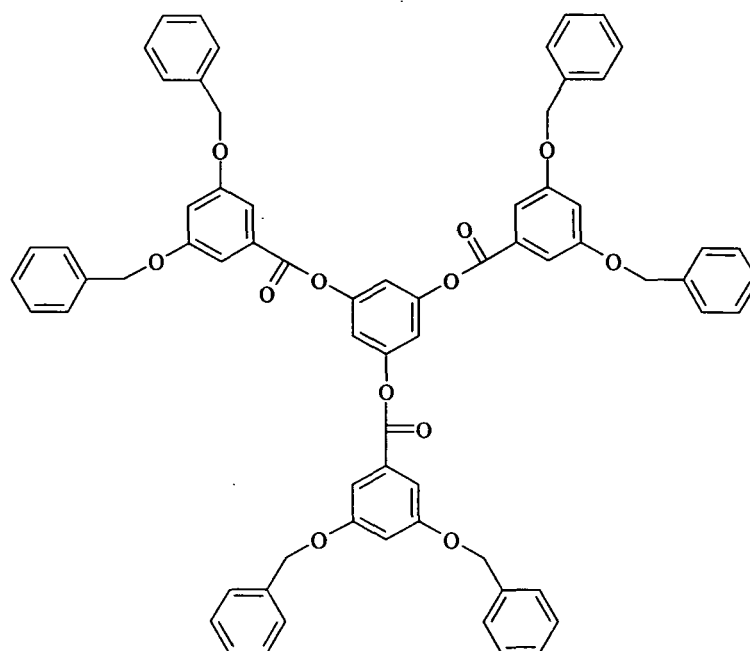


Figure 6.10. Structure of dendrimer G₁P-[6]-Obn (C₆₉H₅₄O₁₂, M_r = 1074)

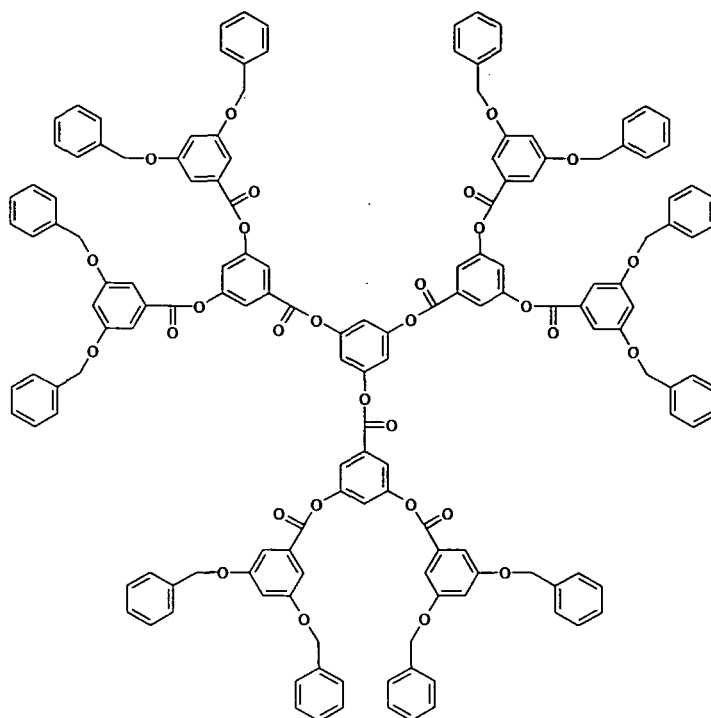


Figure 6.11. Structure of dendrimer G₂P-[12]-Obn (C₁₅₃H₁₁₄O₃₀, M_r = 2430)

6.2.2. Dissolution protocol

The general experimental procedures used for the attempted dissolution of IOM and other substrates, and subsequent analysis of fractionated material are outlined in Figure 6.12. Experimental details are included in Sections 6.2.3 – 6.2.8. General laboratory procedures were as described in Section 2.3.1. In addition, prior to use, glass fibre filters were oven dried (110 °C, overnight); sodium sulphate was pre-extracted (DCM, 24 h) and oven dried (110 °C, 3 days); and cotton wool was pre-extracted (DCM, 24 h).

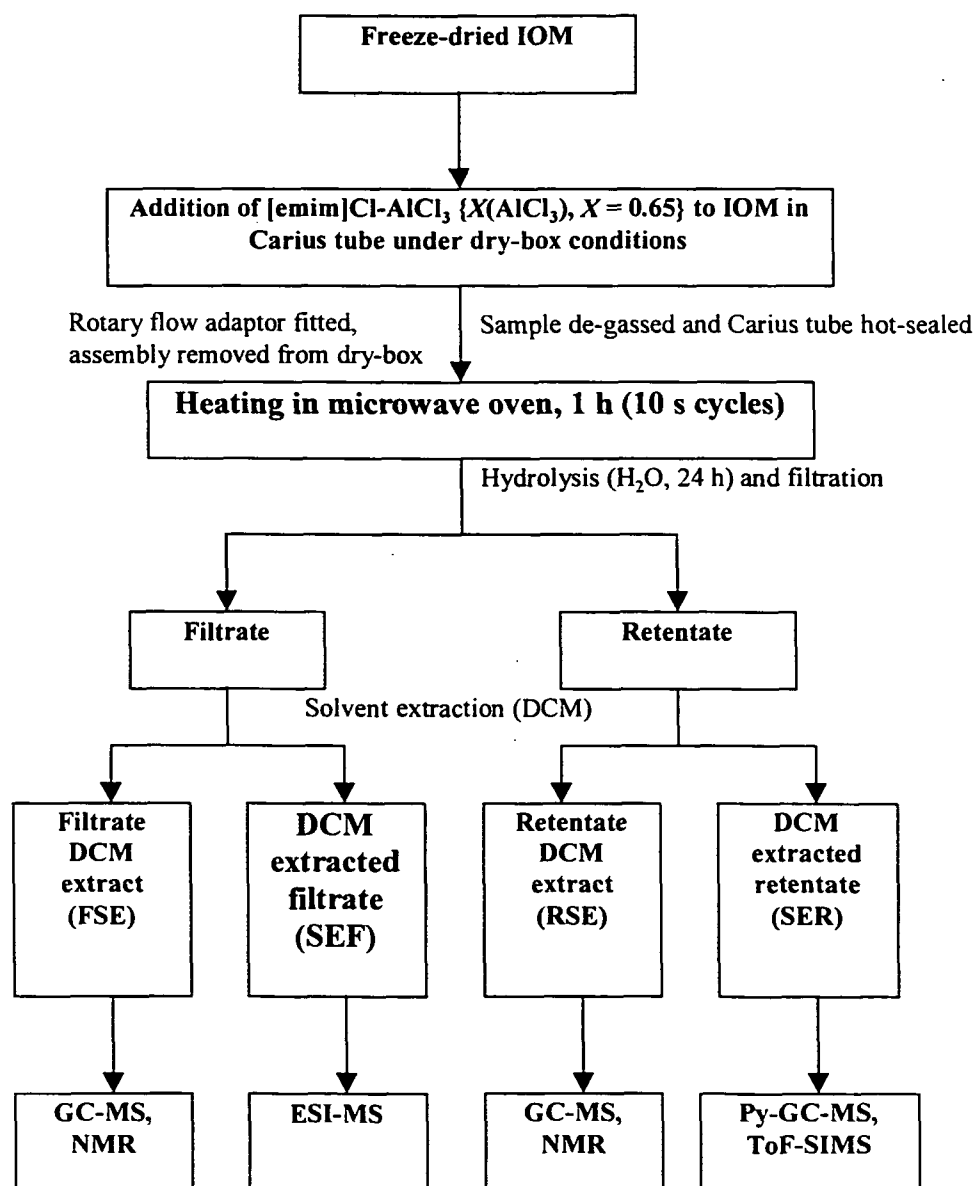


Figure 6.12. Experimental protocol for the attempted dissolution of IOM

The protocol resulted in four important operationally defined fractions *viz*:

- a. Filtrate solvent (DCM) extract (**FSE**)
- b. Solvent-extracted filtrate (**SEF**)
- c. Retentate solvent (DCM) extract (**RSE**)
- d. Solvent-extracted retentate (**SER**)

6.2.3. Addition of [emim]Cl-AlCl₃ {X(AlCl₃), X = 0.65} to samples

Freeze-dried IOM was weighed into a Carius tube (manufactured with an elongated neck and ground glass joint) in a nitrogen dry-box. [emim]Cl-AlCl₃ was added drop-wise into the Carius tube until the ionic liquid/IOM ratio exceeded 10 (w/w). An excess of ionic liquid over IOM was used in order to encourage maximum 'dissolution'. A rotary flow adapter (Young's adapter) was fitted to the Carius tube and the valve closed. After removing the Carius tube/adapter assembly from the dry-box a vacuum line was fitted to the adapter, a vacuum applied, and the valve gently opened to de-gas the sample. Once initial vigorous bubbling subsided, the valve was opened fully and the sample allowed to de-gas for 15 minutes, or until the bubbling ceased. After closing the valve and removing the assembly from the vacuum line, the elongated neck of the Carius tube was heat sealed to maintain the sample under vacuum. This procedure was also repeated for tricyclic aromatic model compounds, dendrimers and melanoidins (Table 6.9). Procedural blanks comprising solely [emim]Cl-AlCl₃ were also prepared in this manner.

Table 6.9. Ratios of substrates and ionic liquid mixtures

Substrate	Ratio ionic liquid: substrate (w/w)
[emim]Cl-AlCl₃	--
Aromatic compounds:	
Anthracene	11:1
Phenanthrene	10:1
Dendrimers:	
G ₁ P-[6]-Obn	11:1
G ₂ P-[12]-Obn	11:1
Rostherne Mere IOM:	
7 – 10 cm bswi	11:1
21 – 24 cm bswi	11:1
33 – 36 cm bswi	11:1
46 – 49 cm bswi	11:1
59 – 62 cm bswi	11:1
82 – 85 cm bswi	11:1
Bacteria:	
<i>M. jannaschii</i>	8:1
Kimmeridge Clay IOM	12:1
Melanoidins:	
Gly/Glu	11:1
His/Glu	11:1

6.2.4. Microwave heating

The sealed Carius tube containing sample and ionic liquid was placed horizontally on a notched cork block in the centre of a microwave oven (Sharp model R-3J58M with turntable, output power 700 W, frequency 2450 MHz) cavity and heated (lowest power setting, 10 s). After heating, the tube was removed from the oven, shaken and left to cool. The heating procedure was repeated for up to one hour (10 s heating cycles). In some instances the Carius tubes became too hot to touch and the procedure was modified. In the modified heating procedure six Carius tubes were placed vertically in separate Teflon

bombs and heated for one hour (1 min heating cycles). Qualitative changes in the appearance of each sample were recorded.

6.2.5. Pre-hydrolysis

Prior to hydrolysis, a Carius tube containing only microwave heat-treated [emim]Cl-AlCl₃ { $X(\text{AlCl}_3)$, $X = 0.65$ } was opened with a glasscutter in a nitrogen flushed and filled glove-bag. The contents were transferred by pipette to a NMR tube and an insert tube containing deuterated solvent (D₂O) was fitted. ¹H and ¹³C NMR spectroscopy was used to examine changes in the ionic liquid following microwave heat treatment. Other samples were not examined in this manner owing to their extreme viscosity and the presence of particulate material that would have interfered with NMR spectroscopy.

6.2.6. Hydrolysis

Once microwave heat treatment was complete, each Carius tube was opened with a glass cutter in a fume cupboard and the contents poured into a beaker of water (*ca.* 20 ml, Milli-Q), complete with washings (3 x 2 ml, Milli-Q), containing a Teflon-coated magnetic stirrer and stirred (24 h). The contents of the beaker were then vacuum filtered, complete with washings, through a pre-dried (*ca.* 110 °C, overnight), pre-weighed glass fibre filter (Whatman GF/A grade) over a sintered glass filter fitted to a side-arm flask attached to a vacuum line. After filtering, the filter was loosely wrapped in foil, dried (*ca.* 60 °C, 24 h) and re-weighed. The filtrate was transferred to a pre-weighed jar, frozen, freeze-dried, and re-weighed.

6.2.7. Solvent extraction of retentate

The dried filter retaining the retentate was placed in a boiling tube and refluxed with solvent (DCM, 15 ml, 2 x 24 h). Solvent was decanted to a round-bottom flask after reflux, the extracts combined, and rotary evaporated to near-dryness. Moisture was

removed from the extract by passing it through a pipette containing sodium sulphate and fitted with a cotton wool plug. The extract was collected in a pre-rinsed, dried and weighed vial before blowing down to dryness (N_2) and re-weighing. Filters retaining solvent-extracted retentate were re-dried ($60\text{ }^\circ\text{C}$, 24 h).

6.2.8. Solvent extraction of filtrate

Solvent (DCM, 2 x 15 ml) was added to freeze-dried filtrate and shaken (15 min, Gallenkamp autoshaker) before decanting off the solvent supernatant. Moisture was removed from the extract by passing it through a pipette filled with sodium sulphate and fitted with a cotton wool plug. The extract was collected in a vial complete with washings and blown down to dryness (N_2) before reweighing.

6.2.9. ^1H and ^{13}C NMR analysis

Samples were either dissolved in a small volume of deuterated solvent and transferred to a NMR tube or transferred to a NMR tube and fitted with an insert containing deuterated solvent. Tetramethylsilane (TMS) was added to provide a reference signal (0 ppm) prior to analysis using NMR. ^1H and ^{13}C spectra were obtained using a Jeol EX270 high resolution FT-NMR spectrometer at constant temperature ($20\text{ }^\circ\text{C}$).

6.2.10. Pyrolysis-gas chromatography-mass spectrometry (Py-GC-MS) of solvent-extracted retentate

Solvent-extracted retentate was carefully scraped from the filter with a micro-spatula and loaded into a capillary tube and analysed using Py-GC-MS as previously described (Section 4.2.1). Procedural blanks comprising unused glass fibre filter and $[\text{emim}]\text{Cl}-\text{AlCl}_3$ solvent-extracted retentate were also analysed using Py-GC-MS.

6.2.11. Gas chromatography-mass spectrometry (GC-MS) of retentate and filtrate solvent extracts

Dried retentate and filtrate solvent extracts were re-dissolved in solvent (DCM) to specific concentrations (0.1 and 0.5 mg ml⁻¹) prior to analysis using a Finnigan MAT GCQ™ ion trap GC/MS system with CTC Analytics A200S liquid sample autosampler. The autosampler method included five pre-injection solvent washes and two sample washes prior to sample uptake (1.0 µl; 0.5 µl, air volume) and injection (pre-injection hold, 3.0 sec; post-injection hold, 2.0 sec). Splitless injection was used with the injector temperature at 250 °C and a carrier gas (He) flow rate of 40 cm sec⁻¹. The GC column was a HP 5 MS (30 m x 0.25 mm; 0.25 µm film thickness, 5% diphenyl, 95% dimethylpolysiloxane) with the oven temperature programmed from 40 to 300 °C at 5 °C min⁻¹ and held at 300 °C for 10 minutes. The mass spectrometer was operated on full scan mode (2 scans sec⁻¹; 40 – 650 amu; mass defect 100.0 mmu amu⁻¹) with a source temperature of 180 °C. A series of external alkane and aromatic standards was also examined. Relative quantification based on peak area was measured automatically and mass spectra were identified by comparison with computerised library spectra (NBS), National Institute of Science and Technology (NIST) spectra, and previously published spectra. Where reference is made to mass spectral ions in the following text, base ions are indicated by underlining.

6.2.14. Analysis of solvent-extracted retentates using time of flight – secondary ion mass spectrometry (ToF-SIMS)

Qualitative analysis of some solvent-extracted retentates was undertaken using TOF-SIMS. Details of sample preparation, instrumentation and operating conditions are given in Section 4.2.2.

6.2.15. Analysis of solvent-extracted filtrates using electrospray ionisation-mass spectrometry (ESI-MS)

Freeze-dried solvent-extracted filtrate was made up to *ca.* 0.1 $\mu\text{g ml}^{-1}$ concentration in methanol (BDH HiPerSolv HPLC grade) and injected into the electrospray chamber of a Finnigan MAT LCQ™ ion trap mass spectrometer (spray voltage, 4 kV; high purity N_2 sheath gas; capillary temperature, 200 °C). Positive and negative ion mass spectra from 100 – 2000 amu were continuously recorded over one minute. Time-averaged mass spectra of the [emim]Cl-AlCl₃ {X(AlCl₃), X = 0.65} procedural blank solvent-extracted filtrate were subtracted from sample time-averaged mass spectra using Xcalibur™ software.

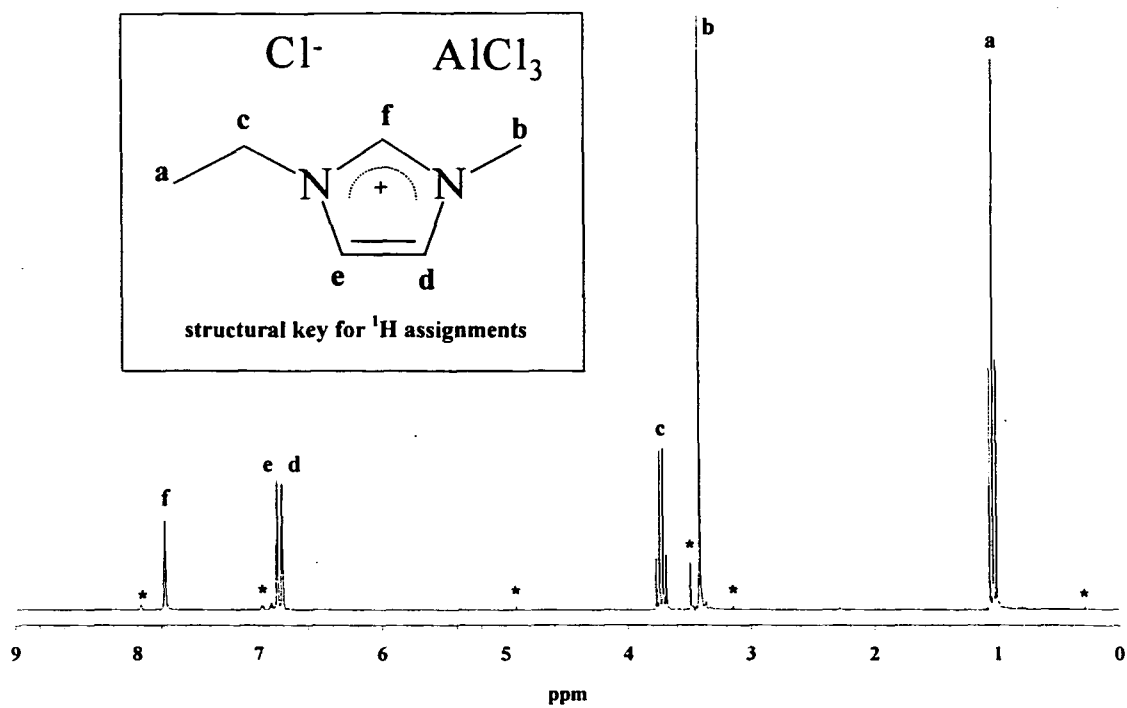
6.3. Results

6.3.1. [emim]Cl-AlCl₃ {X(AlCl₃), X = 0.65} procedural blank

[emim]Cl-AlCl₃ was a light golden brown colour with a fluid, slightly oily consistency, prior to microwave heating. Intermittent ‘sparking’ was noticed within the ionic liquid during some microwave heating cycles. This was also apparent during the microwave heating of some substrate/ionic liquid mixtures. No qualitative changes in either colour or viscosity were noted for the [emim]Cl-AlCl₃ {X(AlCl₃), X = 0.65} procedural blank after microwave heating. ¹H and ¹³C NMR spectra of the ionic liquid blank after heating but prior to hydrolysis were identical to those obtained for the [emim]Cl-AlCl₃ before microwave heating (Figure 6.13). Assignments for proton and carbon resonances made in the current study are given in Tables 6.10 and 6.11, respectively, along with literature values. Carbon assignments were confirmed by CDEPT and 2-D, ¹H-¹³C NMR experiments. More traditional acid/base properties may have been conferred to the ionic liquid by the presence of protic impurities (peaks marked with asterisks in Figure 6.13) which could have provided reaction-initiating proton sources, as previously reported (*e.g.* Pagni, 1987). The ¹H NMR spectrum of the procedural blank solvent-extracted filtrate had

the same pattern as that of the ionic liquid prior to hydrolysis except that all resonances were less well resolved and shifted downfield owing to interaction with water molecules.

(a)



(b)

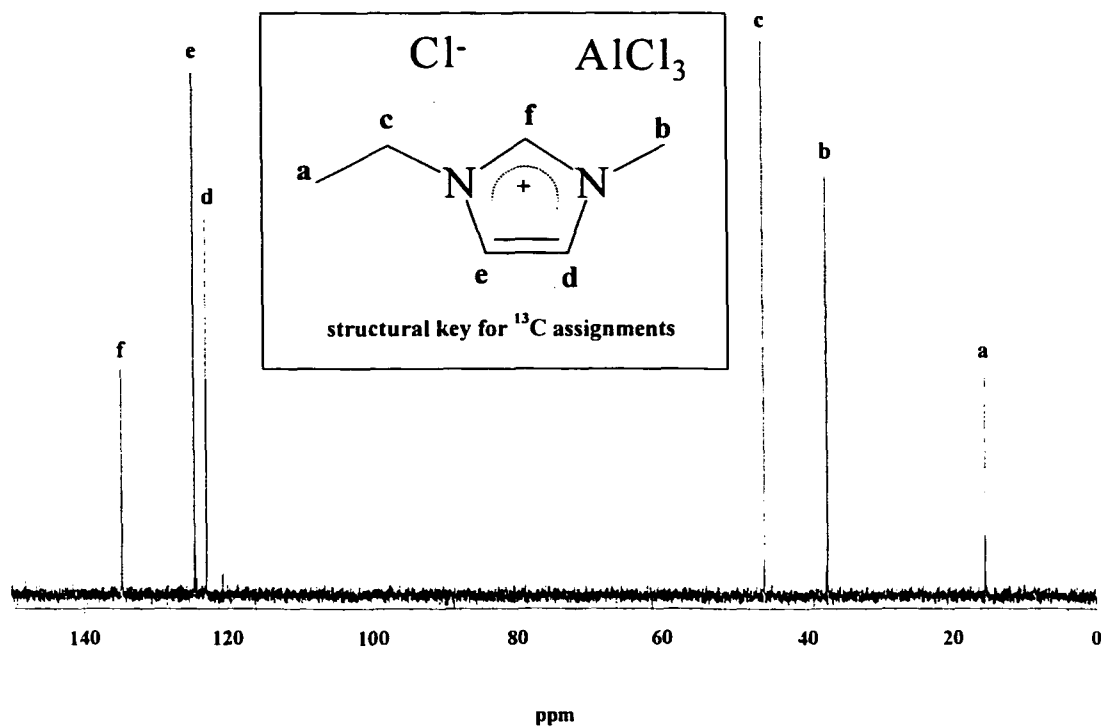


Figure 6.13. NMR spectra of $[\text{emim}]\text{Cl}-\text{AlCl}_3$ (a) ^1H (b) ^{13}C (* protic impurity).

Table 6.10. NMR ^1H assignments of [emim]Cl-AlCl₃

Assignment	δ / ppm		$\Delta\delta$	Multiplicity
	This work	Welton (1990)		
CH ₂ CH ₃ (a)	1.04	0.89	0.15	Triplet
NCH ₃ (b)	3.42	3.26	0.16	Singlet
CH ₂ CH ₃ (c)	3.73	3.58	0.15	Quartet
H ⁴ (d)	6.81	6.65	0.16	Triplet
H ⁵ (e)	6.85	6.69	0.16	Triplet
H ² (f)	7.77	7.61	0.16	Singlet

Table 6.11. NMR ^{13}C assignments of [emim]Cl-AlCl₃

Assignment	δ / ppm		$\Delta\delta$
	This work	Welton (1990)	
CH ₂ CH ₃ (a)	15.40	15.23	0.17
NCH ₃ (b)	37.15	36.98	0.17
CH ₂ CH ₃ (c)	45.83	45.70	0.13
C ⁴ (d)	122.61	122.25	0.36
C ⁵ (e)	124.28	124.28	0.00
C ² (f)	134.45	134.30	0.15

The results of gravimetric measurements of the four fractions obtained following hydrolysis of the procedural blank and substrate/ionic liquid mixtures, and solvent extraction of the retentate and filtrate are presented in Table 6.12. The total mass of the four fractions represented 91 % of the initial mass of ionic liquid with virtually all of the remaining material (> 99 %) present in the solvent-extracted filtrate (SEF). Loss of volatile

material during de-gassing or during the vigorously exothermic hydrolysis stage may have accounted for the 9 % loss. Nevertheless, these results for the procedural blank indicate that products from the hydrolysis of [emim]Cl-AlCl₃ should have provided a minimal contribution to all but the solvent-extracted filtrate fraction. Furthermore, because of the extremely hygroscopic nature of the solvent-extracted filtrate, mass balance data for hydrolysed and fractionated substrate/ionic liquid mixtures is reported in later sections as the yield of the other three fractions in terms of the mass of initial substrate.

Table 6.12. Percentage of initial sample weight in each of the fractions obtained following hydrolysis of substrate/ionic liquid mixtures and solvent extraction of the retentates and filtrates

Sample	SER	RSE	SEF [†]	FSE	% recovery
[emim]Cl-AlCl ₃	< 1	< 1	> 99	< 1	91
Anthracene	6	89	--	< 1	95
Phenanthrene	5	30	--	< 1	35
G ₁ P-[6]-Obn	62	11	--	3	76
G ₂ P-[12]-Obn	7	98	--	< 1	106
7 – 10 cm bswi IOM	103	1	--	< 1	105
21 – 24 cm bswi IOM	93	< 1	--	1	95
33 – 36 cm bswi IOM	85	< 1	--	1	85
46 – 49 cm bswi IOM	100	< 1	--	< 1	100
59 – 62 cm bswi IOM	97	< 1	--	< 1	98
82 – 85 cm bswi IOM	101	< 1	--	< 1	102
<i>M. jannaschii</i> IOM	4	< 1	--	1	5
Kimmeridge clay IOM	92	5	--	1	98
Gly/Glu IOM	93	< 1	--	< 1	94
His/Glu IOM	96	1	--	1	98

SER – solvent-extracted retentate, RSE – retentate solvent extract, SEF – solvent-extracted filtrate, FSE – filtrate solvent extract. [†]calculated by difference.

6.3.2. Ionic liquid-treated aromatic compounds

Anthracene (BDH) and phenanthrene (Koch-Light) were both in silvery-white flake form prior to ionic liquid treatment. Upon addition of [emim]Cl-AlCl₃, anthracene formed a green mixture and phenanthrene a purple one. Both mixtures became progressively darker and more viscous throughout the microwave heating stage.

Most (95 %) of the original mass of anthracene could be accounted for in the two solvent fractions and the solvent-extracted retentate, whereas only 35 % of the initial mass of phenanthrene could be accounted for in this manner. The bulk (89 %) of ionic liquid-treated anthracene was recovered as a black residue from the retentate solvent extract whilst 6 % had become solvent insoluble. Similarly, most of the phenanthrene recovered in the two solvent fractions and the extracted retentate was found in the retentate solvent extract (30 %) whilst some (5 %) was insoluble in DCM following ionic liquid treatment.

Prior to ionic liquid treatment, anthracene eluted as a single peak on a gas chromatogram (RT = 30.02 min) with a characteristic mass spectrum ($M^{+} = 178$). Analysis of the anthracene retentate solvent extract by GC-MS (Figure 6.14) showed that the major component was anthracene (67 %) whilst the remaining products were protonated anthracene species (dihydro-, 8 %; tetrahydro-, 20 %; octahydro-, 1 %), anthraquinone (6 %), an anthracene dimer (4 %; m/z 178, 358) and phenanthrene (< 1 %). The distribution of protonated anthracenes may be accounted for by formation of anthracenium (VI⁺) prior to hydrolysis owing to protic impurities in the ionic liquid (Section 6.3.1) and the subsequent non-quantitative protonation of this intermediate *via* the super-acidic action of the ionic liquid during the initial moment of hydrolysis, similar to that previously reported for anthracene treated with superacidic [emim]Cl-AlCl₃ (Smith *et al.*, 1989; Carlin *et al.*, 1992). If this assumption is correct, then anthraquinone may also have been produced *via*

oxidation of the anthracenium cation during the vigorous exothermic hydrolysis of the ionic liquid-anthracene solution. The production of bianthracene was consistent with the dimerisation of reactive intermediates, similar to the reported formation of anthracene dimers during photolysis of anthracene in ionic liquid solution (Hondrogiannis *et al.*, 1993).

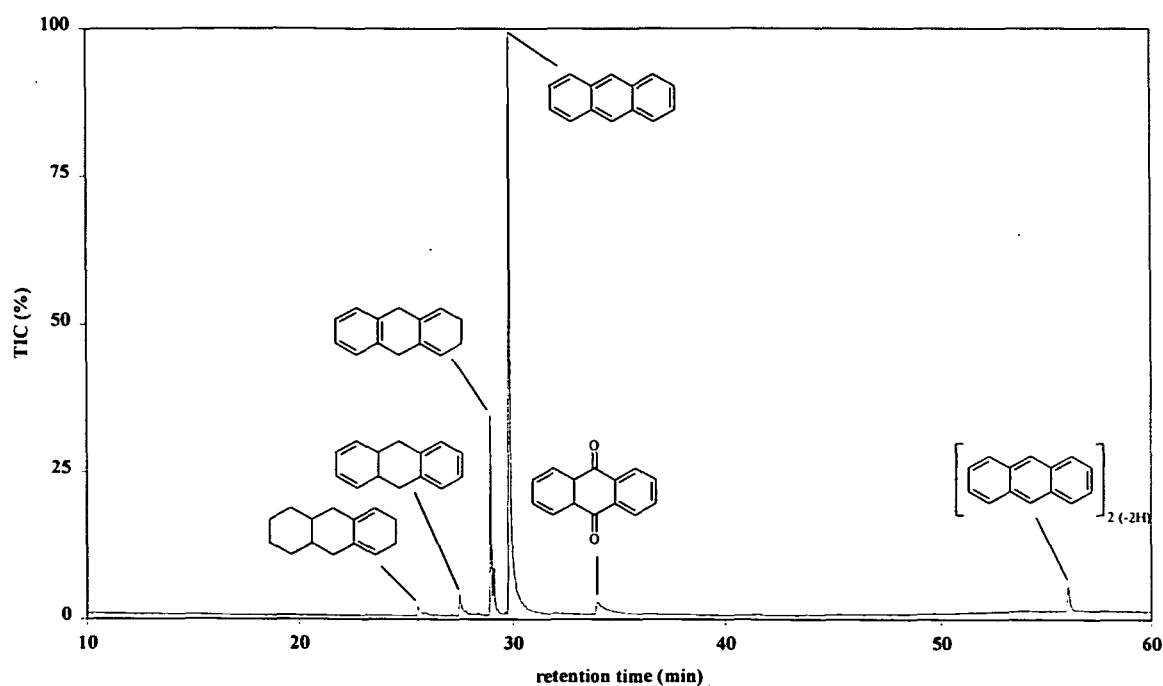


Figure 6.14. Partial GC-MS TIC of anthracene retentate solvent extract (temperature programme: 40 – 300 °C at 5 °C min⁻¹, 10 min at 300 °C; HP5 MS column). Structures shown in generic form.

The single most abundant component in the pyrogram of anthracene solvent-extracted retentate (Figure 6.15) was anthracene (40 %). Other components present in this fraction were not identified in the pyrogram of the unreacted anthracene. These included protonated anthracenes, *i.e.* tetrahydro- (25 %) and octahydro- (6 %), anthraquinone (10 %), several anthracene dimers (7 %) and naphthalenes (< 2 %). Poor chromatographic resolution due to sample overloading was not adjudged to be problematic because the aim of this

pyrolysis experiment was to provide a comparison to the Py-GC-MS analysis of anthracene. With the exception of naphthalenes and some of the anthracene dimers, these products were the same as those found in the retentate solvent extract. Although the presence of naphthalenes in the pyrogram inferred that some ring cleavage had occurred during ionic liquid treatment, an alternative source may have been *via* the polymerisation of trace contaminants in the raw anthracene, *e.g.* C₄-substituted benzene. This latter supposition is the more likely, as electropolymerisation of benzene in ionic liquids has been reported previously (Goldenberg & Osteryoung, 1994), whereas ring cleavage has not. Nevertheless, anthracene derivatives were quantitatively the most important products formed from the ionic liquid treatment of anthracene. Anthraquinone accounted for 10 % of the chromatographic response, possibly due to oxidation of the anthracenium cation during the vigorous hydrolysis reaction with water acting as the oxidising agent.

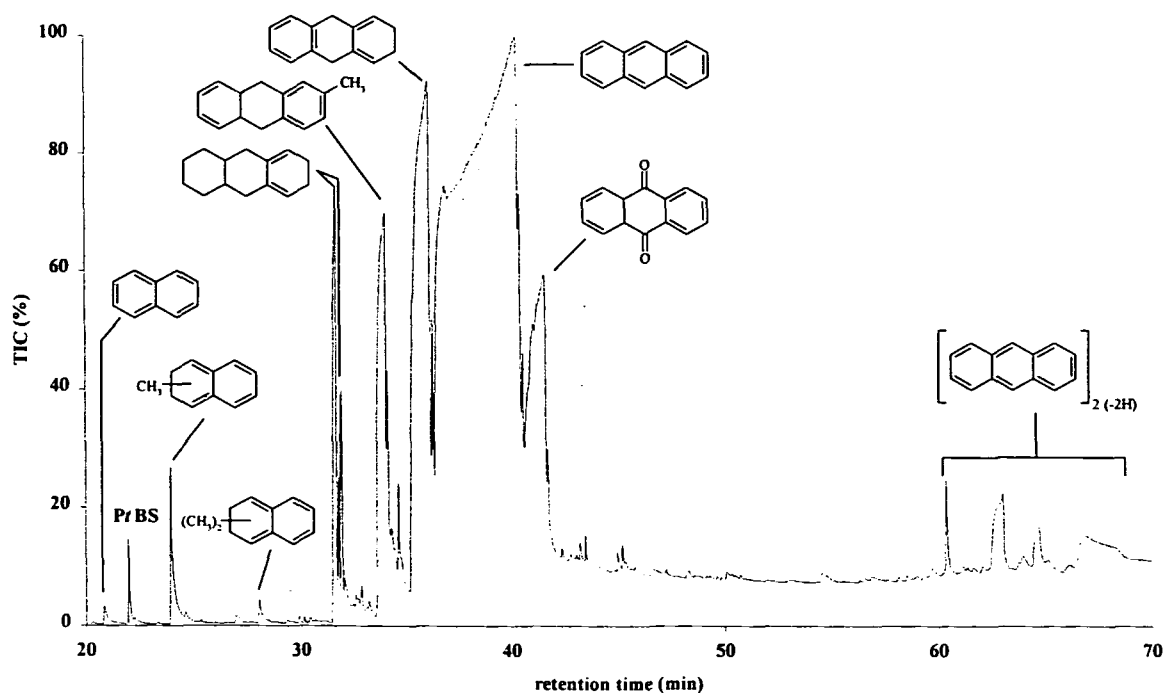


Figure 6.15. Partial Py-GC-MS TIC of anthracene solvent-extracted retentate (pyrolysis at 595 °C 5 °C; GC programme, -10 to 300 °C at 5 °C min⁻¹, hold at 300 °C for 10 min; column Rtx-5; MS at 40 eV). Structures shown in generic form.

The poor recovery of ionic liquid-treated phenanthrene products (35 % of starting material quantified as solvent extracts and solvent-extracted retentate) inferred that a substantial portion of material may have been lost as volatile material upon hydrolysis, or had been retained in the aqueous phase. The solvent-extracted filtrate was analysed using ESI-MS, a soft ionisation technique that tends to produce protonated/de-protonated molecular ions ($M + H)^+$ and $(M - H)^-$ when operated in positive and negative ion modes, respectively (Ascroft, 1997). Examination of the solvent-extracted filtrate using ESI-MS (positive ion mode; Figure 6.16c) indicated the presence of a single ion ($m/z = 1440$) that was not attributable to the solvent (MeOH; Figure 6.16a) or ionic liquid hydrolysis products (Figure 6.16b). Whilst this mass was consistent with a polymerised phenanthrene compound containing eight tetrahydrophenanthrene units, each bonded at two positions, such a compound is unlikely to have been aqueous soluble, although it may have formed as an adduct during ionisation. Alternatively, the ion at $m/z = 1440$ also corresponded to an adduct comprising four hexachlorotetrahydrophenanthrene units bonded together at two positions. Whilst a single ion at $m/z = 1899$ in the negative ion ESI-MS mass spectrum was also consistent with such structures, the possibility remains that these ions may have represented analytical artefacts. Whether this accounted for the entire product deficit is uncertain and some of the original phenanthrene sample may have been converted to gaseous products by ionic liquid treatment.

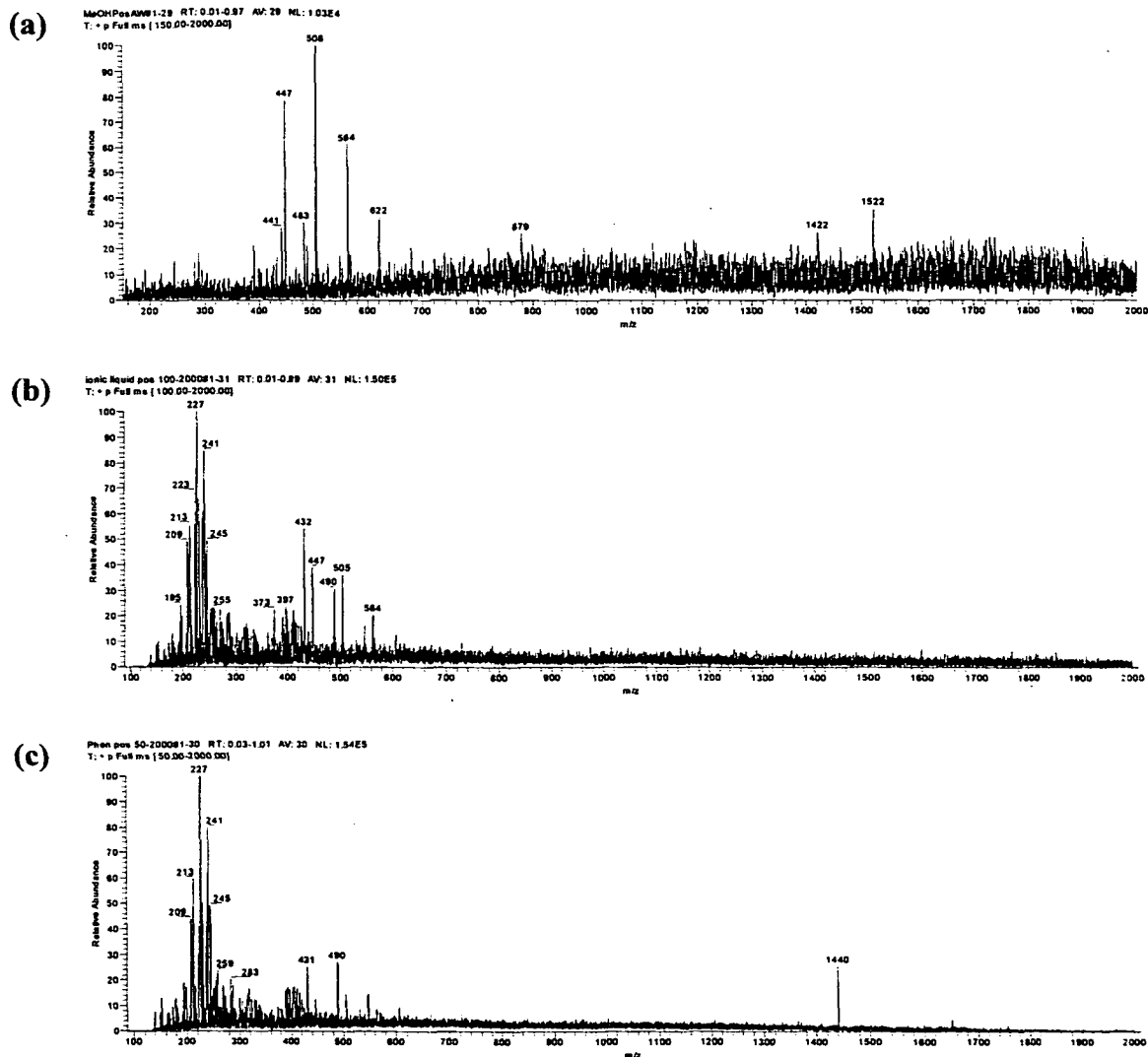


Figure 6.16. Positive ion ESI-MS mass spectra of (a) methanol, and solvent-extracted filtrates (SEF) from (b) [emim]Cl-AlCl₃ and (c) phenanthrene (0.1 g ml⁻¹ in MeOH; 4 kV spray voltage; 200 °C capillary temperature; recorded over 1 min).

Prior to ionic liquid treatment phenanthrene eluted as a single peak (RT = 29.44 min) when examined by GC-MS with a characteristic mass spectrum similar to that of anthracene. Analysis of the phenanthrene retentate solvent extract using GC-MS (Figure 6.17) showed the major GC-amenable components to be phenanthrene (87 %) and protonated phenanthrene species (dihydro-, 8 %; tetrahydro-, < 1 %; hexahydro-, 3 %; octahydro-, 2 %). In addition, trace levels of two isomers of two phenanthrene dimers (ions $m/z = 178$ and 354/356) eluted after the oven temperature had reached its maximum. These results mirrored those found for anthracene, indicating that similar reaction mechanisms

were involved. A noticeable difference between the GC-MS results from anthracene and phenanthrene retentate solvent extracts was the absence of phenanthraquinone from the chromatogram of the latter.

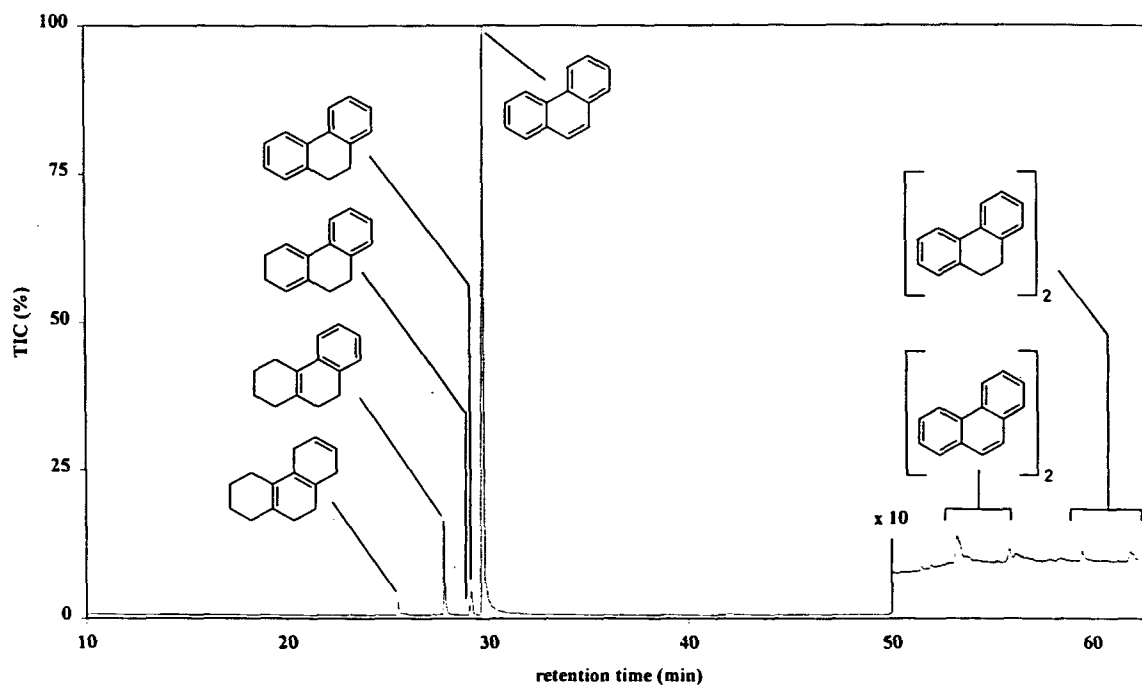


Figure 6.17. Partial GC TIC of phenanthrene retentate solvent extract (temperature programme: 40 - 300°C at 5°C min⁻¹, 10 min at 300°C; HP5 MS column). Structures shown in generic form.

Trace contaminants identified as alkanes, plasticisers and fluorene were present in pyrograms from both the unreacted phenanthrene and the solvent-extracted retentate (Figure 6.18). The principal difference between the pyrolysis chromatogram of phenanthrene solvent-extracted retentate and that of untreated phenanthrene was the presence of naphthalenes in the former, as found from the Py-GC-MS analysis of the anthracene solvent-extracted retentate. In contrast to the pyrogram of anthracene solvent-extracted retentate, the quinonic form was absent from the corresponding phenanthrene pyrogram.

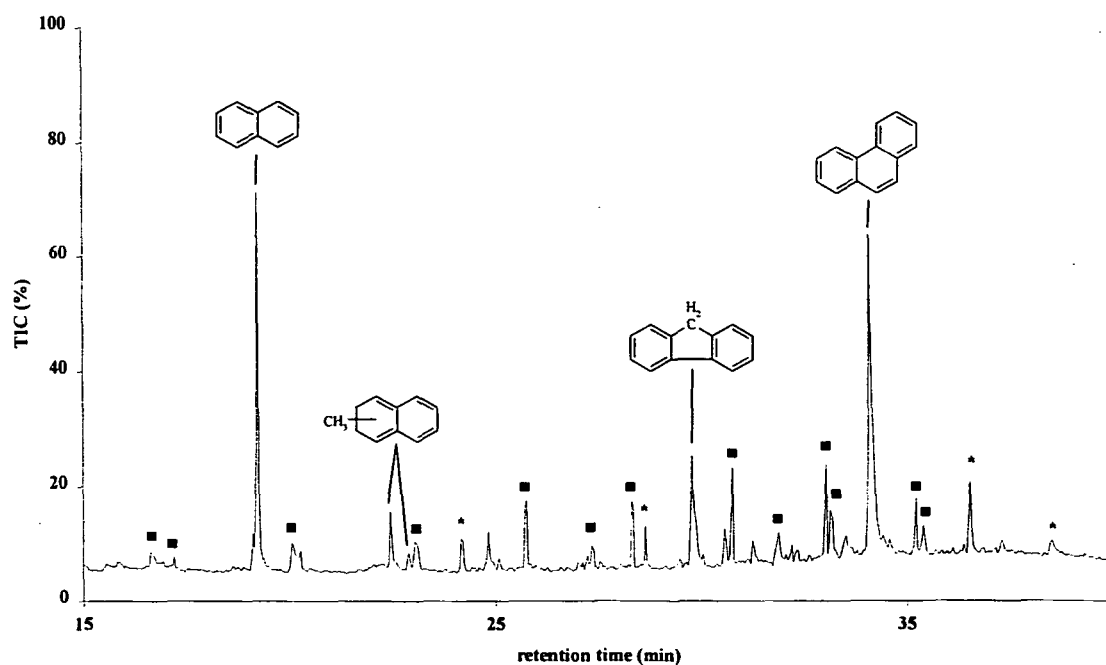


Figure 6.18. Partial Py-GC-MS TIC of phenanthrene solvent-extracted retentate (pyrolysis at 595 °C 5 °C; GC programme, -10 to 300 °C at 5 °C min⁻¹, hold at 300 °C for 10 min; column Rtx-5; MS at 40 eV; ■ alkanes, * phthalates).

6.3.3. Ionic liquid-treated dendrimers

Both dendrimers were DCM soluble, non-GC-MS amenable, white powders prior to the addition of [emim]Cl-AlCl₃. A dark red mixture was formed on addition of the ionic liquid to G₁P-[6]-Obn before microwave heating, during which the mixture darkened and became viscous. Dendrimer G₂P-[12]-Obn was not subjected to microwave heating in order to assess the effect of microwave heating.

Three quarters of the original mass of G₁P-[6]-Obn could be accounted for in the two solvent fractions and the solvent-extracted retentate, of which most (84 %) had become DCM insoluble following ionic liquid treatment. All (106 %) of the initial mass of G₂P-[12]-Obn could be accounted for in the solvent extracts and the extracted retentate, most (92 %) of which was recovered in the retentate solvent extract. Ionic liquid-treated G₂P-[12]-Obn had not been subjected to microwave heating, suggesting that microwave heating

was important in controlling the interaction between [emim]Cl-AlCl₃ and the dendrimer. Previous studies have reported that microwave heating was essential in promoting the ionic liquid dissolution of kerogens and coals (Patell, 1994; Dutta, 1994)

Pyrolysis-GC-MS of untreated G₁P-[6]-Obn yielded in excess of thirty chromatographic peaks (Figure 6.19a), although 90 % of the total resolved chromatographic response was contained in ten peaks. These products were exclusively aromatic in character (benzene, 6 %; toluene, 20 %; xylene, 2 %; ethenyl benzene, 1 %; benzaldehyde, 3%; methylbiphenyl, 3 %; diphenylethane, 28 %; and 1,2-diphenylethenes, 11 %) indicating that substantial ether cleavage and rearrangement of the original dendrimer had occurred during pyrolysis. A proposed formation scheme for the major pyrolysis fragmentation products from the original dendrimer (Figure 6.20) is consistent with the 60 % content of surface benzyl groups forming toluene (XVII), diphenylethane (XVIII) and diphenylethene (XIX), which accounted for 59 % of the chromatographic response, and the 10 % content of the benzyl core forming benzene (XX). Furthermore, there was an apparent reduction in the oxygen content of pyrolysis products compared to the untreated dendrimer, compatible with the loss of volatile components, *e.g.* CO, CO₂, and O₂, during pyrolysis. These results serve to highlight a major drawback associated with analysis of large chemical structures using Py-GC-MS, *i.e.* complex fragmentation patterns may be produced by compounds with even relatively simple architecture and where the parent architecture is unknown it may be extremely difficult to interpret the fragmentation pattern correctly.

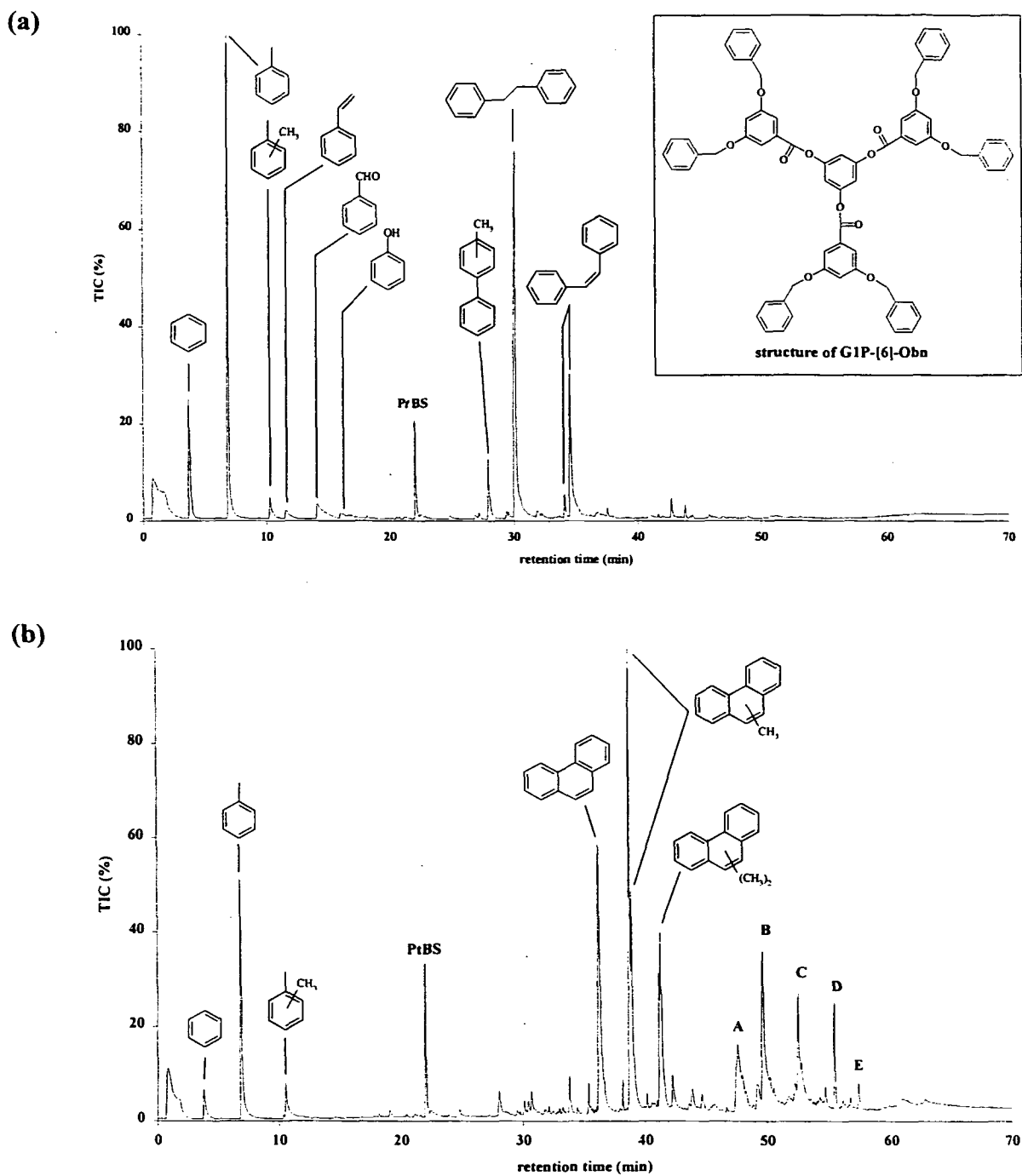


Figure 6.19. Py-GC-MS TIC of G₁P-[6]-Obn (a) Before ionic liquid treatment (b) Solvent-extracted retentate (SER) (pyrolysis at 595 °C 5 °C; GC programme, -10 to 300 °C at 5 °C min⁻¹, hold at 300 °C for 10 min; column Rtx-5; MS at 40 eV).

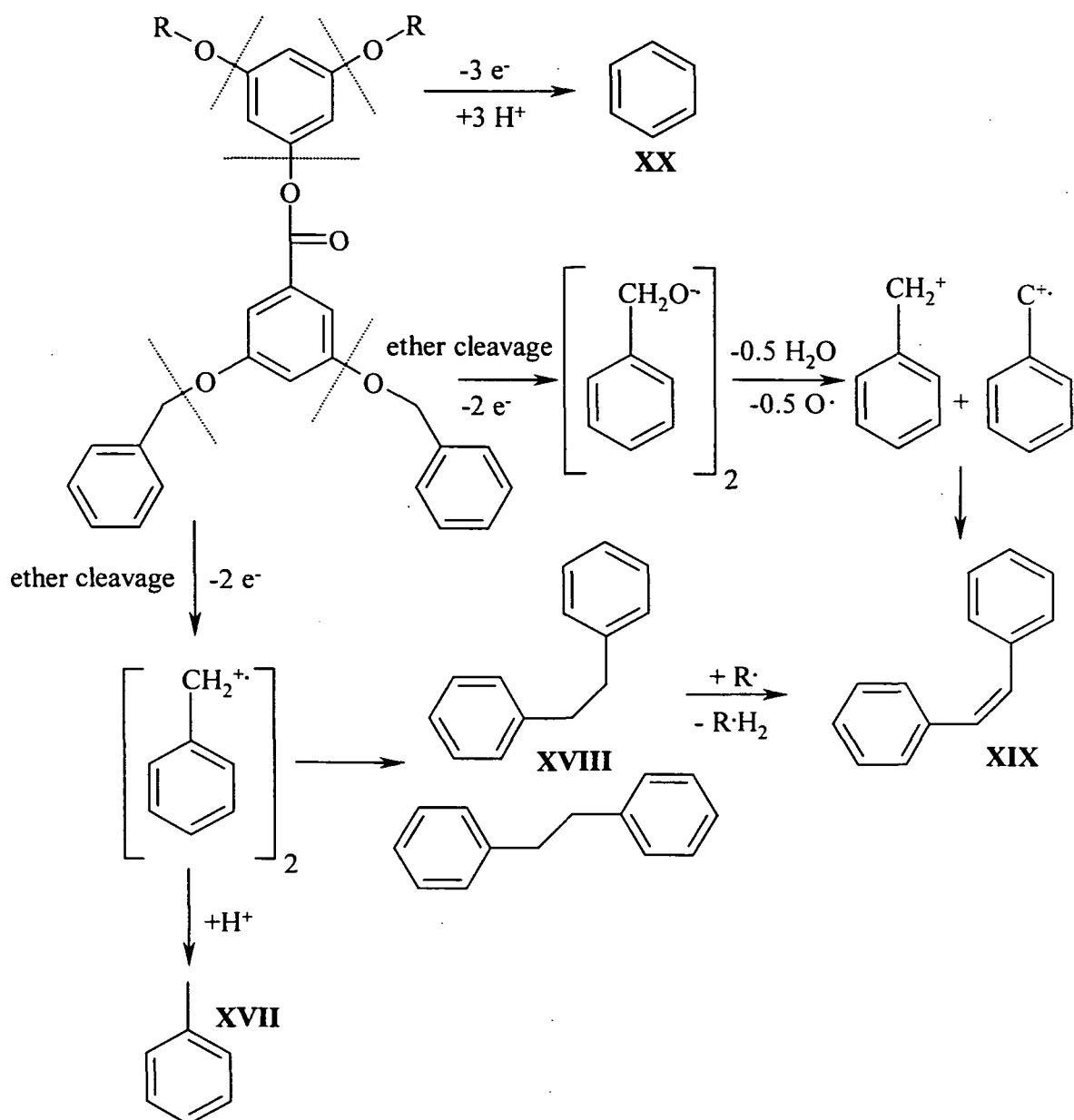


Figure 6.20. Hypothesised fragmentation routes for major products formed during the pyrolysis of untreated G₁P-[6]-Obn

Following ionic liquid treatment 62 % of the initial G₁P-[6]Obn had become insoluble in DCM. The pyrolysis chromatogram of the solvent-extracted retentate (Figure 6.19b) was dominated by seventeen components (87 % of the total chromatographic response). Benzene, toluene and xylene were common components in the pyrograms of the untreated

dendrimer and the solvent-extracted retentate and suggest that they may have been similarly bound in the matrix. However, other monoaromatic and bicyclic species observed in the untreated dendrimer pyrogram were absent from the pyrogram of the treated dendrimer, being replaced by phenanthrene compounds (39 %) and other unidentified higher molecular weight components eluting between 45 and 60 minutes (peaks A-E, Figure 6.19; 26 %). A possible route to the formation of phenanthrene compounds from G₁P-[6]-Obn may have been *via* the formation of stilbenes during microwave heating and subsequent oxidation of the dihydrophenanthrene intermediates by molecular oxygen, similar to that observed when stilbene is subjected to irradiation by UV light in the presence of oxygen (Figure 6.21; March, 1985). Whether this occurred when G₁P-[6]Obn was in ionic liquid solution or upon hydrolysis was not clear. Analysis of the dendrimer-ionic liquid solution, prior to hydrolysis, using NMR produced spectra dominated by [emim] resonances that were of little assistance in answering this question. Alternatively, the production of phenanthrene compounds may be explained by intermolecular Scholl reactions between benzyl groups following ether cleavage, or simply result from pyrolytic heating of the dendrimer-ionic liquid solution during the microwave heating stage. Nevertheless, the apparent overall effect of treating G₁P-[6]Obn with [emim]Cl-AlCl₃ was to remove oxygen (ester and ether) and promote aromatisation.

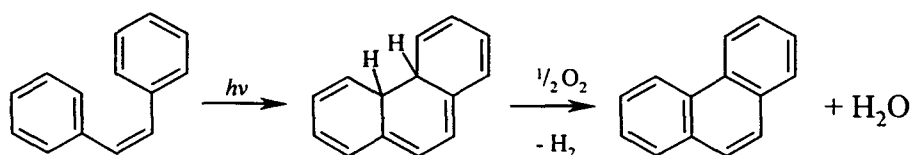


Figure 6.21. Formation pathway of phenanthrene from *cis*-stilbene by UV irradiation in the presence of molecular oxygen (from March, 1985)

Analysis of the G₁P-[6]-Obn retentate solvent extract using GC-MS revealed that whereas the dendrimer had not previously been GC-amenable a number of GC amenable products

were present in this fraction (Figure 6.22). The principal components of the chromatogram, identified from their mass spectra, were phenanthrenes (methyl-, 34 %; dimethyl-, 17 %; trimethyl-, 2 %; dihydro-, 8 %; dihydromethyl-, 22 %; and dihydrodimethyl-, 1 %) and methylated naphthalene dimers (methyl-, 3 %; dimethyl-, 1 %). These results were consistent with those obtained from the Py-GC-MS analysis of the solvent extracted retentate and support the contention that the consequences of ionic liquid treatment of G₁P-[6]-Obn were (1) removal of oxygen *via* ether/ester cleavage, (2) increased aromatisation *via* condensation of cyclised aromatic fragments.

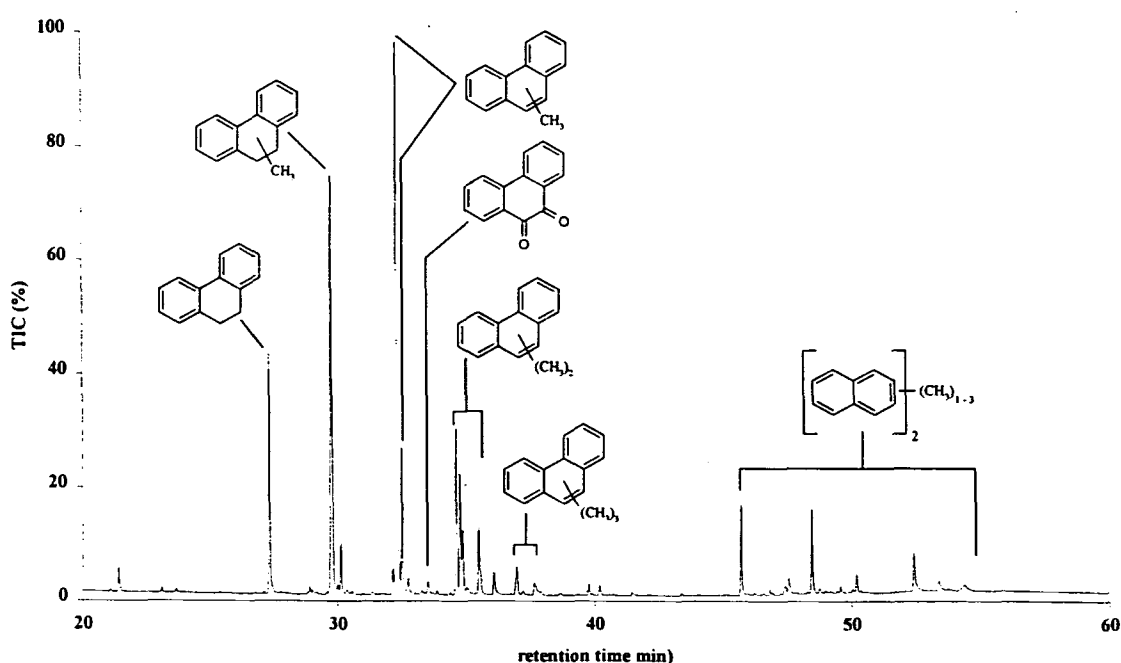


Figure 6.22. Partial GC TIC of G₁P-[6]-Obn retentate solvent extract (temperature programme: 40 - 300°C at 5°C min⁻¹, 10 min at 300°C; column HP5 MS)

The effect of microwave heating during ionic liquid treatment was investigated using the G₂ dendrimer, G₂P-[12]-Obn, which contained identical terminal and functional groups to those in G₁P-[6]-Obn. In contrast to the G₁ dendrimer, the bulk (98 %) of ionic liquid treated G₂P-[12]-Obn remained soluble in DCM following ionic liquid treatment when microwave heating was omitted. However, analysis of the G₂P-[12]-Obn retentate solvent

extract using GC-MS (Figure 6.23) showed that its character had changed substantially. Whereas G₂P-[12]-Obn had not been amenable to GC prior to ionic liquid treatment, soluble material following treatment principally comprised anthracene (56 %) and anthracene derivatives (dihydro-, 6 %; tetrahydro-, 20 %; octahydro-, 3 %; quinonic, 7 %; dimer, 6 %) derivatives, accounting for 98 % of the chromatographic response. These were differentiated from the solubilised phenanthrene products identified in the retentate solvent extract from G₁P-[6]-Obn by their retention times, with the anthracene products eluting later than their phenanthrene counterparts. Clearly, ionic liquid treatment without microwave heating, had a profound effect on the dendritic structure. The ionic liquid appears to have caused cleavage of ether linkages in the G₂ dendrimer with subsequent limited polymerisation/rearrangement of the released benzyl groups, similar to that observed in the G₁ dendrimer. Whilst the major products from ionic liquid treatment of G₁P-[6]-Obn were phenanthrenes, binaphthalenes and their methylated derivatives, the soluble products from G₂P-[12]-Obn were exclusively non-methylated anthracene derivatives. This suggested that, for the soluble products, microwave heating had promoted the formation of phenanthrenes over anthracenes and methylation when methylene groups were present. The loss of volatile material was consistent with the gravimetric results.

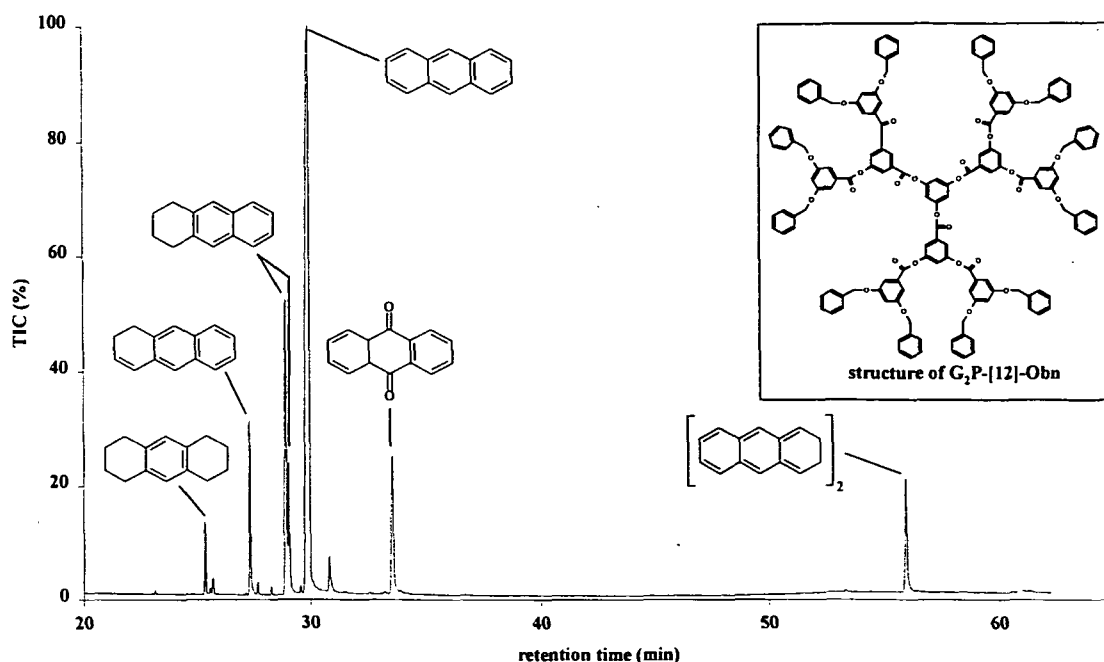


Figure 6.23. Partial GC-MS TIC of G_2P -[12]-Obn retentate solvent extract (temperature programme: 40 – 300 °C at 5 °C min⁻¹, 10 min at 300 °C; column, HP5 MS)

Dendrimer G_2P -[12]-Obn contained identical terminal and functional groups to those in G_1P -[6]-Obn, differing only in their number, owing to a second iterative step in the G_2 dendrimer synthesis. Therefore, it was reasonable to expect that both dendrimers would have fragmented in a similar manner during Py-GC-MS analysis. However, fragmentation of untreated G_2P -[12]-Obn during Py-GC-MS analysis produced a more complex pyrogram (Figure 6.24a) than that of the G_1 dendrimer with over forty peaks present. Integration of the total resolved peaks with respect to the *PtBS* internal standard accounted for 95 % of the pyrolysed sample on a mass basis. Components identified from their mass spectra accounted for 73 % of the total chromatographic response and included benzenes (benzene, 6 %; toluene, 22 %; xylene, 1 %; ethenylbenzene, 1 %; benzaldehyde, 5 %; phenol, 4 %; benzenediol, 3 %) and two and three-ringed aromatic compounds (acenaphthene, 1 %; diphenylmethane, 3%; methylbiphenyl, 3 %; 1,2-diphenylethane, 9 %; 1,2-diphenylethene, 9 %; phenylmethylphenol, 3 %; phenylmethylbenzenediol, 2 %; phenylene-*bis*-phenylmethanone, 1 %). Common components (benzene, toluene, xylene,

ethenylbenzene, benzaldehyde, phenol, methylbiphenyl, 1,2-diphenylethane and 1,2-diphenylethene) in the pyrograms from both dendrimers likely reflected their identical functionality and suggested some consistency in their fragmentation pathways during pyrolysis. However, unidentified higher molecular weight components (eluting between 35 – 65 minutes) in the pyrogram from G₂P-[12]-Obn, which accounted for 23 % of the chromatographic response, comprised < 10 % of the chromatographic response in the G₁ dendrimer pyrogram. In addition, more oxygen-containing compounds were identified in the G₂P-[12]-Obn pyrogram than in the G₁ dendrimer pyrogram. These differences may have reflected differences in molecular conformation, *i.e.* steric factors, or elemental composition (G₁P-[6]-Obn, C, 77 %, H, 5 %, O, 18 %; G₂P-[12]-Obn, C, 75 %, H, 5 %, O, 20 %), either of which could have important implications for the interpretation of Py-GC-MS data obtained from geopolymers.

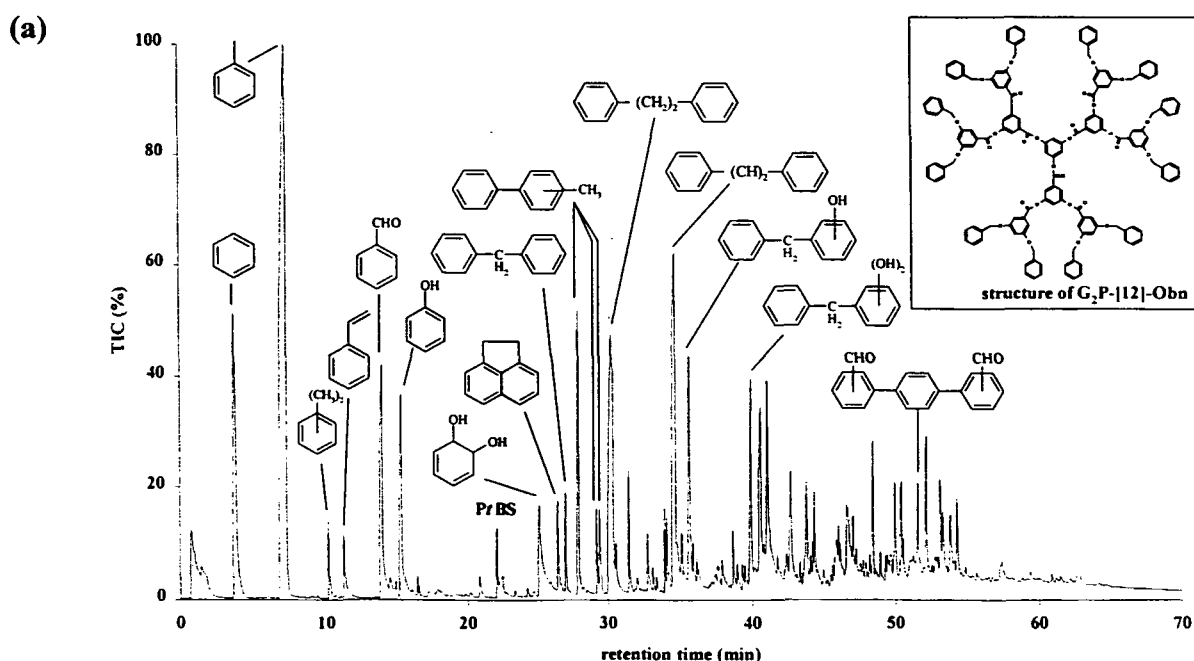


Figure 6.24 cont. overleaf

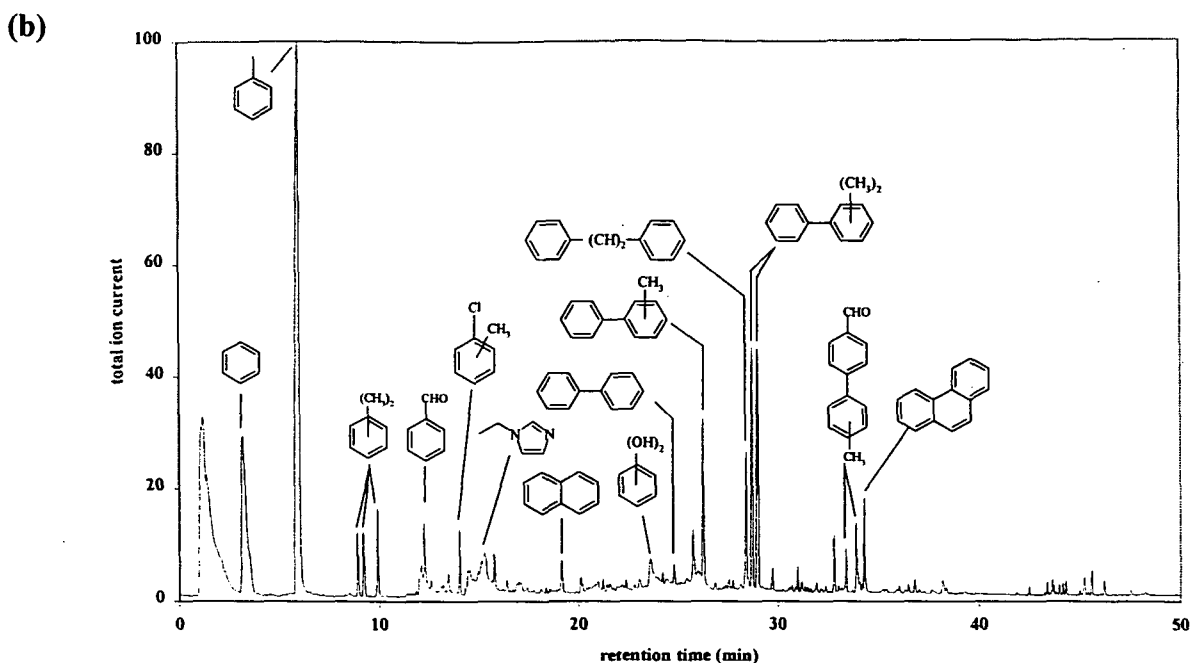


Figure 6.24. Py-GC-MS TIC of G₂P-[12]-Obn (a) Before ionic liquid treatment (b) Solvent-extracted retentate (SER) (pyrolysis at 595 °C 5 °C; GC programme, -10 to 300 °C at 5 °C min⁻¹, hold at 300 °C for 10 min; column Rtx-5; MS at 40 eV).

The pyrolysis chromatogram of the ionic liquid-treated G₂P-[12]-Obn solvent-extracted retentate (Figure 6.24b) was distinctly different to that of the untreated dendrimer, the former being characterised by an obvious reduction in the number of peaks in the higher mass region (beyond 40 minutes). Most of the chromatographic response (81 %) from the pyrolysis of ionic liquid-treated G₂P-[12]-Obn solvent-extracted retentate could be accounted for by fifteen components, mainly volatiles (25 %), mono-aromatic (benzene, 10 %; toluene, 25 %; xylenes, 3 %; benzaldehyde, 2 %; chloromethylbenzene, < 1 %; benzenediol, 2 %) and bi- and tri-cyclic aromatic compounds (naphthalene, < 1 %; biphenyls, 16 %; 1,2-diphenylethane, 2 %; phenanthrene, 1 %). The presence of ethylimidazole (4 % of the chromatographic response) suggested that some of the ionic liquid had become bound to G₂ dendrimer products.

6.3.4. Ionic liquid-treated IOM from Rostherne Mere sediments

Prior to the addition of ionic liquid, IOM obtained from Rostherne Mere sediments was black/brown in colour and had a powdery consistency. Previously, characterisation of this IOM using a range of techniques (ss-NMR spectroscopy, elemental analysis, IR spectroscopy and Py-GC-MS; Chapters 3 and 4), indicated that it was relatively enriched in aromatic components but also contained a significant portion of (C₆₍₁₎ – C₃₀₍₁₎) *n*-alkanes/*n*-alk-1-enes. After two minutes (12 x 10 s heating cycles) microwave heating the sedimentary IOM/ionic liquid mixture became noticeably darker and more viscous, accompanied by an obvious reduction in the size of particulate material. Observation of further change in particle size was hampered by the increasing viscosity of the mixture, although some particulate material was evident in the mixture following completion of the microwave heating stage. A strong sulphurous odour was noted upon hydrolysis of the IOM/ionic liquid mixture. Patell (1994) and Dutta (1994) reported a similar odour when they hydrolysed kerogen/ionic liquid mixtures but surprisingly a test for hydrogen sulphide made by these authors was negative.

The two solvent fractions and the solvent-extracted retentate accounted for 85 – 105 % of the initial mass of IOM. Most importantly, in most cases, almost all (> 98 %) of the IOM remained solvent (DCM) **insoluble** after ionic liquid treatment. Additional solvent extractions carried out on some retentate samples using hexane and methanol also failed to extract any significant amounts of material. Analysis of the retentate solvent extract using ¹H NMR showed that this fraction was dominated by aliphatic resonances (*ca.* 60 %), similar to that reported by Patell (1994) and Dutta (1994), but given its quantitative unimportance this was not analysed further.

Pyrolysis chromatograms obtained from the Py-GC-MS analyses of the solvent-extracted retentates (**SERs**) from Rostherne Mere sediments following ionic liquid treatment of the

respective IOMs were very similar to each other (typical pyrolysis chromatogram shown in Figure 6.25b) but quite distinct to those obtained from the Py-GC-MS analyses of the untreated isolated IOMs (Figure 6.25a). Quantification of the manually integrated total area of peaks against the *Pt*BS internal standard showed that resolvable peaks accounted for 0.7 – 2.7 % of the pyrolysed substrates. Integration of the total response including the unresolved area below the baseline equated to 1 – 5 % of the pyrolysed substrates. The chromatographic response of the resolved components of each of the Rostherne Mere sediment IOM solvent-extracted retentate pyrolysis chromatograms was dominated by the volatiles peak (62 – 76 %) and characterised almost exclusively by a relative enrichment in, or formation of, aromatic compounds, compared to aliphatic and monounsaturated compounds in the untreated IOM (Figure 6.25a). Sulphur (S₈) was evident in the solvent-extracted retentate pyrograms, whereas previously it was absent from the corresponding IOM pyrograms. The appearance of imidazoles and a pyridine dimer in the pyrograms of sediment solvent-extracted retentates implied that some of the ionic liquid had reacted with, and become incorporated into, the IOM matrix. A series of *n*-alkanes from C₉ – C₂₃ and some alk-1-ene homologues were evident in all of the pyrolysis chromatograms of the sediment retentates but were not quantitatively important components, whereas previously in the pyrograms from sedimentary IOM (Section 4.3.2) they had been dominant (Figure 6.25a).

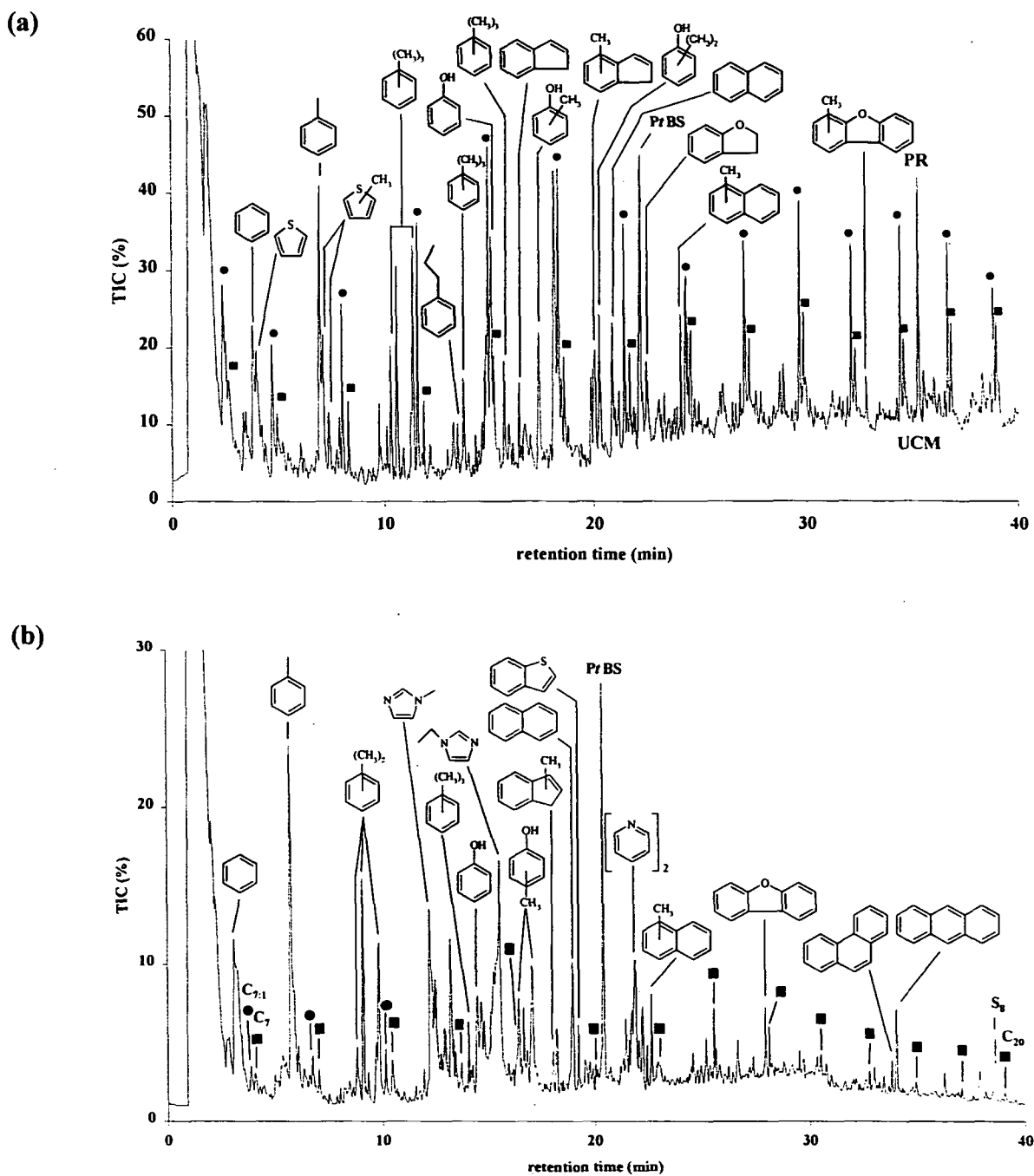


Figure 6.25. Typical partial Py-GC-MS TIC of Rostherne Mere sedimentary IOM (a) Before ionic liquid treatment (b) Solvent-extracted retentate (SER) (pyrolysis at 595 °C 5 °C; GC programme, -10 to 300 °C at 5 °C min⁻¹, hold at 300 °C for 10 min; column Rtx-5; MS at 40 eV; ■ *n*-alkanes; ● *n*-alk-1-enes; PR = prist-1-ene).

Loss of *n*-alk-1-enes from the solvent-extracted retentate pyrograms indicated that the

ionic liquid had attacked the aliphatic precursors of these compounds. A reduction in the bias towards higher molecular weight unresolved components, *i.e.* shifting of the 'hump' maxima towards shorter retention times, suggested that much of the unresolved compounds had been significantly altered. If the ionic liquid had simply caused lysis of IOM macromolecules or dissolved the IOM an increase in the pyrolysis yield might have been expected, but pyrolysis yields increased by only 1 – 2 %. It is more likely that some constituents became more amenable to Py-GC-MS whilst others became more intractable. This would explain the reduction in higher molecular weight unresolved components and aliphatic and unsaturated alkyl chains. Ionic liquid mediated polymerisation, addition and substitution reactions involving these components may have led to the formation of new non-pyrolysable material. Insoluble material, speculated to have been of a macromolecular nature, has previously been reported to form upon hydrolysis of pyrrole from an acidic ionic liquid (Zawodzinski *et al.*, 1988).

ToF-SIMS spectra of solvent-extracted retentates from ionic liquid-treated IOM from Rostherne Mere sediments (21 – 24 and 59 – 62 cmbswi) are presented in Figure 6.26. Polydimethylsiloxane (PDMS) contamination was indicated by the presence of ions at $m/z = 207, 221, 281$ and 355 , and supported by ions at $m/z = 73$ and 147 (not shown). This contamination was not apparent in the ToF-SIMS analyses of silicon wafer procedural blanks or sedimentary IOMs carried out on indium foil (Section 4.2.2) prior to ionic liquid treatment. Therefore, the most likely source of this PDMS was as a contaminant of the ionic liquid. Other than the presence of PDMS, the ToF-SIMS mass spectrum of the solvent-extracted retentates differed substantially from those of the corresponding IOMs (Figure 6.26 and Section 4.3.2). In particular, the absence of the series of alkylated compounds identified in the IOMs and the apparent reduction in some higher molecular weight material following ionic liquid-treatment was entirely consistent with results from Py-GC-MS analyses. In addition, these results support the formation of material of a more

intractable nature than the IOM, *i.e.* it was less susceptible to ionisation and volatilisation under ToF-SIMS conditions than the isolated IOM, possibly as a result of ionic liquid-catalysed graphitisation during the treatment procedure.

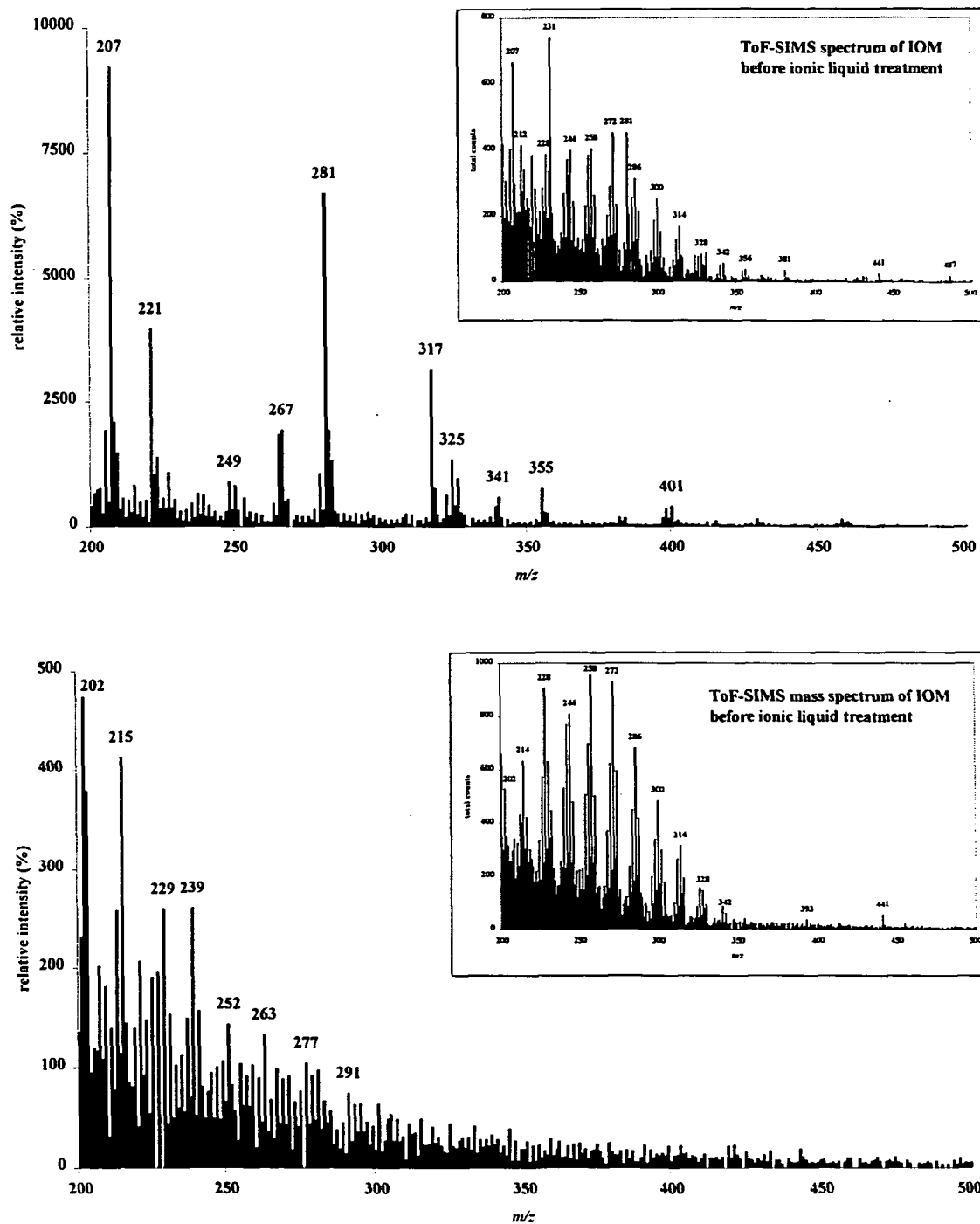


Figure 6.26. Partial positive ion ToF-SIMS mass spectrum of Rostherne Mere sediment IOM solvent extracted retentate (a) 7 – 10 cmbswi (b) 59 – 62 cmbswi (sample on Si wafer; ion source, Ga⁺).

6.3.5. Ionic liquid-treated Kimmeridge Clay IOM

Before ionic liquid treatment, IOM isolated from Kimmeridge Clay was a dark brown powder. Instrumental characterisation of the IOM using IR spectroscopy (Chapter 3), Py-GC-MS and ToF-SIMS (Chapter 4) indicated that it contained alkyl (a series of *n*-alkanes/*n*-alk-1-enes from C₇ – C₃₂) and aromatic components (1 – 3 rings), the latter of which included a number of thiophenes. During microwave heating the IOM/ionic liquid mixture darkened in colour and became more viscous, whilst particulate material diminished in size during the heating process. A strong sulphurous odour was evident when the treated mixture was hydrolysed.

Mass balance calculations showed that 98 % of the initial substrate could be accounted for in the solvent extracts and the solvent insoluble retentate, with most (95 %) of the material still contained in the **insoluble** fraction. Around 5 % of the previously solvent insoluble IOM was recovered in the retentate solvent extract.

The chromatogram from the Py-GC-MS analysis of the solvent-extracted retentate (**SER**) obtained following ionic liquid treatment of the IOM from the Kimmeridge clay sample is presented in Figure 6.27b. Including the unresolved area below the baseline, the entire chromatographic response accounted for 15 % of the pyrolysed sample mass. However, resolved components accounted for 4% of the mass of the pyrolysed sample of which 45 % was contained in the volatiles peak. Despite the low yield of resolved products, others have argued that the pyrolysis chromatogram is representative of the whole material (Larter & Horsfield, 1993), such that differences between the pyrograms before and after ionic liquid treatment should reflect any changes in the composition of the substrate. Other major resolved components comprised principally benzene and C₁ – C₃ substituted derivatives, and thiophenes including C₁ – C₃ and benzyl substituted derivatives. Whilst all of these components were identified in the pyrogram of the Kimmeridge Clay IOM (Figure 6.27a

and Section 4.3.3) a number of the components identified in the pyrogram of the IOM were absent from the pyrogram of the solvent-extracted retentate. In the solvent-extracted retentate pyrogram a noticeable shift in the maximum of the unresolved complex mixture (UCM) from 45 minutes to 35 minutes was accompanied by the loss of the majority of material exceeding 300 amu (Figure 6.28), measured by averaging the pyrogram mass spectra. The major difference between pyrograms obtained before and after ionic liquid treatment of the IOM was the total absence of *n*-alkane and alk-1-ene doublets from the latter pyrogram. This loss of alkyl material from Kimmeridge Clay IOM was even more pronounced than that observed in the immature Rostherne Mere sediments (Section 6.3.4). However, Dutta (1994) previously reported that 50 % of the retentate obtained after ionic liquid treatment of Kimmeridge Clay kerogen comprised aliphatic components, determined using ss-NMR (Table 6.7). Ion plots of $m/z = 57, 71$ and 85 , and $55, 69$ and 83 provided no evidence that the alkyl chains had been substituted onto other components, as may have been expected where the necessary reactants were present to allow AlCl_3 catalysed Friedel-Crafts alkylations to occur. Alkyl material was also absent from the retentate solvent extract. Therefore, it was concluded that ionic liquid treatment had caused substantial alteration to alkyl chains. This supports the previous evidence from ToF-SIMS analyses that alkyl chains were ether linked in the IOM matrix (Section 4.3.3), perhaps undergoing ether cleavage during ionic liquid treatment (as observed in dendrimers) and subsequent rearrangement. The difference between the 50 % aliphatic character of the retentate reported by Dutta (1994) using ss-NMR and the absence of alkanes/alkenes from the pyrolysis chromatogram in the current study could be explained by replacement of ether linkages with other stronger bonds, *e.g.* carbon-carbon bonds. This may explain why aliphatic resonances were preserved in ss-NMR analysis but alkyl fragments were not observed under pyrolysis conditions, *i.e.* alkyl moieties were not cleaved during pyrolysis.

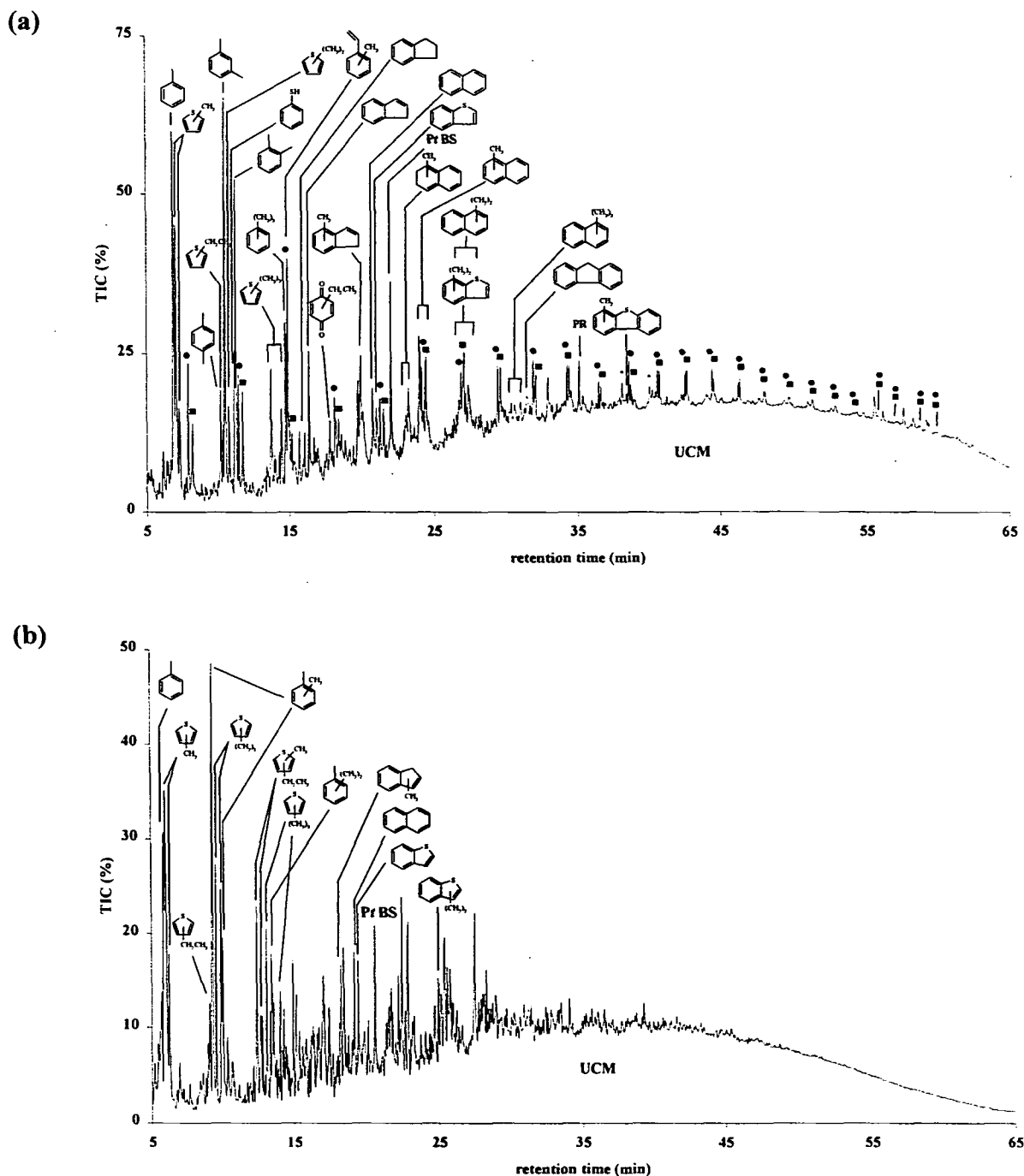


Figure 6.27. Partial Py-GC-MS TIC of ionic liquid-treated Kimmeridge Clay (a) IOM (b) Solvent-extracted retentate (SER) (pyrolysis at 595 °C 5 °C; GC programme, -10 to 300 °C at 5 °C min⁻¹, hold at 300 °C for 10 min; column Rtx-5; MS at 40 eV; ● *n*-alkane; ■ *n*-alk-1-ene; * phthalate; PR = prist-1-ene).

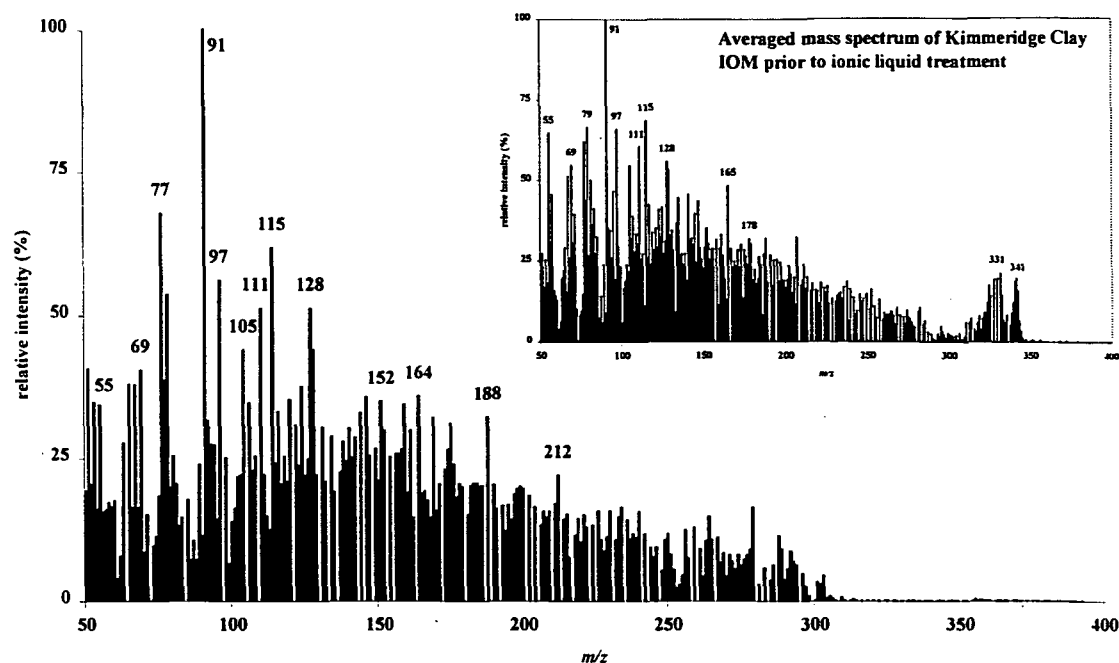


Figure 6.28. Background subtracted averaged mass spectrum (5 – 60 min) of ionic liquid treated Kimmeridge Clay IOM solvent-extracted retentate.

The ToF-SIMS mass spectrum of the solvent-extracted retentate obtained following the ionic liquid treatment of Kimmeridge clay IOM is presented in Figure 6.29. Although differences before and after ionic liquid treatment are less pronounced in the ToF-SIMS spectrum, it does tend to confirm the observations from Py-GC-MS data, *i.e.* general similarity before and after treatment apart from the loss of *n*-alkane/*n*-alk-1-ene doublets and the shift towards lower molecular weight material.

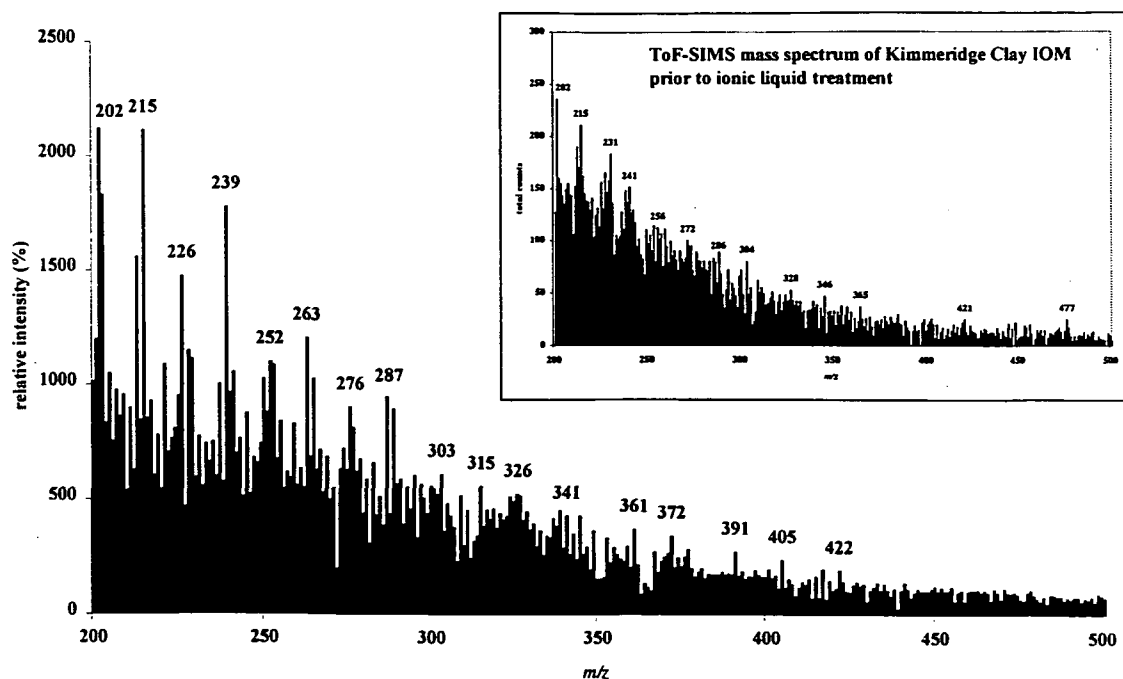


Figure 6.29. Partial positive ion ToF-SIMS mass spectrum of ionic liquid-treated Kimmeridge clay IOM solvent-extracted retentate (sample on Si wafer; ion source, Ga^+).

6.3.6. Ionic liquid-treated bacterial IOM from *M. jannaschii*

IOM isolated from *M. jannaschii* had the same colour and consistency as IOM from Rostherne Mere sediments (Section 6.3.4), but was only poorly characterised using instrumental techniques. IR spectroscopy (Chapter 3) and Py-GC-MS (Chapter 4) indicated that the IOM comprised a significant proportion of branched alkanes/alkenes and one and two ringed aromatic components. Soon after commencement of microwave heating the *M. jannaschii* IOM/ionic liquid mixture darkened and became more viscous. Particle size was observed to reduce during the heating process although some particulate material remained upon completion of microwave heating.

Calculation of the mass balance for products from the ionic liquid treatment of *M. jannaschii* IOM, in the same manner as sedimentary IOM (Section 6.3.1), revealed that only 5 % of the initial substrate could be accounted for by the non-aqueous fractions

(Table 6.12). Of this material, 75 % comprised non-DCM soluble matter whilst 23 % was extractable from the aqueous filtrate. In absolute mass terms, these fractions were only one and-a-half times greater than those measured for the procedural blank. This suggested that either the bulk of organic material was converted to gaseous products and escaped during hydrolysis or that it became aqueous soluble following ionic liquid treatment. Therefore, the solvent-extracted filtrate was analysed using NMR and ESI-MS. The ^1H NMR spectrum of ionic liquid treated *M. jannaschii* IOM solvent-extracted filtrate provided little indication of proton resonances other than those of the hydrolysed $[\text{emim}]\text{Cl}-\text{AlCl}_3$, whilst the ESI-MS mass spectrum (Figure 6.30) contained two prominent ions ($m/z = 609$ and 1784) that could not be attributed to the solvent or hydrolysed ionic liquid products (Figures 6.16a and b, respectively). Although the origin of these ions could not be identified, they do demonstrate the presence of relatively high molecular weight material in the solvent-extracted filtrate, but do not negate the probability that some material was lost as gaseous products during ionic liquid treatment.

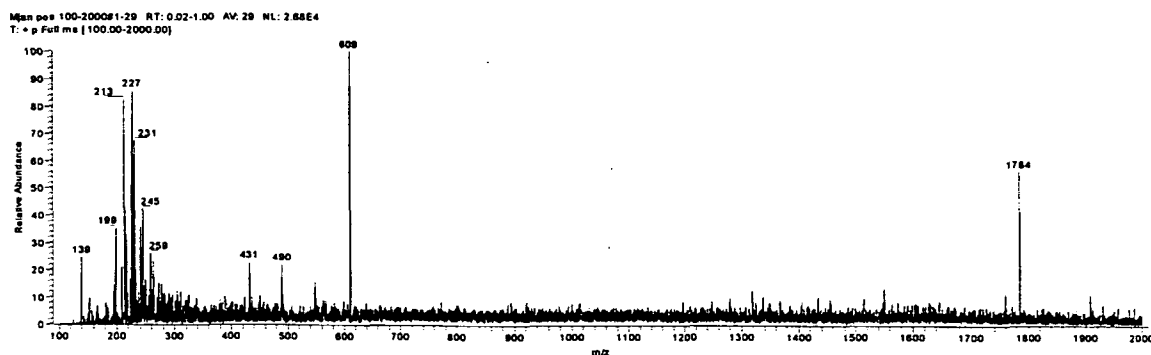


Figure 6.30. Time averaged positive ion ESI-MS mass spectrum of *M. jannaschii* solvent-extracted filtrate (0.1 g ml^{-1} in MeOH; 4 kV spray voltage; $200 \text{ }^\circ\text{C}$ capillary temperature; recorded over 1 min).

The chromatogram obtained from Py-GC-MS of the 5 % solvent-extracted retentate which remained following ionic liquid treatment of *M. jannaschii* IOM (Figure 6.31b) was

nevertheless quite different to that obtained for the IOM prior to ionic liquid treatment (Figure 6.31a). Resolved components accounted for 0.2 % of the pyrolysed sample whereas the entire chromatographic response, including the unresolved fraction below the baseline, accounted for 0.7 % of the pyrolysed sample mass. Overall, the chromatogram was dominated by benzenes and methylbenzenes (methyl-, dimethyl- and trimethyl-) and two- to four-ringed aromatic compounds (naphthalene, methyl- and dimethylnaphthalenes, anthracenone, pyrene, benzanthracenedione). Although a series of *n*-alkanes from C₇ – C₂₀ and monounsaturated alkene homologues were present, they were not quantitatively important components (< 0.1 % of total chromatographic response). Besides the volatiles peak, which accounted for 23 % of the chromatographic response, no single component comprised more than 3 % of the chromatogram. Compared to the pyrogram of *M. jannaschii* IOM (Figure 6.31a), the pyrogram from the solvent extracted retentate exhibited a distinct bias towards higher mass compounds (40 – 60 minutes), although few of these compounds could be unambiguously identified. The increase in higher molecular weight material after ionic liquid treatment may have reflected the removal of lower weight material causing a relative increase in the unresolved 'hump', or represented the formation of more condensed compounds during ionic liquid-treatment. Evidence for the formation of new condensed aromatic material arising from the ionic liquid treatment of the dendrimers tends to support the latter hypothesis (Section 6.3.3).

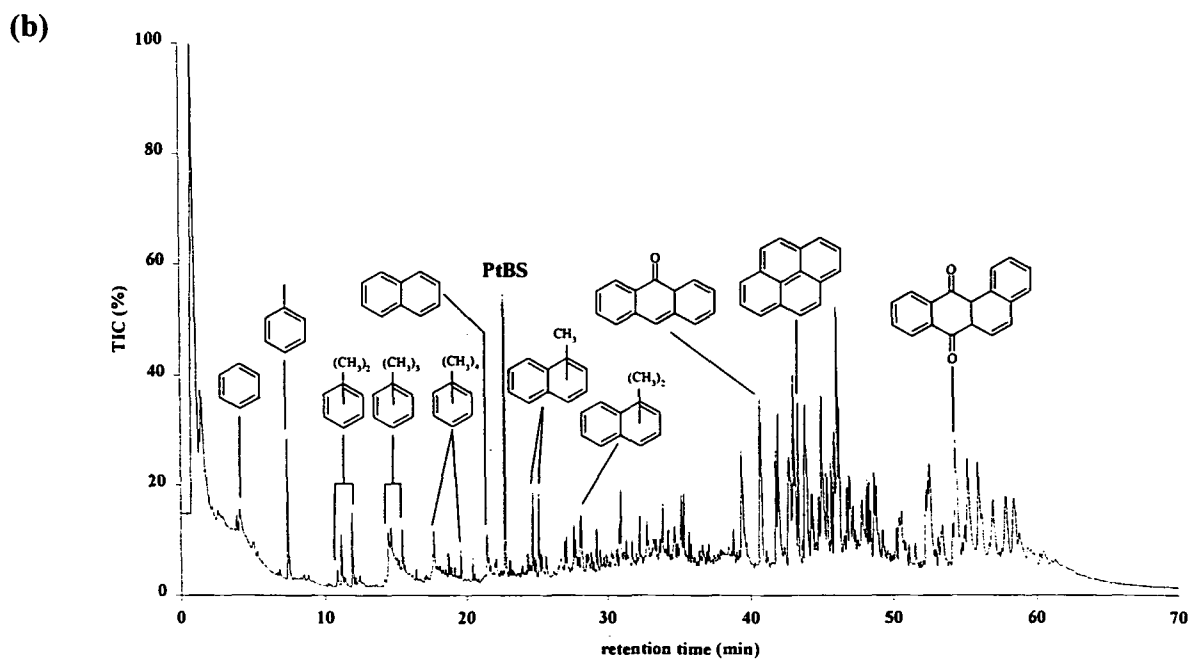
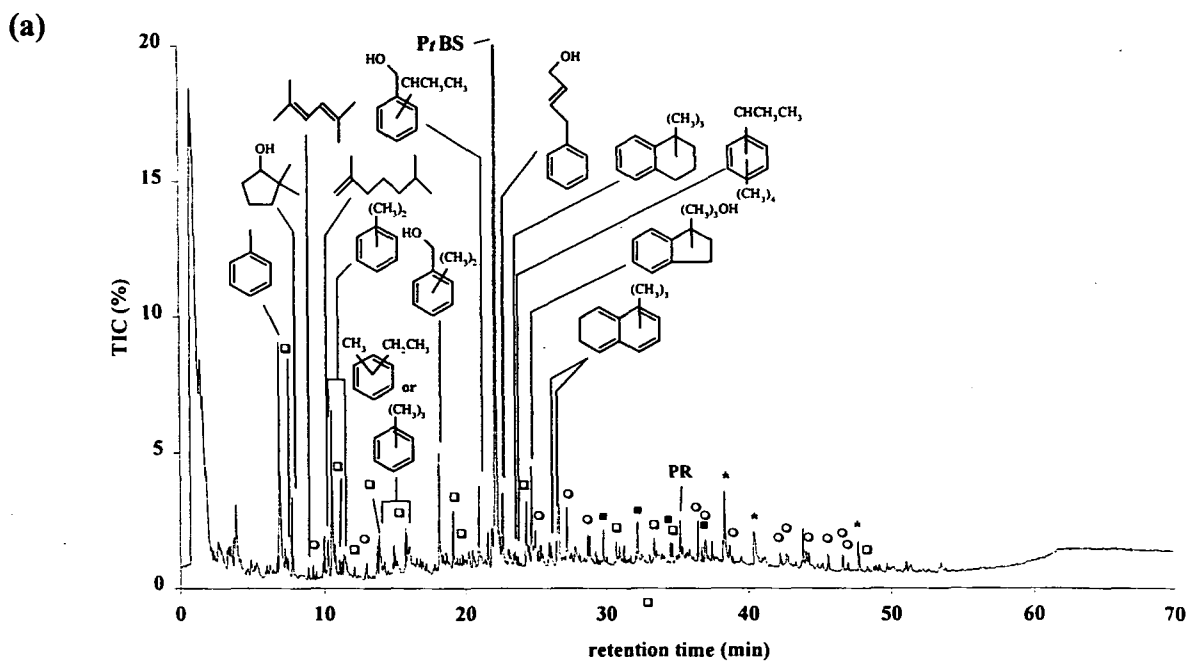


Figure 6.31. Py-GC-MS TIC of *M. jannaschii* (a) IOM (b) Solvent-extracted retentate (SER) (pyrolysis at 595 °C 5 °C; GC programme, -10 to 300 °C at 5 °C min⁻¹, hold at 300 °C for 10 min; column Rtx-5; MS at 40 eV; ○ alkene; ■ *n*-alkane; □ alkane; * phthalate; PR = prist-1-ene).

6.3.7. Ionic liquid-treated acid-synthesised insoluble melanoidins

Acid-synthesised melanoidins (Gly/Glu and His/Glu; Chapter 5) were both dark brown powders before ionic liquid treatment. Characterisation of these insoluble melanoidins using IR spectroscopy and Py-GC-MS (Chapter 5) indicated that they were principally aromatic (1 – 2 ringed and furanyl) and contained significant carbonyl functionality. During microwave heating the melanoidin/ionic liquid mixtures became progressively more viscous and darker in colour. Particulate material reduced in size throughout the heating stage.

Most of the original mass of melanoidins could be accounted for in the two solvent extracts and solvent-extracted retentate (Gly/Glu, 94 %; His/Glu, 98 %). Similarly to the ionic liquid-treated sedimentary IOM, the bulk (> 98 %) of this material was present as **insoluble** material in the solvent-extracted retentate.

The pyrogram of the Gly/Glu solvent-extracted retentate (Figure 6.32b) contained a greater number of resolved peaks than the pyrogram of the melanoidin prior to ionic liquid treatment (Figure 6.32a). In conjunction with a shifting of the UCM maximum to an earlier elution time this suggests that higher molecular weight material had perhaps been broken down by the ionic liquid and lower molecular weight material released. The background subtracted averaged mass spectrum (Figure 6.33) over 34 – 58 minutes retention time was more complex and less well defined than the same region of the isolated melanoidin pyrogram (inset Figure 5.32a). In particular, ions at $m/z > 276$ were less abundant in this region after ionic liquid treatment, indicating that higher molecular weight material had been removed, whilst the relative increase in aromatic ions (*i.e.* $m/z = 91$ and 128) indicated this material had become more condensed. This apparent reduction in higher molecular weight material was similar to that observed for other IOM treated with the ionic liquid. Many of the compounds identified in the pyrogram of Gly/Glu solvent-extracted

retentate were also found in the pyrogram of the isolated melanoidin and as such were of little diagnostic value. However, acetic acid, naphthofuran and fluorene were not detected in the melanoidin before ionic liquid treatment and their presence was consistent with the proposed model of a mode of action of the ionic liquid involving ether cleavage with subsequent condensation, rearrangement or polymerisation of some cleaved moieties.

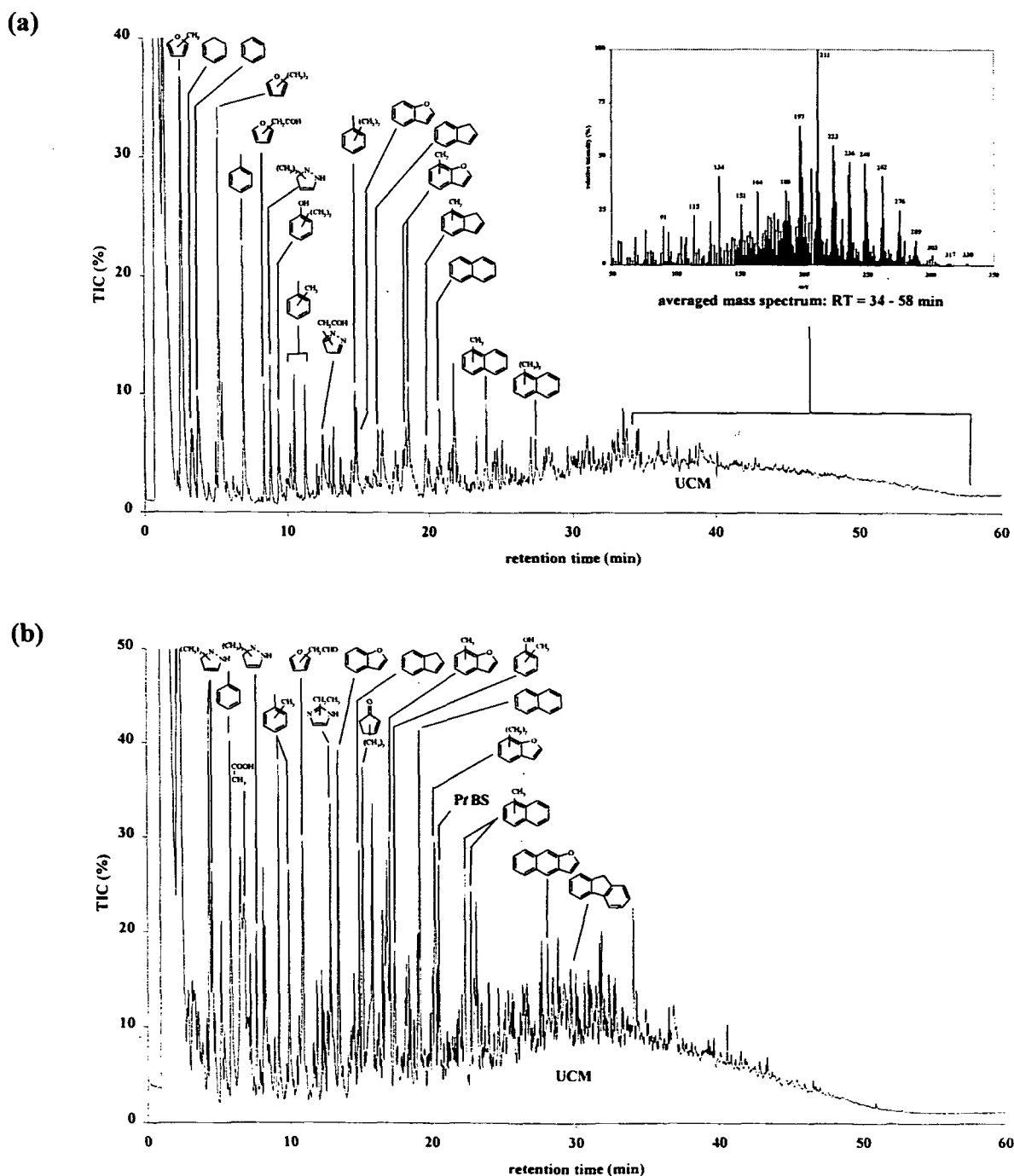


Figure 6.32. Partial Py-GC-MS TIC of (a) Insoluble Gly/Glu melanoidin (b) Solvent-extracted retentate (SER) following ionic liquid treatment (pyrolysis at 595 °C 5 °C; GC programme, -10 to 300 °C at 5 °C min⁻¹, hold at 300 °C for 10 min; column Rtx-5; MS at 40 eV).

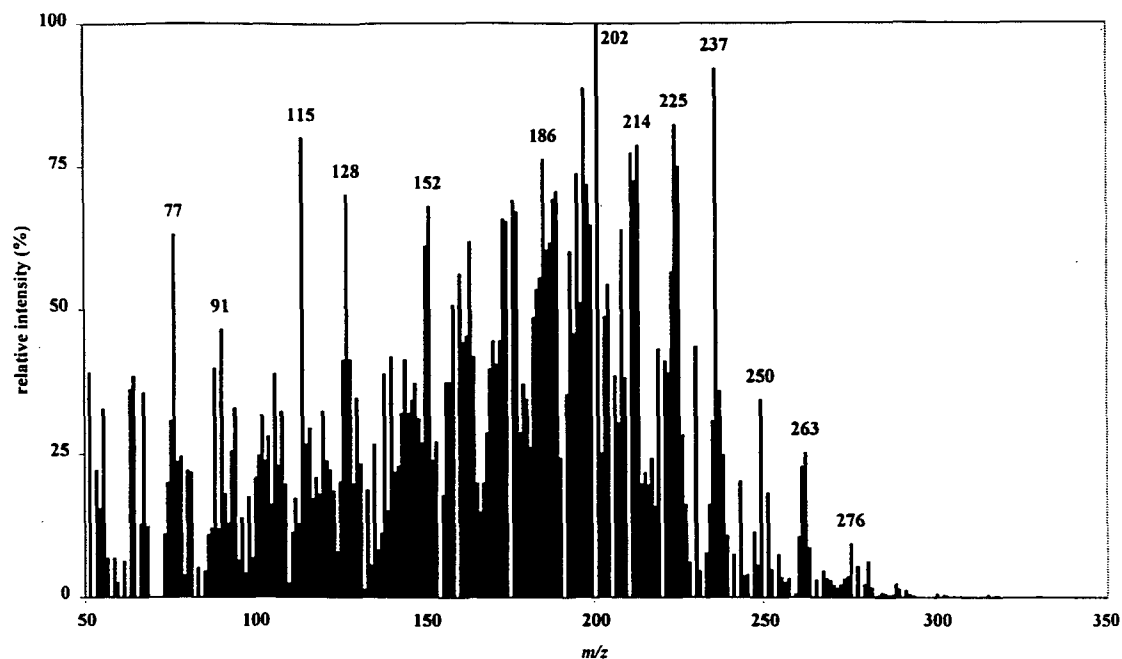


Figure 6.33. Background subtracted averaged mass spectrum of Py-GC-MS analysis of Gly/Glu solvent-extracted retentate (34 – 58 min).

Summary

- Acidic 1-ethyl-3-methyl imidazolium chloride-aluminium (III) chloride does not act as a simple solvent of organic chemicals, dendrimers, IOM from recent sediments and biota or melanoidins, but instead appears to promote chemical reactions such as protonation, ether cleavage, rearrangement, and polymerisation within substrates.
- Evidence from Py-GC-MS, GC-MS and ToF-SIMS analyses suggests that [emim]Cl-AlCl₃ non-quantitatively protonates, and polymerises anthracene and phenanthrene, and promotes the condensation of ether linked benzyl groups in dendrimer molecules.
- Less than 1 % of IOM isolated from immature lacustrine Rostherne Mere sediment and acid-synthesised melanoidins was soluble in solvent following ionic liquid treatment.
- Gravimetric results showed that ionic liquid treatment of organic compounds in fact led to the formation of different insoluble material, accounting for up to 60 % of the initial mass.
- However, 5 % of IOM (kerogen) isolated from Kimmeridge Clay was soluble in

DCM after ionic liquid treatment, similar to that calculated from a previous study into the ionic liquid dissolution of a Liassic shale kerogen (Dutta, 1994).

- The recovery of products after ionic liquid-treatment of *M jannaschii* IOM was poor (5%), suggesting that most of this material was converted to volatile products by the ionic liquid.
- The formation of insoluble material from previously solvent-soluble compounds following ionic liquid treatment, the chemical alteration of soluble components, and the failure to solubilise any substantial quantities of previously insoluble sedimentary organic matter, suggests that ionic liquid 'dissolution' was not applicable as a routine method for furthering the understanding of insoluble geochemical matrices:

Chapter 7: Conclusions and suggestions for further work

6.1. Conclusions

Organic matter which is insoluble in common solvents, non-oxidising acids and bases (IOM) often represents the quantitatively most important fraction of sedimentary organic matter (*e.g.* Klok *et al.*, 1983, 1984). In ancient sediments, broadly similar insoluble (at least in terms of insolubility) material isolated using mineral acids (HF/HCl) and subsequent solvent extractions, is called kerogen, and is the most abundant form of carbon on the planet. The insolubility of this material allied to the restrictions of instrumentation capable of examining solid substrates has, to date, prevented full molecular characterisation, though significant advances have been made using lysis techniques such as chemolysis and pyrolysis (*e.g.* see reviews by Rullkötter & Michaelis, 1990; Larter & Horsfield, 1993; Whelan *et al.*, 1993). Development of a solubilisation technique that could render this previously intractable material amenable to molecular characterisation using traditional solution analytical instrumentation would provide a significant advance in the understanding of geochemical processes leading to kerogen formation. This is of particular importance given the commercial value of fossil fuel deposits for which kerogen and perhaps IOM, are the precursors.

Unfortunately the findings of this study, in contrast to those made earlier (Patell, 1994; Dutta, 1994), suggest that the ionic liquid 1-ethyl-3-methylimidazolium chloride-aluminium (III) chloride is not a simple solvent of IOM and kerogen. Although IOM was isolated from a range of sediments (7 – 30 %, immature lacustrine sediments from Rostherne Mere, Cheshire, UK; 11 – 12 %, Kimmeridge Clay, Dorset, UK), methanogenic bacteria (0.1 - 3 %, *M. jannaschii*, *M. thermoautotrophicum*) and diatomaceous alga (1 – 3 %, *S. Costatum*) using a very logistically demanding mass balance sequential digestion procedure, this material could not be substantially dissolved by treatment with acidic [emim]Cl-AlCl₃ under the conditions used herein.

Monitoring of the sequential isolation procedure using Py-GC-MS demonstrated that sequential removal of major biochemical classes (which accounted for *ca.* 50 % of the total carbon) was not well reflected by qualitative changes in pyrograms from residual material remaining following each digestion stage. However, the pyrogram of IOM obtained following 'mineral' dissolution was characterised by an increase in the range of *n*-alkane/alk-1-ene doublets inferring that aliphatic hydrocarbons had been strongly bound at mineral surfaces. The use of an internal standard (poly-*tert*-butylstyrene) in Py-GC-MS analyses enabled quantification of the total chromatographic response and resolved components. For environmental samples, the total chromatographic response accounted for less than 10 % of the mass of the sample pyrolysed, whereas for pure synthetic compounds the entire mass of the sample pyrolysed could be accounted for in this manner. In addition, resolved components rarely comprised more than 2 % of the total chromatographic response from environmental samples, but in excess of 80 % of pure samples. Thus, it appears that Py-GC-MS analysis only provides molecular information about a minor fragmented part of environmental samples and IOM isolated from them.

ToF-SIMS analysis of untreated sediments and IOM isolated from the same samples suggested that *n*-alkane/alk-1-ene doublets observed in Py-GC-MS analyses of these substrates may have been formed from the pyrolysis of poly-oxygenated alkyl chains. Such observations were consistent with the purported nature of algal kerogens, *i.e.* a network of ether cross-linked methylene chains, and may provide the first direct instrumental evidence of such moieties.

The potential formation of melanoidin-like material during the sequential digestion was addressed by synthesising melanoidins under conditions similar to those employed in the isolation protocol and by monitoring changes between untreated samples and IOM isolated from them using Py-GC-MS, IR spectroscopy and the newer surface-sensitive ToF-SIMS

technique. Of a range of amino acid (Gly, Lys, His, Arg) and saccharide (Glu) mixtures, only Gly/Glu (13 %) and His/Glu (10 %) yielded insoluble melanoidins. Despite common features in the Py-GC-MS pyrograms and IR spectra of acid-synthesised melanoidins and IOMs, *e.g.* alkyl, ester, and aromatic signatures, ToF-SIMS spectra of the sedimentary and bacterial IOMs provided little evidence that higher molecular weight material had been formed from lower weight precursor material during the sequential digestion. Although spectral information obtained from ToF-SIMS analysis was limited to compounds with a mass of < 1000 amu, there was little evidence of any significant quantity of material whose mass exceeded 500 amu in untreated sediments or IOM obtained from them. In contrast, ToF-SIMS analysis of untreated *M. jannaschii* showed that it contained significant amounts of compounds with molecular weight between 500 – 981 amu. These compounds were absent from the ToF-SIMS of the bacterial IOM obtained following sequential digestion, but whether they were removed during the isolation procedure or incorporated into compounds with molecular weight exceeding the capabilities of the ToF-SIMS instrument could not be unequivocally established. Background-subtracted averaged mass spectra of Py-GC-MS pyrograms were found to provide a useful and rapid aid in the bulk characterisation of pyrolysed samples, especially for inter-pyrogram comparisons where much of the pyrolysable material could not be adequately resolved. Comparison of averaged mass spectra of pyrograms from acid-synthesised Gly/Glu and His/Glu melanoidins with those from sedimentary and bacterial IOM showed that melanoidin pyrolysis products generally comprised higher mass ions with distribution maxima at higher masses than observed in sediments.

Previously reported claims of up to 98 % dissolution of kerogens using the ionic liquid 1-ethyl-3-methylimidazolium chloride-aluminium (III) chloride $\{X(\text{AlCl}_3), X = 0.65\}$ (Dutta, 1994; Patell, 1994) were not substantiated in the current study. Rather, almost all (85 - 103 %) of the sedimentary IOMs remained insoluble in DCM following ionic liquid treatment.

Analysis of the solvent soluble material using ^1H NMR showed that it comprised *ca.* 60 % aliphatic components, consistent with previous reports (Dutta, 1994; Patell, 1994), however it was relatively unimportant in quantitative terms (< 1 %). Ionic liquid treatment of bacterial IOM isolated from *M. jannaschii* resulted in a poor yield (5 %), most probably due to conversion of this material to volatile compounds which were subsequently lost during hydrolysis of the ionic liquid.

Treatment of aromatic compounds (anthracene and phenanthrene) with $[\text{emim}]\text{Cl}-\text{AlCl}_3$ $\{X(\text{AlCl}_3), X = 0.65\}$ resulted in the non-quantitative protonation and dimerisation of these substrates, and the formation of DCM-insoluble compounds (6 – 14 % initial mass of reactants) with variable yields. Similarly, ionic liquid treatment of poly-functional dendrimer molecules ($\text{G}_1\text{P}-[6]-\text{Obn}$ and $\text{G}_2\text{P}-[12]-\text{Obn}$) with similar functional groups to those observed in kerogens (*e.g.* benzyl and ester groups and ether linkages) resulted in the formation of newly DCM-insoluble material (7 – 62 %) and a range of products consistent with the ether cleavage of the original molecules and subsequent condensation and polymerisation of the benzyl moieties. Ether cleavage and formation of insoluble compounds apparently occurred even when microwave heating to promote dissolution was not applied. Analysis of the untreated dendrimers using Py-GC-MS indicated that even though they contained identical functionalities (ester groups, ether linkages and benzyl terminal groups) they did not respond in the same manner during pyrolysis under identical conditions. This suggested that steric factors or absolute elemental composition could influence the pyrolysis products of relatively high molecular weight material.

6.2. Suggestions for further work

The use of acidic $[\text{emim}]\text{Cl}-\text{AlCl}_3$ as a solvent to solubilise sequentially isolated sedimentary and bacterial IOM has clearly not produced any significant advancement towards the elucidation of the molecular character of insoluble organic matter. In

particular, the variety and lack of specificity of chemical reactions promoted by the ionic liquid when applied to simple organic substrates, and the production of newly insoluble material from compounds previously soluble in DCM, suggests that continuing research into ionic liquid dissolution would not be worthwhile. However, some other aspects of the present study tend to show more promise.

The sequential digestion procedure used in the current study resulted in the isolation of a reduced proportion of IOM from Kimmeridge Clay compared to the amount of kerogen isolated from the same sample using the 'classical method' (HF/HCl and solvent extraction). This suggests that some kerogens isolated using the 'classical method' may contain between 4 to 8 % of material that could be readily solubilised. It would therefore prove worthwhile to carry out comparison studies into the amount of insoluble material isolated using sequential digestion techniques and the 'classical method'.

Tentative evidence of the presence of ether cross-linked methylene chains in IOM isolated from Rostherne Mere sediments suggests that algal contributors to the organic matter in this sediment may contain non-hydrolysable components similar to algaenans isolated from *B. braunii*. Because algal blooms in Rostherne Mere have previously been reported to be dominated by *Microcystis aeruginosa* (Reynolds, 1979), this species would provide an obvious candidate for such an investigation.

To date, there have been few reported studies into the analysis of insoluble organic matter (*i.e.* kerogen) using soft ionisation techniques coupled with high mass range spectrometers, *e.g.* ToF-SIMS. This field appears quite promising, especially considering the variety of ToF-SIMS techniques available. For example, not only can molecular information be obtained from the surface monolayer of substrates but also depth profiling can be carried out to provide molecular detail about the inner core of insoluble particles. In addition,

coupling of the ToF-SIMS instrument to a SEM means that mass mapping can be related to morphological features of the substrate under analysis. Another soft ionisation technique, laser ablation-mass spectrometry (LA-MS), which is apparently biased towards aromatic compounds, could also be applied to insoluble organic materials. Whilst these techniques are unlikely to directly result in the complete elucidation of the molecular character of IOM they offer promising opportunities to expand our understanding of these complex matrices.

Recent rapid expansion in the field of dendrimer chemistry has led to the synthesis of large numbers of novel organic structures (Newkome *et al.*, 1996). Many of these structures are macromolecular and contain functional groups commonly associated with insoluble geochemical matrices such as kerogen, *e.g.* benzyl and ester groups and ether linkages. The specific architecture and high purity of these compounds, compared to normal polymers, means they could be used to study how instrumental techniques routinely applied to solid geochemical substrates (*e.g.* ss-NMR, pyrolysis techniques and IR) 'perceive' these molecules. Results from such experiments would likely yield useful information regarding how specific components of macromolecules are related to their parent structure and address possible shortcomings in the information obtained from these instrumental techniques, *e.g.* aliphatic bias in Py-GC studies. Dendrimers also offer the potential to be used as internal standards in molecular instrumental studies, *e.g.* ToF-SIMS. Alternatively, the iterative process used in dendrimer synthesis could be exploited to produce synthetic analogues of kerogen, similar to the models proposed by Behar & Vandenbroucke (1987).

References

Abdul-Sada, A.K., Greenway, A.M., Seddon, K.R. and Welton, T. (1989) Upon the existence of $[Al_3Cl_{10}]^-$ in room temperature chloroaluminate ionic liquids. *Org. Mass Spectrom.* **24**, 917 – 918.

Abdul-Sada, A.K., Greenway, A.M., Seddon, K.R. and Welton, T. (1993) A fast atom bombardment mass spectrometric study of room-temperature 1-ethyl-3-methylimidazolium chloroaluminate (III) ionic liquids. Evidence for the existence of the decachloroaluminate (III) anion. *Org. Mass Spectrom.* **28**, 759 – 765.

Abdul-Sada, A.K., Avent, A.G., Parkington, M.J., Ryan, T.A., Seddon, K.R. and Welton, T. (1993a) Removal of oxide contamination from ambient-temperature chloroaluminate (III) ionic liquids. *J. Chem. Soc., Dalton Trans.* **22**, 3283 – 3286.

Adams, C.J., Earle, M.J., Roberts, G. and Seddon, K.R. (1998) Friedel-Crafts reactions in room temperature ionic liquids. *Chem. Commun.* **19**, 2097 – 2098.

Aken, M.E. and Pienaar, R.N. (1985) Preliminary investigations on the chemical composition of the scale-boundary and cyst wall of *Pyramimonas pseudoparkeae* (Prasinophyceae). *S. Afr. J. Bot.* **51**, 408 – 416.

Almendros, G., Dorado, J., González-Villa, F.J. and Martín, F. (1997) Pyrolysis of carbohydrate-derived macromolecules: its potential in monitoring the carbohydrate signature of geopolymers. *J. Anal. Appl. Pyrol.* **40/41**, 599 – 610.

Allard, B., Templier, J. and Largeau, C. (1997) Artifactual origin of mycobacterial bacteran. Formation of melanoidin-like artifact macromolecular material during the usual isolation process. *Org. Geochem.* **26**, 691 – 703.

Allard, B., Templier, J. and Largeau, C. (1998) An improved method for the isolation of artifact-free algaenans from microalgae. *Org. Geochem.* **28**, 543 – 548.

Appleby, D., Hussey, C.L., Seddon, K.R. and Turp, J.E. (1986) Room-temperature ionic liquids as solvents for electronic absorption spectroscopy of halide complexes. *Nature* (London). **323**, 614 – 616.

Ashcroft, A.E. (1997) *Ionization methods in organic mass spectrometry*. p 32. Royal Society of Chemistry, UK.

Atkinson, Jr., A.W., Gunning, B.E.S. and John, P.C.L. (1972) Sporopollenin in the cell wall of *Chlorella* and other algae: Ultrastructure, chemistry, and incorporation of ¹⁴C-acetate, studied in synchronous cultures. *Planta* **107**, 1 – 32.

Avent, A.G., Chaloner, P.A., Day, M.P., Seddon, K.R. and Welton, T. (1994) Evidence for hydrogen bonding in solutions of 1-ethyl-3-methylimidazolium halides, and its implications for room-temperature halogenaluminate (III) ionic liquids. *J. Chem. Soc. Dalton Trans.* **23**, 3405 – 3413.

Beckett, A. (1976) Ultrastructural studies on exogenously dormant ascospores of *Daldinia concentrica*. *Can. J. Bot.* **54**, 689 – 697.

Behar, F. and Vandenbroucke, M. (1987) Chemical Modelling of Kerogens. *Org. Geochem.* **11**, 15 – 24.

Belt, S.T., Cooke, D.A., Hird, S.J. and Rowland, S.J. (1994) Structural determination of a highly branched C₂₅ sedimentary isoprenoid biomarker by NMR spectroscopy and mass spectrometry. *J. Chem. Soc., Chem. Commun.* **18**, 2077 – 2078.

Belt, S.T., Cooke, D.A., Robert, J.-M. and Rowland, S. (1996) Structural characterization of widespread polyunsaturated isoprenoid biomarkers: a C₂₅ triene, tetraene and pentaene from the diatom *Haslea ostrearia* Simonsen. *Tetrahedron Lett.* **37**, 4755 – 4758.

Benninghoven, A., Rüdener, F.G. and Werner, H.W. (1987) Secondary ion mass spectrometry: Basic concepts, instrumental aspects, applications and trends. In, Elving, P.J., Winefordner, J.D. and Kolthoff, I.M. (Eds.) *Chemical Analysis*. Vol. 86. John Wiley & Sons, Inc., USA.

Berkaloff, C., Casadevall, E., Largeau, C., Metzger, P., Peracca, S. and Virlet, J. (1983) The resistant polymer of the walls of the hydrocarbon-rich alga *Botryococcus braunii*. *Phytochem.* **22**, 389 – 397.

Bertenshaw, J. (1996) *The Determination of Trace Metals in Kerogen Using Inductively Coupled Plasma-Mass Spectrometry*. BSc Thesis. University of Plymouth.

Beveridge, T.J. and Schultze-Lam, S. (1996) The response of selected members of the archaea to the Gram stain. *Microbiology* **142**, 2887 – 2895.

- Bintrim, S.B., Donohue, T.J., Handelsman, J., Roberts, G.P. and Goodman, R.M. (1997) Molecular phylogeny of archaea from soil. *Proc. Nat. Acad. Sci. USA*. **94**, 277 – 282
- Blokker, P., Schouten, S., van den Ende, H., de Leeuw, J.W., Hatcher, P.G. and Sinninghe Damsté, J.S. (1998) Chemical structure of algaenans from fresh water algae *Tetraedron minimum*, *Scenedesmus communis* and *Pediastrum boryanum*. In, Horsfield, B., Radke, M., Schaefer, R.G. and Wilkes, H. (Eds.) *Advances in Organic Geochemistry 1997*. pp 1453 – 1468. Elsevier Science Ltd., Oxford, UK.
- Bock, R. (1979) *A Handbook of decomposition methods in Analytical Chemistry*. pp 70 – 71. Blackie Group, Glasgow.

Boon, J.A., Levisky, J.A., Pflug, J.L. and Wilkes, J.S. (1986) Friedel-Crafts reactions in ambient-temperature molten salts. *J. Org. Chem.* **51**, 480 – 483.

Boucher, R.J., Standen, G., Patience, R.L. and Eglinton, G. (1990) Molecular characterisation of kerogen from the Kimmeridge clay formation by mild selective chemical degradation and solid state ^{13}C -NMR. In, Durand, B. and Behar, F. (Eds.) *Advances in Organic Geochemistry 1989*. pp 951 – 958. Pergamon Press plc, Oxford.

Boussafir, M., Gelin, F., Lallier-Verges, E., Derenne, S., Bertrand, P. and Largeau, C. (1995) Electron microscopy and pyrolysis of kerogens from the Kimmeridge Clay Formation, UK: Source organisms, preservation processes, and origin of microcycles. *Geochem. Cosmochim. Acta* **59**, 3731 – 3747

Briggs, D., Brown, A. and Vickerman, J.C. (1989) *Handbook of Static Secondary Ion Mass Spectrometry*. John Wiley & Sons, USA.

Briggs, D. and Hearn, M.J. (1988) Sub-micron molecular imaging. A viability study by time-of-flight SIMS. *Surf. Interface Anal.* **13**, 181 – 185.

Brinkhurst & Walsh (1967)

Brinkhurst, R.O. and Walsh, B. (1967) Rostherne Mere, England, a further instance of guanotrophy. *J. Fish. Res. Bd. Canada* **24**, 1299 – 1309.

Brooks, J. (1971) Some chemical and geochemical studies on sporopollenin. In, Brooks, J., Grant, P.R., Muir, M., van Gijzel, P. and Shaw, G. (Eds.) *Sporopollenin*. pp 351 – 407. Academic Press Inc. (London) Ltd.

Brown, M.R. (1991) The amino-acid and sugar composition of 16 species of microalgae used in mariculture. *J. Exp. Mar. Biol. Ecol.* **145**, 79 – 99.

Bult, C.J., White, O., Olsen, G.J., Zhou, L., Fleischmann, R.D., Sutton, G.G., Blake, J.A., FitzGerald, L.M., Clayton, R.A., Gocayne, J.D., Kerlavage, A.R., Dougherty, B.A., Tomb, J-F., Adams, M.D., Reich, C.I., Overbeek, R., Kirkness, E.F., Weinstock, K.G., Merrick, J.M., Glodek, A., Scott, J.L., Geoghagen, N.S.M., Weidman, J.F., Fuhrmann, J.L., Nguyen, D., Utterback, T.R., Kelley, J.M., Peterson, J.D., Sadow, P.W., Hanna, M.C., Cotton, M.D., Roberts, K.M., Hurst, M.A., Kaine, B.P., Borodovsky, M., Klenk, H-P., Fraser, C.M., Smith, H.O., Woese, C.R. and Venter, J.C. (1996) Complete genome sequence of the methanogenic Archaeon, *Methanococcus jannaschii*. *Science* **273**, 1058 – 1073.

Burczyk, J. (1987) Biogenetic relationships between ketocarotenoids and sporopollenins in green algae. *Phytochem.* **26**, 113 – 119.

- Burdige, D.J. and Martens, C. S. (1988) Biogeochemical cycling in an organic-rich coastal marine basin: 10. The role of amino acids in sedimentary carbon and nitrogen cycling. *Geochem. Cosmochim. Acta* **52**, 1571 – 1584.
- Burkhardt, S. and Riebesell, U. (1997) CO₂ availability affects elemental composition (C:N:P) of the marine diatom *Skeletonema costatum*. *Mar. Ecol. Prog. Ser.* **155**, 67 – 76.
- Cämmerer, B. and Kroh, L.W. (1995) Investigation of the influence of reaction conditions on the elementary composition of melanoidins. *Food Chem.* **53**, 55 – 59.
- Cardoso, J.N., Gaskell, S.J., Quirk, M.M. and Eglinton, G. (1983) Hydrocarbon and fatty acid distributions in Rostherne Mere lake sediment (England). *Chem. Geol.* **38**, 107 - 128
- Carey, F.A. (1992) *Organic Chemistry*. pp 1012 – 1013. McGraw-Hill, Inc., USA.
- Carlin, R.T., Truelove, P.C. and Osteryoung, R.A. (1992) Electrochemical and spectroscopic study of anthracene in a mixed Lewis-Brønsted acid ambient temperature molten salt system. *Electrochim. Acta* **37**, 2615 – 2628.
- Carper, W.R., Keller, C.E., Evangelos, N.A. and Zandler, M.E. (1996) ¹³C and ²⁷Al NMR relaxation studies of an acidic chloroaluminate melt. *Main Group Chem.* **1**, 257 – 263.
- Cheek, G. and Osteryoung, R.A. (1982) Electrochemical and spectroscopic studies of 9, 10-anthraquinone in a room-temperature molten-salt. *J. Electrochem. Soc.: Electrochem. Sci. Tech.* **129**, 2488 – 2496.

Cheek, G. and Osteryoung, R.A. (1982a) An electrochemical and infrared study of chloranil in n-butylpyridinium chloride: aluminium chloride ionic liquid. *J. Electrochem. Soc.: Electrochem. Sci. Tech.* **129**, 2739 - 2745.

Chiavari, G. and Galletti, G.C. (1992) Pyrolysis-gas chromatography/mass spectrometry of amino acids. *J. Anal. Appl. Pyrol.* **24**, 123 – 137.

Clarke, R.H. (1967) Amino-acids in recent sediments off south-east Devon, England. *Nature* (London) **3** – 1005.

Colombo, J.C., Silverberg, N. and Gearing, J.N. (1996) Biogeochemistry of organic matter in the Laurentian Trough, I. Composition and vertical fluxes of rapidly settling particles. *Mar. Chem.* **51**, 277 – 293.

Colombo, J.C., Silverberg, N. and Gearing, J.N. (1996a) Biogeochemistry of organic matter in the Laurentian Trough, II. Bulk composition of the sediments and relative reactivity of major components during early diagenesis. *Mar. Chem.* **51**, 295 – 314.

Combaz, A. (1980) Les kérogènes vus au microscope. In, Durand, B. (Ed.) *Kerogen. Insoluble Organic Matter from Sedimentary Rocks*. pp 55 – 112. Editions Technip, Paris.

Cooke, D.A. (1995) *Structural Characterisation of Highly Branched Isoprenoid Alkenes from Sediments and Algae*. PhD. Thesis. University of Plymouth.

Cranwell, P.A. (1990) Paleolimnological studies using sequential lipid extraction from recent lacustrine sediment: recognition of source organisms from biomarkers. *Hydrobiologia* **214**, 293 – 303.

Crotty, J. (1994) Unpublished data. University of Plymouth.

De Gennes, P.G. and Hervet, H. (1983) Statistics of «starburst» polymers. *J. Physique-Lettres* **44**, L351-L360.

Delcorte, A., Segda, B.G. and Bertrand, P. (1997) ToF-SIMS analyses of polystyrene and dibenzoanthracene: evidence for fragmentation and metastable decay processes in molecular secondary ion emission. *Surf. Sci.* **381**, 18 – 32.

De Leeuw, J.W. and Largeau, C. (1993) A review of macromolecular organic compounds that comprise living organisms and their role in kerogen, coal, and petroleum formation. In, Engel, M.H. and Macko, S.A. (Eds.) *Organic Geochemistry*. pp 23 – 72. Plenum Press, New York.

Derenne, S., Largeau, C., Casadevall, E., Tegelaar, E. and de Leeuw, J.W. (1988) Relationships between algal coals and resistant cell wall biopolymers of extant algae as revealed by Py-GC-MS. *Fuel Process. Technol.* **20**, 93 –101.

Derenne, S., Largeau, C., Casadevall, E. and Berkloff, C. (1989) Occurrence of a resistant biopolymer in the *L* race of *Botryococcus braunii*. *Phytochemistry* **28**, 1137 – 1142.

Derenne, S., Largeau, C., Casadevall, E., Sinninghe Damsté, J.S., Tegelaar, E.W. and de Leeuw, J.W. (1990) Characterization of Estonian Kukersite by spectroscopy and pyrolysis: Evidence for abundant alkyl phenolic moieties in an Ordovician, marine, type II/I kerogen. In, Durand, B. and Behar, F. (Eds.) *Advances in Organic Geochemistry 1989*. Pp 873 – 888. Pergamon Press plc, Oxford.

Derenne, S., Metzger, P., Largeau, C., Van Bergen, P.F., Gatellier, J.P., Sinninghe Damsté, J.S., de Leeuw, J.W. and Berkloff, C. (1992) Similar morphological and chemical variations of *Gloeocapsomorpha prisca* in Ordovician sediments and cultured *Botryococcus braunii* as a response to changes in salinity. In, Eckardt, C.B., Maxwell, J.R., Larter, S.R. and Manning, D.A.C. (Eds.) *Advances in Organic Geochemistry 1991*. pp 299 – 313. Pergamon Press Ltd., Oxford.

De Vries, P.J.R., Simons, J. and Van Beem, A.P. (1983) Sporopollenin in the spore wall of *Spirogyra* (Zygnemataceae, Chlorophyceae). *Acta Bot. Neerl.* **32**, 25 – 28.

Durand, B. (1980) Sedimentary organic matter and kerogen. Definition and quantitative importance of kerogen. In, Durand, B. (Ed.) *Kerogen. Insoluble Organic Matter from Sedimentary Rocks*. pp 13 – 34. Editions Technip, Paris.

Durand, B. and Monin, J.C. (1980) Elemental analysis of kerogens (C, H, O, N, S, Fe). In, Durand, B. (Ed.) *Kerogen. Insoluble Organic Matter from Sedimentary Rocks*. pp 113 – 142. Editions Technip, Paris.

Dutta, L.M. (1994) *The Dissolution of Liassic Kerogen and Coal*. MPhil Thesis. University of Sussex.

Dymek, Jr., C.J., Wilkes, J.S., Einarsrud, M.A. and Øye, H.A. (1988) Spectral identification of $Al_3Cl_{10}^-$ in 1-methyl-ethylimidazolium chloroaluminate molten salt. *Polyhedron* **7**, 1139 – 1145.

Eglinton, T.I., Larter, S.R. and Boon, J.J. (1991) Characterisation of kerogens, coals and asphaltenes by quantitative pyrolysis-mass spectrometry. *J. Anal. Appl. Pyrol.* **20**, 25 - 45.

Elaiwi, A., Hitchcock, P.B., Seddon, K.R., Srinivasan, N., Tan, Y-M., Welton, T. and Zora, J.A. (1995) Hydrogen bonding in imidazolium salts and its implications for ambient-temperature halogenaluminate (III) ionic liquids. *J. Chem. Soc., Dalton Trans.* **21**, 3467 – 3472.

Emery, K.O., Stitt, C. and Saltman, P. (1964) Amino acids in basin sediments. *J. Sed. Petrol.* **34**, 433 – 437.

Engel, M.H., Rafalska-Bloch, J., Schiefelbein, C.F., Zumberge, J.E. and Serban, A. (1986) Simulated diagenesis and catagenesis of marine kerogen precursors: Melanoidins as model systems for light hydrocarbon generation. In, Leythaeuser, D. and Rullkötter, J. (Eds.) *Advances in Organic Geochemistry 1985*. pp 1073 – 1079. Pergamon Journals Ltd.

Fabiano, M. and Danovaro, R. (1994) Composition of organic matter in sediments facing a river estuary (Tyrrhenian Sea): Relationships with bacteria and microphytobenthic biomass. *Hydrobiologia* **277**, 71 – 84.

Fannin, A.A., Floreani, D.A., King, L.A., Landers, J.S., Piersma, B.J., Stech, D.J., Vaughn, R.L., Wilkes, S.J. and Williams, J.L. (1984) Properties of 1,3-dialkylimidazolium chloride aluminium chloride ionic liquids. 2. Phase-transitions, densities, electrical conductivities, and viscosities. *J. Phys. Chem.* **88**, 2614 – 2621.

Faulon, J.L., Vandenbroucke, M., Drappier, J.M., Behar, F. and Romero, M. (1990) 3D Chemical Model for Geological Macromolecules. In, Durand, B. and Behar, F. (Eds.) *Advances in Organic Geochemistry 1989*. pp 981 – 993. Pergamon Press plc., Oxford.

Flaviano, C., Le Berre, F., Derenne, S., Largeau, C. and Connan, J. (1994) First indications of the formation of kerogen amorphous fractions by selective preservation. Role of non-hydrolysable macromolecular constituents of Eubacterial cell walls. In, Telnæs, N., Hydro, N., van Graas, G. and Øygard, K. (Eds.) *Advance in Organic Geochemistry 1993*. Elsevier Science Ltd.

Franklin, E.C. (1905) Reactions in liquid ammonia. *J. Am. Chem. Soc.* **27**, 820 – 851.

Franzen, G., Gilbert, B.P., Pelzer, G. and DePauw, E. (1986) The anionic structure of room-temperature organic chloroaluminate melts from secondary ion mass spectrometry. *Org. Mass Spec.* **21**, 443 – 444.

Fuhrman, J.A. and Davis, A.A. (1997) Widespread *Archaea* and novel *Bacteria* from the deep sea as shown by 16S rRNA gene sequences. *Mar. Ecol. Prog. Ser.* **150**, 275 – 285.

Gelin, F., de Leeuw, J.W., Dinninghe Damsté, J.S., Derenne, S., Largeau, C. and Metzger, P. (1994) The similarity of chemical structures of soluble aliphatic polyaldehyde and insoluble algaenan in the green microalga *Botryococcus braunii* race A as revealed by analytical pyrolysis. *Org. Geochem.* **21**, 423 – 435.

Gelin, F., Boogers, I., Noordeloos, A.A.M., Sinninghe Damsté, J.S., Riegman, R. and de Leeuw, J.W. (1997) Resistant biomacromolecules in marine microalgae of the classes

Eustigmatophyceae and *Chlorophyceae*. Geochemical implications. *Org. Geochem.* **26**, 659 – 675.

Gelin, F., Volkman, J.K., Largeau, C., Derenne, S., Sinninghe Damsté, J.S. and de Leeuw, J.W. (1999) Distribution of aliphatic, nonhydrolyzable biopolymers in marine microalgae. *Org. Geochem.* **30**, 147 – 159.

Gold, T. (1999) *The deep hot biosphere*. Springer-Verlag, New York.

Goldenberg, L.M. and Osteryoung, R.A. (1994) Benzene polymerization in 1-ethyl-3-methylimidazolium chloride-AlCl₃ ionic liquid. *Synthetic Metals* **64**, 63 – 68.

Good, B.H. and Chapman, R.L. (1978) The ultrastructure of phycopeltis (Chroolepidaceae: Chlorophyta). I. Sporopollenin in the cell walls. *Amer. J. Bot.* **65**, 27 – 33.

Gormly, J.R. and Mukhopadhyay, P.K. (1983) Hydrocarbon potential of kerogen types by pyrolysis-gas chromatography. In, Bjorøy, M. *et al.*, (Eds.), *Advances in Organic Geochemistry 1981*. pp 597 – 606. John Wiley Heyden Ltd., Chichester.

Goth, K., de Leeuw, J.W., Püttmann, W. and Tegelaar, E.W. (1988) Origin of Messel Oil Shale kerogen. *Nature* (London) **336**, 759 – 761.

Guilford, W.J., Schneider, D.M., Labovitz, J. and Opella, S.J. (1988) High resolution solid state ¹³C NMR spectroscopy of sporopollenins from different plant taxa. *Plant Physiol.* **86**, 134 – 136.

Haddleton, D.M., Sahota, H.S., Taylor, P.C. and Yeates, S.G. (1996) Synthesis of polyester dendrimers. *J. Chem. Soc., Perkin Trans. 1*, 649 – 656.

Hatcher, P.G., Spiker, E.C., Szeverenyi, N.M. and Maciel, G.E. (1983) Selective preservation and origin of petroleum-forming aquatic kerogen. *Nature* (London) **305**, 498 – 501.

Hayase, F., Kim, S.B and Kato, H. (1986) Analyses of the chemical structures of melanoidins by ^{13}C NMR, ^{13}C and ^{15}N CP-MAS NMR spectrometry. *Agric. Biol. Chem.* **50**, 1951 – 1986.

Hedges, J.I. and Keil, R.G. (1995) Sedimentary organic matter preservation: an assessment and speculative synthesis. *Mar. Chem.* **49**, 81 – 115.

Hemsley, A.R., Scott, A.C., Barrie, P.J. and Chaloner, W.G. (1996) Studies of fossil and modern spore wall biomacromolecules using ^{13}C solid state NMR. *Annals. Bot.* **78**, 83 – 94.

Henrichs, S.M. and Farrington, J.W. (1979) Amino acids in interstitial waters and marine sediments. *Nature* (London) **279**, 319 – 322.

Henrichs, S.M. and Farrington, J.W. (1987) Early diagenesis of amino acids and organic matter in two coastal marine sediments. *Geochim. Cosmochim. Acta* **51**, 1 – 15.

Hershberger, K.L., Barns, S.M., Reysenbach, A.L., Dawson, S.C. and Pace, N.R. (1996) Wide Diversity of Crearchaeota. *Nature* (London) **384**, 420.

Hondrogiannis, G., Lee, C.L., Pagni, R.M. and Mamantov, G. (1993) Novel photochemical behaviour of anthracene in a room temperature molten salt. *J. Am. Chem. Soc.* **115**, 9828 – 9829.

Honegger, R. and Brunner, U. (1981) Sporopollenin in the cell walls of *Coccomyxa* and *Myrmecia* phycobionts of various lichens: an ultrastructural and chemical investigation. *Can. J. Bot.* **59**, 2713 – 2734.

Hou, X., Ren, D., Mao, H., Lei, J., Jin, K., Chu, P.K., Reich, F. and Wayne, D.H. (1995) Application of imaging TOF-SIMS to the study of some coal macerals. *Int. J. Coal Geol.* **27**, 23 – 52.

Huc, A.Y. and Durand, B.M. (1977) Occurrence and significance of humic acids in ancient sediments. *Fuel* **56**, 73 – 80.

Ikan, R., Rubinsztain, Y., Nissenbaum, A. and Kaplan, I.R. (1996) Geochemical aspects of the Maillard reaction. In, Ikan, R. (Ed.), *The Maillard Reaction*. pp 1 – 25. John Wiley & Sons Ltd., England.

Ioselis, P., Rubinsztain, Y. and Ikan, R. (1983) Pyrolysis of natural and synthetic humic substances. In, Bjorøy, M. *et al.* (Eds.) *Advances in Organic Geochemistry 1981*. pp 824 – 827. John Wiley Heyden Ltd., Chichester.

Irwin, W.J. (1982) Analytical pyrolysis: A comprehensive guide. In, Cazes, J. (Ed.) *Chromatographic Science. Vol. 22*. pp 333 – 352. Marcel Dekker, Inc., New York.

Johns, L., Wraige, E.J., Belt, S.T., Lewis, C.A., Massé, G., Robert, J.-M. and Rowland, S. J. (1999) Identification of a C₂₅ highly branched isoprenoid (HBI) diene in Antarctic sediments, sea-ice diatoms and cultured diatoms. *Org. Geochem.* **30**, 1471 – 1475.

Johns, L., Belt, S., Lewis, C.A., Rowland, S., Massé, G., Robert, J.-M. and König, W.A. (2000) Configurations of polyunsaturated sesterterpenoids from the diatom, *Haslea ostrearia*. *Phytochemistry* **53**, 607 – 611.

Johns, R.B. (Ed.) (1986) *Biological Markers in the Sedimentary Record: Methods in Geochemistry and Geophysics*, 24. Elsevier Science Publishers B.V., The Netherlands.

Jones, H.L. and Osteryoung, R.A. (1975) Organic reactions in molten tetrachloroaluminate solvents. *Adv. Molten Salt Chem.* **3**, 121 – 176.

Jones, W.J., Leigh, J.A., Mayer, F., Woese, C.R. and Wolfe, R.S. (1983) *Methanococcus jannaschii* sp. nov., an extremely thermophilic methanogen from a submarine hydrothermal vent. *Arch. Microbiol.* **136**, 254 – 261.

Kadouri, A., Derenne, S., Largeau, C., Casadevall, E. and Berkaloff, C. (1988) Resistant biopolymer in the outer walls of *Botryococcus Braunii*, B race. *Phytochemistry* **27**, 551 – 557.

Klok, J., van der Knaap, J.M.M., de Leeuw, J.W., Cox, H.C. and Schenck, P.A. (1983) Qualitative and quantitative characterization of the total organic matter in a recent marine sediment. In, (Bjørøy, M. et al., Eds.) *Advances in Organic Geochemistry 1981*. pp 813 - 818. John Wiley Heyden Ltd., Chichester.

Klok, J., Baas, M., Cox, H.C., de Leeuw, J.W. Rijpstra, W.I.C. and Schenck, P.A. (1984) Qualitative and quantitative characterization of the total organic matter in a recent marine sediment (Part II). In, Schenck, P.A., de Leeuw, J.W. and Lijmbach, G.W.M. (Eds.) *Advances in Organic Geochemistry 1983*. pp 265 – 278. Pergamon Press Ltd., Oxford.

Klok, J., Cox, H.C., Baas, M., de Leeuw, J.W. and Schenck, P.A. (1984a) Carbohydrates in recent marine sediments – II. Occurrence and fate of carbohydrates in a recent stromatolitic deposit: Solar Lake, Sinai. *Org. Geochem.* 7, 101- 109.

Koch, V.R., Miller, L.L. and Osteryoung, R.A. (1976) Electroinitiated Friedel-Crafts transalkylations in a room-temperature molten-salt medium. *J. Am. Chem. Soc.* 98, 5277 – 5284.

Koga, Y., Nishihara, M., Morii, H. and Akagawa-Matsushita, M. (1993) Ether polar lipids of methanogenic bacteria: Structures, comparative aspects, and biosyntheses. *Microbiol. Rev.* 57, 164 – 182.

Largeau, C., Casadevall, E., Kadouri, A. And Metzger, P. (1984) Formation of *Botryococcus*-derived kerogens – Comparative study of immature torbanites and of the extant alga *Botryococcus braunii*. In, Schenck, P.A., de Leeuw, J.W. and Lijmbach, G.W.M. (Eds.) *Advances in Organic Geochemistry 1983*. pp 327 –332. Pergamon Press Ltd., UK.

Larter, S.R. and Douglas, A.G. (1982) Pyrolysis methods in organic geochemistry: An overview. *J. Anal. Appl. Pyrol.* 4, 1 – 19.

Larter, S.R. and Horsfield, B. (1993) Determination of structural components of kerogens by the use of analytical pyrolysis methods. In, Engel, M.H. and Macko, S.A. (Eds.) *Organic Geochemistry: Principles and Applications*. pp 271 – 287. Plenum Press, New York.

Larter, S.R., Solli, H. and Douglas, A.G. (1983) Phytol-containing melanoidins and their bearing on the fate of isoprenoid structure in sediments. In, Bjorøy, M. *et al.* (Eds.) *Advances in Organic Geochemistry 1981*. pp 513 – 523. John Wiley Heyden Ltd., Chichester.

Le Berre, F., Derenne, S., Largeau, C., Connan, J. and Berkaloff, C. (1991) Occurrence of non-hydrolysable, macromolecular, wall constituents in bacteria. Geochemical implications. In, Manning, D.A.C. (Ed.) *Organic Geochemistry. Advances and Applications in Energy and the Natural Environment*. pp 428 – 431. University Press, Manchester.

Lee, C., Winston, T., Unni, A., Pagni, R.M. and Mamantov, G. (1996) Photoinduced electron transfer chemistry of 9-methylanthracene. Substrate as both electron donor and acceptor in the presence of the 1-ethyl-3-methylimidazolium ion. *J. Am. Chem. Soc.* **118**, 4919 – 4924.

Leenheer, M.J. and Meyers, P.A. (1983) Comparison of lipid compositions in marine and lacustrine sediments. In Bjorøy, M. *et al.* (Eds.) *Advances in Organic Geochemistry 1981*. pp 309 – 316. John Wiley Heyden Ltd., Chichester.

Lewis, C.A. and Rowland, S.J. (1993) Quantitative assessment of changes occurring in organic matter during early diagenesis. *Phil. Trans. R. Soc. Lond. A.* **344**, 101 – 111.

Lewis, C.A. Analytical techniques in organic chemistry. In, Gill, R. (Ed.) *Modern Analytical Geochemistry*. pp 243 – 272. Addison Wesley Longman Limited, England.

Livingstone, D. and Cambray, R.C. (1978) Confirmation of ^{137}Cs dating by algal stratigraphy in Rostherne Mere. *Nature (London)* **276**, 259 – 260.

Livingstone, D. and Reynolds, C.S. (1981) Algal sedimentation in relation to phytoplankton periodicity in Rostherne Mere. *Br. Phycol. J.* **16**, 195 – 206.

Livingstone, D. (1984) The preservation of algal remains in recent lake sediments. In, Haworth, E.Y. and Lund, J.W.G. (Eds.) *Lake Sediments and Environmental History*. 1984. pp 191 – 202. Leicester University Press.

Lonfei, J., Jingling, W. And Shuman, X. (1986) Mechanisms of pyrolysis of fluoropolymers. *J. Anal. Appl. Pyrol.* **10**, 99 – 106.

Maillard, L.C. (1913) *C. R. Acad. Sci. Paris* **156**, 1159.

Marty, D.G. (1993) Methanogenic bacteria in seawater. *Limnol. Oceanogr.* **38**, 452 – 456.

Meuzelaar, H.L.C., Haverkamp, J. and Hileman, F.D. (1982) Pyrolysis mass spectrometry of recent and fossil biomaterials: compendium and atlas. In, *Techniques and Instrumentation in Analytical Chemistry. Volume 3*. pp 15 – 19. Elsevier Scientific Publishing Company, Amsterdam.

Middleditch, B.S. (1989) Analytical Artifacts: GC, MS, HPLC, TLC, and PC. *Journal of Chromatography Library*; Vol. 44. Elsevier Science Publishers B.V., Netherlands.

Milić, B.L. (1987) CP-MAS ^{13}C NMR spectral study of the kinetics of melanoidin formation. *Analyst* (London) **112**, 783 – 785.

Moers, M.E.C., de Leeuw, J.W. and Baas, M. (1994) Origin and digenesis of carbohydrates in ancient sediments. *Org. Geochem.* **21**, 1093 – 1106.

Moss, B., Beklioglu, M., Carvalho, L., Kilinc, S., McGowan, S. and Stephen, D. (1997) Vertically-challenged limnology; contrasts between deep and shallow lakes. *Hydrobiologia* **342/343**, 257 – 267.

Muddiman, D.C., Gusev, A.I., Proctor, A., Hercules, D.M., Venkataramanan, R. and Diven, W. (1994) Quantitative measurement of cyclosporin A in blood by time-of-flight mass spectrometry. *Anal. Chem.* **66**, 2362 – 2368.

Newkome, G.R., Baker, G.R., Young, J.K. and Traynham, J.G. (1993) A systematic nomenclature for cascade polymers. *J. Polym. Sci.: A: Polym. Chem.* **31**, 641 – 651.

Newkome, G.G., Moorefield, C.N. and Vögtle, F. (1996) *Dendritic Molecules: Concepts, syntheses, perspectives*. pp 261. VCH Verlagsgesellschaft GmbH, Weinham (Federal Republic of Germany).

Ni, S. and Boone, D.R. (1998) Extremophilic methanogenic *Archaea* and their adaptation mechanisms. In, Horikoshi, K. and Grant, W.D. (Eds.) *Extremophiles. Microbial Life in Extreme Environments*. pp. 211 – 232. Wiley – Liss, Inc., USA.

Nip, M., Tegelaar, E.W., Brinkhuis, H., de Leeuw, J.W., Schenck, J.P.A. and Holloway, P.J. (1986a) Analysis of modern and fossil plant cuticles by Curie point Py-GC and Curie point Py-GC-MS: Recognition of a new highly aliphatic and resistant biopolymer. In, Leythaeuser, D. and Rullkötter, J. (Eds.) *Advances in Organic Geochemistry 1985*. pp 769 – 778. Pergamon Journals Ltd., Oxford.

Nip, M., Tegelaar, E.W., de Leeuw, J.W., Schenck, J.P.A. and Holloway, P.J. (1986b) A new non-saponifiable highly aliphatic and resistant biopolymer in plant cuticles. Evidence from pyrolysis and ^{13}C -NMR analysis of present-day and fossil plants. *Naturwissenschaften* **73**, 579 – 585.

Pagni, R.M. (1987) Organic and organometallic reactions in molten salts and related melts. In, Mamantov, G. and Braunstein, J. (Eds.) *Advances in Molten Salt Chemistry, Vol. 6*. pp 211 – 346. Elsevier, Amsterdam.

Parkes, R.J., Cragg, B.A., Fry, J.C., Herbert, R.A. and Wimpenny, J.W.T. (1990) Bacterial biomass and activity in deep sediment layers from the Peru margin. *Phil. Trans. R. Soc. Lond. A*. **331**, 139 – 153.

Parkes, R.J., Cragg, B.A., Getliff, J.M., Harvey, S.M., Fry, J.C., Lewis, C.A. and Rowland, S.J. (1993) A quantitative study of microbial decomposition of biopolymers in Recent sediments from the Peru Margin. *Mar. Geol.* **113**, 55 – 66.

Parkes, R.J., Cragg, B.A., Bale, S.J., Getliff, J.M., Goodman, K., Rochelle, P.A., Fry, J.C., Weightman, A.J. and Harvey, S.M. (1994) Deep bacterial biosphere in Pacific Ocean sediments. *Nature* (London) **371**, 410 – 413.

Parkes, R.J., Cragg, B.A. and Wellsbury, P. (2000) Recent studies on bacterial populations and processes in subseafloor sediments: A review. *Hydrogeol. J.* **8**, 11 – 28.

Parsons, T.R., Stephens, K. and Strickland, J.D.H. (1961) On the chemical composition of eleven species of marine phytoplankters. *J. Fish. Res. Bd. Canada* **18**, 1001 – 1016.

Patell, Y. (1994) *The Dissolution of Kerogens*. MPhil. Thesis. University of Sussex.

Patience, R.L., Clayton, C.J., Kearsley, A.T., Rowland, S.J., Bishop, A.N., Rees, A.W.G., Bibby, K.G. and Hopper, A.C. (1990) An integrated biochemical, geochemical, and sedimentological study of organic diagenesis in sediments from Leg 112. In, Suess, E., von Huene, R. *et al.* (Eds.). *Proceedings of the Ocean Drilling Program, Scientific Results*. Volume 112. pp 135 - 152. College Station, Texas, USA. Ocean Drilling Program.

Peters, K.E. and Moldowan, J.M. (1993) *The Biomarker Guide*. Prentice-Hall, Inc., USA.

Peulvé, S., de Leeuw, J.W., Sicre, M.-A., Baas, M. and Saliot, A. (1996) Characterization of macromolecular organic matter in sediment traps from the northwestern Mediterranean Sea. *Geochim. Cosmochim. Acta* **60**, 1239 – 1259.

Philp, R.P. (1985) *Fossil Fuel Biomarkers*. Elsevier Science Publishers B.V., The Netherlands.

Prartono, T. (1995) *Organic Geochemistry of Lacustrine Sediments: A Case Study of the Eutrophic Lake, Rostherne Mere, Cheshire, UK*. PhD. Thesis. University of Liverpool.

Prartono, T. and Wolff, G.A. (1997) Organic geochemistry of lacustrine sediments: A record of the changing trophic status of Rostherne Mere, U.K. *Org. Geochem.* **28**, 729 – 747.

Puel, F., Largeau, C. and Giraud, G. (1987) Occurrence of a resistant biopolymer in the outer walls of the parasitic alga *Prototheca wickerhamii* (Chlorococcales): Ultrastructural and chemical studies. *J. Phycol.* **23**, 649 – 656.

Reimers, C.E. and Suess, E. (1983) Late Quaternary fluctuations in the cycling of organic matter off central Peru: a proto-kerogen record. In, Suess, E. and Thiede, J. (Eds.) *Coastal Upwelling, Part A: Responses of the Sedimentary Regime to Present Coastal Upwelling*. pp 497 – 526. Plenum Press, New York.

Reynolds, C.S. (1979) The limnology of the eutrophic meres of the Shropshire-Cheshire Plain: a review. *Fld. Stud.* **5**, 93 – 173.

Ripley, M. (1994) *Quantitative & Qualitative characterisation of Organic Matter from a Sedimentary Shelf Environment Offshore Peru: A Correlation with Bacterial Necromass*. MSc Thesis. University of Plymouth.

Risatti, J.B., Rowland, S.J., Yon, D.A. and Maxwell, J.R. (1984) Stereochemical studies of acyclic isoprenoids – XII. Lipids of methanogenic bacteria and possible contributions to sediments. *Org. Geochem.* **6**, 93 – 104.

Robertson, D.E., Roberts, M.F., Belay, N., Stetter, K.O. and Boone, D.R. (1990) Occurrence of β -glutamate, a novel osmolyte, in marine methanogenic bacteria. *Appl. Environ. Microbiol.* **56**, 1504 – 1508.

Rosen, H. (1957) A modified ninhydrin colorimetric analysis for amino acids. *Arch. Biochem. Biophys.* **67**, 10 – 15.

Rosenfield, J.K. (1979) Amino acid diagenesis and adsorption in nearshore anoxic marine sediments. *Limnol. Oceanogr.* **24**, 1014 – 1021.

Round, F.E., Crawford, R.M. and Mann, D.G. (1990) *The Diatoms*. pp 4, 140 – 141, 576 - 577. Cambridge University Press.

Rouxhet, P.G., Robin, P.L. and Nicaise, G. (1980) Characterization of kerogens and of their evolution by infrared spectroscopy. In, Durand, B. (Ed.) *Kerogen. Insoluble Organic Matter from Sedimentary Rocks*. pp 301 – 338. Editions Technip, Paris.

Rowland, S.J., Lamb, N.A., Wilkinson, C.F. and Maxwell, J.R. (1982) Confirmation of 2,6,10,15,19-pentamethyleicosane in methanogenic bacteria and sediments. *Tetrahedron Lett.* **23**, 101 – 104.

Rubinsztain, Y., Ioselis, P., Ikan, R. and Aizenshtat, Z. (1984) Investigations on the structural units of melanoidins. In, Schenck, P.A., de Leeuw, J.W. and Lijmbach, G.W.M. (Eds.), *Advances in Organic Geochemistry 1983*. pp 791 – 804. Pergamon Press Ltd., UK.

Rubinsztain, Y., Yariv, S., Ioselis, P., Aizenshtat, Z. and Ikan, R. (1986) Characterization of melanoidins by IR spectroscopy – I. Galactose-glycine melanoidins. *Org. Geochem.* **9**, 117 – 125.

Rullkötter, J. and Michaelis, W. (1990) The structure of kerogen and related materials. A review of recent progress and future trends. In, Durand, B. and Behar, F. (Eds.) *Advances in Organic Geochemistry 1989*. pp 829 – 852. Pergamon Press plc., Oxford.

Sahota, H.S., Lloyd, P.M., Yeates, S.G., Derrick, P.J, Taylor, P.C. and Haddleton, D.M. (1994) Characterisation of aromatic polyester dendrimers by Matrix-assisted Laser Desorption Ionisation Mass Spectrometry. *J. Chem. Soc., Chem. Comm.* **21**, 2445 – 2446.

Saiz-Jimenez, C. (1992) Applications of pyrolysis-gas chromatography/mass spectrometry to the study of humic substances: evidence of aliphatic biopolymers in sedimentary and terrestrial humic acids. *Sci. Tot. Env.* **117/118**, 13 – 25.

Sánchez-Saavedra, M.d.P. and Voltolina, D. (1996) Effect of blue-green light on growth rate and chemical composition of three diatoms. *J. Appl. Phycol.* **8**, 131 – 137.

Seddon, K.R. (1996) Room-temperature ionic liquids: Neoteric solvents for clean catalysis. *Kinetics and Catalysis* **37**, 693 – 697.

Seddon, K.R. (1997) Ionic liquids for clean technology. *J. Chem. Tech. Biotechnol.* **68**, 351 – 356.

Smith, G.P., Dworkin, A.S., Pagni, R.M. and Zingg, S.P. (1989) Brønsted superacidity of HCl in a liquid chloroaluminate. AlCl₃-1-Ethyl-3-methyl-1*H*-imidazolium chloride. *J. Am. Chem. Soc.* **111**, 525 – 530.

Steele, A., Summons, R.E., Toporski, J.K.W., Guidry, S.A., Avci, R., Sutton, P.A., Wynn-Williams, D.D. and McKay, D.S. (in preparation) ToF-SIMS analysis of isolated bacterial hopanols.

Stetter, K.O. (1998) Hyperthermophiles: Isolation, classification and properties. In, Horikoshi, K. and Grant, W.D. (Eds.) *Extremophiles. Microbial Life in Extreme Environments*. pp. 1 – 24. Wiley-Liss, Inc., USA.

Sprott, G.D., Meloche, M. and Richards, J.C. (1991) Proportions of diether, macrocyclic diether, and tetraether lipids in *Methanococcus jannaschii* grown at different temperatures. *J. Bacteriol.* **173**, 3907 – 3910.

Standen, G., Boucher, R.J., Rafalska-Bloch, J. and Eglinton, G. (1991) Ruthenium tetroxide oxidation of natural organic macromolecules: Messel kerogen. *Chem. Geol.* **91**, 297 – 313.

Stoneley, R. and Selley, R.C. (1986) *A Field Guide to the Petroleum Geology of the Wessex Basin*. Imperial College of Science and Technology, London.

Strohl, W.R., Larkin, J.M., Good, B.H. and Chapman, R.L. (1977) Isolation of sporopollenin from four myxobacteria. *Can. J. Microbiol.* **23**, 1080 – 1083.

Surette, J.K.D., Green, L. and Singer, R.D. (1996) 1-Ethyl-3-methylimidazolium halogenoaluminate melts as reaction media for Friedel-Crafts acylation of ferrocene. *J. Chem. Soc., Chem. Comm.* **24**, 2753 – 2754.

Suzuki, N. and Philp, R.P. (1990) Formation of melanoidins in the presence of H₂S. *Org. Geochem.* **15**, 361 – 366.

Tegelaar, E.W., de Leeuw, J.W., Largeau, C., Derenne, S., Schulten, H.R., Müller, R., Boon, J.J., Nip, M. and Sprenkels, J.C.M. (1989a) Scope and limitations of several pyrolysis methods in the structural elucidation of a macromolecular plant constituent in the leaf cuticle of *Agave americana* L. *J. Anal. Appl. Pyrol.* **15**, 29 – 54.

Tegelaar, E.W., Derenne, S., Largeau, C. and de Leeuw, J.W. (1989b) A reappraisal of kerogen formation. *Geochim. Cosmochim. Acta* **53**, 3103 – 3106.

Tegelaar, E.W., Hollman, G., van der Vegt, P., de Leeuw, J.W. and Holloway, P.J. (1995) Chemical characterization of the periderm tissue of some angiosperm species: Recognition of an insoluble, non-hydrolyzable highly aliphatic biomacromolecule (suberan). *Org. Geochem.* **23**, 239 – 251.

Tissot, B.P. and Welte, D.H. (1984) *Petroleum Formation and Occurrence*. 2nd Ed. pp 31 – 54. Springer-Verlag, Berlin, Heidelberg, New York, Tokyo.

Tomalia, D.A. (1994) StarburstTM/cascade dendrimer: Fundamental building blocks for a nanoscopic chemistry set. *Aldrichimica Acta* **26**, 91 – 101.

Tomalia, D.A. (1995) Dendrimer molecules. *Sci. Am.* **272**, 42 – 46.

Truelove, P.C. and Osteryoung, R.A. (1992) Proton speciation in ambient-temperature chloroaluminate ionic liquids. *Inorg. Chem.* **31**, 3980 – 3985.

Uribe, F.A. and Osteryoung, R.A. (1988) Electrochemical and spectroscopic studies of 1,4-benzoquinone in ambient-temperature chloroaluminate ionic liquids. *J. Electrochem. Soc.: Electrochem. Sci. Tech.* **135**, 378 – 381.

Van Bergen, P.F., Collinson, M.E., Damst, J.S.S. and De Leeuw, J.W. (1994) Chemical and microscopic characterization of inner seed coats of fossil water plants. *Geochim. Cosmochim. Acta* **58**, 231 – 239.

Van Vaeck, L., Adriaens, A. and Gijbels, R. (1999) Static secondary ion mass spectrometry: (S-SIMS) Part 1. Methodology and structural interpretation. *Mass Spec. Rev.* **18**, 1 – 47.

Vitorović, D. (1980) Structure elucidation of kerogen by chemical methods. In, Durand, B. (Ed.) *Kerogen. Insoluble Organic Matter from Sedimentary Rocks*. pp 301 – 338. Editions Technip, Paris.

Volkman, J.K., Farrington, J.W., Gagosian, R.B. and Wakeham, S.G. (1983) Lipid composition of coastal marine sediments from the Peru upwelling region. In, Bjorøy, M. *et al.* (Eds.) *Advances in Organic Geochemistry 1981*. pp 228 – 240. John Wiley Heyden Ltd., Chichester.

Wedzicha, B.L. and Kaputo, M.T. (1992) Melanoidins from glucose and glycine: Composition, characteristics and reactivity towards sulphite ion. *Food Chem.* **43**, 359 – 367.

Welton, T. (1990) *The Chemistry and Spectroscopy of ionic liquids*. PhD Thesis. University of Sussex.

Wershaw, R.L., Pinckney, D.J., Llaguno, E.C. and Vicente-Beckett, V. (1990) NMR characterization of humic acid fractions from different Philippine soils and sediments. *Anal. Chim. Acta* **232**, 31 – 42.

Whelan, J.K. and Thompson-Rizer, C.L. (1993) Chemical methods for assessing kerogen and protokerogen types and maturity. In, Engel, M.H. and Macko, S.A. (Eds.) *Organic Geochemistry: Principles and Applications*. pp 289 – 353. Plenum Press, New York.

White, R.H. (1997) Occurrence and biosynthesis of 5-aminoimidazole-4-carboxamide ribonucleotide and N-(β -D-ribofuranosyl) formamide 5'-phosphate in *Methanobacterium thermoautotrophicum* Δ H. *J. Bacteriol.* **179**, 563 – 566.

Wien, K. (1997) TOF-SIMS analysis of polymers. *Nucl. Instrum. Meth. Phys. Res. B* **131**, 38 – 54.

Wilkes, J.S., Levisky, J.A., Wilson, R.A. and Hussey, C.L. (1982) Dialkylimidazolium chloroaluminate melts: A new class of room-temperature ionic liquids for electrochemistry, spectroscopy, and synthesis. *Inorg. Chem.* **21**, 1263 – 1264.

Wilson, M.A. (1987) *N.M.R. Techniques and Applications in Geochemistry and Soil Chemistry*. pp 62 – 94. Pergamon Press, Oxford.

Woese, C.R. and Fox, G.E. (1977) Phylogenetic structure of the prokaryotic domain: The primary kingdoms. *Proc. Natl. Acad. Sci. USA.* **74**, 5088 – 5090.

Woese, C.R., Kandler, O. and Wheelis, M.L. (1990) Toward a natural system of organisms: Proposal for the domains *archaea*, *bacteria* and *eucarya*. *Proc. Natl. Acad. Sci. USA.* **87**, 4576 – 4579.

Wraige, E.J., Belt, S.T., Lewis, C.A., Cooke, D.A., Robert, J.-M., Massé, G. and Rowland, S.J. (1997) Variations in structures and distributions of C₂₅ highly branched isoprenoid (HBI) alkenes in cultures of the diatom, *Haslea ostrearia* (Simonsen). *Org. Geochem.* **27**, 497 – 505.

Wraige, E.J., Belt, S.T., Massé, G., Robert, J.-M. and Rowland, S.J. (1998) Variations in distributions of C₂₅ highly branched isoprenoid (HBI) alkenes in the diatom, *Haslea ostrearia*: influence of salinity. *Org. Geochem.* **28**, 855 – 859.

Wraige, E.J., Johns, L., Belt, S.T., Massé, G., Robert, J.-M. and Rowland, S. (1999) Highly branched C₂₅ isoprenoids in axenic cultures of *Haslea ostrearia*. *Phytochemistry* **51**, 69 – 73.

Yaylayan, V.A. and Kaminsky, E. (1998) Isolation and structural analysis of Maillard polymers: caramel and melanoidin formation in glycine/glucose model system. *Food Chem.* **63**, 25 – 31.

Zawodzinski, Jr., T.A., and Osteryoung, R.A. (1987) Aspects of the chemistry of water in ambient-temperature chloroaluminate ionic liquids: ¹⁷O NMR studies. *Inorg. Chem.* **26**, 2920 – 2922.

Zawodzinski, Jr., T.A., Janiszewska, L. and Osteryoung, R.A. (1988) On the chemistry of pyrrole in room-temperature chloroaluminate melts. *J. Electroanal. Chem.* **255**, 111 – 117.

Zawodzinski, Jr., T.A., and Osteryoung, R.A. (1990) Oxide and hydroxide species formed on the addition of water in ambient-temperature chloroaluminate melts: An ^{17}O NMR study. *Inorg. Chem.* **29**, 2842 – 2847.

Zegouagh, Y., Derenne, S., Largeau, C., Bertrand, P., Sicre, M-A., Saliot, A. and Rousseau, B. (1999) Refractory organic matter in sediments from the North-West African upwelling system: Abundance, chemical structure and origin. *Org. Geochem.* **30**, 101 – 117.

Zelibor, Jr., J.L., Romankiw, L., Hatcher, P.G. and Colwell, R.R. (1988) Comparative analysis of the chemical composition of mixed and pure cultures of green algae and their decomposed residues by ^{13}C nuclear magnetic resonance spectroscopy. *Appl. Environ. Microbiol.* **54**, 1051 – 1060.